Case No. 84739

IN THE SUPREME COURT OF THE STATE OF NEVADA

ADAM SULLIVAN, P.E., NEVADA
STATE ENGINEER, et al.

Appellants,

vs.

LINCOLN COUNTY WATER
DISTRICT, et al.

JOINT APPENDIX

VOLUME 39 OF 49

Transient Numerical Model of Groundwater Flow for the Central Carbonate-Rock Province: Clark, Lincoln, and White Pine Counties Groundwater Development Project

November 2009

SE ROA 50751

PREFACE

This report was prepared by the Southern Nevada Water Authority. The U.S. Geological Survey served as technical advisor to the Bureau of Land Management in the review of this report.

This Page Intentionally Left Blank

CONTENTS

SE ROA 50754

JA_16155

CONTENTS *(CONTINUED)*

JA_16156

CONTENTS (CONTINUED)

CONTENTS *(CONTINUED)*

CONTENTS (CONTINUED)

CONTENTS (*CONTINUED*)

CONTENTS *(CONTINUED)*

JA_16162

FIGURES

SE ROA 50762

JA_16163

JA_16164

FIGURES *(CONTINUED)*

FIGURES (CONTINUED)

NUMBER   TITLE   PAGE

6-15   Groundwater Flow through External Boundaries for Hydrographic Areas Simulated and Target with ±2 Standard Deviations. 6-18

6-16   Groundwater Flow through External Boundaries for Individual Flow Boundaries Simulated and Target with ±2 Standard Deviations. 6-19

6-17   Groundwater Discharge by ET and Springs for Flow Systems Simulated and Target with ±2 Standard Deviations. 6-22

6-18   Groundwater Discharge by ET and Springs for Hydrographic Areas Simulated and Target with ±2 Standard Deviations. 6-23

6-19   Groundwater Discharge by ET and Springs for Sub-Basins Simulated and Target with ±2 Standard Deviations. 6-24

6-20   Groundwater Discharge by ET and Springs in Flow Systems for Shrubland Simulated and Target with ±2 Standard Deviations. 6-25

6-21   Groundwater Discharge by ET and Springs in Flow Systems for Wetland Simulated and Target with ±2 Standard Deviations. 6-26

6-22   Groundwater Discharge by ET and Springs in Flow Systems for Playa Simulated and Target with ±2 Standard Deviations. 6-27

6-23   Groundwater Discharge by ET and Springs in Flow Systems for Open Water Simulated and Target with ±2 Standard Deviations. 6-28

6-24   Groundwater Discharge by ET and Springs in Hydrographic Areas for Shrubland Simulated and Target with ±2 Standard Deviations. 6-29

6-25   Groundwater Discharge by ET and Springs in Hydrographic Areas for Wetland Simulated and Target with ±2 Standard Deviations. 6-30

6-26   Groundwater Discharge by ET and Springs in Hydrographic Areas for Playa Simulated and Target with ±2 Standard Deviations. 6-31

6-27   Groundwater Discharge by ET and Springs in Hydrographic Areas for Open Water Simulated and Target with ±2 Standard Deviations. 6-32

6-28   Groundwater Discharge by ET and Springs in Sub-Basins for Shrubland Simulated and Target with ±2 Standard Deviations. 6-33

SE ROA 50765

JA_16166

FIGURES (CONTINUED)

SE ROA 50766

JA_16167

FIGURES (CONTINUED)

PLATES

This Page Intentionally Left Blank

TABLES

SE ROA 50772

JA_16173

SE ROA 50773

JA_16174

TABLES (CONTINUED)

TABLES (CONTINUED)

ACRONYMS

3D	three-dimensional
BARCASS	Basin and Range Carbonate Aquifer System Study
BLM	Bureau of Land Management
CCRP	Central Carbonate-Rock Province
CHD	Time-Variant Specified-Head (package)
CHOB	Specified-Head Flow Observation (package)
CONDFACT	conductance modifier
COV	coefficient of variation
CRP	Carbonate-Rock Province
CSS	composite-scaled sensitivity
CWP	Cooperative Water Project
DEM	digital elevation model
DRN	Drain (package)
DROB	Drain observation module
DTW	depth to water
DVFS	Death Valley Flow System
DVRFS	Death Valley Regional Flow System
EIS	environmental impact statement
ET	evapotranspiration
GIS	geographic information system
GSLDFS	Great Salt Lake Desert Flow System
GVFS	Goshute Valley Flow System
HA	hydrographic area
HFB	Horizontal Flow Barrier (package)
HGU	hydrogeologic unit
HOB	head observation
HUF2	Hydrogeologic-Unit Flow (package)
K	hydraulic conductivity
KDEP	hydraulic-conductivity depth-dependence
LVVWD	Las Vegas Valley Water District
MAE	mean absolute error
MDF	moderate-displacement fault
ME	mean error
MNW	Multi-Node Well
MVFS	Meadow Valley Flow System

ACRONYMS (CONTINUED)

MVWD	Moapa Valley Water District
NA	not applicable
NCDC	National Climatic Data Center
NDWR	Nevada Division of Water Resources
NWIS	National Water Information System
NWS	National Weather Service
PDSI	Palmer Drought Severity Index
PLSS	Public Land Survey System
POD	point of diversion
PRISM	Parameter-elevation Regressions on Independent Slopes Model
RASA	Regional Aquifer-System Analysis
RCH	MODFLOW-2000 recharge (package)
RE	recharge efficiencies
RMSE	root mean square error
RMU	regional modeling unit
SFR2	Streamflow-Routing (package)
SNWA	Southern Nevada Water Authority
SoSWR	sum of squared weighted residual
UDWR	Utah Division of Water Rights
USGS	U.S. Geological Survey
UTM	Universal Transverse Mercator
VANI	vertical anisotropy
WRCC	Western Regional Climate Center
WRFS	White River Flow System

ABBREVIATIONS

af	acre-foot
afy	acre-feet per year
amsl	above mean sea level
bgs	below ground surface
cfs	cubic feet per second
d	day
ft	foot
ft^2	square foot

ABBREVIATIONS (CONTINUED)

in.	inch
km	kilometer
km^2	square kilometer
m	meter
m^2	square meter
m^3	cubic meter
mi	mile
yr	year

This Page Intentionally Left Blank

1.0 INTRODUCTION

This report describes the development of a num erical groundwater flow m odel of the C entral Carbonate-Rock Province (CCRP) in N evada and Utah. The CCRP numerical groundwater flow model supports the Sout hern Nevada Water Authority's (SNWA) Clark, Lincoln, a nd White Pine Counties Groundwater Development Project (hereinafter referred to as the Project). The extent of the Project study area (i.e., the regional model area) is shown in Figure 1-1. This numerical model is based on a conceptual model primarily described in a separate report (SNWA, 2009a) and was used as part of the e nvironmental analysis for the Project. Spe cifically, the nume rical model was used to simulate groundwater development scenarios to evaluate the range of potential water-related effects of the Project's groundwater production at the regional scale. Two previous models for this region, the Death Valley Regional Flow S ystem (DVRFS) Model (Belcher, 2004) a nd the Great Basin Regional Aquifer-System Analysis (RASA) model (Prudic et al., 1995), provided the foundation for much of the modeling approach, methodology, and documentation for the CCR P model. The se models are summarized in Section 1.3 and cited throughout this report. Summaries of the P roject background, previous models, purpose and scop e, general assumptions and model limitations, and Bureau of Land Ma nagement (BLM) review process are presented in this sec tion, followed by a description of the contents of this report.

1.1 Background

A brief description of the ba ckground of the Projec t is presented, followed by a summary of the historical background of the study area.

1.1.1 Project Background

To reduce reliance on Colorado River water resources and buffer the impacts of long-term droughts on the Colorado River system, S NWA has identified plans to deve lop in-state non-Colorado River water resources (SNWA, 2004). These potential additional resources will augment the current water resource portfolio i dentified in the S NWA Water Resource Plan (SNWA, 2009c). The Project will develop and conve y groundwater rights and applications held by S NWA in five basins in eastern Nevada. Figure 1-2 shows the project basins and current points of diversion.

The Project consists of groundwat er production, c onveyance and treatm ent facilities, and power conveyance facilities, most of which will be located on Federal lands managed by BLM. Consequently, in 2004, SNWA applied to BLM for r ights-of-way to construct, operate, and maintain the Project facilities. BLM issua nce of these rights-of-way is a Federal action, which must comply with the National Environmental Policy Act of 1969, the Endangered Species Act of 1973, and other Federal regulations. BLM has determined that pr eparation of an Envi ronmental Impact Statement (EIS) is required to assess the potential effects that may r esult from permitting the r ights-of-way,
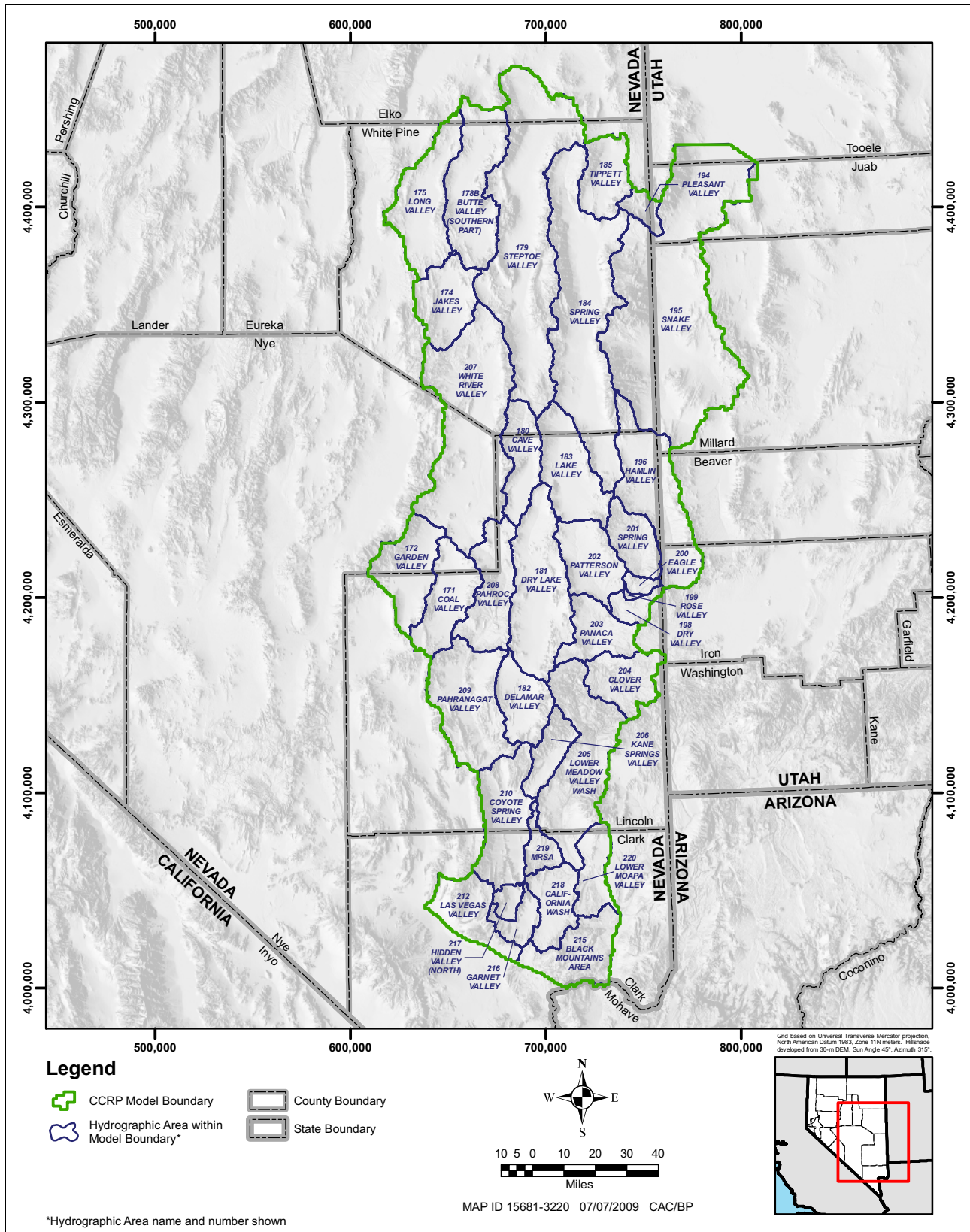
Figure 1-1
Location of Study Area
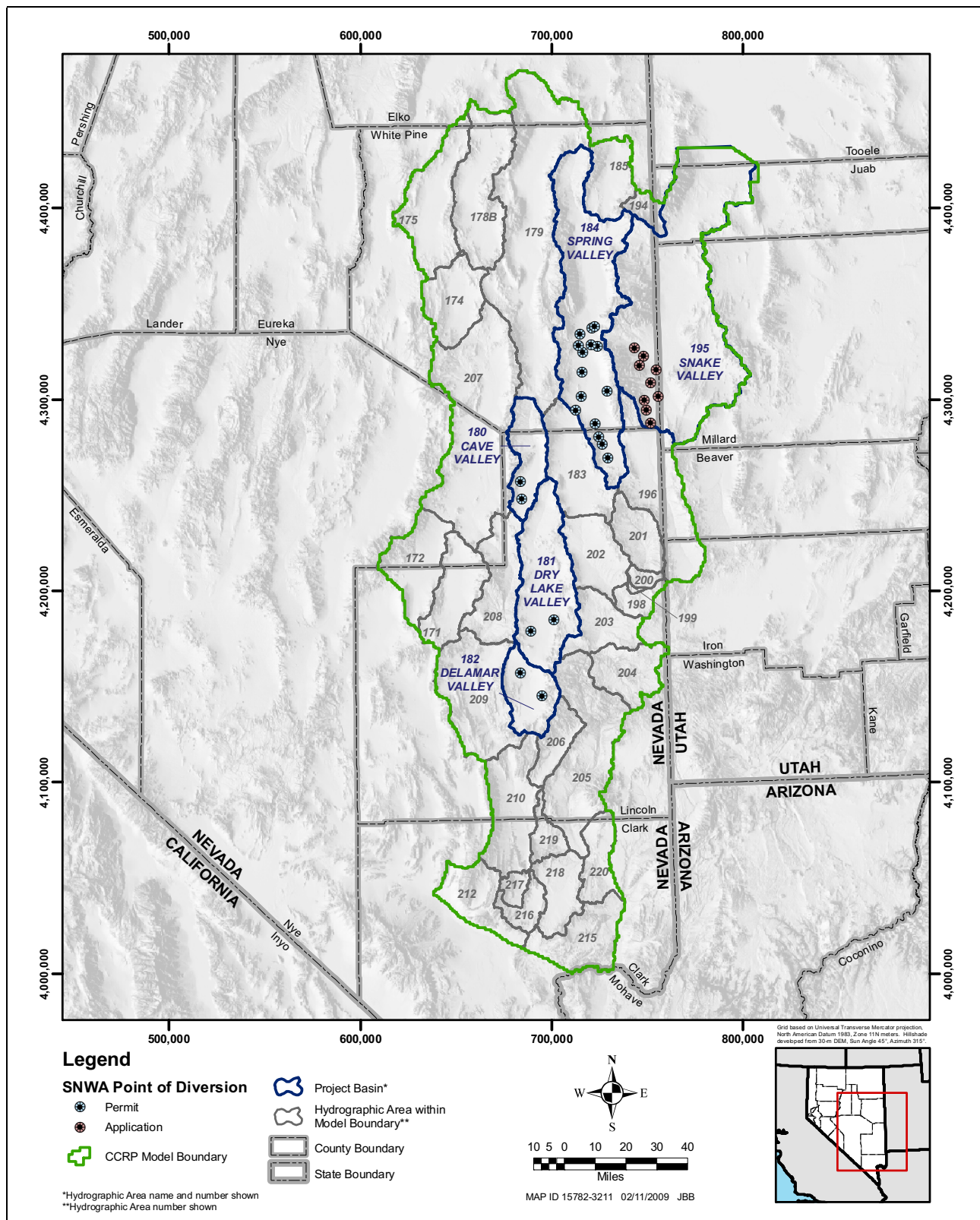
Figure 1-2
Location of Project Basins and Current SNWA Water Rights/
Application Points of Diversion

including the potential indirect effects of the proposed groundwater development. A groundwater flow model was used in the analysis of potential indirect effects for the EIS.

1.1.2   Study Area Background

As described in the Conceptual Model Report (SNWA, 2009a), major historical events include early settlements, the creation of Lake Mead, and increasing historical water use.

According to the Nevada State Engineer (Smales and Harrill, 1971), the first major water use in Nevada coincides with the mining boom starting in 1849. Most of the water was diverted from streams to nearby mills to process the mining ores. Some water was used for irrigation purposes to support the mining community. From 1849 to 1860, the mining community was the main water user in Nevada. The livestock industry began in Nevada around 1870. Irrigation by surface water to produce forage crops started to increase then. Water use continued to expand in Nevada with the building of dams and reservoirs starting in 1903. Major water needs continued to be satisfied by surface water up to the early 1940s when the state began experiencing notable growth. At that time, groundwater use became more significant.

The development history of the basins in the study area is documented in more detail in the Nevada Division of Water Resources (NDWR)/U.S. Geological Survey (USGS) Ground-Water Resources—Reconnaissance Series and the NDWR water-rights database. Boulder Dam, now Hoover Dam, was built in the 1930s during the period when the major source of water in Nevada was surface water. Filling of the reservoir (Lake Mead) was completed in 1937. Spring flow records at the Muddy River Springs Area (Eakin, 1966, p. 264) and Rogers and Blue Point springs (USGS, 2006a and b) indicate that filling the lake has not significantly affected the majority of the flow systems of the study area. Based on the water-rights database, groundwater use by man did not become significant until about 1945 in basins of the study area. Thus, although Lake Mead is man-made, approximate predevelopment groundwater conditions are assumed to prevail up to 1945 and include Lake Mead.

Since the 1940s, groundwater use in the study area has been increasing, as indicated by the water-rights database and the water-use records, although these records are sparse. The rate of increase, however, has slowed down considerably within the last 10 to 15 years. Currently, the main uses of groundwater are irrigation of croplands and rangelands. Other less significant groundwater uses are industrial, mining and milling, municipal, stock watering, and domestic (SNWA, 2008).

1.2   Terminology Used in this Report

The following is a list of definitions for technical terminology used in this report.

Anthropogenic stresses: actions imposed on a flow system by humans. These actions consist of water withdrawals from or additions to a flow system. Water withdrawals may be made directly from wells penetrating the aquifer system, from springs, or from diversion of stream flow of groundwater origin. Water additions to the flow system may result from application of irrigation water to croplands or from artificial recharge.

Anthropogenic effects: the effects that anthropogenic stresses have on the aquifer system. These effects consist of declines or i ncreases in hydraulic heads and flows (discharge by groundwater evapotranspiration [ET], lateral boundary fluxes, and spring and stream flow of groundwater origin).

Predevelopment groundwater conditions: state of a flow system before any anthropogenic stresses occur. When applied to the CCRP model area, this term refers to the state of the flow system when anthropogenic stresses and effects were assumed negligible, i.e., prior to 1945. This term may also be applied to localized areas at any time during the historical period of concern if negligible or no anthropogenic stresses and effects occurred in that area.

Steady-state model or pre development steady-state numerical model: numerical groundwater flow model designed to sim ulate the state of the flow system under equilibrium assuming no anthropogenic stresses. The simulated state represent s the averag e flow s ystem conditions based solely on natural variations caused by natural stresses. Thi s condition is assumed to occur prior to 1945 in this report.

Transient model or transie nt numerical model: numerical groundwater flow model designed to simulate the changing behavior of the flow system under anthropogenic stresses. The time continuum is subdivided into stress pe riods. A transient m odel may or may not incl ude a steady-state stress period. In the transient model prese nted in this report, the first st ress period repr esents predevelopment steady-state conditions similarly to a steady-state model and provides the i nitial conditions for the transient stre ss periods. During the transient stress periods, average stresses are imposed on the flow system and their effects simulated by the model.

1.3   Previous Numerical Models

Several numerical models have been developed for regions that include the entire CCRP model area or parts of the study area. These models are summarized in this section. Other models developed for neighboring flow systems that may be useful to thi s study are also mentioned. Relevant de tails will be cited in the body of the report as appropriate.

Carlton (1985) de veloped a numerical model for the Fish Springs Flow System as part of the Great Basin RASA study. The purpose of the study was to evaluate groundwater flow in the carbonate-rock province of e astern Nevada and we stern Utah. Carlton (1985) der ived interpretations of major controls on groundwater flow and estimates of groundwater-budget components for the Fish Springs Flow System. However, the recharge distribution used in the model was derived using a method developed by Hood and Waddell (1968) and was not varied during model calibration.

As part of the Great Basin RASA study, Prudic et al. (1995) present a conceptual evaluation of regional groundwater flow in the region based on a numerical model. The two-layer numerical model was used to simul ate the concept of numerous shallow-flow regions superimposed upon f ewer deep-flow regions (Prudic et al., 1995). The R econnaissance Series provided the basic estimates of recharge and discharge (Prudic et al., 1995) for this regional flow model. Of particular interest are the interpretations of interbasin flow and flow-system boundaries derived from the modeling results.

Schaefer and Harrill (1995) used the steady-state numerical model developed by Prudic et al. (1995) and made transient simulations of the effects of pumping the points of diversion proposed by SNWA. The simulations were performed without calibration to transient conditions. Instead, storage-property values deemed reasonable were used; therefore, like any model based on this approach, the predictions are even more uncertain than in the case of transient models that are calibrated for transient conditions. No evaluation of the uncertainty associated with the predictions was made.

The Las Vegas Valley Water District (LVVWD, 2001) developed a numerical model in support of the Coyote Spring Valley water-right hearing. The model areas include the southern part of the current model area and compose the White River and Meadow Valley flow systems (LVVWD, 2001). This model was calibrated to predevelopment steady-state and transient conditions using the available data and estimates of historical water use in the area. Using this transient model, LVVWD (2001) evaluated the potential effects of SNWA's proposed groundwater withdrawals in Coyote Spring Valley.

SNWA (2006) developed a numerical model of predevelopment steady-state conditions in support of the Spring Valley water-right hearing. The model area covers much of the northern part of the current model area. The model was developed to serve as a management tool for planning the development of the water resources of Spring Valley (SNWA, 2006). The initial recharge was derived by applying the standard Maxey-Eakin (Maxey and Eakin, 1949) method to an updated spatial precipitation distribution for Spring Valley. Other components of the groundwater budget were based on the Reconnaissance Series of reports.

In the early 1990s, LVVWD developed numerical models for 19 single basins in Nevada, representing predevelopment steady-state conditions. No transient calibration or simulations were performed because the available data were limited. However, analyses were conducted to evaluate the sensitivity of the model to the uncertain parameters. The data and information used in these models are mainly from the Reconnaissance Series and information reported by Harrill et al. (1988). The simulated groundwater budgets were essentially the same as the ones reported in the Reconnaissance reports. The models were documented in the Cooperative Water Project (CWP) Report Series published by LVVWD in support of groundwater applications filed with the Nevada State Engineer's Office in 1989 and as part of its CWP. Brothers et al. (1993, 1994, and 1996) are part of this series of reports and focused on the project basins. The reports were prepared in support of water-rights applications by LVVWD. Other numerical models developed for single basins in the study area include that developed by Frick (1985) for Steptoe Valley and those developed by Leeds, Hill, and Jewett, Inc., (in 1983) for Steptoe and Spring valleys.

Other numerical models of interest were developed for the Death Valley Flow System (DVFS) by D'Agnese et al. (1997, 2002), DOE/NV (1997), and Belcher (2004). The DVFS is contiguous with the CCRP model area, is part of the same region, and has many of the same characteristics. Because of the many similarities between the two study areas, the models developed to represent their flow regimes are very similar, as described throughout this report. For instance, the results derived from these models can be used for comparison purposes in this study.

1.4   Purpose and Scope

This section describes the overall purpose and scope of both the hydrologic evaluation conducted in support of the EIS analysis and the numerical model presented in this report.

1.4.1   Overall Purpose and Scope

The purpose of the hydrologic evaluation was to compile and analyze the available hydrogeologic information to support the EIS analysis. The hydrologic evaluation includes the development of a regional three-dimensional (3D) numerical model of the flow systems underlying the study area. These flow systems consist of three subsystems identified by their depth and the lengths of their flow paths: regional, intermediate, and local, as described by Tóth (1963) and Freeze and Cherry (1979).

The numerical model focuses on the regional flow system. Intermediate systems may also be addressed if they are in contact with the regional flow system. Perched or local flow systems are not modeled. The model will ultimately be used, along with other analyses, to evaluate the potential water-related effects on the environment. As pumping, monitoring, and testing data become available in the future, the model will be improved and used as a management tool.

The CCRP model is specifically designed to simulate historical, existing, and reasonably foreseeable, future groundwater withdrawals, including the proposed SNWA pumping and EIS alternatives, to evaluate the potential effects on the following:

- Potential drawdowns in the regional and intermediate portions of the flow system within the model area

- Regional (primarily) and intermediate (secondarily) springs, groundwater ET areas, streams, or wells that are hydraulically connected to regional and intermediate parts of the flow system

- Flow boundaries

The CCRP model is NOT designed for the following uses:

- Simulation of perched (local) portions of the flow system, including perched springs, groundwater ET areas, streams, or wells or the effects that pumping from the regional flow system would have on these features

- Derivation of accurate predevelopment steady-state groundwater budgets for individual basins or flow systems within the study area or estimates of interbasin flow (directions and volumes) across boundaries

- Derivation of new delineations of groundwater basin or flow-system boundaries

The overall scope of work of the hydrologic evaluation includes four major tasks:

1. Preparation of a report documenting the site baseline conditions titled *Baseline Characterization Report for Clark, Lincoln, and White Pine Counties Groundwater Development Project* (SNWA, 2008).

2. Development of a conceptual model of groundwater flow in the flow system underlying the study area. This step is primarily documented in a report titled *Conceptual Model of Groundwater Flow for the Central Carbonate-Rock Province - Clark, Lincoln, and White Pine Counties Groundwater Development Project* (SNWA, 2009a). Additional information supporting this step is included in SNWA (2008) and this report.

3. Analysis of the data necessary to describe the historical behavior of the flow system and development of the transient numerical model calibrated to the available observation data. This step is documented in this report. The data describing the historical behavior of the flow system include additional estimates of aquifer properties, observation data (water levels, spring flow, and stream flow), and anthropogenic stress data (historical well pumping and stream flow diversions). These data analyses are presented in Appendixes A through C, respectively.

4. Use of the resulting transient model to evaluate future water-use scenarios including SNWA's proposed groundwater withdrawals and EIS alternatives as well as the cumulative effects associated with groundwater development in the model area. These evaluations are documented in a report titled *Simulation of Groundwater Development Scenarios Using the Transient Numerical Model of Groundwater Flow for the Central Carbonate-Rock Province: Clark, Lincoln, and White Pine Counties Groundwater Development* (SNWA, 2009b).

The approach followed to conduct each of the tasks listed above and the associated results have been subjected to detailed peer reviews by BLM and a panel assembled by BLM as described in Section 3.0.

The study area extends over parts of Lincoln, White Pine, Elko, Nye, and Clark counties in Nevada and over Tooele, Juab, Millard, Beaver, and Iron counties in Utah, and encompasses the five project basins: Cave Valley (Hydrographic Area [HA] 180), Dry Lake Valley (HA 181), Delamar Valley (HA 182), Spring Valley (HA 184), and Snake Valley (HA 195) (Figure 1-1). The study area also includes basins where the water-conveyance pipelines and associated facilities will be constructed to move the water from the project basins to the intended places of use in Lincoln County and the Las Vegas Valley. Originally, the eastern boundary of the model area coincided with the boundary of Snake Valley. During the course of this work, the model boundary was extended to include the portion of Fish Springs Flat that comprises Fish Springs.

1.4.2   Purpose and Scope of Numerical Model

The purpose of the work described in this document is the development of a calibrated transient numerical model of the flow systems underlying the study area of the Project (Figure 1-1).

The scope of work includes model construction, calibration, and evalua tion. This work was conducted in two major ph ases with all of its major aspects subjected to review by the Hydrology Technical Group (discussed in Section 1.6) throughout the process. The two major numerical model development phases were as follows:

- Phase 1: Testing of a preliminary numerical model
- Phase 2: Calibration of a transient numerical model

The first p hase consisted of model construction ac tivities and preliminary simulations to derive a numerical representation of the conc eptual model that approximately matched the response of the flow systems under predevelopment conditions. In the preliminary versions of the numer ical model, predevelopment conditions were interpreted from data spanning the f ull period of re cord to supplement the sca rce data available from years prior to 1945. For example, in a reas where no significant anthropogenic stress occurred (no major groundwater use), the fluctuations observed in the water levels were interpreted to be caused by natural stresses only. For such a location, the water levels were statistically reduced to a mean a nd standard deviation to approximate the hydraulic head and hydrograph error at that location. The mea n value was then a ssumed to represent the mean predevelopment hydraulic head at that location. The hydrograph error was added to other sources of error (e.g., land-surface elevation) to represent the error associated with the mean hydraulic-head value. M ore details are provided in the Baseline Report (SNWA, 2008). Many simulations were conducted using this pre liminary numerical model to test and refine the numerical representation of the conceptual model. This preliminary version of the numerical model was then used as the starting point for the development of the transient model.

The transient model was actually designed to simulate the steady-state and transient behaviors of the flow systems. Steady-state conditions were assumed to prevail prior to 1945. Initially, except for a few aspects mostly relating to th e simulation of tr ansient conditions, this version of the model is identical to the preliminary version of the numer ical model representing predevelopment conditions. The exceptions are as follows: (1) the transient capability is activated and transient stress periods are added, (2) the stress da ta are added for each stress period, (3) storage parameters for regional modeling units (RMUs) are added, and (4) the observation data (calibration targets) are rearranged to fit the stress per iods. The model construction, including the fr amework, the boundary c onditions, recharge from precipitation, and values of all hydraulic parameters other than the storage properties, is initially as in the preliminary numerical model.

Both phases of num erical model development were implemented following the modeling approach described in Section 2.0. Phase 1 is summ arized in Section 3.0, and Phase 2 is discussed in the remainder of this report. Most of the information used to develop the numerical model is contained in the Conceptual Model Report (SNWA, 2009a). Many of the interpretations derived by the Basin and Range Carbonate Aquifer System Study (BARCASS) (Welch et al., 2008) for the northern part of the model area were incorporated in the conceptual model. Some of the information used in the numerical model was obtained from SNWA (2008). Som e of the information ne eded (aquifer properties derived from inverse analytical solutions, aquifer response data, and aquifer stress data) is provided in Appendixes A through C. Specific references to these documents, along with additional information used for the de velopment of the CCR P numerical model, ar e provided throughout this report.

1.5   General Assumptions

As stated by Prudic et al. (1995), it is difficult to use computer models to describe groundwater flow in an area as geographically large and geologically complicated as the Carbonate-Rock Province of Nevada and western Utah. Howe ver, as has bee n demonstrated by previous investigators who conducted groundwater modeling studies of the Great Basin or portions of it (Prudic et al., 1993, 1995; D'Agnese et al., 1997, 2002; and Faunt et al., 2004), it is possible and useful to develop such models. As reiterated by these investigators, many arguments can be invoked concerning the validity of the assumptions and hydrologic values used in simulating groundwater flow when such complex geology and hydrology are involved. Inevitably, simplifying assumptions must be used to ada pt the complex conceptual model for numerical simulation. Thr ee major assumptions were used in the development of the CCRP numerical groundwater flow model:

- Groundwater in the region flows t hrough fractures and solution openings of consoli dated rocks, as well as in porous basin-fill deposits. Fracture-flow simulation is, however, impractical at a regional scale; therefore, a porous medium model is used. This assumption is reasonable as long as the grid-cell size is sele cted to be within the range of r epresentative elementary volumes of the media (Bea r, 1979). Repr esentative elementary volumes occ ur over the range of volumes for which media properties do not change with volume.

- The flow system is assumed to have been under predevelopment steady-state conditions before 1945, prior to la rge-scale groundwater development, but a fter the construction of Hoover Dam in the 1930s. As a result, estimates of groundwater recharge are assumed to equal estimates of natural g roundwater discharge prior to 1945. That is, no groundwater withdrawals are simulated for that period. Several conditions exist, however, that may violate this assumption:

  - Regional flow systems of the Gr eat Basin Region may be undergoing a drying-out sequence following a wet ter climate cycle related to the late Pleist ocene period (Prudic et al., 1993). As a re sult, groundwater levels and groundwater discharges being us ed as calibration targets for pre-1945 in this model may not be in equilibrium with present-day groundwater recharge and interbasin flow estimates.

  - Flow systems are subject to natural seasonal or annual fluctuations that are reflected in the uncertainty of pre-1945 target hydraulic heads and groundwater discharge estimates but are not explicitly represented in t he simulation. As a r esult, pre-1945 conditions are represented by average pre-1945 conditions.

  - Lake Mead is historically a significant new regional hydrologic feature in the re gion, and flows in the CCRP model area may not have come into equilibrium with its presence. Well observations taken over the years since its construction may also have some temporal bias.

  - Some irrigation and municipal pumping did occur prior to 1945, on a localized basis, in the study area. This may bias the pre-1945 hydraulic heads and flow observations assumed to be subject to only natural stresses at that time.

JA_16190

- For the post-1945 time per iod, the f low systems were assumed to be under transient conditions due to stresses imposed by man through well pumping and diversion of spring and stream flow originating from groundwater. The stresses and effects of natural fluctuations on the flow systems, namely those associated with variations in precipitation, were not simulated.

1.6   BLM Review Process

A Hydrology Technical Group wa s assembled by BLM in t he early stages of the technica l work conducted in support of the EIS. The primary objective of this group was to provide technical advice and recommendations to BLM, so they could ensure that the hydrologic data analysis and numerical model development satisfy the analysis requirements of the EIS.

The BLM Hydrology Technical Group members are as follows:

- BLM (Nevada, Utah, and Denver regional offices)
- USGS
- ENSR/AECOM (BLM EIS consultant)
- Nevada State Engineer's Office (Observing)

The Hydrology Technical Group r eview process included meetings and c onference calls to discuss and resolve technical issues. I t also included formal reviews of pr eliminary reports and work products, including da ta compilation and a nalysis and modeling f iles or results. This group conducted the report reviews and provided review comments to SNWA and Earth Knowledge, Inc., a consultant to SNWA. ENSR/AECOM was selected by BLM as a third-party contractor to assist in the preparation of the EIS. The Nevada State Engineer's Office participated in the technical meetings but in an observation capacity only.

Major comments provided by the Hydrology Technical Group throughout the development of the CCRP model and their resolution are summarized in Section 3.0 of this report.

1.7   Document Contents

This document consists of nine sections and three appendixes. A brief description of the contents of each is provided:

- Section 1.0 is this introduction.

- Section 2.0 describes the approach followed to develop the numer ical model. This section includes descriptions of the general modeling approach, code sele ction, model construction, and the methods used in the model calibration and evaluation processes.

- Section 3.0 provides a summary of the preliminary testing of the CCRP model before the start of transient calibration, including descriptions of the major issues identified by the Hydrology Technical Group and their resolutio n. All previous work was essentially focused on refining the conceptual model and nume rical model construction and identifying appropriate initial

parameter estimates through preliminary simulations and review. The resulting model serves as the initial configuration for the transient model described in this report.

- Section 4.0 describes the construction of the transient model, which includes grid definition, external boundary conditions, representation of the hydrogeologic system, and observation data.

- Section 5.0 describes the model-calibration process and the refinements of the conceptual model during calibration.

- Section 6.0 describes the model-evaluation process in detail, along with the final parameter-estimation simulations. The evaluation process includes the assessment of the model fit, the estimated parameters, and the simulated flow systems.

- Section 7.0 describes model limitations and uncertainties.

- Section 8.0 provides a summary of this report.

- Section 9.0 provides a list of references cited in this report.

- Appendix A describes local analytical and numerical models developed independently to analyze local site-specific irrigation data to derive estimates of aquifer properties at scales larger than aquifer tests.

- Appendix B describes the analysis of transient observation data (water levels and spring and stream flow). The data sets are provided on the DVD.

- Appendix C describes the analysis of the available water-use data to derive estimates of historical groundwater use in the study area. The data set is provided on the DVD.

JA_16192

2.0   CCRP MODEL DEVELOPMENT APPROACH

The general approach followed to develop the CCRP model is presented in this section, followed by a description of the numerical model construction and calibration approach. The specific computer codes and processes of model construction and calibration are then presented, followed by a description of the process of model fit evaluation.

2.1   General Approach

The general approach for the development of the CCRP model consisted of the following steps:

1. Development of a three-dimensional conceptual model for the flow systems of the study area, including estimates of groundwa ter-budget components (e.g., pr ecipitation, recharge, groundwater discharge by ET, and interbasin inflow and outflow).

2. Development of a numerical model for the flow systems of the study area, including:

   - Construction of the numerical model based on the conceptual model.
   - Preliminary testing of the numerical model.
   - Calibration of the numerical model to transient conditions.

3. Simulation of development scenarios using the transient numerical model to evaluate:

   - Effects of proposed pumping and alternatives.
   - Cumulative effects of historical groundwater use and proposed pumping.

The approach followed to de velop the c onceptual model (Step 1) is described in S NWA (2009a). Additional information relating to the conceptualization of the flow systems, including the specific approaches followed, is presented in Appendixes A through C of this document. The approa ch followed to complete Step 2 is described in the remainder of this section. The approach to Step 3 is described in the corresponding report (SNWA, 2009b).

2.2   Numerical Model Calibration Approach

The numerical model was deve loped by approxima tely following the 14 gui delines for e ffective model calibration advanced by Hill (1998) and recently updated by Hill and Tiedeman (2007). Relevant guidelines were applied to all stages of development of the numerical model.

SE ROA 50792

JA_16193

The 14 guidelines were organized into four major modeling sta ges—model development, model testing, potential new data, and prediction uncertainty—by Hill and Tiedeman (2007, Table 1.3) and are as follows:

- Stage 1 - Model Development

  1. Apply the principle of parsimony (start very simply; build complexity slowly).

  2. Use a broad range of system information (soft data) to constrain the problem.

  3. Maintain a well-posed, comprehensive regression problem.

  4. Include many kinds of observations (hard data) in the regression.

  5. Use prior information carefully.

  6. Assign weights that reflect errors.

  7. Encourage convergence by making the m odel more accurate and evalua ting the observations.

  8. Consider alternative models.

- Stage 2 - Model Testing

  9. Evaluate model fit.

  10. Evaluate optimized parameter values.

- Stage 3 - Potential New Data

  11. Identify new data to improve simulated processes, features, and properties.

  12. Identify new data to improve predictions.

- Stage 4 - Prediction Uncertainty

  13. Evaluate prediction uncertainty and accuracy using deterministic methods.

  14. Quantify prediction uncertainty using statistical methods.

This general modeling approach is applicable to any process model, not just groundwater models. It is consistent with the iterative nature of the development of groundwater flow models as described by Bredehoeft (2003).

2.3   *Description of Selected Codes and Supporting Software*

The finite-difference modeling code, MODFLOW-2000 (Harbaugh et al., 2000), was selected as the platform for construction of the numerical model. More specifically, a customized version of MODFLOW-2000, Version 1.18.01, was used to construct the CCRP model. Given that MODFLOW-2000 has sever al limitations for sensitivity analysis and param eter-estimation capabilities, a custom ized version of UCODE_2005 (Poeter et al., 2005), a parameter-estimation code, was selected for these purposes. UCODE_2005 adds significant flexibility in parameter definition, allowing application of formulas to create derived parameters that may be dependent on a function or multiplier. This feature was used specifically for the recharge runoff parameters. Two other programs, SIM_ADJUST (Poeter and Hill, 2008) and a customized version of ZONBUD, were also used in calculating intermediate statistics for UCODE_2005 processing. The codes wer e executed in the Cygwin e nvironment. Several utility codes were also developed to pre - and post-process the input and output data.   The code changes made to MODFLOW -2000, UCODE_2005, and Z ONBUD are provided electronically on the DVD accompanying this report. The installation and execution of modeling codes and supporting software as well as a description of the model files are also provided on t he DVD. Summary descriptions of the m ain computer codes that were used follow.

2.3.1   *MODFLOW-2000*

MODFLOW-2000 (Harbaugh et al., 2000) was selec ted because of i ts ability to simulate a wide variety of flow systems, its publicly available source code and documentation, and its rigorous USGS peer review. MODFLOW-2000 and earlier versions of MODFLOW have also been used extensively in this region of the United States for regional m odeling (Prudic et al., 1995; Schaefer and Harrill, 1995; D'Agnese et al., 1997, 2002).

The numerical modeling code MODFLOW-2000 (Harbaugh et al., 2000; Hill et al., 2000) is a 3D, block-centered, finite-difference code of groundwater flow. MODFLOW-2000 is an enhanced version of the US GS 3D, finit e-difference, modular groundwater flow modeling code MODFLOW (McDonald and Harbaugh, 1988; Hill, 1992) and MODFLOW-96 (Harbaugh and McDonald, 1996). Enhancements include:

- Restructuring of the code to add processes to packages, procedures, and m odules used in previous versions of MODFLOW. This facilitates the solution of additional equations, such as transport equations or automatic parameter-estimation equations.

- Addition of automatic parameter estimation using nonlinear regression.

Code capabilities in the latest version of MODFLOW-2000 (Version 1.18.01) are as follows:

- Steady and nonsteady flow simulation in a layered 3D and irregularly shaped flow system
- Confined, unconfined, or a combination of confined and unconfined model layers
- Heterogeneous aquifer properties
- Anisotropy of hydraulic conductivities (principal directions restricted to grid axes)
- Depth-decay of hydraulic conductivity

SE ROA 50794

JA_16195

- Specification of hydraulic properties by hydrogeologic unit
- Barriers to groundwater flow
- Several types of lateral boundary conditions:

  - Specified-head boundaries (steady-state and transient)
  - Specified-flux boundaries (steady-state and transient)
  - Head-dependent flux (general head)

- Simulation of flow from external stresses (wells, areal recharge, ET, and drains)
- Simulation of streams, including unsaturated flow beneath streams
- Simulation of lakes and reservoirs
- Time-varying parameters
- Observation, sensitivity, and parameter-estimation processes
- Compatible post-processors, such as RESAN-2000, YCINT-2000, and BEALE-2000

This version of MODFLOW (MODFLOW-2000) includes the following processes:

- GWF1: Ground-Water Flow Process
- SEN1: Sensitivity Process
- OBS1: Observation Process
- PES1: Parameter-Estimation Process

This version of MODFLOW (MODFLOW-2000) includes the following packages:

- BAS6: Basic Package
- BCF6: Block-Centered Flow Package
- LPF1: Layer-Property Flow Package
- RIV6: River Package
- DRN6: Drain Package
- WEL6: Well Package
- GHB6: General Head Boundary Package
- RCH6: Recharge Package
- EVT6: Evapotranspiration Package
- CHD6: Time-Variant Specified-Head Package
- HFB6: Horizontal Flow Barrier Package
- SIP5: Strongly Implicit Procedure Package
- SOR5: Slice Successive Over-Relaxation Package
- PCG2: Version 2 of Preconditioned Conjugate Gradient Package
- DE45: Direct solver
- LMG1: Multigrid solver (for USGS use only)
- STR6: Streamflow-Routing Package
- ADV2: Advective-Transport Observation Package
- RES1: Reservoir Package (RES is the file type in the name file)
- FHB1: Flow and Head Boundary Package (FHB is file type in the name file)
- IBS6: Interbed Storage (subsidence) Package (IBS is the file type in the name file)
- HUF2: Hydrogeologic-Unit Flow Package

- LAK3: Lake Package
- ETS1: Evapotranspiration with a Segmented Function Package
- DRT1: Drains with Return Flow Package
- LMT6: Link to MT3DMS contaminant-transport model
- MNW1: Multi-Node Well Package
- DAF1: Diffusion Analogy Surface-Water Flow Package
- SUB1: Subsidence and Aquifer-System Compaction Package
- SFR2: Stream-Flow Routing Package, version 2
- GMG1: Geometric MultiGrid Solver Package
- SWT1: Subsidence and Aquifer-System Compaction Package for Water-Table Aquifers

Additional capabilities are as follows:

- HYDMOD: Hydrograph option
- GAGE: Hydrograph option for lakes (LAK3 Package) and streams (SFR Package)

2.3.2   UCODE_2005

Although MODFLOW-2000 has built-in parameter-estimation capabilities, UCODE_2005 (Poeter et al., 2005) provides additional flexibility and, therefore, was used in this study. UCODE_2005 (Poeter et al., 2005) is a universal-analysis code and represents updates of the methods implemented in MODFLOW-2000 (Harbaugh et al., 2000) and UCODE (Poeter and Hill, 1998). The methods implemented in these codes follow the guidelines for effective model calibration (Hill, 1998; Hill and Tiedeman, 2007) (see Section 2.2).

UCODE_2005 and associated codes (Poeter et al., 2005) were developed by the USGS, in cooperation with the U.S. Environmental Protection Agency and the International Ground Water Modeling Center of the Colorado School of Mines. The objective was to enhance inverse modeling by expanding the functionality of UCODE (Poeter and Hill, 1998). The resulting software package not only performs parameter estimation but can also be used to conduct residual analysis, linear uncertainty, and a test for model linearity. UCODE_2005 also may be run under two additional modes (advanced-test-model linearity and nonlinear uncertainty). The two additional modes are based on the methods of Christensen and Cooley (2006). The two modes allow for advanced residual analysis and model-linearity testing and adjustment of confidence intervals for nonlinearity. UCODE_2005 also allows for the calculation of linear and nonlinear uncertainties on model predictions.

UCODE_2005 solves parameter-estimation problems using nonlinear regression. It can be used with any process model that has ASCII or text input and output files, and it can be executed in batch mode. The parameters being estimated can primarily be identified in the input files of the application model(s). However, parameters can also be used in conjunction with user-defined functions to calculate a quantity defined in the input files. Quantities simulated by the application model(s) are compared to observations in the regression process. Observations may be selected to correspond to values simulated by the process model or simulated-equivalent values calculated by UCODE_2005 using values simulated by the process model. Prior information on parameters can also be included in the regression, if available.

SE ROA 50796

JA_16197

The computer codes that are part of the UCODE_2005 package are documented in Poeter et al. (2005), Christensen and Cooley (2006), and Hill and Tiedeman (2007). Limited discussions of most of the methods used may also be found in Hill (1994, 1998) and Cooley (2004).

2.3.3   SIM_ADJUST

SIM_ADJUST is a FOR TRAN-90 computer code de veloped by P oeter and Hill (2008) to adjust simulated equivalents for observations or predictions.

Universal-analysis computer codes such as UCODE_2005 (Poeter et al., 2005) are programmed to read simulated equivalents from an out put file generated by the process model being used (MODFLOW-2000 in this case). Under certain conditions (no useful solution), values needed by the universal code (UCODE_2005 in thi s case) are missing or assigned de fault values that ar e not appropriate for the problem at hand. SIM_ADJUST (Poeter and Hill, 2008) alleviates this problem by allowing the user to easily identify missing or default observations in the process model output file and replace them with appropriate values or defaults specified by the user.

2.3.4   ZONBUD

ZONBUD (Harbaugh, 1990) is a FORTRAN computer program developed by the USGS to compute subregional groundwater budgets for MODFLOW groundwater flow models. Documentation about changes to the original version of the code (Harbaugh, 1990) is available from the USGS website (http://water.usgs.gov/nrp/gwsoftware/zonebud3/zonebudget3.html).

Given an input file de fining numbered zones as complex areas in terms of MODFLOW grid cells, ZONBUD calculates groundwater-budget components for each zone using the MODFLOW output files. ZONBUD reads cell-by-cell budget data written by MODFLOW, sums each flow component for all the cells in each specified zone, and writes the zone budgets to an output file.

2.3.5   Cygwin and Utility Codes

Cygwin is a UNIX/Linux-like environment th at runs concurrently with Microsoft Windows XP or Windows Vista. Most of the Cygwin tools are covered by the GNU General Public License, so they can be freely distributed. Specific details regarding the licenses can be found at the Cygwin website (http://www.cygwin.com/ and http://cygwin.com/licensing.html).

Many scripts and utility codes were developed to execute the codes in the Cygwin e nvironment. While the Cygwin environment is not st rictly needed to run the CCRP steady-state model, many of the scripts and support codes require its use.

2.4   Numerical Model Construction

The Conceptual Model Report (SNWA, 2009a), Baseline Report (SNWA, 2008), and Appendixes A through C of this report include data and information necessary for numerical model construction and calibration. Numerical model construction consisted of simplifying the components of the conceptual

model, selecting the appropriate MODFLOW-2000 packages, and preparing the files necessary for MODFLOW-2000, UCODE_2005, and ZONBUD. Besides the setup of the physical aspects of the flow system, other important infor mation included in the input files is the identification of the parameters and t heir initial values and t he observations and their weights. Nume rical model construction consisted of the following steps (MODFLOW-2000 package or supporting code shown in parentheses):

1. Discretization of the model domain to define a 3D finite-difference grid (DIS)

2. Representation of the hydrogeologic framework in the model to include:

   - RMUs (HUF2)
   - RMU zones (HUF2)
   - Structural features affecting groundwater flow (HFB) and RMU zones (HUF2)

3. Definition of external model-boundary conditions (CHD)

4. Representation of groundwa ter discharge in the model including groundwater ET and major springs and streams as:

   - Evapotranspiration (DRN)
   - Springs and streams (DRN and SFR2)
   - Groundwater use (well pumping and stream baseflow diversions)

5. Representation of areal recharge from precipitation in the model (RCH)

6. Addition of hydraulic-head and flow observations (CHOB, DROB, GAGE, UCODE_2005, and ZONBUD)

Information compiled and evaluated in the Baseline and Conceptual Model reports (SNWA, 2008, 2009a) and in the appendixes of this report was used in the de velopment of the numer ical model. This information consists of the following:

- Hydrogeologic framework
- Simplified hydrogeologic framework
- Aquifer-property data
- Major surface-water features (springs and Muddy River stream flow)
- Precipitation distribution
- Initial estimates of groundwater recharge efficiencies (RE) (from precipitation)
- Initial distribution of potential recharge from precipitation
- Locations and rates of groundwater ET under predevelopment conditions
- Locations and discharge rates of major springs under predevelopment and transient conditions
- Hydraulic-head data under predevelopment and transient conditions
- Locations and rates of interbasin flow under predevelopment conditions
- Groundwater budgets under predevelopment conditions
- Historical anthropogenic stresses on the aquifer system

SE ROA 50798

JA_16199

Additional information was obt ained from o ther studies in a few instances. References to t hese studies are provided where appropriate.

2.5   Numerical Model Calibration

Because the CCRP conceptual and numerical models are complex, inconsistencies may occur. The calibration process enabled inconsistencies between the numerical model and field observations to be identified as var ious features of the conceptual model were tested. As a result, refinements to the conceptual and numerical models were necessary during the calibration process. The calibration processes included both a utomated parameter-estimation and tria l-and-error manual calibration approaches.

UCODE_2005 (Poeter et al., 2005) prove d useful for estimating parameter sensitivities, calculating observation residuals, estimating parameters, and indirectly identifying problems with the conceptual model and numerica l model implementation. The manua l trial-and-error approach was usef ul for testing alternative scenarios or for fitting the model to local but important areas of the model that might be overlooked or be mishandled by UC ODE_2005. Optimized solutions estimated by UCODE_2005 could produce unreasonable solutions because of issues of model nonlinearity, model design, and inherent difficulties associated with weighting the accuracy of field data and weighting the relative importance of different types of observations, The iterative use of automated and manual techniques minimized the limitations of the automated approach and allowed a reasonable calibration of the transient numerical model to be achieved.

After a given refinement to the conceptual model was made, a set of MODFLOW-2000 simulations were performed through UCODE_2005. The sensitivities, residuals, and fit statistics gene rated by UCODE_2005 were then used to evaluate the m odel results and to identify pot ential additional refinements to the conceptual model. The following sections describe the nonlinear regression methods, parameters, parameter sensitivities, and observations.

2.5.1   Nonlinear Regression Objective Function

Parameter estimation using nonlinear regression consists of finding parameter values that minimize the Sum of Squared Weighted Residuals (SoSWR) objective function. In UCODE_2005 (Poeter et al., 2005; Hill and Tiedeman, 2007), this objective function may be expressed as follows:

$$S(b) = (y - y')^T W (y - y') \qquad \text{(Eq. 2-1)}$$

where,

$S(b)$ = Objective function
b = $np \times 1$ vec tor containing pa rameter values (where np = the number of pa rameters estimated by regression)
y and y' = $n \times 1$ ve ctors with elements equal to observed and simulated (using b) values respectively (for the CCR P model, the observed and simulated quantities are hydraulic heads and groundwater discharge)

$y - y'$	=	vector of residuals, defined as the observed minus simulated values
W	=	$n \times n$ weight matrix (where n = the number of measured and simulated hydraulic heads and flows
T	=	Superscript indicating the transpose of the vector

The parameters being esti mated are assigned ini tial values t hat are then change d during the optimization process using a modified version of the Gauss-Newton method (Hill, 1998, p. 7–13; Hill and Tiedeman, 2007) to minimize the objective function (Equation 2-1). The resulting values are called optimal parameter values. This procedure is repeated for each conceptual model considered.

For the CCRP model, the weight matrix is diagonal; each diagonal entry is equal to the inverse of the estimated variance of the observation measurement error, where measurement error is defined more broadly than might be expected in that some types of model error are included. This weighting will result in parameter estimates with the smallest possible variance if (1) the estimated variances and the model are accurate, (2) the model is ef fectively linear, and (3) the number of obser vations is asymptomatically large (Bard, 1974). In addition to variances, UCODE_2005 permits the designation of standa rd deviations or c oefficients of va riation (COV), from which va riances are calculated as des cribed by Hill et al. (2000) and Hi ll and T iedeman (2007). These i ndicators of measurement precision are based on an analysis of likely measurement error.

2.5.2 Parameter Definition

Parameters may be defined to represent most physical quantities of i nterest, such as hydr aulic conductivity and recharge. MODFLOW-2000 allows these spatially distributed physical quantities to be represented using zones over wh ich the parameter is c onstant or by using more sophisticated interpolation methods. In either case, multipliers and/or multiplication arrays can be used to modify parameter values in a predictable way.

2.5.3 Parameter Sensitivities

As part of the regression, sensitivities are calculated as $(\partial y'_i)/(\partial b_j)$, the partial derivative of the simulated hydraulic head or flow; y'_i, with resp ect to the jth estimated parameter; and b_j, using the sensitivity-equation method as de scribed by Hil l et al. (2000, p. 67–70) and Hill and T iedeman (2007). Bec ause the groundwater flow e quations are nonlinear with respect to many pa rameters, sensitivities calculated for the same parameter for different sets of parameter values will be different.

Besides being used in the regression calculations, sensitivities are useful to the modeler because they reflect how important each measurement is to the estimation of each parameter. The composite-scaled sensitivity (CSS) is a statistic that summarizes all the sensitivities for one parameter and therefore indicates the cumulative amount of information that the me asurements contain toward the estimation of that parameter. Because they are dimensionless, composite-scaled sensitivities can be used to compare the amount of information provided by various types of data for different types of parameters. Using the weight matrix W in Equation 2-2, CSS for parameter j, CSS_j, is calculated as:

SE ROA 50800

JA_16201

$$CSS_j = \{[\Sigma_{i=n} W_i (\partial y'_i / \partial b_j)^2 b_j^2] / n\}^{1/2} \qquad \text{(Eq. 2-2)}$$

Parameters with la rge CSS values relative to th ose for ot her parameters are likely to be e asily estimated by the regression; parameters with smaller CSS values are likely to be dif ficult or impossible to estimate. Generally, parameters with a CSS less than 1 or a CSS that is more than two orders of magnitude smaller than the largest CSS are difficult to estimate. For some parameters, the available measurements may not provide enough info rmation for e stimation. In this circumstanc e, the parameter value will need to be se t by the modeler, or more he ad and flow me asurements will need to be added to the regression. Parameters with values set by the modeler are called unestimated parameters. If the parameters are insensitive or correlated, they can be left as unestimated during the regression and their uncertainty included as parameters for prediction in UCODE. Composite-scaled sensitivities calculated for different sets of parameter values will be different (Hill, 1998), but in this work, they a re rarely different enough to indi cate that a previously un estimated parameter can subsequently be estimated. An alternative to setting a parameter value is to use prior information on the parameter. This alternative is es pecially important when evaluating prediction uncertainty because it allows measures of uncertainty in model predictions, such as confidence intervals, to reflect uncertainty in the unestimated parameter.

Linear and nonlinear confidence and prediction intervals on simulated values may be calculated using equations shown i n Hill (1998, e q. 28), Christ ensen and Cool ey (2006), and Hill and T iedeman (2007). If the model is sufficiently linear and a dequately represents the flow system, the linea r estimates of these intervals may be good indica tors of prediction uncertainty. Otherwise, the stated significance level of the linear intervals becomes questionable. In such cases, estimates of the confidence intervals may be derived using the nonlinear option of UCODE _2005, or other means such as sensitivity analysis using low and high estimates of the most important parameters.

2.5.4   Observations

Observations are required input to pa rameter-estimation codes such as UCODE_2005. They are weighted and used in the objective function (Equation 2-1).

Observations consist of estimates of hydraulic heads, drawdowns, and flow r ates derived from the available measurements. Values of hydraulic heads were derived from the available water-level data and land-surface elevations at spring locations. Flow rates include fluxes estim ated for permeable segments of the external model boundary, mean annual volumes of groundwater ET, and mean annual spring flow rates.

Weights are calculated based on the uncertainty associated with the observations and are calculated based on the inverse of the varianc e reported for each observation. Observation weights may be manually adjusted dur ing model calibration by the m odeler. This re weighting of the observations must be conducted carefully (Hill and Tiedeman, 2007).

JA_16202

2.6   *Evaluation of Model Fit*

Model fit is e valuated through analyses of weighted and unweighted residuals of hydraulic heads, drawdowns, and flows. More detailed analyses of the simulated values provide additional insight into the calibrated model.

Weighted and unweighted residuals (defined after Equation 2-1) are important indicators of model fit and depend somewhat on data quality and model accuracy. Consideration of unweighted residuals is intuitively appealing because the values have the dimensions of the observations and indicate, for example, that a hydraulic head is matched to within 33 ft (10 m). However, unweighted residuals can be misleading because observations are measured with different accuracies.

Weighted residuals demonstrate model fit relative to what is expected in the calibration based on the precision, or noise, of the data. They are less intuitively appealing because they are dimensionless quantities that equal the number of standard deviations or coefficients of variation needed to equal the unweighted residual.

Unweighted hydraulic-head residuals tend to be larger in areas (1) with moderate to large hydraulic gradients than in areas with flat gradients (e.g., at the mountain-front and alluvial-fan interface) and (2) where surface topography varies dramatically (e.g., along mountain range s). Howe ver, these areas are not always coincident.

Residual analyses primarily include summary statistics, probability distributions, and spatial distributions of residuals. Distributions of weighted residuals relative to unweighted simulated values are also a useful part of the evaluation.

More detailed eva luations generally include graphical analyses comparing simulated values to observed ranges of observations but vary depending on the type of observations as described below:

1. Evaluations of estimated hydraulic-head distribution:

    -   Review simulated hydraulic-head distribution at the water table. Evaluate gene ral flow directions.

    -   Review simulated hydraulic-head distribution of the regional potentiometric surface for the lower carbonate aquifers. Note regions, groundwater divides, and flow directions.

2. Evaluations of estimated groundwater discharge:

    -   Review ET rate distribution and range by ET type.
    -   Review simulated ET rates by type, flow system, and hydrographic area.
    -   Review simulated spring discharge.
    -   Review simulated stream flow rates.

3. Evaluations of estimated groundwater budgets:

   - Review groundwater budget organized by flow system.
   - Review groundwater budget organized by hydrographic area.

4. Evaluations of model-simulated general flow directions

5. Evaluations of estimated model parameters

   - Review K and transmissivity (T) by layer.
   - Review cumulative transmissivities.
   - Review storage parameters.
   - Review calibrated total, in-place, and runoff recharge distribution.
   - Review calibrated recharge efficiencies by flow system.

3.0 PRELIMINARY NUMERICAL MODEL TESTING

This section describes the preliminary testing of the numerical model up to the start of the transient calibration phase conducted as par t of the development of the CCRP model. The development process was initiated with the formulation of a conceptual model, followed by its translation into a numerical model, and subsequent model calibration phases. Results from the preliminary testing were presented to the Hydrology Technical Group for review throughout the development of the CCRP model in the form of presentation and draft reports. Review comments were also incorporated in the CCRP model throughout the process. Results from the last test simulation of predevelopment conditions were used as the starting point for the transient model. The major issues identified by the Hydrology Technical Group in the conc eptual and numerical models and their re solution are described in this section.

3.1 Major Issues and Their Resolution

The development of the CCRP model included several review and revision cycles. The Hydrology Technical Group primarily reque sted improvements in t his model. Comments relating to the conceptual model and the preliminary numerical model are summarized in the remainder of t his section. Comments re lating to the transient version of the numerical model have bee n considered during the construction and calibration of the transi ent numerical model presented in the remaining sections of this document. The issues identified by the Hydrology Technical Group were subdivided into two groups: (1) conceptual model issues resolved in the Conceptual Model Report (SNWA, 2009a) and (2) numerical model issues resolved in the preliminary numerical model (construction and preliminary calibration).

3.1.1 Conceptual Model Issue Resolution

Comments on the conceptual model pertained to the hydrogeologic framework, groundwater flow patterns in the model domain including the external boundaries, and groundwater-budget components.

3.1.1.1 Hydrogeologic Framework

Issues identified in the hydrogeologic fra mework concern the hypothesis that extensional terrains may be subdivided into zones of hydraulic properties and the lack of discussion of storage properties in the document (SNWA, 2009a).

3.1.1.1.1   Extensional Terrains

The Hydrology Technical Group c ommented that if no hydra ulic-property data are available to support the zonation of the carbonate aquifer based on exte nsional terrains, the z ones should be removed.

As discussed in the Baseline Report (SNWA, 2008), most of the effects of the extensional period have already been incor porated into the hydrogeologic framework of t he model. These effects include interpreted unit thicknesses and locations of structural features, such as faults. Another effect of the extension that was not included in the hydrogeologic framework is the potential impact on the spatial variation of hydraulic c onductivity. It wa s postulated that (1) the hydra ulic conductivities are expected to be moderate in c arbonate terrains that are slightly e xtended and thick and (2) the hydraulic conductivities are expected to be larger if any significant thickness of the carbonate rock is present in extremely extended carbonate terrains.

The available data on the hydraulic conductivity of the carbonate aquifer are insufficient to prove or disprove this assumption. Howeve r, the delinea tion of slightly and extremely extended terrains interpreted by Dettinger and Schaefer (1996) was used in the zonation of the carbonate aquifer in the numerical model. A dding these zones to the mode l does not nec essarily mean that the calibrated hydraulic-conductivity distribution will follow this logi cal expectation but it allows testing of its validity at the re gional scale. The additi onal zones also provide more flexibility to the calibration process just in case these zones are needed.

The preliminary simulations revealed that assigni ng different hydraulic conductivities to the two types of zones did not significantly affect simulation results. Thus, the hydraulic conductivities assigned to the two types of zones are approximately the same. This e ssentially removes the extensional-terrain zones from the numerical model.

3.1.1.1.2   Hydraulic Properties

The Hydrology Technical Group commented that the documentation of the storage properties should be revised to include a detailed review of the available storage-property data applicable to the study area. Furthermore, the group requested that a summary of the expected values and uncertainty ranges by RMU be included in the Conceptual Model Report (SNWA, 2009a).

A discussion of the data analysis of storage properties compiled in the aquifer-property database was added to Appe ndix C a nd summarized in S ection 4.0 of the Conce ptual Model Report (SNWA, 2009a). Unfortunately, the available data are scarce, and the estimated values derived may not reflect the large scales represented in the numerical model. Therefore, an additional analysis was conducted to derive estimates of T and S using long-term irrigation-pumping estimates together with water-level records in wells determined to be affected by irrigation pumping (Appendix A). Ranges of vertical anisotropy of hydraulic c onductivity were also summarized from the available data. However, these ranges may not be representative of large portions of the aquifer systems because of scarce data. Thus, a value between 10 and 100 wa s used in the numerical model, a s recommended by the Hydrology Technical Group. This range is withi n the vertical anisotropy of 2 t o 100 re ported by Walton (1988).

SE ROA 50805

JA_16206

3.1.1.2   Groundwater Flow Patterns and External Flow Boundaries

Initially, the simplified conceptual model consisted of a single interpretation of regional groundwater flow configuration and corresponding locations of external flow boundaries. Annual boundary flows were derived from the literature only for these model-boundary segments. Other interpretations of flow patterns, including other potential loc ations of boundary flow, had been considered for comparison purposes only. The uncertainty associated with the boundary flows was quantified using only literature ranges.

Issues identified with this appr oach were (1) the estimates of boundary flow were not de rived independently but were derived from previous conceptual models, and (2) BARCASS interbasin flow estimates were not considered in the derivation of the conceptual model.

These issues were addressed as follows:

- The simplified interpretation of regional patterns of groundw ater flow was still used to describe the simpl ified conceptual model. A specific interpretation of groundwater flow is necessary to derive an initial distribution of precipitation recharge for the numerical model. Groundwater flows ac ross the corresponding model-boundary segments wer e estimated independently using Monte Carlo simulations of Darcy's equation where possible.

- Other major interpretations of groundwater flow in the model domain, such as the one derived for BARCASS, were incorporated within the uncertainty envelope of the conceptual model (SNWA, 2009a). This mea ns that no pre vious interpretation was dismissed from the conceptual model. The spa rse data available for the model area do not permit a single accurate interpretation of flow everywhere in the flow system.

In summary, the CCRP conceptual model of groundwater flow now described in SNWA (2009a) is not only represented by the simpli fied interpretation but a lso by the uncertainties associated with every component of the conceptual model, including flow directions where information is insufficient.

3.1.1.3   Groundwater Budget

Groundwater-budget issues identified in the conceptual model relate to estimates of groundwater ET in Lower Meadow Valley Wash and excess water in Hamlin Valley. The methods used to estimate these quantities link these two components of the groundwater budget. The first is sue was that the estimated annual rate of groundwater ET from Lower Meadow Valley Wash was too large and should be replaced with the estimate de rived by D eMeo et al. (2008), r educed by surface water . The resulting value of groundwater ET must be less than 10,000 af y. The second issue wa s that the amount of interbasin flow from Hamlin Valley to Snake Valley was too large. The excess water was due to the large annual recharge volumes estimated for Hamlin Valley.

- These issues were resolved by (1) adjusting the groundwater ET estimates for Meadow Valley Flow System (MVFS) to be consistent with those estimated by DeMeo et al. (2008), adjusted for surface water as nece ssary; (2) recalculating the recharge efficiencies for MVF S;

SE ROA 50806

JA_16207

(3) assigning these efficiencies to the southern portion of Hamlin Valley (volcanic rocks); and (4) recalculating the recharge efficiencies for the remainder of the Great Salt Lake Desert Flow System (GSLDFS). The corresponding solution also yielded a new lesser estimate of outflow through the Confusion Range. The details are provided in SNWA (2009a).

3.2   Numerical Model Issue Resolution

Revisions to the construction of the numerical model included modification of the model-domain discretization and representation of the conceptual model.

3.2.1   Model-Domain Discretization

Initially, the model domain was discretized into 474 rows, 202 columns, and 15 layers. In addition, in the preliminary calibration runs, the top model layer was simulated as a convertible layer between confined and unconfined conditions to accommodate the unconfined portions of the flow system. Under this setup, when the simulated hydraulic head falls below the top of a convertible-layer cell, water-table conditions are assumed to prevail in that cell. Consequently, saturated thickness and transmissivity are recalculated at each iteration based on the simulated hydraulic head. This setup of the top model layer caused numerical instabilities and prevented model convergence.

To resolve these instabilities, the top four layers were removed, and the tops of the upper layers were adjusted to approximate the elevation of the water table. As a result, the number of model layers was reduced to 11 layers. This was accompanied by a simplification of the top layers from convertible to confined. The last version of the model spatial discretization is described in Section 4.0.

3.2.2   Conceptual Model Representation

Four major types of changes were made to the conceptual model represented in the numerical model during calibration. These changes pertained to (1) hydrogeologic framework, (2) boundary conditions, (3) definition of recharge processes, and (4) definition of discharge areas.

3.2.2.1   Hydrogeologic Framework

Issues included in this category pertain to (1) hydrogeologic structures, (2) RMU zonation, and (3) hydraulic properties.

3.2.2.1.1   Hydrogeologic Structures

Faults important to groundwater flow act as conduits or barriers or both. Practically no data are available to accurately identify the role of the faults present in the model domain. Generally, faults that are oriented in the dominant direction of flow may be assumed to be conduits of variable permeability along their strikes. However, these faults may also act as barriers to groundwater flow across them. Faults are discussed in greater detail in Section 4.2.3.2.

JA_16208

3.2.2.1.2   RMU Zonation

Preliminary calibration runs revealed that the RMUs provided an overly s implified hydrogeologic framework of the model domain. As a result, the RMUs were subdivided into zones based on natural regional spatial variations. In addition to these re gional variations, more localized variations were tested and incorporated into the model.   Refinements to the RMUs are summarized below and details are provided in Section 4.0.

- The Upper Valley Fill (UVF) RMU was subdi vided into several zones re presenting the lithologic variations of this unit.

- The Lower Valley Fill (LVF) RMU was subdivided into zones to separate volcanic rocks from the consolidated basin fill.

- The Upper Carbonate (UC) and Lower Carbonate (LC) RMUs were subdivided into several zones to delineate various regions within the carbonate rocks based on regional variations.

- Geographic zonations of the "basement" rock (BASE or BAS) and pluton (PLUT) RMUs were based on regional-scale structural features.

- The Upper Aquitard (UA) and LC RMUs in the areas of Long, Jakes, Steptoe, Butte, and White River valleys were subdivided into zones mainly to add and test a possible groundwater flowpath from Long Valley to White River Valley, via Jakes Valley.

- Zones were added to some RMUs to represent local hydrogeologic features to better simulate flows at some springs. This zonation is designed to improve, but still only approximate, the representation of local geologic features controlling spring flow.

3.2.2.1.3   Hydraulic Properties

Issues associated with hydraulic properties in the pr eliminary numerical model included the spatial distributions of transmissivity and hydraulic conductivity, the values of anisotropy ra tios, the variation of horizontal hydraulic conductivity with depth, and t he hydraulic conductivity of structures. The following text reflects comments made by the Hydrology Technical Group.

In many ar eas, transmissivity values were too high, while in other areas they we re too low. For example, the thickness of the carbonate rocks near the eastern boundary along the Confusion Range in Snake Valley was large. However, the simulated values of transmissivity in this area were on the order of only 500 ft^2/day, while they ranged from 5,000 to 50,000 ft^2/day in the RASA model (Prudic et al., 1995). Simulated transmissivities should be compared to field values to ensure that they are reasonable.

- This issue was addressed by deriving reasonable estimates of transmissivity at scales larger than aquifer tests. This was accomplished by deriving ranges of transmissivities from historical agricultural groundwater-use and aquifer-response data collected over long, dry periods for are as where sufficient data were available (Appendix A). The derived

transmissivity ranges were interpreted to represent the aquifer properties at the appropriate scale for the numerical model. The transmissivity values simulated by the model were compared to these values during calibration.

The spatial distribution of hydraulic conductivity in the preliminary numerical model was inconsistent with the conceptual model. In the conceptual model, the most conductive areas were located along the structural zones or in the carbonates. However, in the numerical model, the most conductive units were simulated in the basin fill.

- The numerical model was revised to correct this issue. The spatial hydraulic-conductivity distribution in the numerical model was revised to follow the conceptualization of groundwater flow.

The preliminary numerical model did not include a decrease of horizontal hydraulic conductivity with depth. However, consolidation of the geologic materials is expected to occur and increase with depth. As a result the hydraulic conductivities of the RMUs should decrease with depth. The Hydrology Technical Group requested that the results of the analysis of hydraulic conductivity versus depth reported in the Conceptual Model Report (SNWA, 2009a) be used to set up the variation of hydraulic-conductivity depth-dependence (KDEP) capability of MODFLOW-2000. The Hydrology Technical Group stated that this should have been included in the numerical model, primarily in the UVF RMU.

- Decrease of horizontal hydraulic conductivity with depth was added where appropriate as recommended by the Hydrology Technical Group, using the KDEP capability of MODFLOW-2000. Details are provided in Section 4.2.4.

3.2.2.2 Boundary Conditions

The flow patterns, particularly across some lateral boundaries of the model domain, could not be simulated as depicted in the simplified conceptual model. The available information is insufficient to support unique interpretations. Therefore, several interpretations of external boundary flows were derived from the available water-level data, interpretive hydrogeologic framework information, and estimates from previous studies. The following modifications were made to the external boundaries based on testing during the model-calibration process.

- Steptoe Valley to Goshute Valley: This boundary was shifted slightly to the east, from its identified location in the simplified conceptual model (SNWA, 2009a), to account for lower hydraulic heads near the model boundary in this area.

- Snake Valley to Tule Valley: The length of this flow segment located along the Confusion Range is uncertain. Initially, it was lengthened to represent the extent of the Confusion Range but was later reduced to match the length of Cowboy Pass.

- Garden Valley to Penoyer Valley: This flow-boundary segment was shifted more to the south, from its identified location in the simplified conceptual model (SNWA, 2009a), to better coincide with a larger section of carbonate rock.

JA_16210

- Tikaboo North Valley to Coyote Spring Valley, Snake Valley to Pine Valley, and Snake Valley to Wah Wah Valley: These flow-boundary segments were deactivated in the preliminary versions of the numerical model. They were, however, reactivated in the numerical model and assigned the flows estimated in the conceptual model as calibration targets as requested by the Hydrology Technical Group.

The following flow-boundary segments were added to the numerical model to improve calibration. These additions are within the uncertainty envelope of the conceptual model (SNWA, 2009a).

- Pahranagat Valley to Tikaboo Valley: This flow-boundary segment was added to the southwest side of Pahranagat Valley to allow potential flow out to Tikaboo Valley.

- Long Valley to Ruby Valley: This flow-boundary segment was added to the northwest boundary between Long Valley and Ruby Valley to allow potential flow out to Ruby Valley.

- Tippett Valley to Antelope Valley South: This flow-boundary segment was added between Tippett Valley and Antelope Valley to allow potential flow out to Antelope Valley.

- Snake Valley to Fish Springs Flat: This flow-boundary segment was added to allow potential west-to-east flow within the carbonate-rock aquifer through the Fish Springs Range.

The Hydrology Technical Group commented that the hydraulic head at Lake Mead was assigned the average lake level between 1937 and 2007. However calibration of the numerical model during preliminary testing was to steady-state predevelopment conditions (pre-1945). The average elevation of Lake Mead between 1937 and 1945 should have been used as the boundary condition.

- The effect of the constant-head value assigned to Lake Mead was tested as part of the preliminary numerical model simulations. After the numerical model reached an acceptable level of calibration to predevelopment conditions assuming post-lake hydraulic heads, a UCODE-2005 optimization run was conducted after changing the constant head at that boundary to pre-lake conditions. Except for minor differences in the UVF aquifer located south of the Muddy Springs, the results were practically the same as for the post-lake version of the numerical model. It was then concluded that using a post-lake hydraulic head for that boundary would not introduce significant additional errors in the numerical model.

3.2.2.3   Recharge and Discharge Processes

The Hydrology Technical Group commented that the preliminary numerical model simulated excess water in several parts of the model area. This water excess results in groundwater discharge values that are larger than expected. The group stated that in the White River Flow System (WRFS), the simulated excess water was apparent as excess discharge in Pahranagat Valley. In the GSLDFS, the excess recharge was evidenced by the large interbasin groundwater flow from Hamlin Valley to Snake Valley. Excess water in the MVFS was evidenced by excess discharge in Lower Meadow Valley Wash.

- Adjustments were made to recharge within the WRFS, and modifications were made to the representation of Pahranagat Valley as described in Section 4.4.4.2.2. These adjustments reduced the excess water in the WRFS.

- Adjustments were made to the discharge targets used for Lower Meadow Valley Wash (SNWA, 2009a), which resulted in a new set of recharge efficiencies for both MVFS and GSLDFS, as described in SNWA (2009a). The recharge in Hamlin Valley was also adjusted during model calibration as described in Section 5.3.3.4. These adjustments reduced the excess water in the MVFS as well as the excessive interbasin groundwater flow from Hamlin to Snake valleys in the GSLDFS.

4.0 NUMERICAL MODEL CONSTRUCTION

This section describes the construction of the transient numerical groundwater flow model, including the abstraction process of the flow system s in the model area into MODFLOW-2000 and UCODE_2005. This process includes the selec tion of the MODFLOW -2000 packages and the preparation of the necessary input files. The construction steps discussed a re (1) numerical model discretization, (2) representation of hydroge ologic framework, (3) de finition of e xternal model boundary conditions, (4) representation of natural surface and groundwater discharge, (5) representation of areal recharge from precipitation, (6) estimation of anthropogenic stresses, and (7) derivation of observation data sets. Parameters associated with the various components of the numerical model are presented, where appropriate.

4.1 Numerical Model Discretization

The discretization of the numerical model is applied to the 3D spatial domain and the simulated time period.

4.1.1 Spatial Discretization

The spatial discretization includes the definition of a horizontal gr id and layers in the ve rtical direction. The layers are then assigned the appropriate hydraulic conditions.

The horizontal discretization of the numerical model domain consisted of defining a finite-difference grid including appropriate grid orientation and grid-cell size.

- The grid orienta tion was se lected to be north-south to approximately match the gener al direction of r egional groundwater flow. R egional flow direc tions follow the north-south orientation of the prominent basins and ranges and dominant structures present in the mode l domain.

- A grid-cell size of approximately 3,281 ft (1,000 m) was selected. Factors considered in the selection of an appropriate grid-cell size were (1) computational efficiency, (2) appropriate representation of the available data, and (3) ability to effectively simulate regional-scale groundwater flow. Thus, t he model grid us ed to simulate regional flow re sults in the averaging of hydraulic properties over grid-cell areas of about $3,281 \times 3,281$ ft ^{2} $(1,000 \times 1,000$ m$^2)$.

The vertical discretization of the numerical model consisted of subdividing the total thickness of the model into layers.

SE ROA 50812

JA_16213

A total of 11 model layers were selected. Table 4-1 lists the grid layer tops and bottoms represented in the numerical model. Cross sections for each numerical model row were developed by sampling the RMU grids, a 30-m resolution surface-elevation grid, and several fault layers (see DVD). In general, the model layers cannot coincide with the RMUs because of the complex geometries of the RMUs, which were caused by folding, faulting, volcanism, and other processes.

Table 4-1
Thickness and Elevation of Top and Bottom of Each Layer of the Numerical Model

Model Layer[a]	Top of Layer ft amsl (m amsl)	Bottom of Layer ft amsl (m amsl)	Thickness ft (m)
1	12,631 (3,850) or lower	6,070 (1,850)	328 (100) to 6,562 (2,000)
2	6,070 (1,850) or lower	5,085 (1,550)	328 (100) to 984 (300)
3	5,085 (1,550) or lower	4,101 (1,250)	328 (100) to 984 (300)
4	4,101 (1,250) or lower	3,117 (950)	328 (100) to 984 (300)
5	3,117 (950) or lower	2,133 (650)	328 (100) to 984 (300)
6	2,133 (650) or lower	1,148 (350)	328 (100) to 984 (300)
7	1,148 (350)	164 (50)	984 (300)
8	164 (50)	-1,312 (-400)	1,476 (450)
9	-1,312 (-400)	-3,527 (-1,075)	2,215 (675)
10	-3,527 (-1,075)	-6,726 (-2,050)	3,199 (975)
11	-6,726 (-2,050)	-10,000 (-3,048)	3,274 (998)

[a]The top or bottom of a layer may be 328 ft (100 m) lower to ensure top model layer is at least 328 ft (100 m) thick.

The north-south-oriented model grid consists of 474 rows, 202 columns, and 11 layers (Figure 4-1). The model domain corresponds to 589,391 active cells and encompasses an area of about 20,688 mi^2 (53,581 km^2) (Figure 4-1). The lower, left-corner origin of the grid is located at Universal Transverse Mercator (UTM) coordinates (X = 607069.1 15225 m; Y = 3998858.038990 m). Grid dimensions along both rows and columns are constant at 3,281 ft (1,000 m). The model extends vertically from -10,000 ft amsl (-3,048 m amsl) to the water table, which varies from about 1,148 ft amsl (350 m amsl) to more than 9,022 ft amsl (2,750 m amsl).

Ideally, the numerical model would have been modeled under confined and unconfined conditions. However, the use of convertible layers (unconfined) resulted in instabilities in model convergence. To address this issue, all model layers were treated as confined, and the model grid was adjusted in two ways:

- The top elevation of the top model layer was adjusted to approximately match the expected water-table surface. Thus, the confined layer thickness approximates the unconfined saturated thickness, and calculated flows are similar. The transmissivity (T) will be similar as it equals the hydraulic conductivity (K) times the saturated thickness (b; $T = Kb$). During model calibration, the top of the model was adjusted to the last calculated steady-state water table.

JA_16214
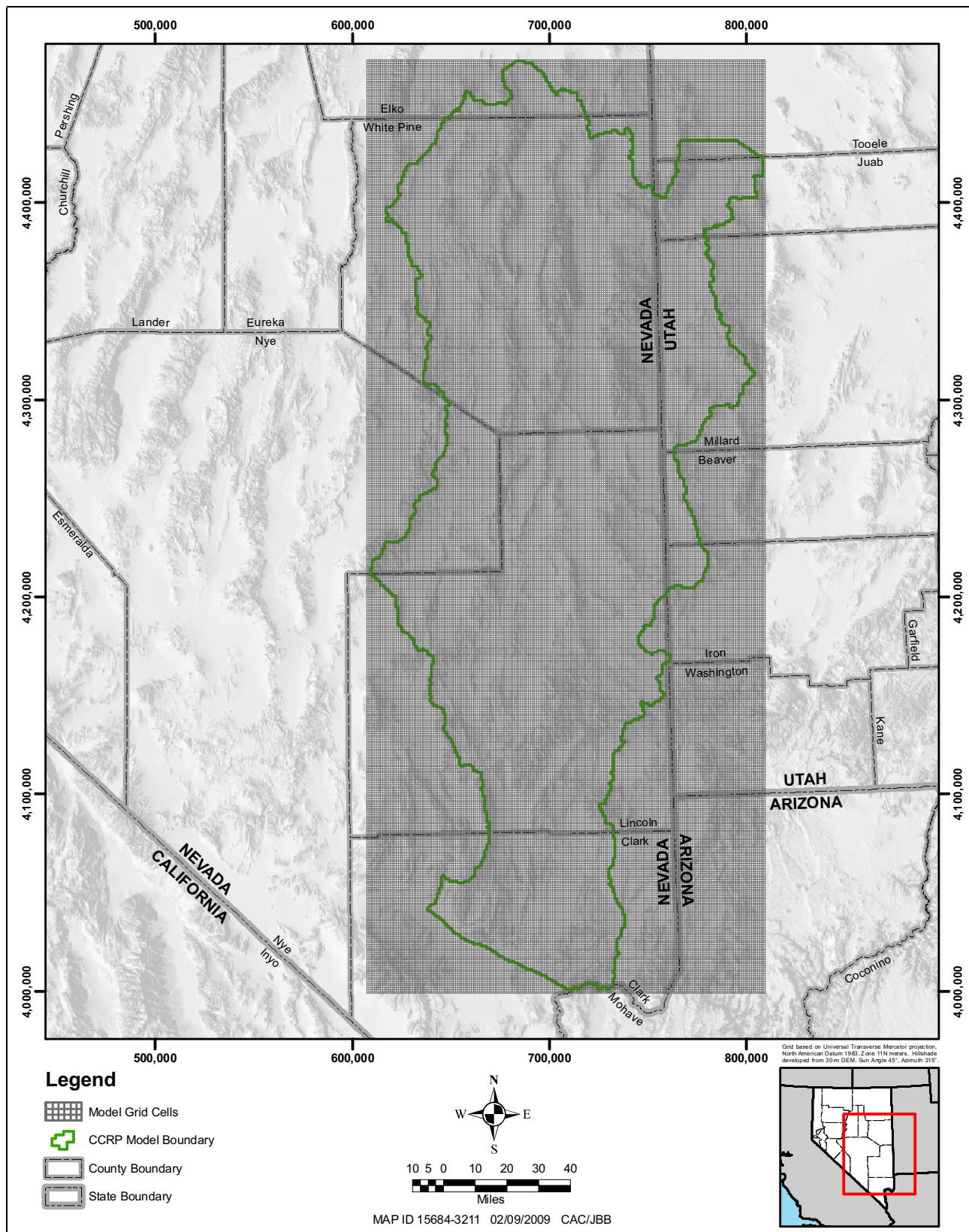
Figure 4-1
Numerical Model Finite-Difference Grid

JA_16215

- Under steady-state conditions, adjusting the top elevation of the model minimizes many of the problems. Under transient conditions, the water table can change, and the assumption of confined flow can become less accurate. For example, if the calculated hydraulic head in the uppermost saturated layer decreases because of a stress (e.g., pumping), the transmissivity does not change, but the effective *K* increases. To minimize the impact of this issue, the top model layer was defined to have a minimum thickness of 328.1 ft (100 m). In areas where the model layer would normally be less than 328.1 ft (100 m), the underlying layers were adjusted to maintain the 100-m thickness in the upper layer. The underlying layers are typically 984.3 ft (300 m) thick. The grid adjustments described reduced the underlying layer thickness a maximum of approximately 656.2 ft (200 m). Except in places of large drawdown, this approach maintains a large saturated thickness, minimizing numerical inaccuracies of the confined assumption.

4.1.2   Time Discretization

The numerical model combines steady-state and transient stress periods. The initial stress period is steady-state and represents predevelopment conditions prior to January 1, 1945. The transient portion of the model extends over the period from January 1, 1945, through December 31, 2004. The 60-year time period was subdivided into 60 transient 1-year stress periods, each lasting 365 or 366 days, as appropriate. Each stress period was subdivided into 12 equal-length time steps.

4.2   Hydrogeologic Framework

The simplified hydrogeologic framework described by SNWA (2009a) consists of eight RMUs (Table 4-2) and major structural features. This hydrogeologic framework was discretized based on the model grid described earlier in the previous section. Figure 4-2 illustrates an oblique view of the discretized hydrogeologic framework model. The RMUs are illustrated in the cross sections across each numerical model row (see DVD). In addition to model layers, the framework was represented in the numerical model using the hydrogeologic-unit flow (HUF2) package (Anderman and Hill, 2003) and the horizontal flow barrier (HFB) package (Hsieh and Freckleton, 1993). These two software packages are described, followed by a description of how the hydrogeologic framework was represented using these packages.

Table 4-2
RMUs Represented in the Numerical Model

RMU Description	RMU Abbreviation
Upper Valley Fill	UVF
Lower Valley Fill and Volcanic Rocks	LVF
Upper Carbonate	UC
Upper Aquitard	UA
Cretaceous Plateau Sediments	Kps
Lower Carbonate	LC
Basement Rocks	BASE (or BAS)
Plutonic Rocks	PLUT

Section 4.0

JA_16216
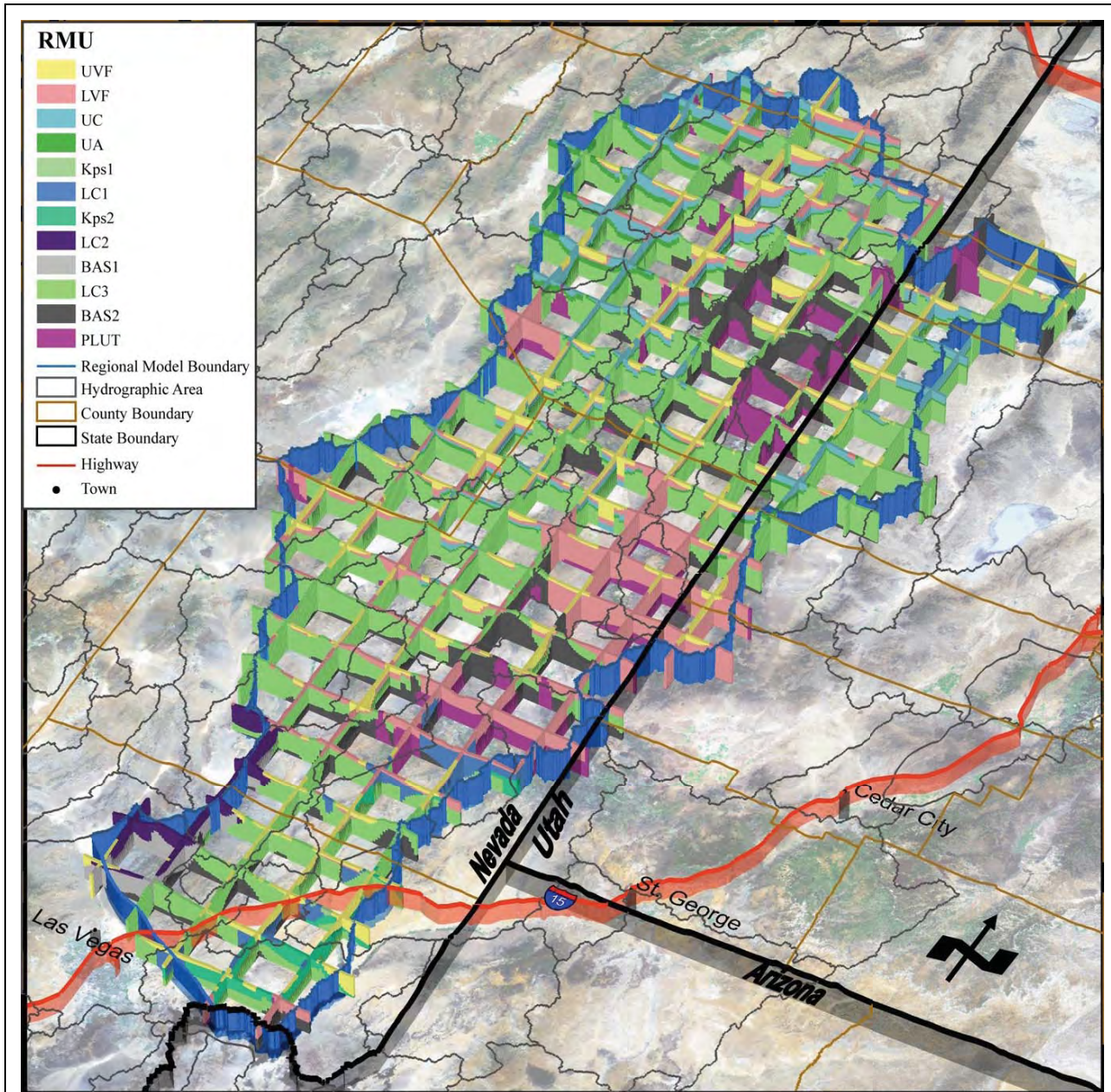
Note: Three times the vertical exaggeration.

Figure 4-2
Oblique View of 3D Framework of RMUs Using a Series of
North-South and East-West Cross Sections Oriented at 20 km

4.2.1   HUF2 Package Description

The HUF2 computer code (Anderman and Hill, 2003) builds on the HUF package (Anderman and Hill, 2000). Three additions are documented by Anderman and Hill (2003): (1) alternative storage for the uppermost active cells (SYTP parameter type), (2) modified calculation of flows in hydrogeologic units, and (3) the KDEP capability. The HUF2 package allows the vertical geometry of the flow system to be different from the model layers. An advantage of the HUF2 package is that

the hydrogeologic framework is set up in the numerical model independently of the model grid. In other words, the model grid can be modified without affecting the hydrogeologic framework.

When using the HUF2 package, the hydraulic properties are assigned to the hydrogeologic units. Initial estimates of all hydraulic properties must be provided for each hydrogeologic unit. Hydraulic properties are treated as parameters and include hydraulic conductivity and storage characteristics. Hydraulic-conductivity characteristics consist of horizontal and vertical hydraulic conductivities (K_h and K_v) and the KDEP factor. The vertical hydraulic conductivity, K_v, can also be represented as a ratio relative to K_h. There are some advantages to keeping the K_v value proportional to K_h during model calibration. Given that the horizontal and vertical hydraulic-conductivity values of a material are typically correlated, it is reasonable that when one value is adjusted, the other should be as well. This tied behavior is defined by the vertical anisotropy ratio (the ratio of horizontal to vertical hydraulic conductivity). The vertical anisotropy (VANI) is expressed as follows:

$$VANI = \frac{K_h}{K_v} \qquad \text{(Eq. 4-1)}$$

where,

$VANI$ = Vertical anisotropy (-)
K_h = Horizontal hydraulic conductivity (L/T)
K_v = Vertical hydraulic conductivity (L/T)

Using the hydraulic properties specified for the hydrogeologic units, HUF2 internally calculates hydraulic properties for every cell in the model grid that are adjusted to depth using Equation 4-2. If a model cell contains a single hydrogeologic unit, the properties of the cell are the same as for the hydrogeologic unit. If a grid cell contains multiple hydrogeologic units, HUF2 calculates the hydraulic properties for that cell by averaging the hydraulic properties of the hydrogeologic units occurring in that cell. The K_h values are calculated using the thickness-weighted arithmetic mean, and the K_v values are calculated using the geometric mean.

The same hydraulic properties may be assigned to an entire hydrogeologic unit. However, for large numerical models, it is reasonable to expect local variations or variation controlled by geologic structure within a given hydrogeologic unit. To account for these variations, the hydrogeologic unit may be subdivided into zones. Zones allow the user to assign different hydraulic parameters to different portions of the hydrogeologic unit.

The variation of hydraulic conductivity with depth is handled by the KDEP capability of the HUF2 package (Anderman and Hill, 2003). This capability allows the horizontal hydraulic conductivity of the hydrogeologic units (RMUs in the numerical model) to decrease with depth using an exponential decay function. The equation is as follows:

$$K_{Depth} = K_{Surface} 10^{-\lambda d} \qquad \text{(Eq. 4-2)}$$

JA_16218

where,

K_{Depth} = Hydraulic conductivity at depth d [L/T]
d = Depth below the reference surface [L]
$K_{Surface}$ = Hydraulic conductivity projected to a reference surface [L/T]
λ = Depth-dependence coefficient [1/L]

The reference surface may be the ground surface or other surface, such as the top of the top model layer. The depth-dependence coefficients, λ, can be treated as parameters in MODFLOW-2000. If the *VANI* option is used to calculate vertical hydraulic conductivity, the values of vertical hydraulic conductivities are automatically adjusted with depth too.

4.2.2   HFB Package Description

The HFB package was added to the MODFLOW code by Hsieh and Freckleton (1993). The HFB package is designed to simulate thin, vertical, low-permeability geologic features that impede horizontal groundwater flow.

These features are represented in the model "as a series of horizontal flow barriers conceptually situated on the boundaries between pairs of adjacent cells in the finite-difference grid" (Hsieh and Freckleton, 1993, p. 1). The only function of these features is to lower the horizontal branch conductance between the two adjacent cells they separate. The storage capacity of the features is assumed to be zero.

The width of the thin barrier is assumed to be negligible relative to the horizontal dimensions of the grid cells and is implicitly included in the expression of the hydraulic property of the flow barrier. This hydraulic property may be expressed in two ways:

- If the flow barrier is located within a constant-transmissivity layer, its hydraulic property is defined as its transmissivity divided by its width.

- If the barrier is located within a variable-transmissivity layer, its hydraulic property is defined as its hydraulic conductivity divided by its width.

4.2.3   Representation of Framework

The RMUs are represented as zones of variable hydraulic properties in the HUF2 package. The major faults are also represented in the HUF2 package as zones of larger permeability along their strikes within the RMUs. The HFB package is used to simulate the potential ability of selected faults represented in the model to also act as barriers to cross flow. Regional faults can be simulated as both conduits along their strike (HUF2) and barriers to cross flow (HFB).

4.2.3.1 Hydrogeologic Features Represented in HUF2 Package

The HUF2 package was used to represent the distribution of RMUs and their hydraulic properties in the model domain (hydraulic conductivity and storage properties). The RMUs were subdivided into zones based on natural features of the hydrogeologic framework conceptualized to affect groundwater flow. A description of the natural features forming the basis of RMU zonation is presented, followed by a discussion of the parameter zones associated with each RMU.

4.2.3.1.1 RMU Zonation Basis

All RMUs were subdivided into parameter zones. Although the zonation was based on natural features conceptualized to affect groundwater flow, the resulting zones are not necessarily supported by aquifer-property data, as such data are scarce in this region. The features are, however, supported by other sources of information and interpretations. Nonetheless, incorporating these zones into the construction of the model allowed variation of the hydraulic properties within a given RMU during model calibration, if necessary. The zones were delineated based on the following features:

- Mountain blocks, structural basins, and normal faults
- Alluvial deposition zones
- Extensional terrains
- Plutonic intrusion events
- Subregional features

Mountain blocks, structural basins, moderate-displacement faults, and large-displacement faults form natural zones of increasingly disturbed materials. Within a given RMU, the portions forming the mountain blocks are the least disturbed materials and therefore form zones of relatively lower hydraulic conductivities. Portions of the same RMU located with the structural basins are more disturbed than the mountain blocks and generally have relatively larger hydraulic conductivities. The moderate- and large-displacement faults (normal faults) are the most disturbed zones and are interpreted to be zones of increased hydraulic conductivity along the strike of the normal faults.

Alluvial deposition zones are natural zones of varying hydraulic properties in the UVF RMU only. Four such zones were delineated: alluvial fans, fluvial deposits, valley bottoms, and playa deposits. The alluvial fans and fluvial sediments are expected to be zones of larger hydraulic conductivity, whereas the playa deposits are expected to be zones of lower hydraulic conductivity. The valley bottoms encompass all other alluvial deposits in a given basin and generally have moderate hydraulic conductivities.

Brittle rocks, such as the carbonate rocks, were extended to varying degrees during extensional deformation. Most of the effects of this extension (thicknesses and faults) were incorporated into the framework model. However, the effects of the extension on the hydraulic conductivity of the RMU blocks were not accounted for. Based on geologic interpretations, Dettinger and Schaefer (1996) have delineated areas of slight and extreme extension in the Carbonate-Rock Province. Carbonate rocks located within the areas of slight extension are interpreted to essentially have their original thicknesses and moderate hydraulic conductivities. Carbonate rocks located within the areas of

JA_16220

extreme extension are interpreted to be thinner to absent and have larger hydraulic conductivities when present.

Plutonic intrusion events cause hydrothermal and thermal alterations to the materials surrounding the intrusion sites. The altered materials form an aureole or halo around the plutonic intrusion. Such areas occur around a number of plutonic intrusions (PLUT RMU) present in the model area. In the numerical model, it was assumed that an alteration aureole could exist in surrounding materials extending 1.2 mi (2 km) laterally around plutonic intrusions that are more than 3,281 ft (1,000 m) thick (from base of model). This alteration is expected to affect all the RMUs except the UVF. The effect of the alteration is a reduction in the hydraulic conductivity. To manage this attribute, the ALT_FACT parameter was added. Cells affected by these alteration zones have their *K* values divided by ALT_FACT using derived UCODE parameters and specially designated HUF2 parameters.

Additional zones were added at the basin and subregional scales as needed during the calibration to improve the fit of the numerical model to the target observations. These zones were based on the available information and included adding zones to reflect local hydrogeology, including texture changes or the presence of faults not already included in the numerical model.

4.2.3.1.2   Parameter Zones

This section discusses the subdivision of the individual RMUs into parameter zones. All RMUs, except the UVF, were assumed to be altered within the halos surrounding the plutons described in the previous subsection. Table 4-3 lists the zone types used to add detail to the hydrogeologic framework. The hydraulic parameters were named by zone and assigned initial values (see DVD).

Table 4-3
Zones Applied to RMUs in the Numerical Model

Zone Type	UVF	LVF	UC	UA	Kps	LC	BASE	PLUT
Mountain Block	---	X	X	---	---	X	---	---
Structural Basin	---	X	X	---	---	X	---	---
Normal Faults[a]	---	X	X	---	---	X	---	---
Alluvial Deposition Zones[b]	X	---	---	---	---	---	---	---
Extension Terrain	---	---	X	---	---	X	---	---
Plutonic Intrusion Events	---	X	X	X	X	X	X	X
Subregional Zones[c]	X	X	X	X	---	X	X	X

[a]Large- or Moderate-Displacement Faults (LDF and MDF)
[b]Streams, alluvial fans, valley bottoms, and playas
[c]Zones applied at basin and subregional scale

SE ROA 50820

JA_16221

Upper Valley Fill

Zones were defined in the numerical model to represent variation within the UVF RMU based on the types of alluvial deposits or on the geographic distribution of the unit. These zones include playas and playa deposits, stream channels, valley bottom materials, alluvial fans, and subregional zones. Figure 4-3 illustrates the UVF parameter zones. The spatial distribution of the detailed hydrogeologic units forming the UVF RMU was obtained from published maps, including county geologic maps.

Lower Valley Fill

The LVF RMU consists of discontinuous Tertiary and Cretaceous sediments as well as middle-Tertiary volcanic rocks. These rocks are composed of conglomerates, sandstones, siltstones, nonwelded to densely welded ash-flow tuffs, ash-fall tuffs, and lava flows. LVF zones represented in the model are calderas and consolidated basin fill. The LVF zones allow materials with different origin and different material properties (volcanic rocks versus various sedimentary basin deposits) to be estimated separately. Sedimentary basin deposits (such as lithified Tertiary basin-fill deposits) and volcanic basin deposits (such as ash and lava flows outside the caldera complexes) are grouped into a single zone. Figure 4-4 illustrates LVF parameter zones. The spatial distribution of the detailed hydrogeologic units forming the LVF RMU was obtained from published maps, including county geologic maps.

Upper Aquitard

The UA RMU consists predominantly of the Eleana and Chainman Formations. These rocks are composed of siltstones and shales. The UA consists of low-permeability, fine-grained sedimentary deposits that restrict vertical flow between the lower carbonate and the upper carbonate and other shallow units. Figure 4-5 illustrates the UA parameter zones. The spatial distribution of the detailed hydrogeologic units forming the UA RMU was obtained from the hydrogeologic framework described in the Baseline Report (SNWA, 2008). Little data are available for the UA, particularly in Butte Valley South, Jakes Valley, and Long Valley. Thus, the UA was assigned a uniform thickness of 3,000 ft (914 m) throughout its extent. Because of the large uncertainty associated with its thickness, the UA composition (all shale versus shale and sandstone interbeds), its competence (degree of faulting), and corresponding hydrologic conditions were allowed to strongly influence its hydraulic-conductivity values.

Upper Carbonate and Lower Carbonate

The UC and LC RMUs consist of Cambrian to Pennsylvanian carbonate rocks, including limestone and dolomite with lesser amounts of shale, siltstone, sandstone, and quartzite. The LC is present throughout the study area, while the UC is predominantly present in the northern areas. Overthrown blocks caused by major thrust faults disrupt the LC's regional continuity (SNWA, 2008). Therefore, three RMUs (LC1, LC2, and LC3) form the LC RMU (SNWA, 2009a). The carbonate RMUs were further subdivided into zones based on their location relative to major basin structures. As shown in Table 4-3, the UC and LC RMUs were subdivided into multiple zones. The zones identified for the UC and LC1 RMUs are shown in Figures 4-6 and 4-7, respectively. The zones identified for the LC2 and LC3 RMUs are shown in Plate 1.
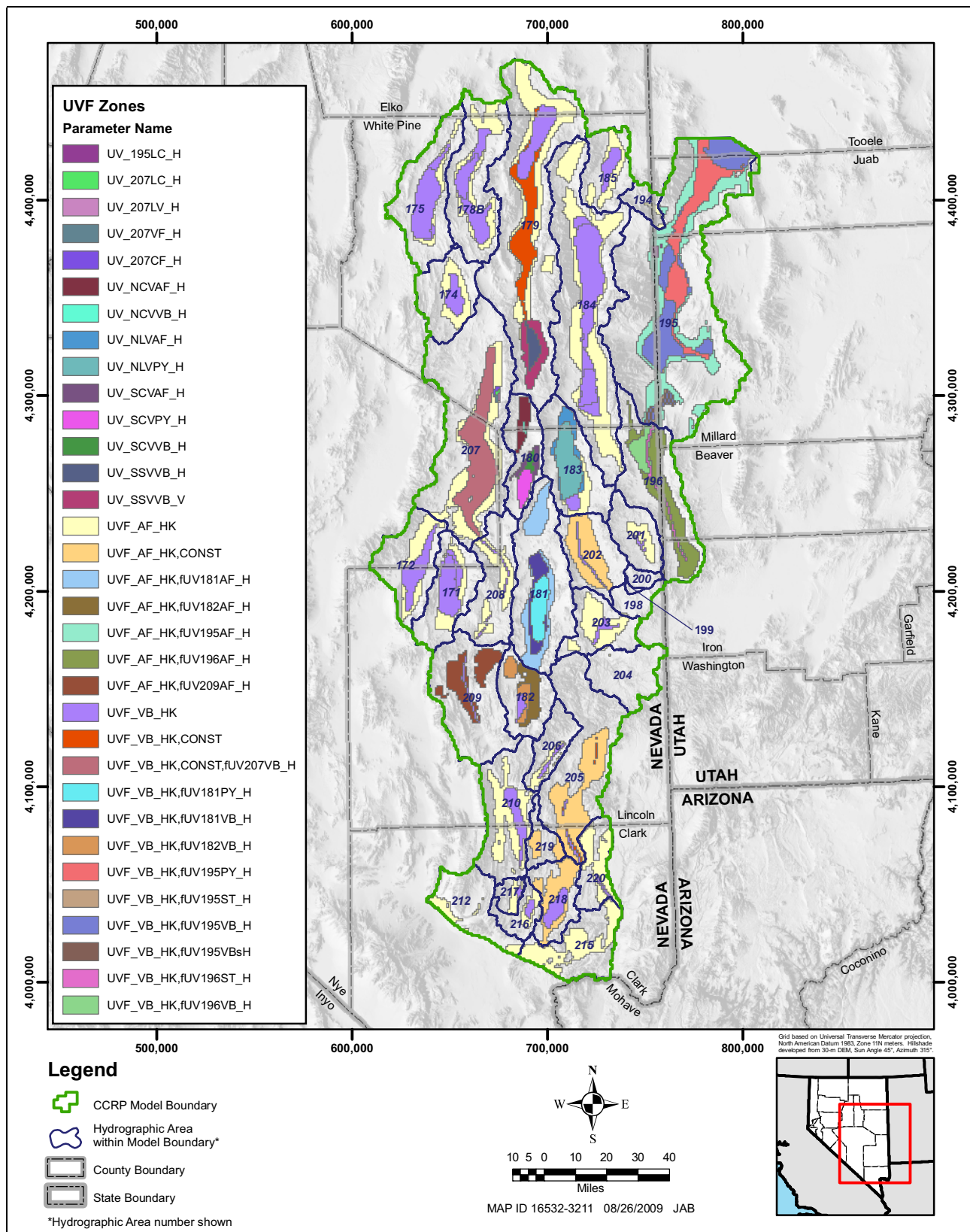
Figure 4-3
Parameter Zones Defined for the UVF RMU in the Numerical Model
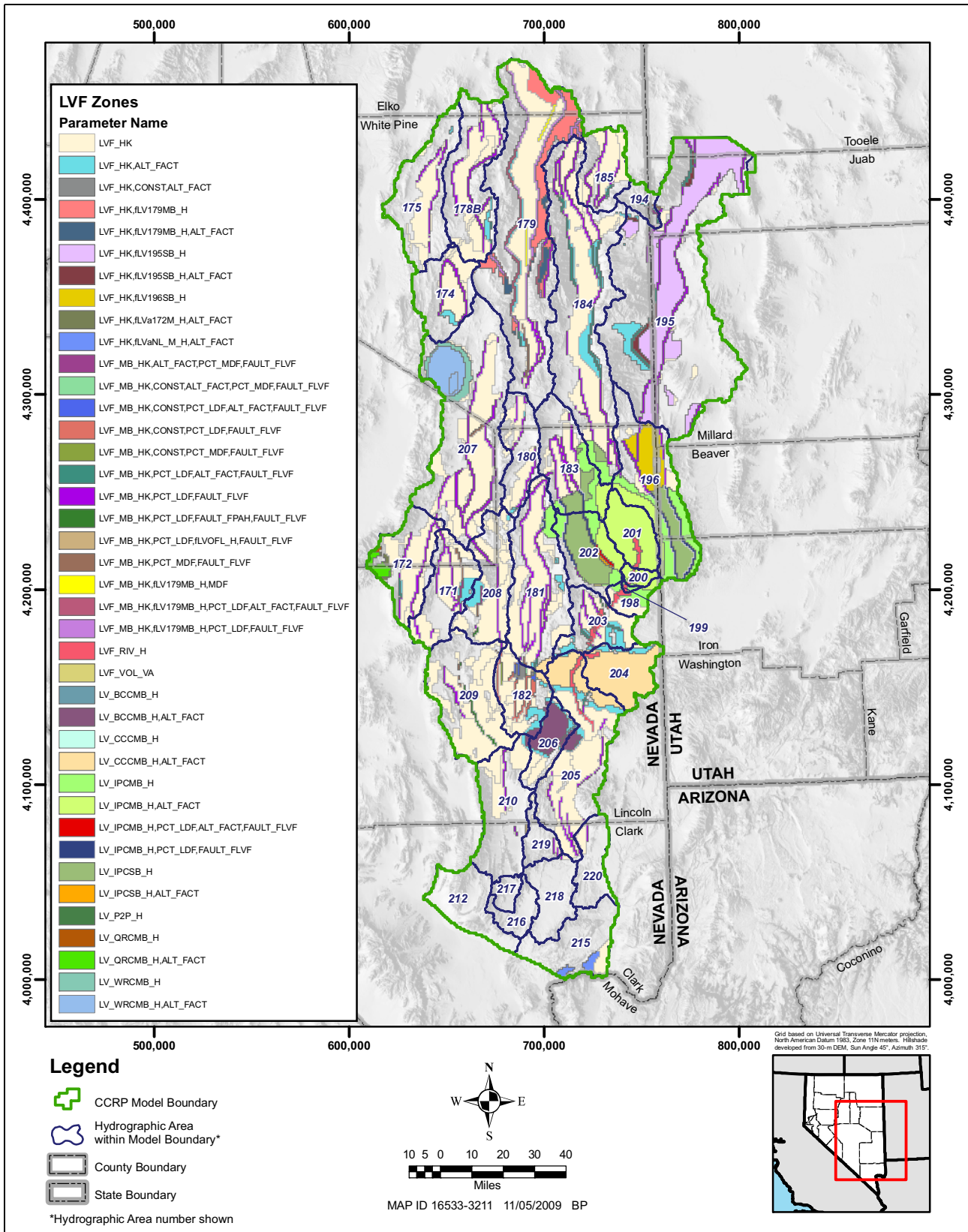
Figure 4-4
Parameter Zones Defined for the LVF RMU in the Numerical Model

SE ROA 50823

JA_16224
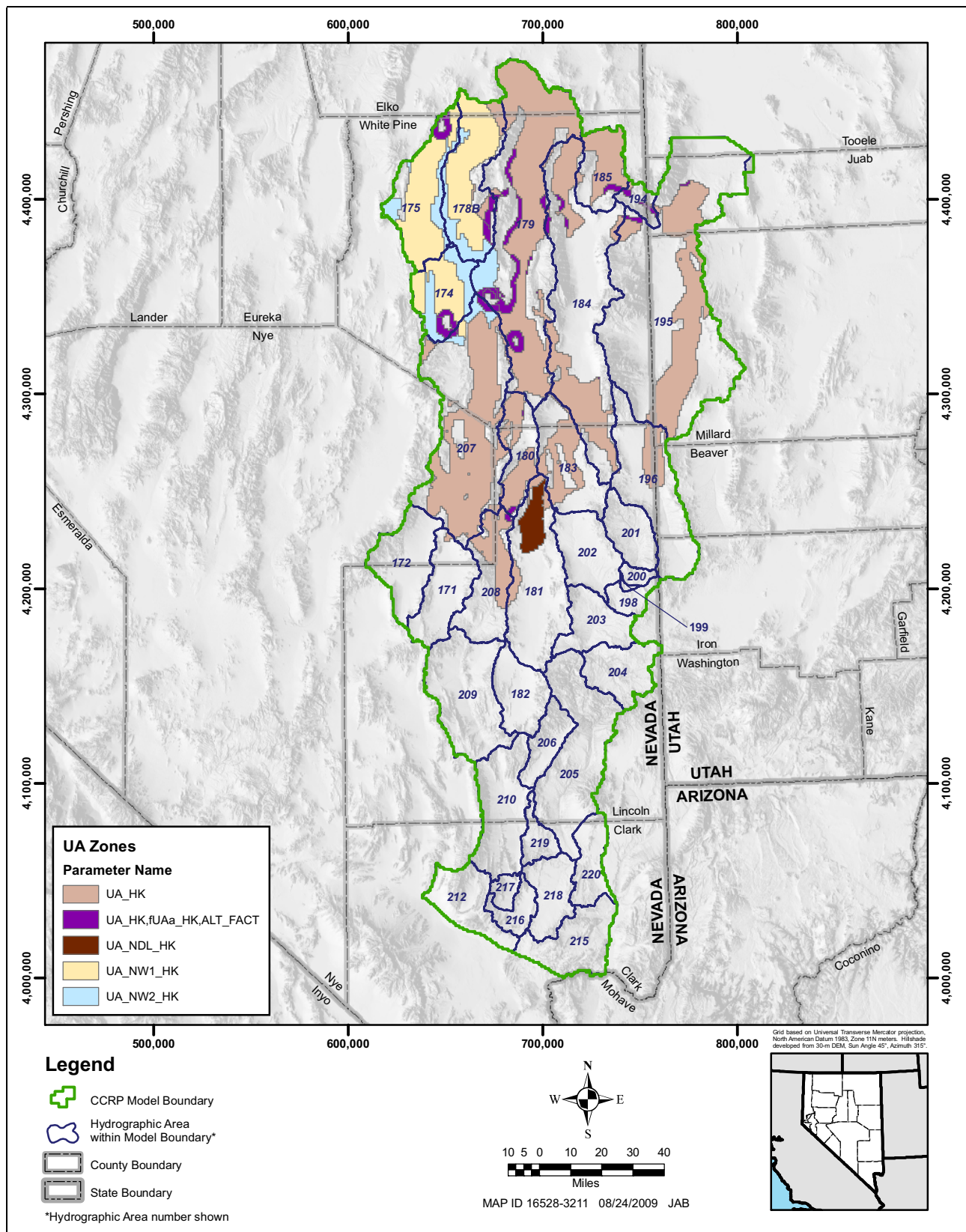
Figure 4-5
Parameter Zones Defined for the UA RMU in the Numerical Model

SE ROA 50824

JA_16225

UC Zones

Parameter Name

- CA_SBSD_HK
- CA_SBSD_HK,ALT_FACT
- CA_SBSD_HK,CONST
- CA_SBSD_HK,TP2SNK_FCT
- CA_SBSD_HK,TP2SNK_FCT,ALT_FACT
- CA_SBSD_HK,fUd195SB_H
- CA_SBSD_HK,fUd195SB_H,ALT_FACT
- CA_SBSD_HK,fUd195SB_H,TP2SNK_FCT
- UC_HK
- UC_HK,ALT_FACT
- UC_HK,CONST
- UC_HK,CONST,ALT_FACT
- UC_HK,CONST,PCT_LDF,ALT_FACT,FAULT_FDUC
- UC_HK,CONST,PCT_LDF,FAULT_FDUC
- UC_HK,CONST,PCT_MDF,ALT_FACT,FAULT_FDUC
- UC_HK,CONST,PCT_MDF,FAULT_FDUC
- UC_HK,CONST,fUwMB_HK
- UC_HK,CONST,fUwMB_HK,ALT_FACT
- UC_HK,PCT_LDF,ALT_FACT,FAULT_FDUC
- UC_HK,PCT_LDF,FAULT_FDUC
- UC_HK,PCT_MDF,ALT_FACT,FAULT_FDUC
- UC_HK,PCT_MDF,FAULT_FDUC
- UC_HK,TP2SNK_FCT
- UC_HK,TP2SNK_FCT,ALT_FACT
- UC_HK,fUdCS_LF_H,PCT_LDF,FAULT_FDUC
- UC_HK,fUw174MB_H,fUw174MB_H
- UC_HK,fUw174MB_H,fUw174MB_H,ALT_FACT
- UC_HK,fUwMB_HK
- UC_HK,fUwMB_HK,ALT_FACT
- UC_HK,fUwMB_HK,PCT_MDF,FAULT_FDUC
- UC_HK,fUwMB_HK,fUw174MB_H
- UC_HK,fUwMB_HK,fUw174MB_H,ALT_FACT

Legend

- CCRP Model Boundary
- Hydrographic Area within Model Boundary*
- County Boundary
- State Boundary

*Hydrographic Area number shown

Grid based on Universal Transverse Mercator projection, North American Datum 1983, Zone 11N meters. Hillshade developed from 30-m DEM, Sun Angle 45°, Azimuth 315°.

MAP ID 16535-3211 08/25/2009 BP

Figure 4-6
Parameter Zones Defined for the UC RMU in the Numerical Model

4-14

Section 4.0

SE ROA 50825

JA_16226
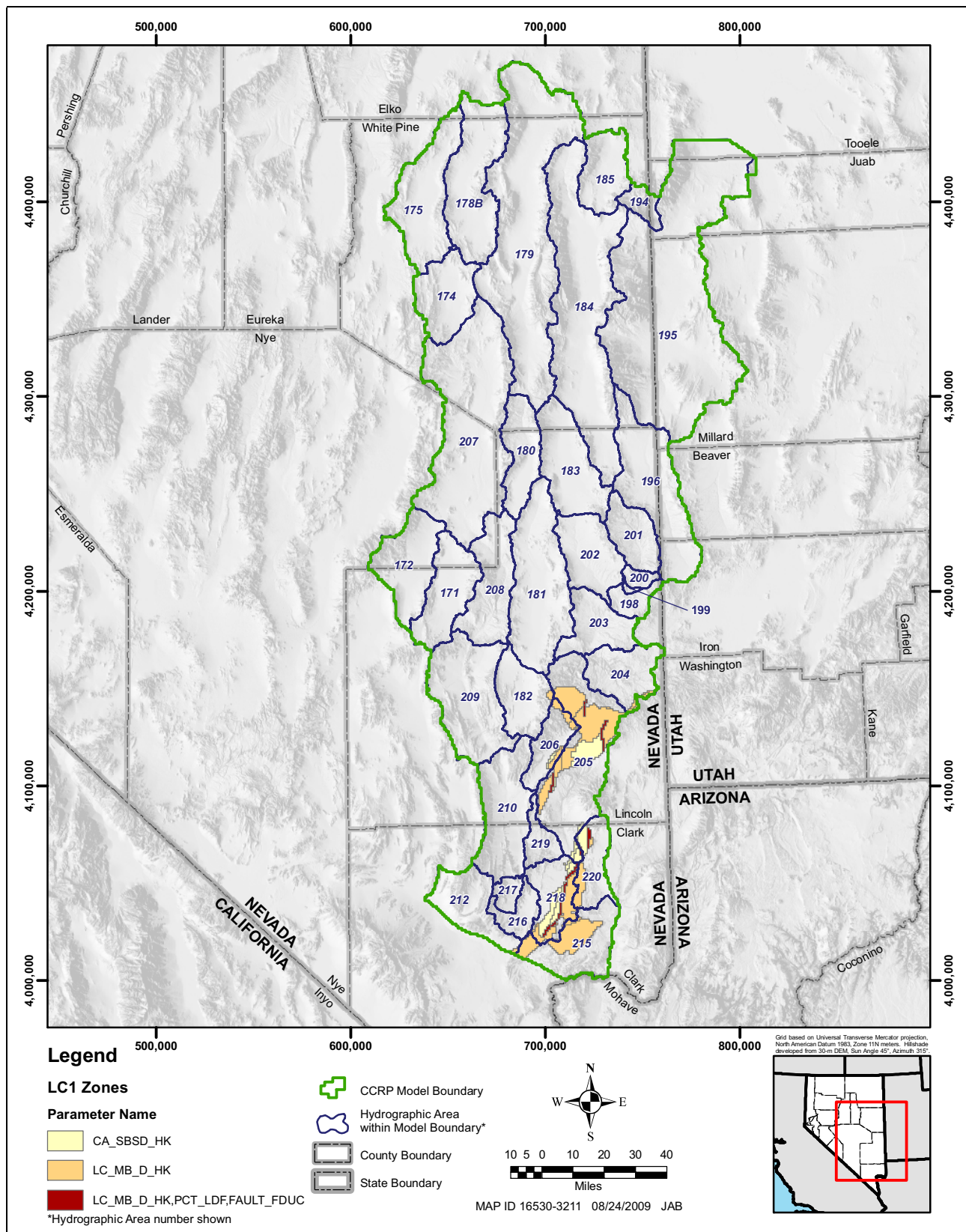
Figure 4-7
Parameter Zones Defined for the LC1 RMU in the Numerical Model

Plateau Sediments

The Kps RMU consists of Cretaceous to T riassic siliciclastic rocks and is ge nerally of low permeability. The K ps RMU is present only in the souther n part of the study ar ea. Figure 4-8 illustrates the Kps RMU parameter zone. The Kps RMU was subdivided into two parts, as shown in Figure 4-8.

Plutons

The PLUT RMU c onsists of all intrusive rocks, including granodiorite, quartz monzonite, and granitic rocks. The PLUT RMU is found sporadicall y in the study ar ea as several large irregularly shaped bodies within the area. This R MU generally has small hydrau lic conductivities unless fractured. The PLUT RMU was subdivided into four parameter zones as shown in Figure 4-9.

Basement

The BASE RMU (also referred to as BAS in the model files) consists of Precambrian metamorphic and Precambrian and early Cambrian clastic rocks. This unit occurs at significant depths in most, but not all, areas. Much like the LC, overthrown blocks of basement rock are present at the Gass Peak thrust fault. BASE1 and BASE2 account for the repeating units caused by this thrust fault. BASE1 represents the basement rock present at the hanging wall of the Gass Peak thrust fault. The extent of BASE1 is very similar to the LC1 extent with the exception of an outcrop band of basement rock in the Las Vegas Range. The B ASE2 extent covers the entire model area with the exception of areas where the PLUT RMU has replaced it and where the model thickness is not sufficient to extend to the top of the BASE RMU. BASE2 also represents the basement rock of the footwall at the Gass Peak thrust fault. The BASE RMU zones were defined based on their areal isolation, structural separation, or the thermal alteration halo around a given pluton (Figure 4-10).

4.2.3.2 Structural Features Represented with HFB Package

The HFB package (Hsieh and Freckleton, 1993) was used to represent barriers to flow i n the numerical model across selected lateral and norma l faults where these faults are conceptualized as barriers to groundwa ter flow across these geologic features. The se flow ba rriers are located along cell boundaries approximating the location of selected mapped lateral and normal faults. Horizontal flow barriers, in most cases, penetrate all RMUs and have a vertical orientation (see DVD). For two cases in White River Valley, the HFBs cross valley basin material, and it was assumed that the low K barriers did not extend into the UVF. The normal faults in the model are typically represented by moderate- or large-displacement faults zones where K *is* expected to be higher to the basin side of the HFB.

Figure 4-11 illustrates lateral and normal faults represented using the HFB package. Horizontal flow barriers are illustrated in cross sections for each model row (see DVD). Table 4-4 describes the lateral faults represented as flow barriers and their parameters. Table 4-5 describes the normal faults represented as flow barriers and their parameters. Fifty fault groups are represented in the numerical model using the HFB pac kage. The thickness of all flow ba rriers was assumed to be 3.28 ft (1 m). Their hydraulic conductivities were treated as pa rameters and, therefore, were estimated during the calibration process. The initial hydraulic conductivity of HFBs was set to 1×10^{-6} m/d.
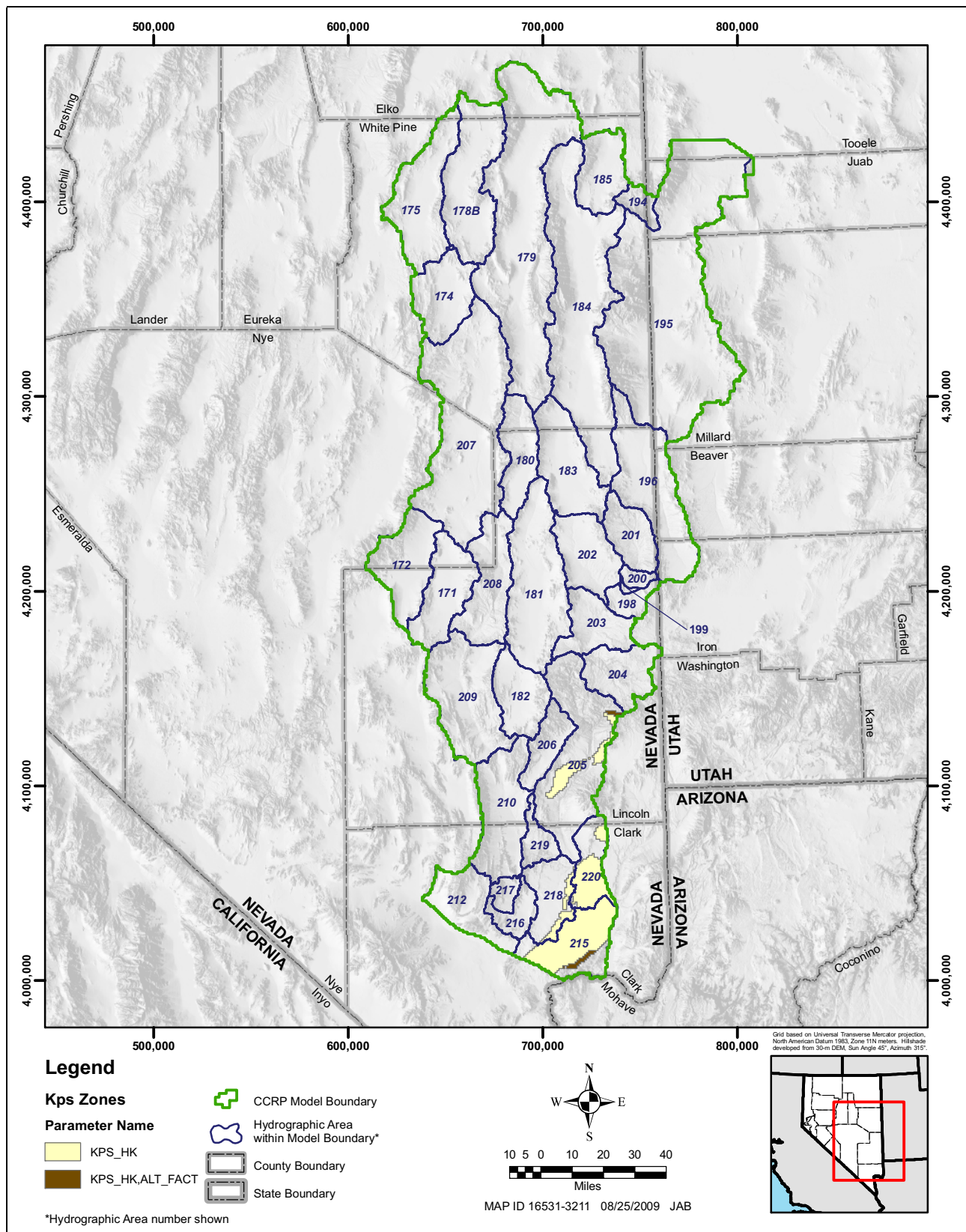
Figure 4-8
Parameter Zones Defined for the Kps RMU in Numerical Model

SE ROA 50828

JA_16229
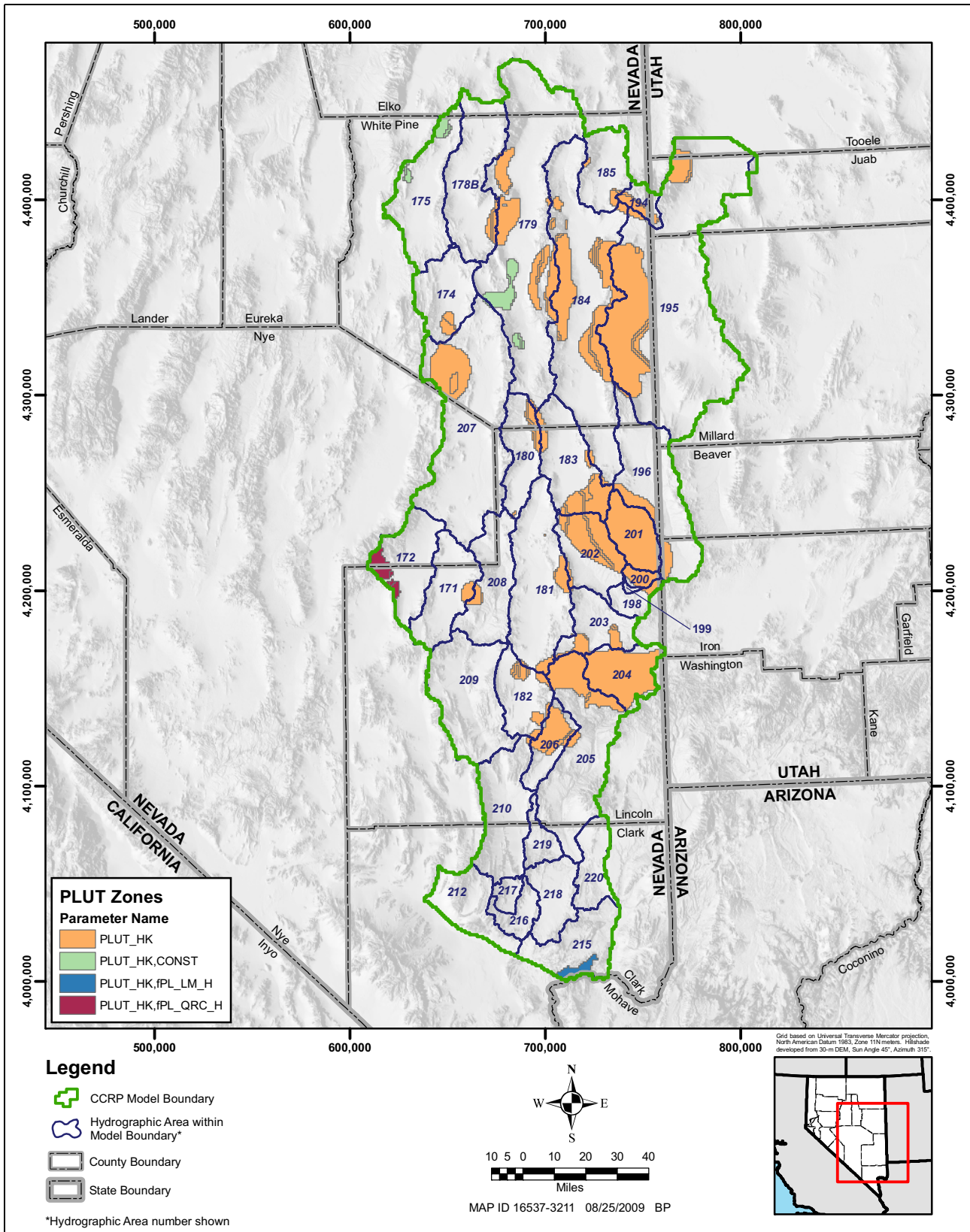
Figure 4-9
Parameter Zones Defined for the PLUT RMU in Numerical Model
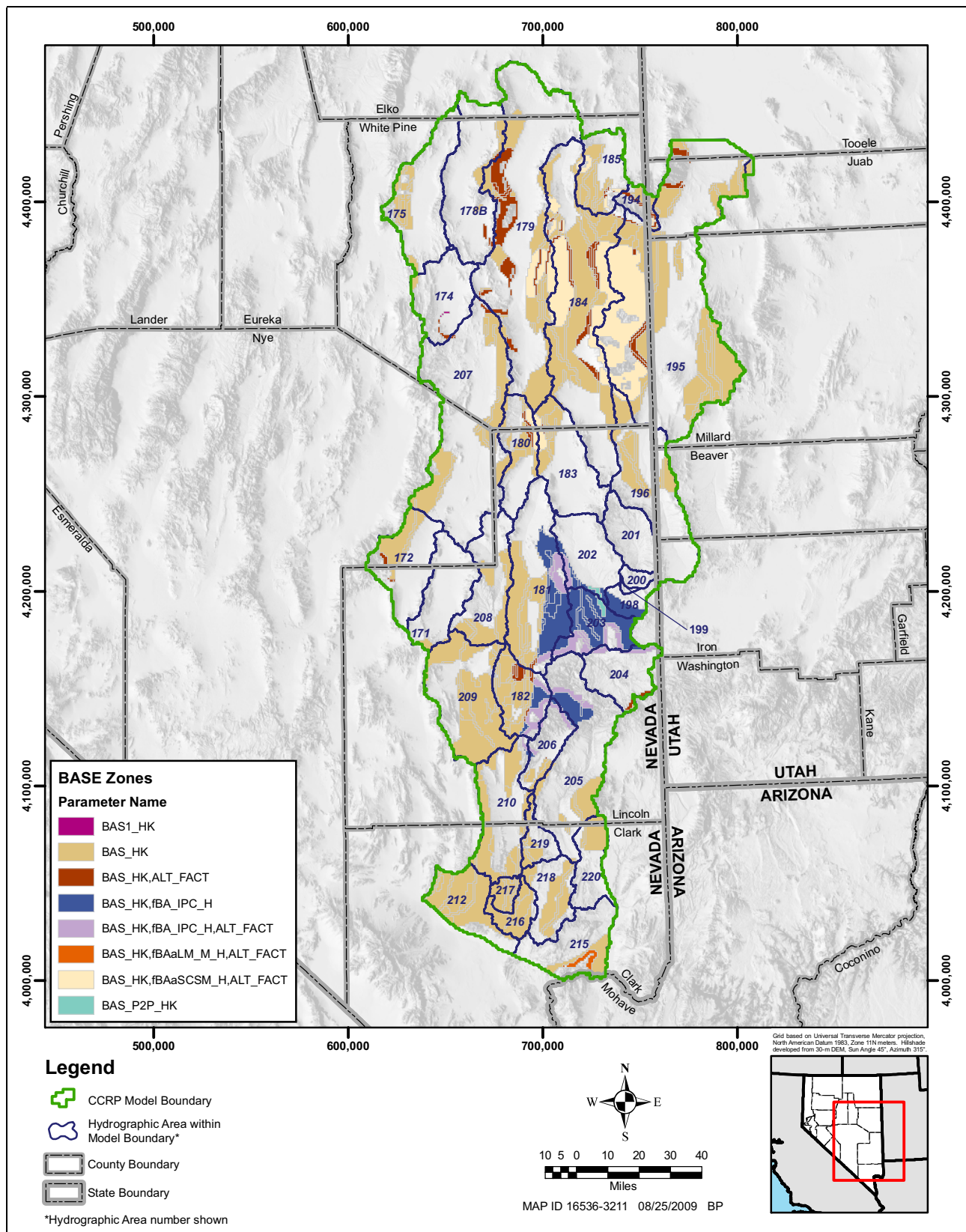
Figure 4-10
Parameter Zones Defined for the BASE RMU in Numerical Model

SE ROA 50830

JA_16231
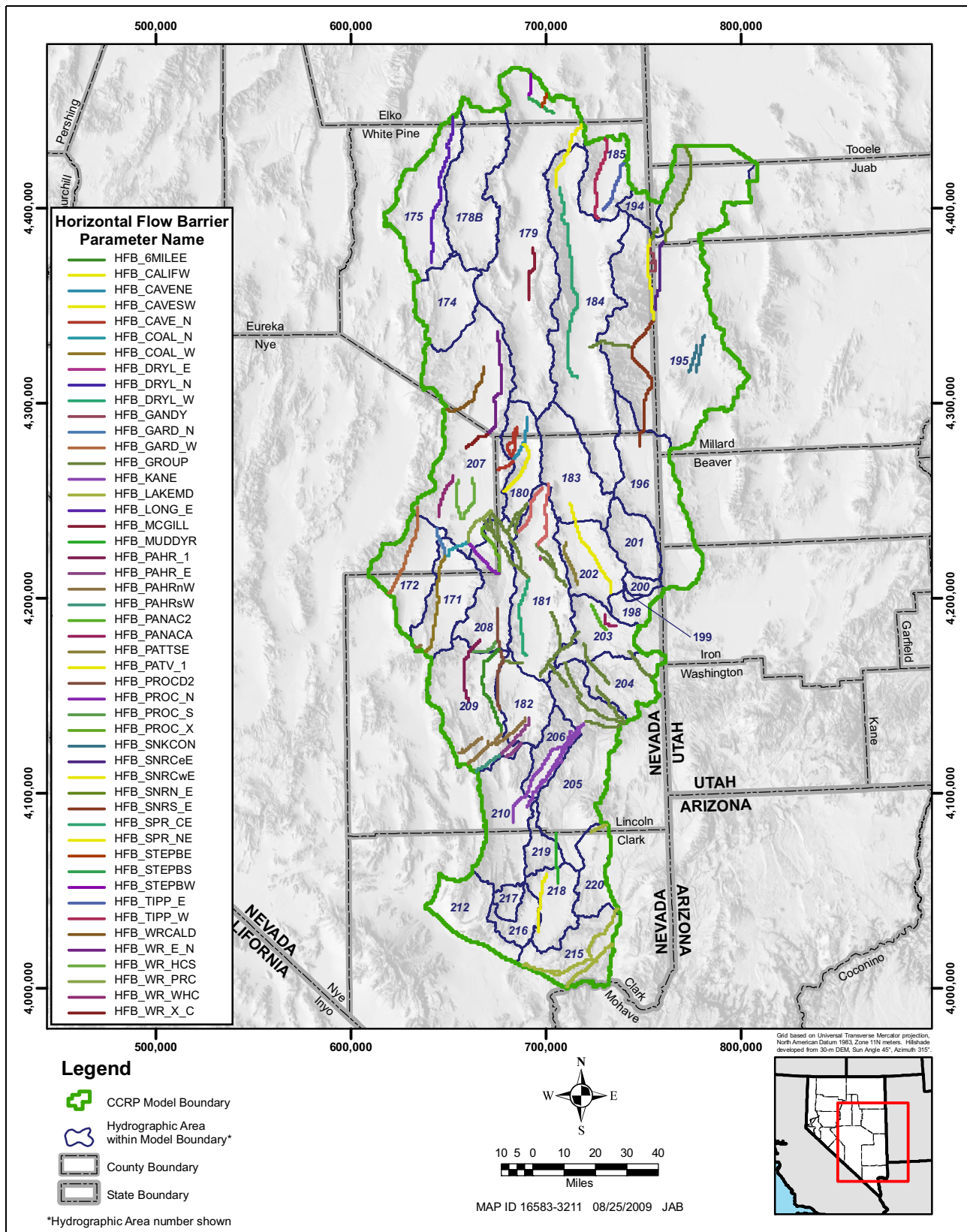
Figure 4-11
Lateral and Normal Faults Defined as Horizontal Flow Barriers in the Numerical Model

SE ROA 50831

JA_16232

Table 4-4
Description of Lateral Faults Defined as
Horizontal Flow Barrier (HFB) Package Parameters

Feature Description	MODFLOW-2000 Parameter Name	UCODE_2005 Parameter Definition
Black Mountains Area	HFB_LAKEMD	HFB_HK * fHFBLAKEMD
Caliente Caldera Area	HFB_GROUP	HFB_HK
Kane Springs Area	HFB_KANE	HFB_HK
North Dry Lake Area	HFB_GROUP	HFB_HK
Snake Range	HFB_GROUP	HFB_HK
South Dry Lake Area	HFB_GROUP	HFB_HK
Pahranagat Shear Zone		
Eastern Section	HFB_PAHR_E	tHFBPAHR_E
Northwestern Section	HFB_PAHRnW	HFB_HK * fHFBPAHRNW
Southwestern Section	HFB_PAHRsW	HFB_HK

Horizontal flow barriers, in most cases, penetrate all RMUs and have a vertical orientation (see DVD). The UVF was assumed to be unfaulted, or if faulted, the faults were assumed to not form barriers to flow. Two cases occur in White River Valley where HFBs extend across basin-fill material, and the low-*K* barriers do not extend into the UVF. A third case occurs west of Warm Springs near Gandy, Utah, in Snake Valley.

Faulting in the Gandy area is complex. However, because of the regional nature of the hydrogeologic framework described in the Baseline Report (SNWA, 2008), the rather complex geology of the immediate vicinity around Gandy Warm Springs is overly simplified. In the Baseline Report (SNWA, 2008), a carbonate horst is described. This feature and faults associated with this feature contribute to the spring discharge at Gandy Warm Springs. Given the magnitude of the flow at Gandy Warm Springs, additional faulting besides that described by the large-displacement faults in the framework is needed. It also appears faulting to the west helps direct subsurface flow from Indian George Wash and Tangstinia Wash toward Gandy Warm Springs.

4.2.4   KDEP Parameters - HUF2 Package

In addition to using the HUF2 module (Anderman and Hill, 2003) to define hydrogeologic units and their material properties, a modified version of the KDEP submodule of HUF2 (Anderman and Hill, 2003) was used to model depth decay for the UVF and for carbonate fault zones. KDEP describes how materials under load are compressed and how this causes *K* to decrease with depth. In the Conceptual Model Report (SNWA, 2009a), while the correlation is minimal, evidence suggests depth decay occurs in the basin-fill deposits of the model area.

In the numerical model, depth decay was assumed to occur only in the UVF and the carbonate moderate- and large-displacement fault zones (MDF and LDF). The UVF deposits are unconsolidated. It is therefore reasonable to expect that compaction due to burial reduces hydraulic

SE ROA 50832

JA_16233

Table 4-5
Description of Normal Faults Defined as
Horizontal Flow Barrier (HFB) Package Parameters
(Page 1 of 2)

Feature Description	MODFLOW-2000 Parameter	UCODE_2005 Parameter
Cave Valley		
Cave Valley - Northern	HFB_CAVE_N	HFB_HK
	HFB_CAVENE	HFB_HK
	HFB_CAVESW	HFB_HK
California Wash		
California Wash - Western	HFB_CALIFW	HFB_HK
Coal Valley		
Northern	HFB_COAL_N	HFB_HK * fHFBCOAL_N
Western	HFB_COAL_W	tHFBCOAL_W
Dry Lake Valley		
Eastern	HFB_DRYL_E	HFB_HK
Northern	HFB_DRYL_N	HFB_HK
Western	HFB_DRYL_W	HFB_HK
Garden Valley		
Northern	HFB_GARD_N	HFB_HK * fHFBGARD_N
Western	HFB_GARD_W	HFB_HK * fHFBGARD_W
Long Valley		
Northeast	HFB_LONG_E	HFB_HK
Muddy River Springs Area		
Muddy River Springs Area	HFB_MUDDYR	HFB_HK * fHFBMUDDYR
Pahranagat Valley		
East Side Near Ash Springs	HFB_PAHR_1	HFB_HK
Eastern Sixmile Flat	HFB_6MILEE	HFB_HK
Pahroc Valley		
Central Valley into Delamar	HFB_PROCD2	HFB_HK
Cross Valley	HFB_PROC_X	HFB_HK * fHFBPROC_X
Northern	HFB_PROC_N	HFB_HK * fHFBPROC_N
Southern	HFB_PROC_S	HFB_HK
Panaca Valley		
Northern	HFB_PANACA	HFB_HK
	HFB_PANAC2	HFB_HK

SE ROA 50833

JA_16234

Table 4-5
Description of Normal Faults Defined as
Horizontal Flow Barrier (HFB) Package Parameters
(Page 2 of 2)

Feature Description	MODFLOW-2000 Parameter	UCODE_2005 Parameter
Patterson Valley		
Southeast	HFB_PATTSE	HFB_HK
Central	HFB_PATV_1	HFB_HK
Snake Range and Snake Valley		
Near Confusion Range	HFB_SNKCON	HFB_HK
Eastern Flank – Southern Section	HFB_SNRS_E	HFB_HK
Eastern Flank – Central Section: East	HFB_SNRCeE	HFB_HK * fHFBSNRN_E
Eastern Flank – Central Section: West	HFB_SNRCwE	HFB_HK * fHFBSNRCwE
Eastern Flank – Northern Section	HFB_SNRN_E	HFB_HK * fHFBSNRN_E
Warm Spring near Gandy	HFB_GANDY	HFB_HK
Spring Valley		
North	HFB_SPR_NE	HFB_HK
Central	HFB_SPR_CE	HFB_HK
Steptoe Valley		
McGill Springs Area	HFB_MCGILL	HFB_HK
Northern Boundary: East Flank	HFB_STEPBE	HFB_HK
Northern Boundary: West Flank	HFB_STEPBW	HFB_HK
Northern Boundary: South Flank	HFB_STEPBS	HFB_HK
Tippett Valley		
Eastern	HFB_TIPP_E	HFB_HK
Western	HFB_TIPP_W	HFB_HK
White River Valley		
Caldera Area	HFB_WRCALD	HFB_HK
Crossing Central Valley	HFB_WR_X_C	HFB_HK
Eastern Side, Northern End	HFB_WR_E_N	HFB_HK
Eastern Side, Southern End	HFB_WR_E_S	HFB_HK
Hot Creek Springs Area	HFB_WR_HCS	HFB_HK
West of Hot Creek Springs Area	HFB_WR_WHC	HFB_HK
To Pahroc	HFB_WR_PRC	HFB_HK

conductivity in this RMU. The fault zones we re assumed to be co mposed of fra ctured material, which would fuse with depth, thereby reducing the hydraulic conductivity of the material.

A potential shortcoming of the KDEP method, as implemented in HUF2, is that there is no lower limit on how much the hydraulic conductivity of the source material may be re duced. For example, the numerical model has some sections of UVF that are more than 16,400 ft (5,000 m) thick. Using the KDEP f unction and a depth-dependence coefficient of va lley-fill deposits (0.0123 m/day) reported in the DVRFS model analysis (Belcher, 2004), K reduces to 3E-62 m/day at the base of the model. At a depth of 1,640 ft (500 m), the K reduces almost six orders of magnitude (Figure 4-12).

Plots illustrating K versus depth presented in the Conceptual Model Report (SNWA, 2009a) suggest a possible lower limit to the reduction of hydraulic conductivity as a result of confining pressures. Based on these observations and the unlikely reduction of hydraulic conductivity to ne ar zero, the KDEP function was modified so that the lower limit of K reduces to a user-defined percentage of the base K value (see DVD). The reduction in K was limited to two orders of magnitude in the numerical model. In other words, if the initial K value were 1 ft/day, KDEP could not reduce the K value to less than 0.01 ft/day (Figure 4-12).
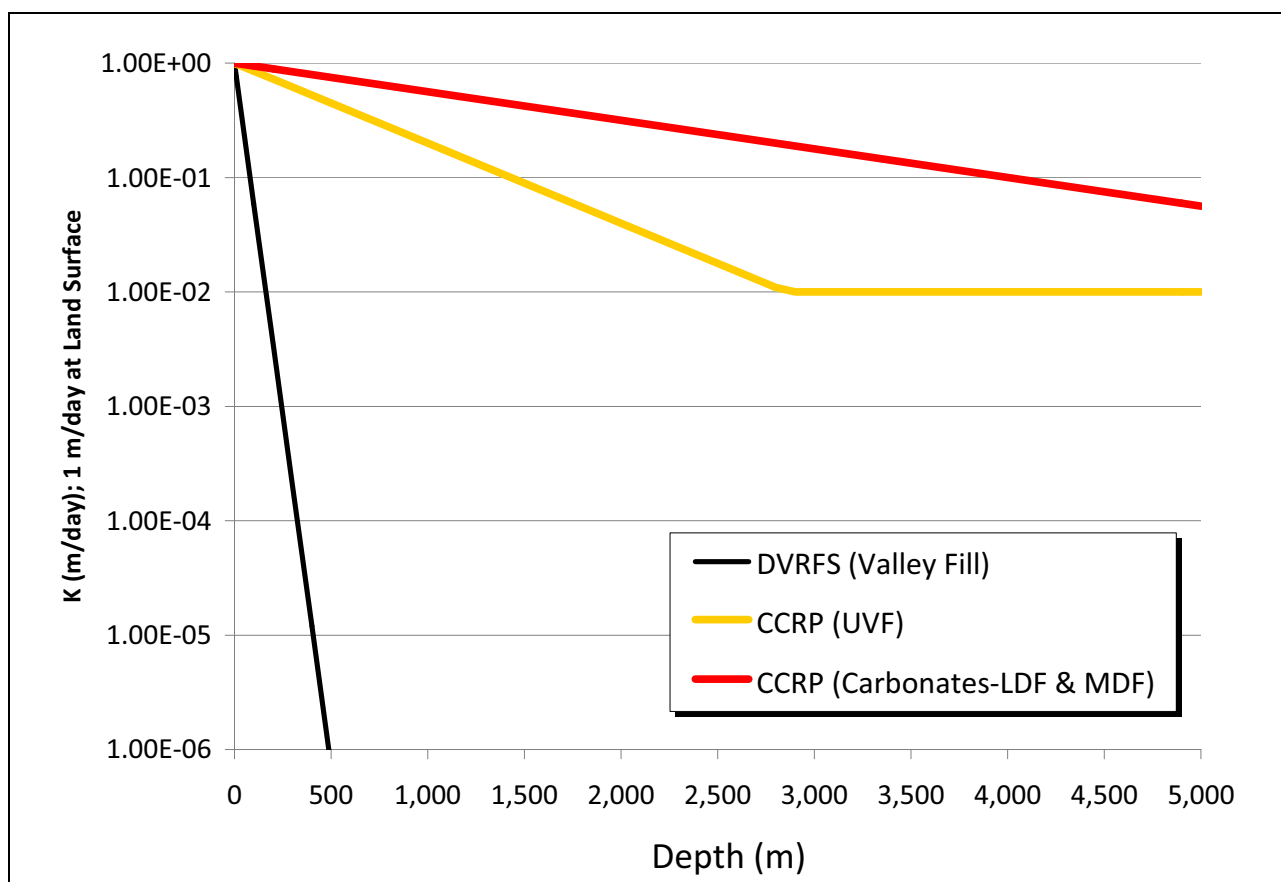
Figure 4-12
Hydraulic Conductivity versus Depth Used in Numerical Model

4.2.5   Specific Storage and Specific Yield

The transient numerical model simulates the aquifer-system response, assuming confined conditions for all model layers. This assumption does not affect the simulated results under predevelopment steady-state conditions.   However, this assumption greatly affects the results simulated under transient conditions when anthropogenic stresses are imposed on the flow system: well yields are underestimated, and drawdowns are overestimated. If the aquifer system were actually confined, the only storage parameters that would need to be defined would be the specific storage (S_s) for each hydrogeologic unit (HGU) and/or RMU. However, the flow system underlying the study area is actually composed of a mixture of confined and unconfined aquifers. Therefore, the transient numerical model must be set up to simulate unconfined conditions using specific yield (S_y).

An alternate method was used in the numerical model to assign S_y to the top model layer using the SYTP property type of HUF2. This alternate method allows the averaging of S_y values assigned to RMUs, when multiple RMUs occur within a single model cell, in a manner similar to the averaging of *HK*, *VANI*, and *S* by the HUF2 module. The averaging in the alternate method uses the thicknesses of the RMUs as weights. In this method, the averaging of the S_y values for each RMU must be implemented outside of MODFLOW-2000, as the S_y values are input as an array that must be generated before MODFLOW-2000 starts. If the S_y for an RMU is changed during manual calibration, for example, the average SYTP array must be adjusted before MODFLOW-2000 is executed again.

The easiest way to update the SYTP array was to create a modified version of MODFLOW-2000 that implements SYTP in the same way it implements *HK*, *VANI*, and *S*. However, this is a significant change to the MODFLOW-2000 code, so the modified code was limited to only producing the updated SYTP array. The modified MODFLOW program was then terminated, and the original, unadjusted version of MODFLOW-2000 was started. The unadjusted version of MODFLOW then read the updated SYTP array and executed as originally designed.

In the study area, and even in most of Nevada, few S_s and S_y data exist. As a result, initial estimates were based on a combination of the information provided in SNWA (2009a), in Appendix A of this report, and from the literature.

4.3   External Boundary Conditions

The Time-Variant Specified-Head (CHD) package (Leake and Prudic, 1991; Harbaugh et al., 2000) was used in conjunction with the Specified-Head Flow Observation Package (CHOB) of the observation process to represent the boundary conditions in the numerical model. A summary of the CHD package is presented, followed by brief descriptions of the external flow boundaries represented using this package. The CHOB portion is described at the end of this section.

4.3.1 CHD Package Description

Before Leake and Prudic (1991) created the CHD package, constant-head cells were part of the finite-difference solution formulation of MODFLOW. McDonald and Harbaugh (1988, p. 3-15) describe constant-head cells as follows:

> A finite-difference equation…is formulated for each variable-head cell in the mesh. For constant-head cells, no equation is formulated; however, the equation for each variable-head cell adjacent to a constant-head cell contains a term describing flow to and from the constant-head cell…

Leake and Prudic (1991) designed the CHD package to simulate constant-head boundary conditions with time-dependent, constant-head values. However, the creation of the CHD package does not affect the formulation of the constant-head boundaries in the finite-difference equations of MODFLOW.

Harbaugh et al. (2000) further modified the CHD package in MODFLOW-2000 to allow the specified heads to be treated as parameters during model calibration.

4.3.2 External Flow Boundaries Represented in Numerical Model

The external model boundaries represented by constant-head cells in the numerical model are shown on Figure 4-13. Constant hydraulic heads were specified for all model layers containing the UVF, LVF, or UC/LC RMUs. Maps showing the constant-head boundaries for each model layer are presented in electronic form (see DVD). The following sections describe the sources of the initial estimates of constant-head values. The constant-head boundaries simulated in the numerical model are then discussed by hydrographic area. Target observations are composed of flows across these boundary segments and are presented in Section 4.7.

4.3.2.1 Constant-Head Values

Except for Lake Mead, no data were available along the model boundary to provide values of hydraulic heads assigned to the constant-head cells. Thus, the constant-head values assigned to the boundaries were derived from the interpreted hydraulic-head distributions made by Prudic et al. (1995), Bedinger and Harrill (2004), Welch et al. (2008), and SNWA (2009a). For the boundary representing Lake Mead, the constant-head value was set to 1,169.3 ft (356.4 m), which is the average water level for the reservoir from January 1937 to April 2007 (USBR, 2007). The constant-head values were treated as parameters and were estimated during the model calibration process. The MODFLOW-2000 parameter names for the constant-head boundary segments are listed in Table 4-6. The constant-head parameters are multiplication factors applied to designated boundary hydraulic heads.

4.3.2.2 Description of Constant-Head Boundaries

The constant-head boundaries included in the numerical model are described by basin.

JA_16238
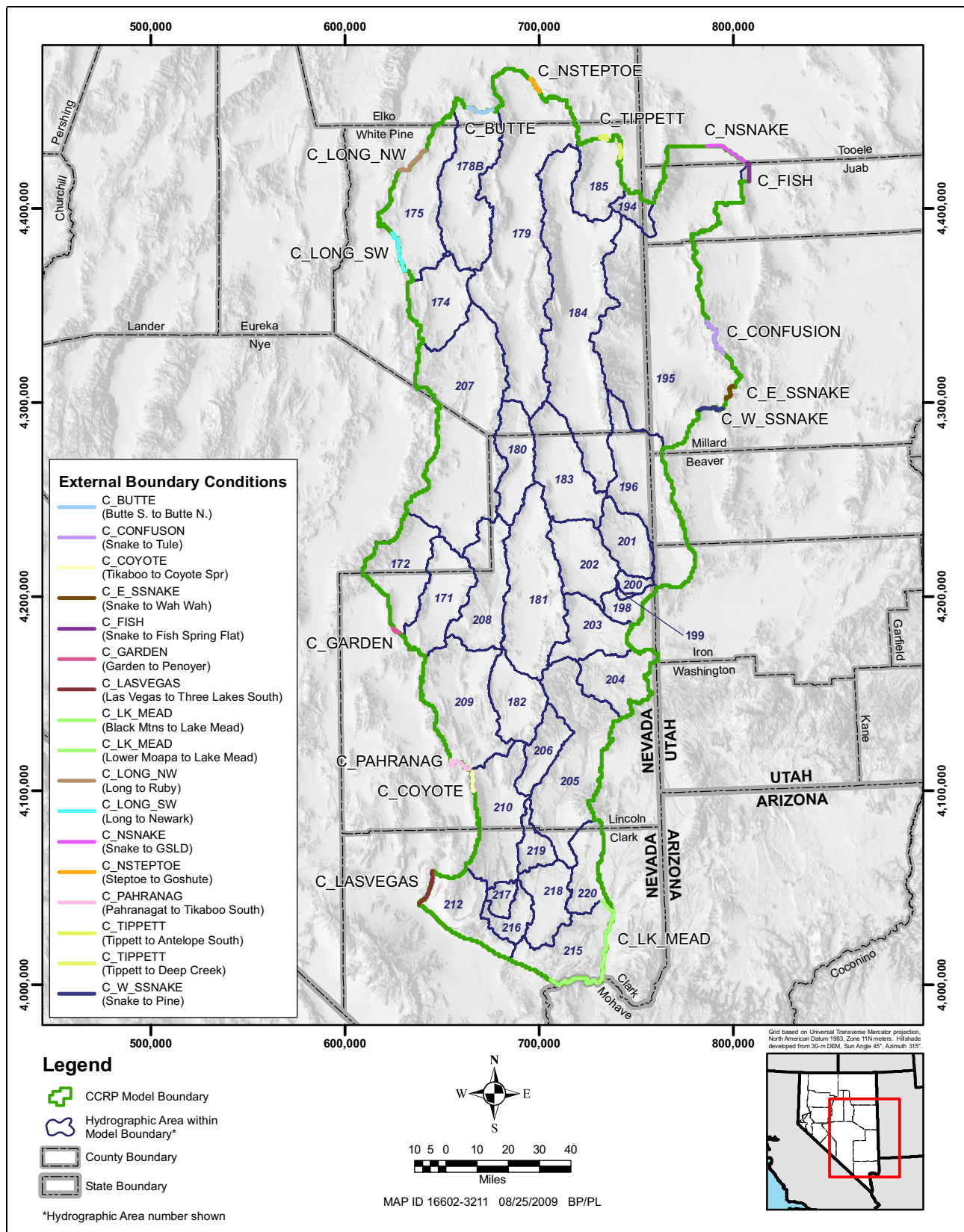
Figure 4-13
Location and Parameter Names of Constant-Head Boundaries in Numerical Model

SE ROA 50838

JA_16239

Table 4-6
Parameters for Constant-Head Boundaries
in Numerical Model

Boundary Name	Parameter Name
Steptoe to Goshute	C_NSTEPTOE
Snake to Great Salt Lake Desert (deep)	C_NSNAKE
Snake to Great Salt Lake Desert (shallow)	C_NSNAKE_G
Snake to Fish Springs Flat (deep)	C_FISH
Snake to Fish Springs Flat (shallow)	C_FISH_G
Tippett to Antelope Valley South	C_TIPPETT
Snake to Tule	C_CONFUSON
Butte South to Butte North	C_BUTTE
Garden to Penoyer	C_GARDEN
Long to South Newark	C_LONG_SW
Long to Ruby	C_LONG_NW
Coyote Spring to Tikaboo	C_COYOTE
Snake to Wah Wah	C_E_SSNAKE
Snake to Pine	C_W_SSNAKE
Lower Moapa to Lake Mead	C_LK_MEAD
Black Mountains to Lake Mead	
Las Vegas to Three Lakes South	C_LASVEGAS
Pahranagat to Tikaboo South	C_PAHRANAG

Butte Valley South

One segment of the northern boundary of Butte Valley South (Figure 4-14) was defined as a constant-head boundary in the numerical model. This boundary segment is positioned to permit groundwater flow through the basin-fill and bedrock aquifers. Most of the groundwater flow across this boundary segment appears to pass through the structural basin from Butte Valley South toward Butte Valley North.

Steptoe Valley

One segment of the northeastern boundary of Steptoe Valley (Figure 4-14) was defined as a constant-head boundary. This boundary segment is positioned to permit groundwater flow through the basin-fill aquifer and the bedrock aquifer. The lowest observed hydraulic heads in this valley are not in the structural basin but are actually in the mountain-block material to the east. Thus, groundwater flow from Steptoe Valley to Goshute Valley is interpreted to occur in the mountain block.

Tippett Valley

Tippett Valley is interpreted to have groundwater flow moving out of the model area through the northern and eastern boundaries of the valley. These two outflow locations are represented by constant-head boundaries in the numerical model (Figure 4-15). The outflows are as follows:

- Groundwater flow from Tippett Valley to Antelope Valley is through a structural basin.

- Groundwater flow from Tippett Valley to Deep Creek Valley is through fractured mountain block.
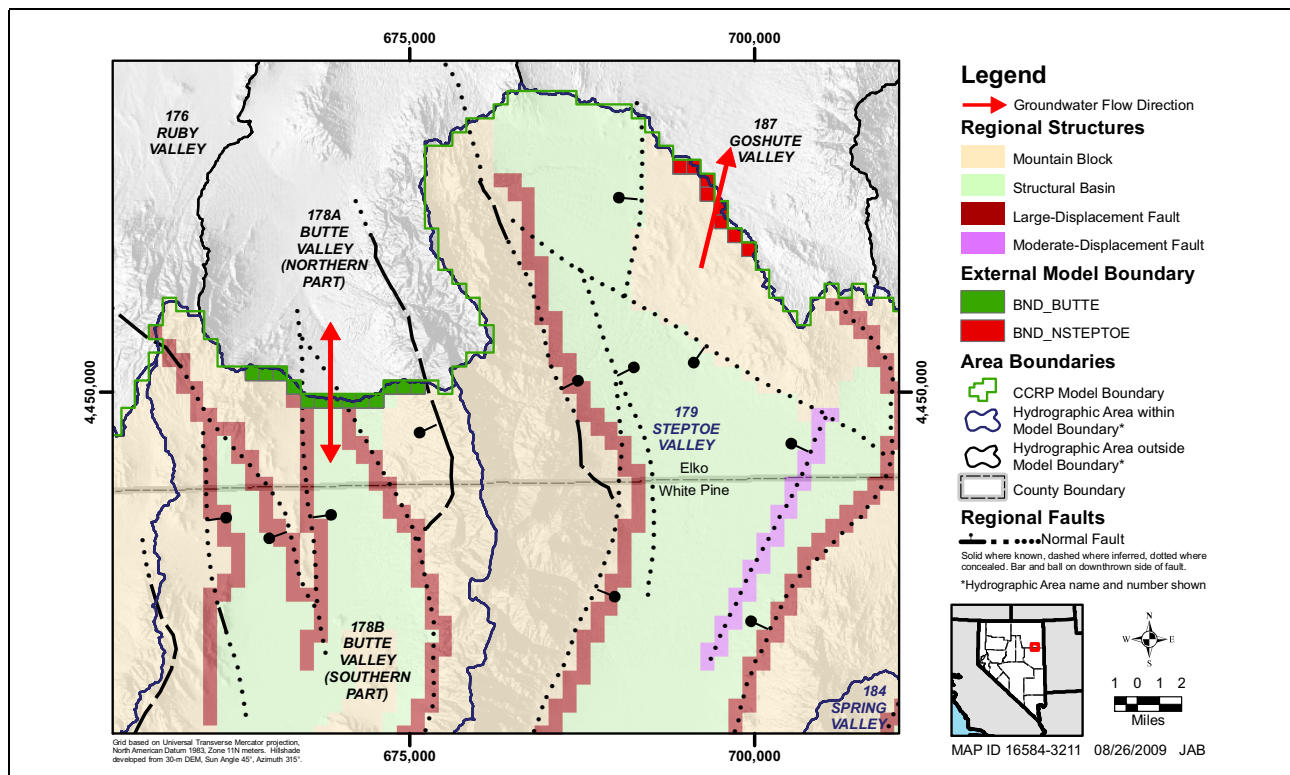
Figure 4-14
Butte Valley South and Steptoe Valley Constant-Head Boundaries
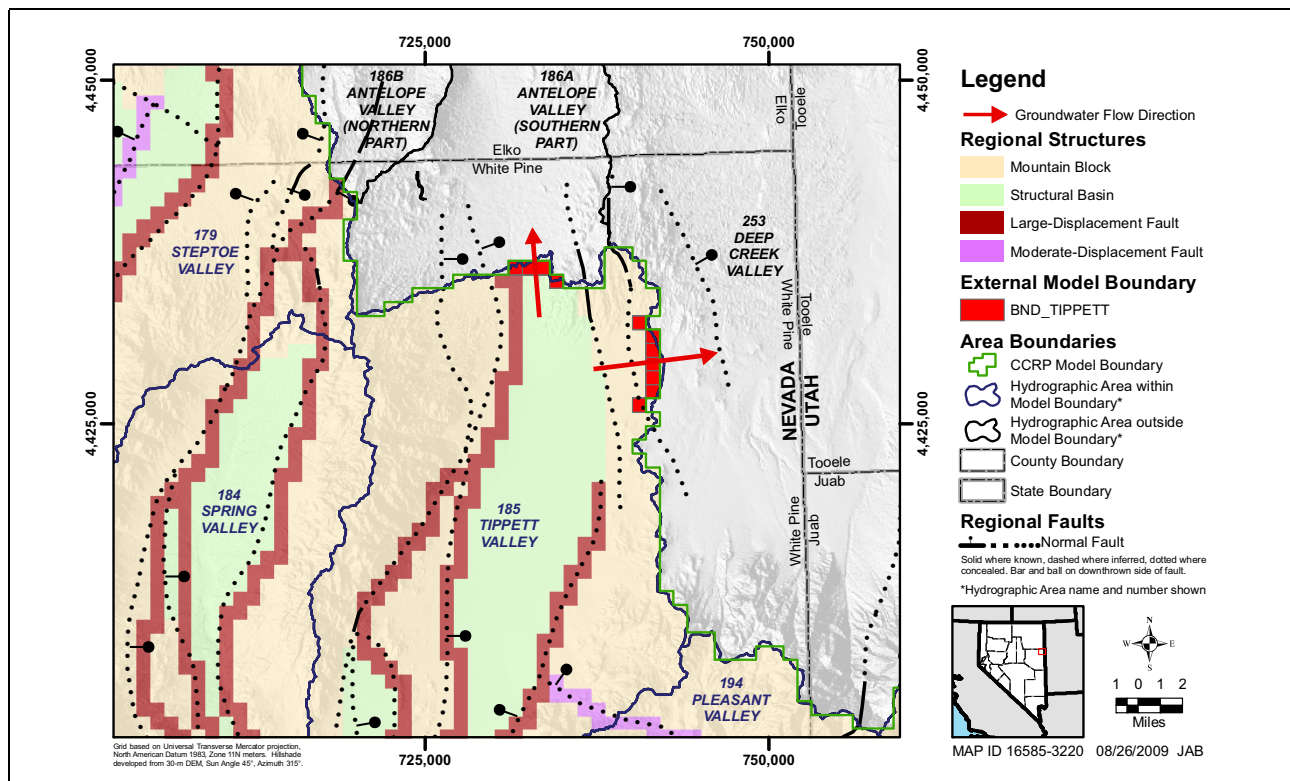
Figure 4-15
Tippett Valley Constant-Head Boundaries

SE ROA 50840

JA_16241

Snake Valley

Snake Valley is interpreted to have groundwater flow moving out of the model area through boundary segments located in the northern and southern parts of the valley (Figure 4-16). These outflow locations are represented as constant-head boundaries in the numerical model. The flow boundaries are as follows:

- The two constant-head boundaries defined in the northern part of Snake Valley consist of one segment along the boundary of Snake Valley with the Great Salt Lake Desert to the north and one segment along the boundary with Fish Springs Flat to the east (Figure 4-16A).

- The three constant-head boundaries defined in the southern part of Snake Valley consist of one segment located along a portion of the Confusion Range on the eastern boundary of Snake Valley, one segment located along the boundary between Snake Valley and Pine Valley, and one segment located along the boundary between Snake Valley and Wah Wah Valley at the southeastern end of the valley (Figure 4-16B).

Long Valley

Long Valley was interpreted to have two constant-head boundaries allowing flow out of the valley (Figure 4-17). Both flow boundaries are consistent with the interpretations of Prudic et al. (1995) and are as follows:

- The first boundary allows flow from Long Valley to Newark Valley.

- The second boundary, located on the northwestern and western edge of Long Valley, allows flow from or to Ruby Valley.

Garden Valley

The Garden Valley constant-head boundary is located along the hydrographic boundary between Garden Valley and Penoyer Valley. This boundary segment is interpreted to be highly transmissive as it coincides with a significant thickness of the LC3 RMU. Groundwater flow is interpreted to be from Garden Valley to Penoyer Valley (Figure 4-18).

Coyote Spring Valley

In the conceptual model report (SNWA, 2009a), water is interpreted to flow from Tikaboo Valley into the north end of Coyote Spring Valley (see Figure 4-19). Some of this water is suspected to be from Pahranagat Valley, flowing along the Pahranagat Shear Zone to Tikaboo Valley. Some of the flow may have more regional sources from the northwest. The boundary of Coyote Spring Valley and Tikaboo Valley parallels the Gass Peak thrust fault. Head values in the area suggest the Gass Peak thrust fault is a barrier to flow, as heads to the west of the fault can be hundreds of feet higher than those measured east of the fault in the central valley area. It has been suggested that for flow to move across this boundary, it may have to move at depth under the shallow-angle thrust fault.
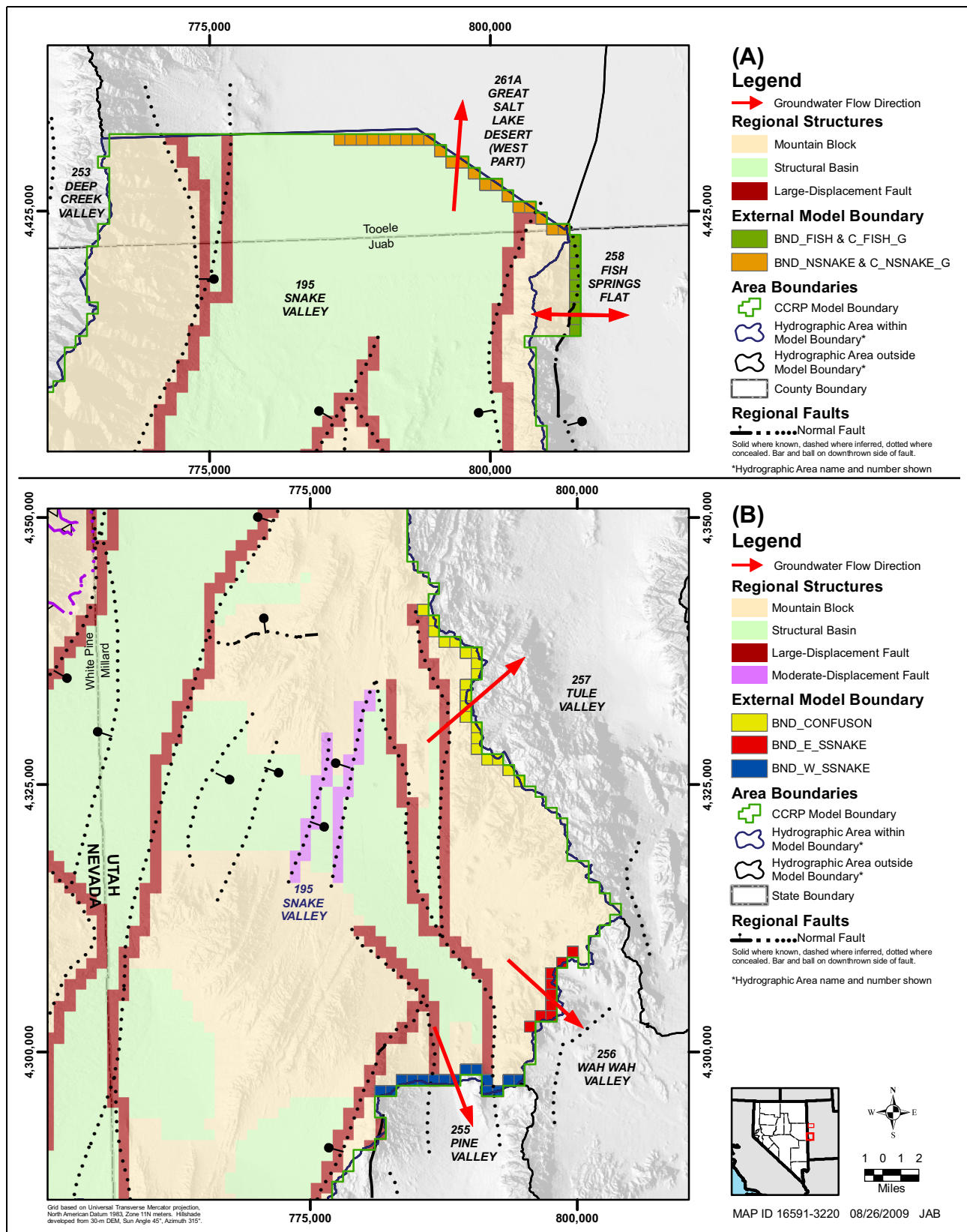
Figure 4-16
Northern and Southern Snake Valley Constant-Head Boundaries
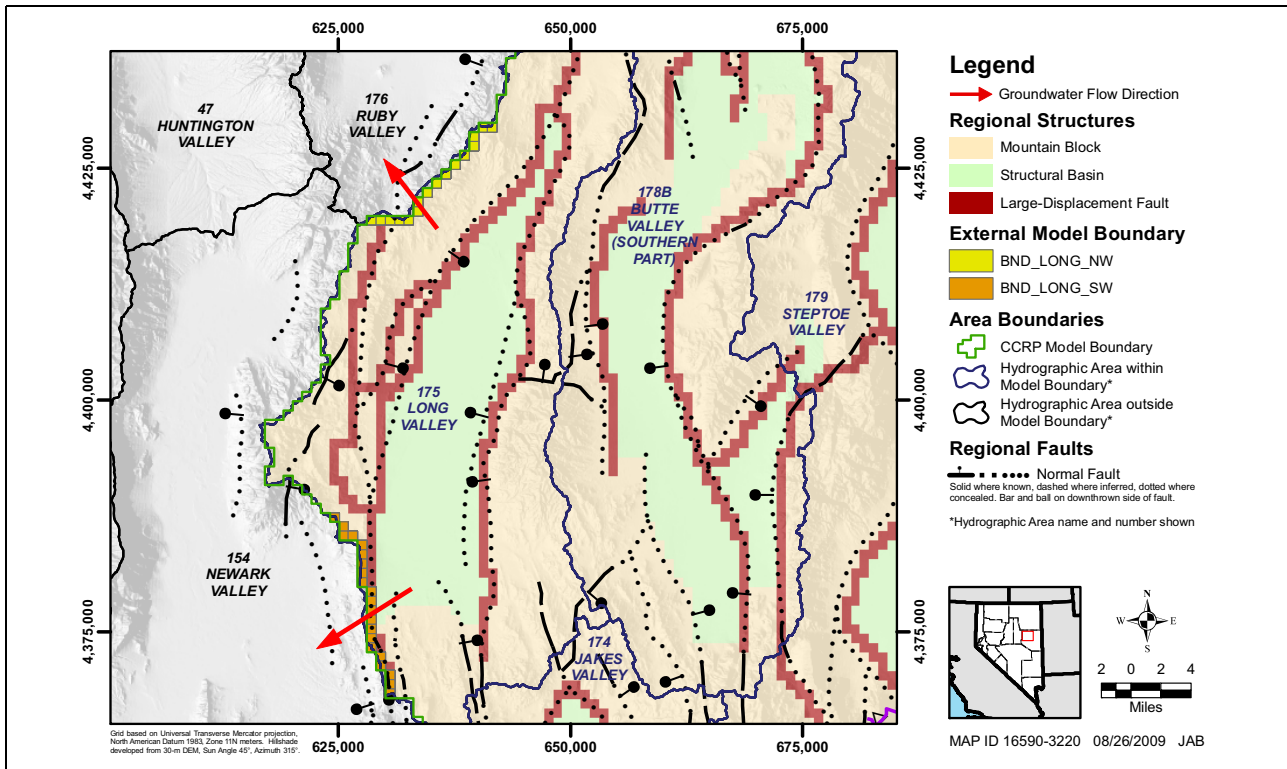
Figure 4-17
Long Valley Constant-Head Boundaries
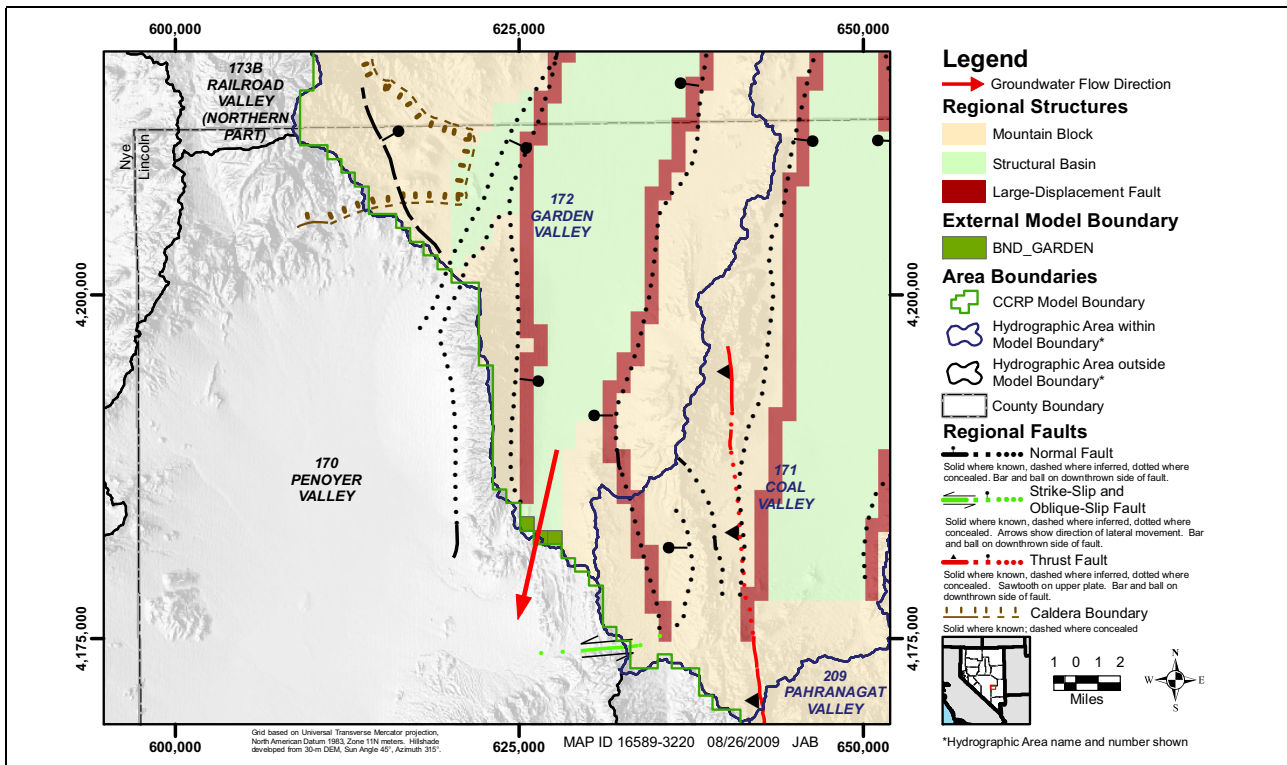
Figure 4-18
Garden Valley Constant-Head Boundary

SE ROA 50843

JA_16244
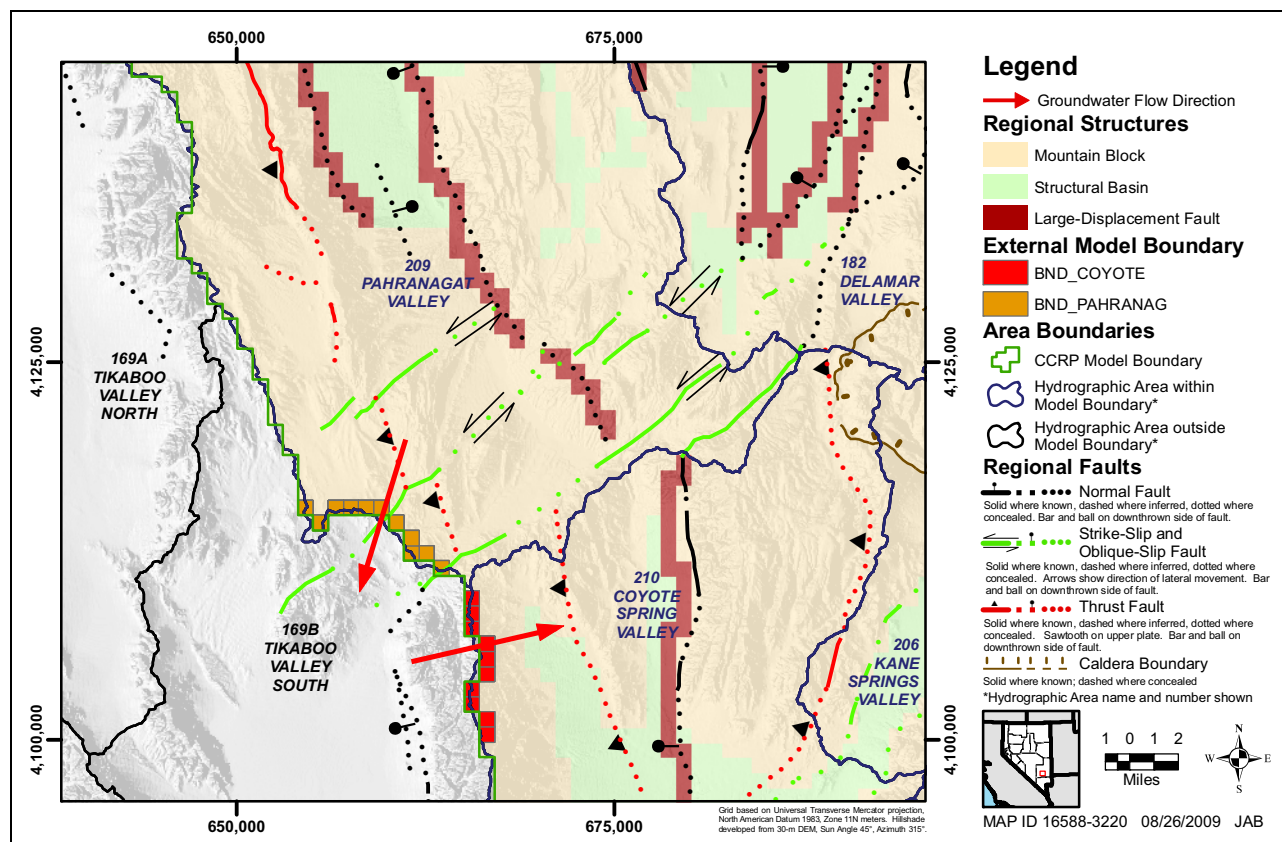
Figure 4-19
Coyote Spring Valley and Pahranagat Valley Constant-Head Boundaries

Pahranagat Valley

In the simplified conceptual model (SNWA, 2009a), groundwater flows roughly parallel to Pahranagat Valley and the North and South Tikaboo Valley boundaries. It was assumed that some of this southwesterly flow then moves into northern Coyote Spring Valley, southwest of the Pahranagat Shear Zone. It has also been suggested that flow from Pahranagat Valley moves out to South Tikaboo Valley. This flow may be going around the southwest side of the Pahranagat Shear Zone and into Coyote Spring Valley. Significant flow may also move farther southwest toward the Amargosa Desert. This interpretation had previously been postulated by D'Agnese et al. (2002) and Belcher (2004) and falls within the uncertainty of the conceptual model. This new flow-boundary segment was also defined as a constant-head boundary (Figure 4-19).

Lower Moapa Valley

A constant-head boundary is interpreted along the boundary between Lower Moapa Valley and Lake Mead (Figure 4-20). The Lower Moapa Valley constant-head boundary accounts for groundwater flow out of the model domain.
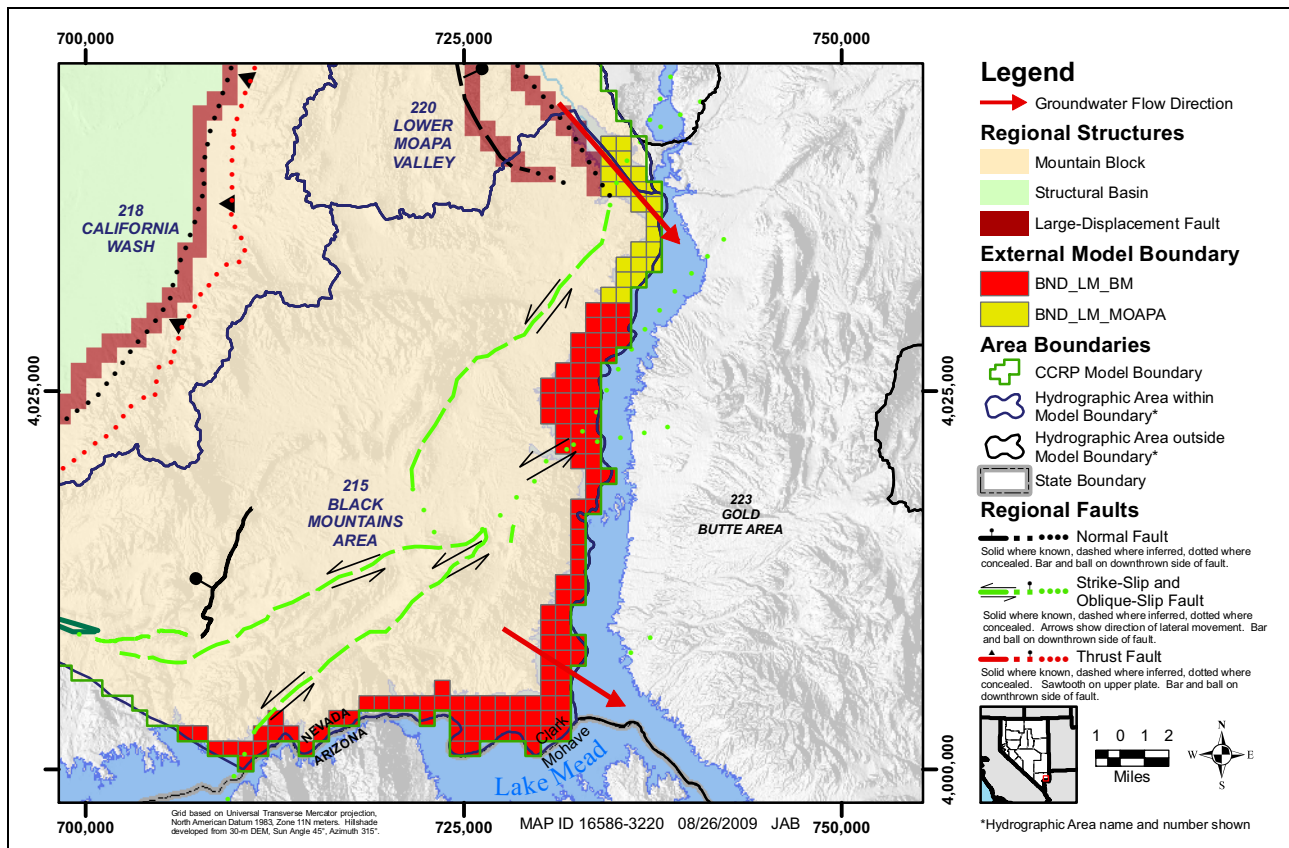
Figure 4-20
Lower Moapa Valley and Black Mountains Area Constant-Head Boundaries

Black Mountains Area

A constant-head boundary wa s defined along the boundary of this area with Lake Me ad (Figure 4-20). Groundwater flow is interpreted as moving out of the f low system across this boundary.

Las Vegas Valley

Groundwater flow is interpreted to occur across the boundary along the northwest end of Las Vegas Valley (Figure 4-21). The direction of flow is uncertain and may be into or out of the numerical model domain.

4.4   Natural Groundwater Discharge

Groundwater discharge, including ET and spring flow, was simulated in MODFLOW-2000 using the Drain (DRN) and Streamflow-Routing (SFR2) packages (Harbaugh et al., 2000). B rief descriptions of the DRN and S FR2 packages are provided, followe d by a pre sentation of how g roundwater-discharge components were represented in the numerical model using these packages.
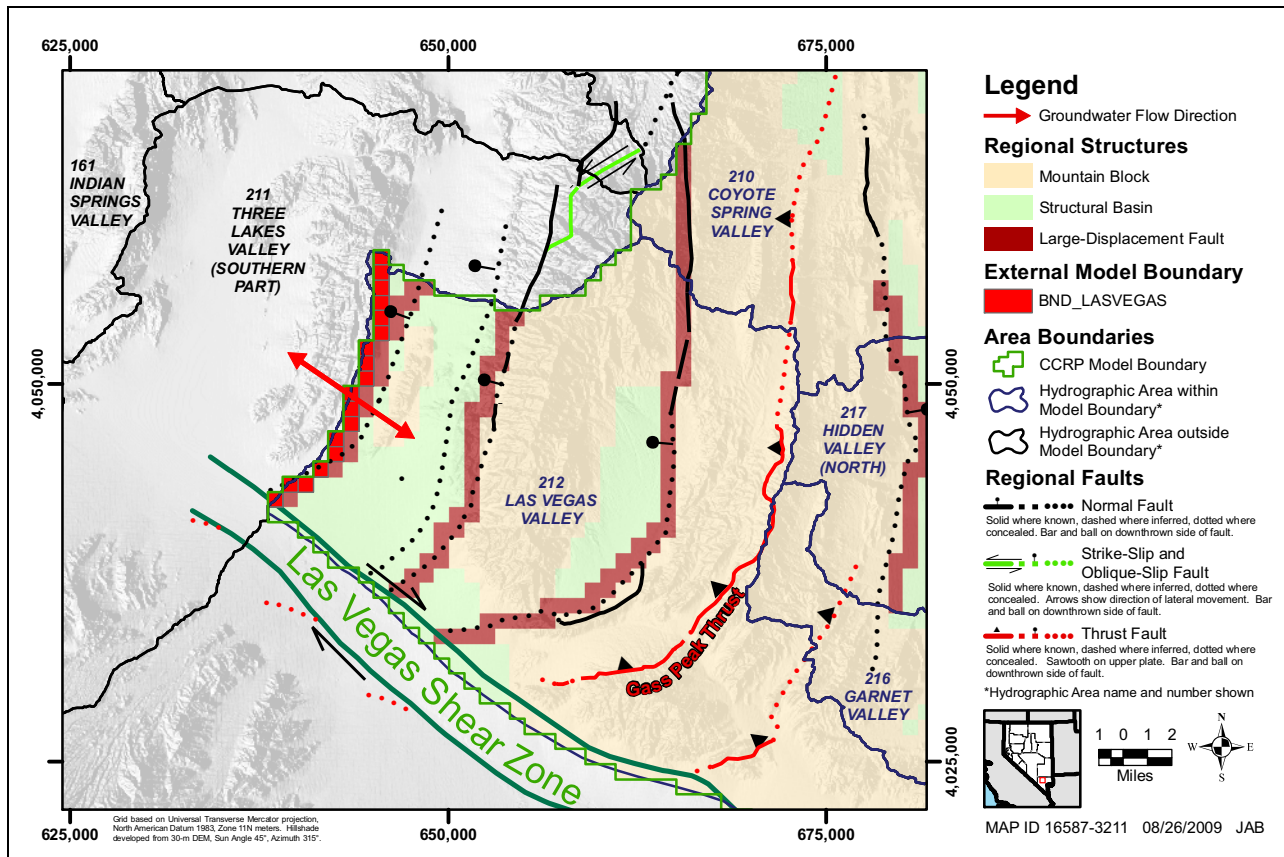
Figure 4-21
Las Vegas Valley Constant-Head Boundary

4.4.1   DRN Package

The DRN package simulates groundwater discharge through a head-dependent flow boundary. The DRN package is used to represent groundwater discharge from groundwater ET areas and springs.

Groundwater discharges from a cell specified as a drain when the simulated hydraulic head in the cell rises above a threshold level, ca lled the drain el evation. The rate of flow is dependent on the conductance term, which i s a comb ination of several parameters used i n Darcy's law. The conductance across a pr ism in a given direc tion is expressed as follows (McD onald and Har baugh, 1988):

$$C = Q/(h_A - h_B)$$ (Eq. 4-3)

where,

C = Conductance (L^2/T)
Q = Flow rate across the prism (L^3/T)
$h_A - h_B$ = Hydraulic-head change across the prism (L)

SE ROA 50846

JA_16247

In the case of a drain, flow is oriented vertically and represents discharge to the surface—h_A is the hydraulic head at the top, and h_B is the hydraulic head at the bottom of the drain—or the drain elevation.

4.4.2   SFR2 Package

The SFR2 package (Niswonger and Prudic, 2006) simulates stream-aquifer interactions like the SFR1 package (Prudic et al., 2004) but has the ext ended ability to simulate unsat urated flow beneath streams.   Stream flow is rout ed in t he same way as in SFR 1 based on the continuity equation assuming steady, uniform flow (i.e., the vo lumetric inflow is equal to the outflow minus all sources and sinks to the channel).

In both SFR1 and SFR2, the streams are represented by a network of channels, and each channel is subdivided into s egments (Figure 4-22A). The c ross-sectional geometry of each segment is represented by several points (Figure 4-22B). The case where an unsaturated zone exists between the stream and the water table (functionality exists within SFR2 only) is depicted in Figure 4-22C.

Niswonger and Prudic (2006, p. 6) describe the flow process in the SFR2 package:

> In SFR2 (as in SFR1), flows are routed through a network of channels where flow is always in the same direction along channels, and where seepage (ground-water recharge or discharge) is constant for each MODFLOW time step. Gr ound-water recharge resulting from streambed seepage and flow through the unsaturated zone may be variable within a MODFLOW time step, because the time steps used in calculating flow through the unsaturated zone may be shorte r than those used in the saturated zone. Thus, all water reaching the water table from the unsaturated zone is totaled over the MODFLOW time step.

In the numerical model, SFR2 simulates groundwater discharge of large-volume regional springs to a stream channel, which then redistributes this water downstream as surface water. Ultimately, the surface water evaporates or recharges the groundwater system, which can then be consumed by ET.

4.4.3   Groundwater Evapotranspiration

This section describes the way in which the groundwater ET process was performed under predevelopment steady-state conditions and transient conditions in the numerical model.

4.4.3.1   Steady-State Conditions

Groundwater ET for st eady-state conditions was set up i n the numerica l model as esti mated for natural conditions prior to development by man in the Conceptual Model Report (SNWA 2009a).

The estimates of groundwater ET derived by SNWA (2009a) for the model area included four ET regions (Wetland, Shrubland, Playa, and Ope n Water) and annual discharge rates. The groundwate r ET regions were grouped into three categories. Category 1 consists of groundwater ET areas

JA_16248
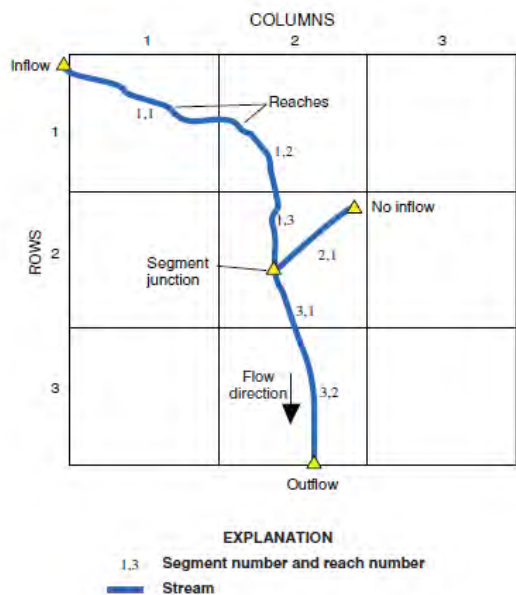
(A) Simple stream network having three segments and six reaches in a finite difference model grid consisting of three rows and three columns
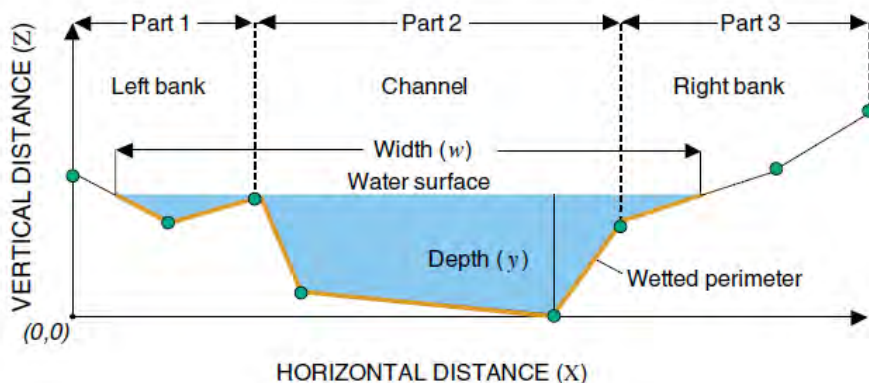
(B) Example Cross-Section Used to Compute Depth, Width, and Wetted Perimeter for a Stream in SFR1/SFR2
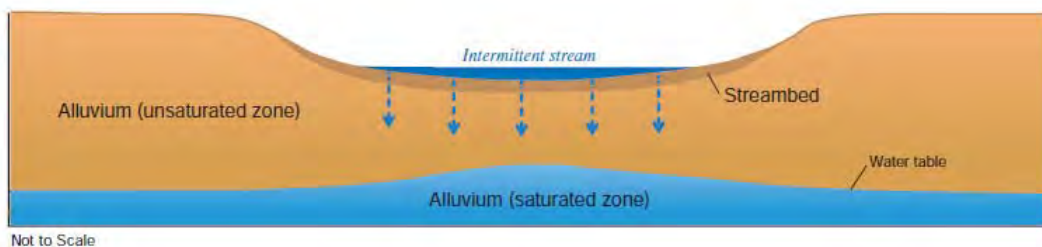
(C) Example cross section of stream separated from the water table by an unsaturated zone

Source: Adapted from Prudic et al. (2004) and Niswonger and Prudic (2006)

Figure 4-22
Example Representation of Streams in MODFLOW-2000 Using SFR2 Package

intersecting the regional groundwater table. Category 2 consists of groundwater ET areas tapping intermediate aquifers. Categor y 3 consists of groundwater ET areas tapping local or perched aquifers. O nly Category 1 and 2 groundwater ET areas were represented in the numerical model. The groundwater ET ar eas were further subdivided by sub-basin and their extents approximated by grid cells as shown in Figure 4-23. The DRN package was used to represent groundwater ET as four groups of drains corresponding to the four types of ET zones. The groundwater ET area within each grid cell was represented by a single drain. The representation of groundwater ET areas as drains is presented in this section. The annual discharge rates were used as tar get observations and ar e presented in Section 4.7.4.

4.4.3.1.1 Drain Elevations

The drain elevation was assumed to appr oximate the ET-extinction depth. The drain elevation in a given ET ce ll corresponds to the e levation of the ET-extinction-depth surface at the loc ation of the drain. The drain elevation is calculated as the difference between the ground-surface elevation and the extinction depth. Two values of extinctio n depths were used, depending on the location of the groundwater ET ar ea. For ET grid ce lls located in low-topographic relief, the extinction depth was assumed to be 16.4 ft bgs (5 m bgs). For all other ET grid cells, the extinction depth was assumed to be 32.8 ft bgs (10 m bgs). The ground-surface elevations for the ET grid cells were derived from the USGS 30-m digital elevation model (DEM). A single grid cell has an area of 247.1 acres (1 km^2) and includes about 900 DEM points. The ground-surface elevations for the ET grid cells were calculated as follows:

- For a given ET grid cell located in low-topographic relief, the l and-surface elevation was calculated as the m ean of the DEM poi nts in that grid ce ll. The extinction depth was set to 16.4 ft bgs (5 m bgs) for these grid cells.

- For a given ET grid cell located in other areas, the land surface of a given grid cell was set equal to the minimum DEM elevation within that grid cell. The e xtinction depth was set to 32.8 ft bgs (10 m bgs) for these grid cells.

The drain elevation is an approximation of the ET-extinction depth. This approach of using the DRN package to simulate gr oundwater ET has pr eviously been used in oth er regional Great Basin modeling studies, such as Prudic et al. (1995) and D'Agnese et al. (2002).

4.4.3.1.2 Drain Conductances

The drain conductance was set up to approximate the maximum ET rate corresponding to the type of ET region (i.e., Wetland, Shrubland, Playa/Wet Soil, or Open Water). In some instances, the ET drain conductances were modified. The dr ain conductances were treated as par ameters during the calibration of the numerical model. Init ial estimates of drain conduc tances were cal culated as the quotient of the estim ated discharge and the difference of int erpolated hydraulic head and drain elevation. The dr ain conductances were estimated by ET -region type. Thus, four values were calculated to represent Open Water, Wetland, Shrubland, and Playa. The four values were adjusted using conductance-modifier parameters (Table 4-7) representing Wetland, Shrubland, Playa, and
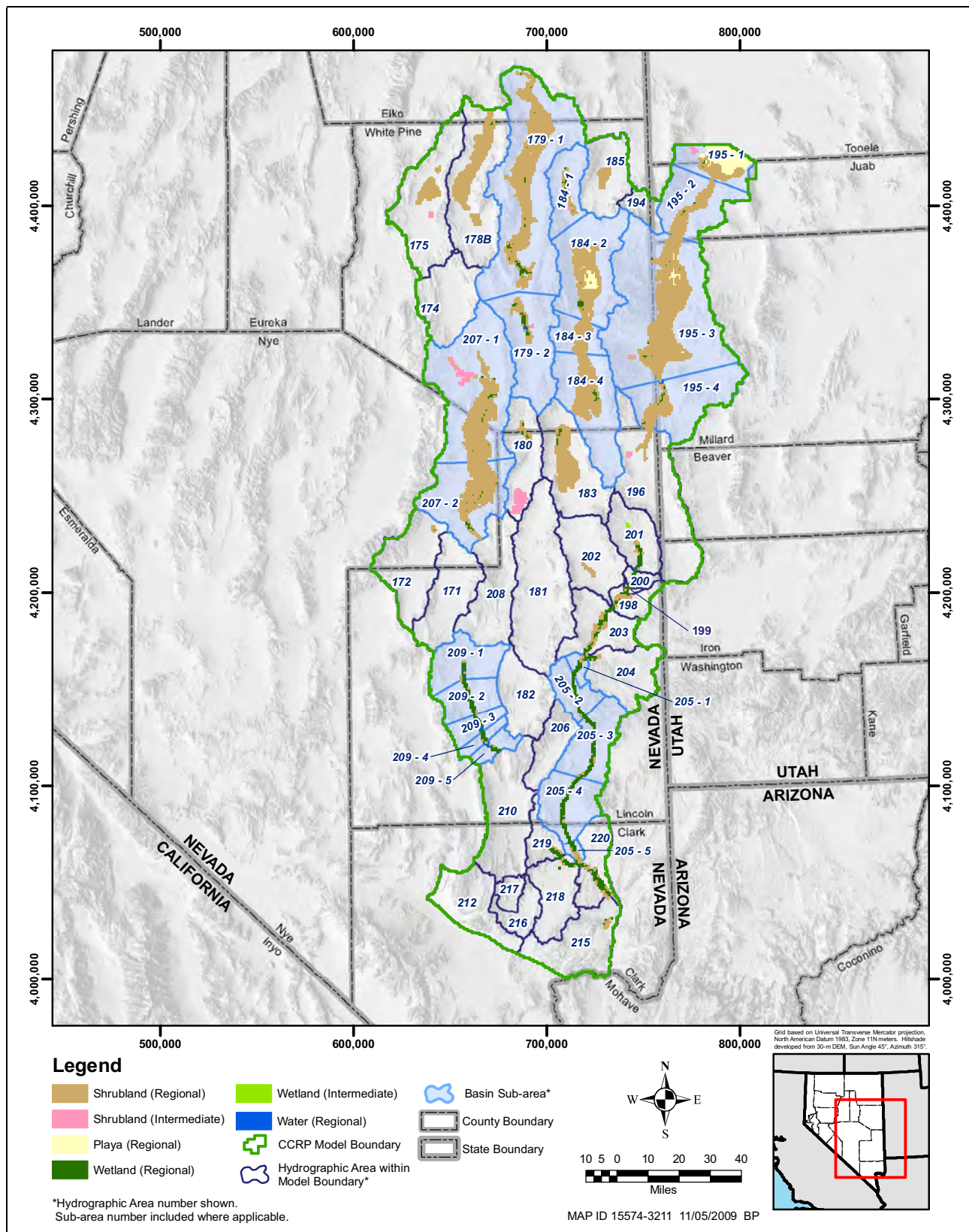
Figure 4-23
Groundwater ET Areas Represented as DRN Cells in the Numerical Model

SE ROA 50850

JA_16251

Open Water for both regional- and intermediate-discharge areas. Note that it was assumed regional and intermediate ET rates were identical; hence, their parameters were combined (Table 4-7). The initial estimates of the conductance-modifier values for the ET grid cells are described in the following text.

Table 4-7
ET Regions and Conductance Modifier Parameters

ET Regions	Parameter Name
Wetland	ETrWET and ETiWET
Shrubland	ETrSHR and ETiSHR
Playa/Wet Soil	ETrPLY
Open Water	ETrWAT
HA 209 Wetland	ETr209WET
HA 209 Open Water	ETr209WAT

Note: There are no intermediate Playa and Open Water ET areas.

Groundwater ET areas covered grid cells either entirely or partially. The partial coverage was accounted for by scaling the conductance of the ET drain in that grid cell by the percentage of grid cell ET coverage, using the conductance modifier (CONDFACT) in the DRN cell. The default value of CONDFACT was set equal to 1,000,000, reflecting the total area of a model grid cell (1,000,000 m^2). Several cases arose and were handled as follows:

- For ET grid cells that were entirely covered with a single ET-region type, the grid cell was assigned the conductance value corresponding to the ET-region type present. In this case, the ET coverage is 100 percent of the area of the cell; thus, the default conductance modifier of 1,000,000 was assigned.

- For ET grid cells that were partially covered by a single ET-region type, the grid cell was assigned the conductance value corresponding to the ET-region type and an adjusted conductance modifier. For example, cells with 10 percent ET coverage have a conductance modifier of 100,000.

- In cases where multiple ET regions corresponded to a single cell and entirely covered the cell, the most prevalent ET-region type in the grid cell was assumed to control the conductance of the ET drain. For example, if a cell contains 15 percent Playa, 1 percent Open Water, 30 percent Shrubland, and 54 percent Wetland, the cell is assigned to Wetland, with the Wetland conductance value and the default conductance modifier of 1,000,000.

- In cases where multiple ET regions corresponded to a single cell and partially covered the cell, the most prevalent ET-region type in the grid cell was assumed to control the conductance of the ET drain. The conductance modifier was, however, adjusted to reflect the ET-covered area only. For example, if a cell contains 5 percent Playa, 10 percent Wetland, 1 percent Open Water, 30 percent Shrubland, and 54 percent non-ET area, the cell was

SE ROA 50851

JA_16252

assigned the S hrubland conductance value. The c onductance modifier was 460,000, corresponding to the 46 percent of the cell area where groundwater ET occurs.

This approach resulted in the exclusion of certain limited ET zones in the model. This situation occurs when a particular ET type ne ver dominates any cell within a basin or sub-ba sin but ha s a significant area in the entire basin or sub-ba sin. This occurs in W hite River Valley, for example, where open-water evaporation accounts for over 2,961 afy (10,000 m^3/d) discharge, but no single cell is designated as Open Water in the model grid. Although such areas were not explicitly represented in the model, the corresponding volume of groundwater was accounted for by assuming that it was removed by the Wetland or Shrubland ET cells. Two additional ET zones were created in Pahranagat Valley to account for ET rates in Pahranagat Wash. Pahranagat Wash is configured as a semiperched riparian zone. Most of the ET derives its source from the outflows of Ash, Crystal, and Hiko springs. Some ET, however, is still derived from groundwater. To restrict the amount of ET from regional groundwater and to show the weak connection between the regional aquifer system and the perc hed flow system, the ET ra tes in Pahranagat Wash were set to 50 percent of the re gional ET rates. Section 4.4.4.2.2 describes the re presentation of dischar ge in Pahranagat Valley further. This is described in more detail in the observations in Section 4.7.4. The ET units not represented in the numerical model as a result of this simplification are listed in Table 4-8.

Table 4-8
ET Zones Not Represented in the Numerical Model[a]

Open Water	Wetland	Shrubland	Playa
ER178B_WATER	EI175_WET	EI201_SHRUB	EI195a_PLAYA
ER179a_WATER	EI179b_WET	---	ER183_PLAYA
ER183_WATER	EI180_WET	---	ER184c_PLAYA
ER184b_WATER	EI195a_WET	---	ER184d_PLAYA
ER195b_WATER	EI196_WET	---	ER185_PLAYA
ER195c_WATER	ER175_WET	---	ER195b_PLAYA
ER198_WATER	ER184c_WET	---	ER207a_PLAYA
ER205d_WATER	ER185_WET	---	ER207b_PLAYA
ER205e_WATER	ER196_WET	---	---
ER207b_WATER	---	---	---

[a]Indicates ET type does not occur in any cell in the model. Occurs when an ET type is dominated spatially by other types within a model cell.

4.4.3.2   *Transient Conditions*

Conceptually, when anthropogenic stresses (described in Section 4.6) are imposed on a flow system, particularly within or near natural ET areas, the rates and areal extents of groundwater ET areas may decrease. Portions of the groundwater ET areas are converted to agricultural areas to be irrigated with groundwater obtained from nearby wells. In such cases, natural groundwater ET would likely decrease substantially, or ce ase, depending on t he depth to water . The c rops replacing the phreatophytes would, initially , use the groundwater available at the water table and requi re an

additional amount of water supplied by pumping from nearby irrigation wells. At later times, if the drawdown caused by the irrigation pumping wells under the irrigated areas were to increase, the croplands would likely require more irrigation water until all their needs were eventually satisfied by irrigation water from wells. If pumping were stopped during this transitional period, natural groundwater discharge within the converted areas would gradually resume as the water table rose back to prepumping conditions.

An accurate representation of this process cannot be simulated in the numerical model, not only because the data are not available at that level of detail but also because the processes of ET and agricultural activities are very simplified in the model. The two processes can be approximately simulated in the numerical model in different ways but the question is how to simulate the conversion from groundwater ET to agricultural areas without irreversibly turning off natural groundwater ET. The conversion of the groundwater ET areas to agricultural areas may be simulated by using one of three options: (1) by setting the drain conductances at the ET cells to zero, (2) by completely removing the ET drains from the model cells at the time they are converted, or (3) by decreasing the water table below the drain elevations.

Although Options 1 and 2 were considered, Option 3 appeared to be the most viable. Options 1 and 2 would essentially remove natural ET from the specified model cells but would not allow the groundwater ET process to resume if pumping for agricultural purposes were stopped in some areas. In addition, the Option 1 is infeasible in the numerical model as constructed because ET drain conductances are assigned by type of vegetation, rather than by ET cell. The model was set up this way to minimize the number of parameters, as the drain conductances associated by the four types of vegetation are calibration parameters. Option 3, though not exactly representative of reality, does allow the ET process to resume, should agricultural pumping cease, and therefore was selected.

Groundwater pumping is the only way to decrease the water table in the converted agricultural areas under Option 3. This process does not accurately represent reality because the conversion does not occur rapidly as it would actually. The water table under the former groundwater ET area decreases gradually as pumping from agricultural wells within or near the agricultural areas is started. The error associated with Option 3 is that the ET drain cells continue to discharge groundwater as long as the water table is above the ET drain. However, this error is relatively negligible because, as described in the next paragraph, the converted areas are relatively small. In addition, as pumping continues and the water levels decrease, the ET rates in the converted areas decrease further.

The extents of the groundwater ET areas under natural conditions and the irrigated croplands for the period 2001 to 2004 are shown in Figure 4-24. As can be seen from this figure, the extent of the irrigated croplands located within the ET areas (converted areas) is relatively small. In fact, the total area of irrigated croplands located within the ET areas represent about 3 percent of the total ET area for the period 2001 to 2004.

In terms of volumes, the maximum volume of ET discharging from all irrigated croplands located within the ET areas represents 4 percent of the total groundwater discharge from all ET areas for the period 2001 to 2004. As listed in Table 4-9, the relative importance of the converted areas and the corresponding annual volume of lost groundwater ET are small for basins with the largest converted areas.
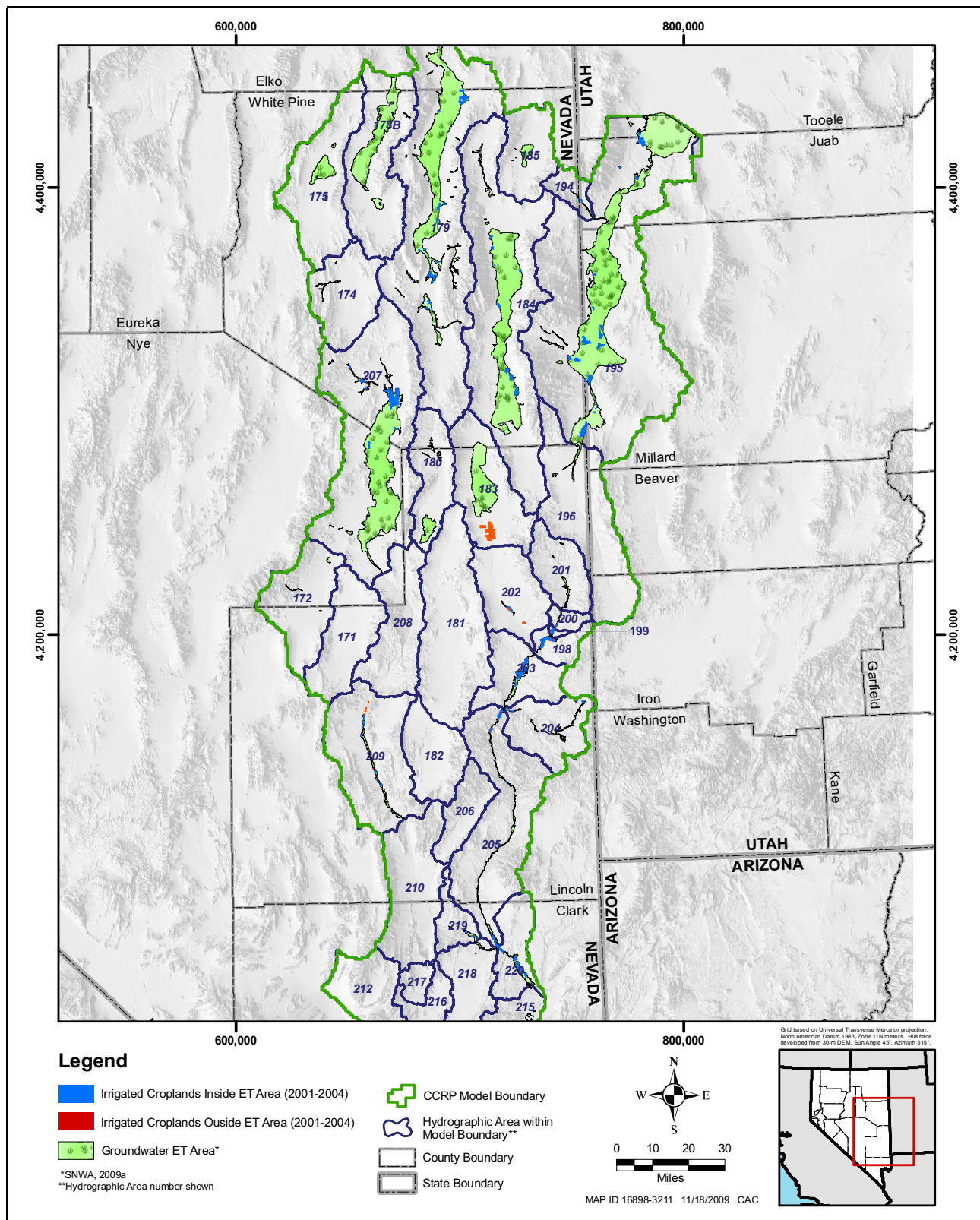
Figure 4-24
Extents of Irrigated Croplands (2001-2004) and
Groundwater ET Areas under Natural Conditions

SE ROA 50854

JA_16255

Table 4-9
Relative Importance of ET Areas Converted to Croplands

HA	Basin Name	Total Extent of ET Area (acres)	Total Annual ET Volume (af)	Areal Extent of Croplands Inside the ET Areas (acres)	Annual Volume of ET from Croplands Inside the ET Areas[a] (af)	Converted Areas (% of Total ET Area)	Converted Areas (% of Total Annual ET Volume)
179	Steptoe Valley	174,614	101,715	4,249	1,900	2	2
184	Spring Valley	177,772	75,436	2,568	600	1	1
195	Snake Valley	320,269	129,350	8,222	3,800	3	3
207	White River Valley	178,172	76,446	5,542	1,200	3	2

Source: SNWA (2009a)
[a]Calculated value using areal extent of croplands and ET rate information.

4.4.4   Springs

This section describes the setup of springs in the numerical model. No special considerations were needed to sim ulate spring flow under transient conditions. The c hanges in hydraulic heads determined flow rates, which were calibrated to the spring flow tar get observations presented in Section 4.7. The elevations at the spring locations were also included as hydraulic-head observations for tracking purposes onl y (see Section 4.7.3). Table 4-10 lists the springs considered in t he numerical model.

Except for a fe w, all regional and selected intermediate springs loc ated in the model area were simulated in the num erical model using the DRN or SFR2 packages. The e xceptions consist of springs that lie within or are adjacent to a model-boundary cell. Table 4-10 defines how the springs were represented in the model. The springs were categorized into se veral spring model type s as follows:

- DRN: Represented in the MODFLOW-2000 Drain package
- SFR2: Represented in the MODFLOW-2000 Streamflow-Routing package
- CHD: Represented in the MODFLOW-2000 Constant-Head package

Figure 4-25 illustrates the location of springs modeled with the DRN and SFR2 package.

Most of the springs included in the numerical model were simulated using the DRN package. Exceptions occur in Pahranagat Valley, Muddy River Springs Area, and at Big Springs, where spring discharge can flow as surface water for significant distances. The SF R2 package was use d to simulate the springs in these areas. Exceptions were also made for very small springs with flows less than 0.05 cfs that occurred in active ET areas already represented as ET DRN cells. It was assumed that the flow from these springs would be accounted for by the ET DRN cells.

JA_16256

Table 4-10
Setup of Regional and Intermediate Springs
in the Numerical Model of the Central Carbonate-Rock Province
(Page 1 of 2)

Model Type[a]	Spring Name	DRN and SFR2 Spring Name[b]	Observation Type	Comment
CHD	Deadman Spring	---	---	---
CHD	North Springs	---	---	In an active cell next to CHD
CHD	Walter Spring	---	---	---
CHD	Wilson Hot Spring 1	---	---	---
CHD	Wilson Hot Spring 2	---	---	---
CHD	Wilson Hot Spring 3	---	---	In an active cell next to CHD
CHD	Wilson Hot Spring 5	---	---	---
DRN	Arnoldson Spring	SPiw07_2_01	Flow	---
DRN	Blue Point Spring	SDiw15_2_##	Flow	---
DRN	Brownie Spring	SPis09_4_01	Flow	---
DRN	Butterfield Spring	SPib07_10_01	Flow	---
DRN	Caine Spring	SPis95_3_01	Flow	---
DRN	Campbell Ranch Springs	SPib79_5_01	Flow	---
DRN	Cherry Creek Hot Springs	SPr79_2_01	Flow	---
DRN	Cold Spring	SPiw07_3_01	Flow	---
DRN	Cold Spring	SPis79_4_01	Flow	---
DRN	Currie Spring	SPib79_6_01	Flow	---
DRN	Emigrant Springs	SPib07_15_01	Flow	---
DRN	Flag Springs 1	SPiw207_7	Flow	Flag Springs 1, 2, and 3 in same cell; flow aggregated in one observation
DRN	Flag Springs 2			
DRN	Flag Springs 3			
DRN	Foote Res. Spring	SPib95_12_01	Flow	---
DRN	Four Wheel Drive Spring	SPis84_11_01	Flow	---
DRN	Hardy Spring NW	SPis07_11_01	Flow	Hardy and Hardy NW in same cell; flow aggregated in one observation
DRN	Hardy Springs			
DRN	Hot Creek Spring	SPr07_1_01	Flow	---
DRN	Keegan Spring	SPis84_12_01	Flow	---
DRN	Kell Spring	SPis95_13_01	Flow	---
DRN	Knoll Spring	SPis95_4_01	Flow	---
DRN	Layton Spring	SPis84_7_01	Flow	---
DRN	Lund Spring	SPib07_5_01	Flow	---
DRN	McGill Spring	SPiw79_1_01	Flow	---
DRN	Minerva Spring	SPis84_13_01	Flow	---
DRN	Monte Neva Hot Springs	SPr79_3_01	Flow	---
DRN	Moon River Spring	SPr07_14_01	Flow	---
DRN	Moorman Spring	SPr07_6_01	Flow	---
DRN	Nicholas Spring	SPiw07_13_01	Flow	---

Table 4-10
Setup of Regional and Intermediate Springs
in the Numerical Model of the Central Carbonate-Rock Province
(Page 2 of 2)

Model Type[a]	Spring Name	DRN and SFR2 Spring Name[b]	Observation Type	Comment
DRN	North Millick Spring	SPis84_3_01	Flow	---
DRN	North Spring	SPiw84_8_01	Flow	---
DRN	Osborne Springs	SPis84_10_01	Flow	---
DRN	Panaca Spring	SPr03_1_01	Flow	---
DRN	Preston Big Spring	SDr07_4_##	Flow Change	---
DRN	Preston Big Spring	SDr07_4_58	Flow Change	---
DRN	Preston Big Spring	SPr07_4_01	Flow	---
DRN	Rogers Spring	SDiw15_1_##	Flow Change	---
DRN	Rogers Spring	SPiw15_1_01	Flow	---
DRN	South Bastian Spring	SPis84_5_01	Flow	---
DRN	South Bastian Spring 2	SPis84_6_01	Flow	---
DRN	South Millick Spring	SPib84_4_01	Flow	---
DRN	Stonehouse Spring	SPis84_14_01	Flow	---
DRN	The Seep	SPiw84_15_01	Flow	---
DRN	Twin Spring	SPib95_15_01	Flow	---
DRN	Unnamed 5 Spring	SPis84_16_01	Flow	---
DRN	Unnamed Spring	SPis95_14_01	Flow	---
DRN	Warm Creek near Gandy, UT	SPiw95_2_01	Flow	---
DRN	Willard Springs	SPis84_2_01	Flow	---
DRN	Willow Spring	SPiw84_1_01	Flow	---
SFR2	Ash Springs	GdASH_61	Flow	---
SFR2	Big Springs	GdBIG_SPR_61	Flow	---
SFR2	Crystal Springs	GdXTL_61	Flow	---
SFR2	End of Lake Creek	GdLKCK_END_##	Flow	---
SFR2	End of Pahranagat Wash	GdPW_7_##	Flow	---
SFR2	Hiko Spring	GdHIKO_01	Flow	---
SFR2	Muddy River at Lake Mead	GdLK_MEAD_01	Flow	---
SFR2	Muddy River at Overton	GdOVERTON_61	Flow	---
SFR2	Muddy River near Glendale	GdmrGLEND_08	Flow	---
SFR2	Muddy River near Moapa	GdmrMOAPA_##	Flow	Baldwin Spring, Jones Spring, M-10, M-11, M-12, M-13, M-15, M-16, M-19, M-20, Muddy Spring, Pederson East Spring, Pederson Spring, and Warm Springs East aggregated in Muddy River near Moapa SFR2 gage observation

[a]DRN: MODFLOW-2000 Drain package; SFR2: MODFLOW-2000 Streamflow-Routing package;
 CHD: MODFLOW-2000 Constant-Head package (Springs within CHD cells not represented in the model).
[b]Used as MODFLOW-2000 and UCODE_2005 observation names in DRN and SFR2 packages. ## indicates two-digit number corresponding to stress period.
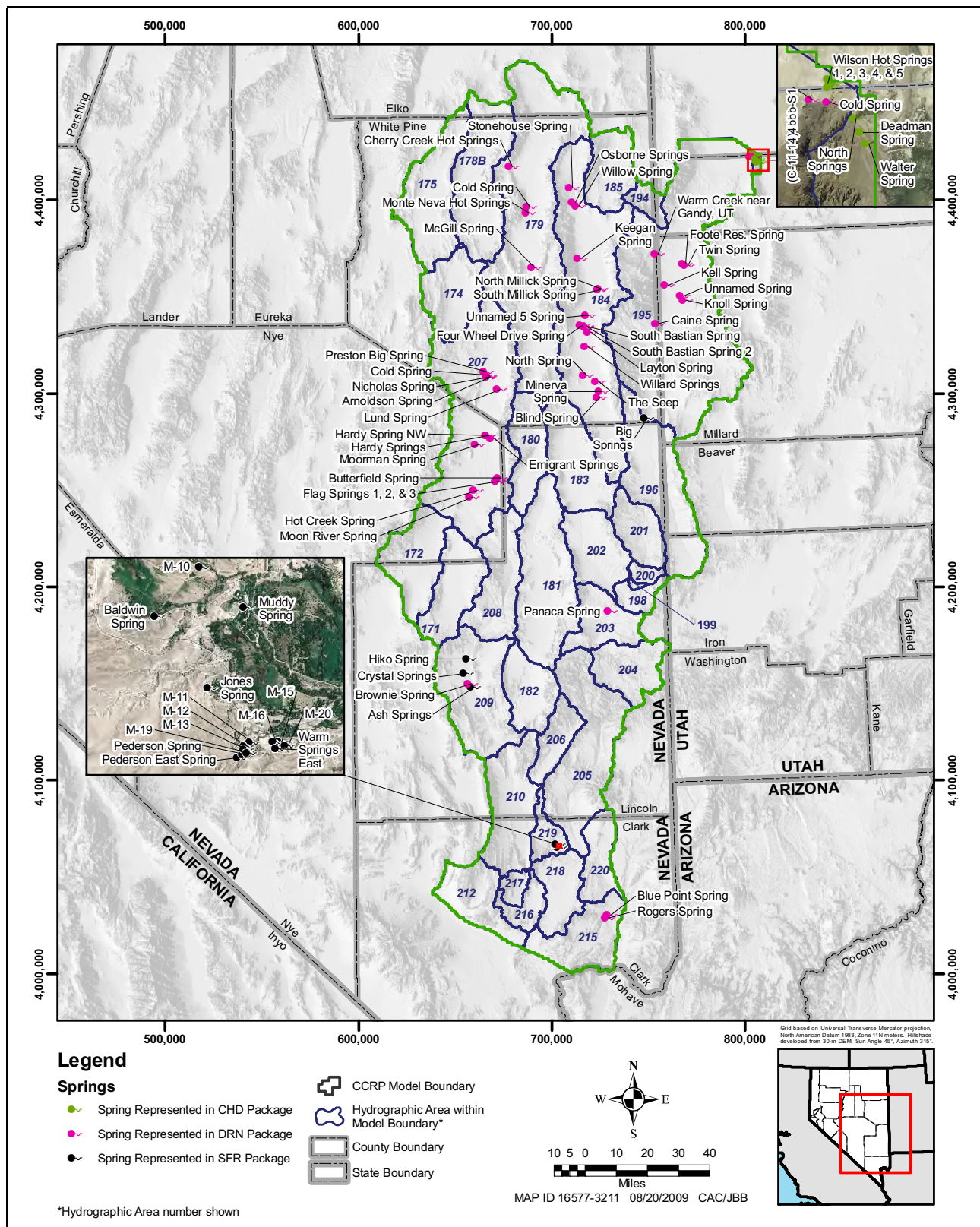
Figure 4-25
Locations of Springs Simulated with the CHD, DRN,
and SFR2 Packages in the Numerical Model

4.4.4.1 Springs Simulated Using DRN Package

Spring discharge at selected springs was simulated using the MODFLOW-2000 DRN package. The corresponding observations are included in the drain observation (DROB) module discussed later in this section. Each spring was assigned to a particular model cell. Where multiple springs occupy the same model cell, the springs were simulated as a group. A given spring (or group of springs) was represented by one or more drains linked to a different model layer. A single spring could, therefore, be represented by a maximum of 11 drains. However, all drains representing the spring were assigned the same drain elevation.

The depths of the spring drains were assumed to be at 32.8 ft bgs (10 m bgs). The ground surface was assumed to equal the minimum 30-m DEM elevation within the 1 km^2 grid cell in which the spring is located. The elevation of a given spring drain was calculated as this value of the ground surface minus the depth of the spring drain. This method of calculating the spring drain elevations was used because spring cells in the model are typically surrounded by ET drain cells. In such cases, when the drain elevation is set to the pool elevation or the land surface, surrounding ET drain cells effectively restrict flows to the spring drain cell. Lowering the spring drain to 32.8 ft bgs (10 m) provides a preferential gradient to the spring cell. If a spring occupies the same cell as an ET drain cell, the ET drain cell is reassigned to a Wetland ET DROB observation, regardless of its original type. A similar approach was used in the DVFS model (Faunt et al., 2004).

Spring conductance was estimated using the following equation:

$$C = (Q/(GS - DE))/L \qquad\qquad\qquad\text{(Eq. 4-4)}$$

where,

C	=	Conductance (L^2/T)
Q	=	Pre-1945 target discharge rates (L^3/T)
GS	=	Spring head elevation approximated by ground surface (L)
DE	=	Drain elevation (L)
L	=	Number of layers that contain spring cells

Spring conductances were treated as pa rameters. Initial estimates of drain conductance were calculated as the quotient of me asured spring discharge and the difference of interpolated field hydraulic-head and drain elevation. The values of initial estimates of spring conductance are listed in Table 4-11. Individual spring conductances were adjusted during manual portions of the model calibration to better approximate spring discharge. Conductance adjustments are generally limited to within one order of magnitude of the starting value.

4.4.4.2 Springs and Streams Simulated Using SFR2 Package

If all springs were represented as drains usi ng the DRN package, groundwater ET from basins with significant surface-water flow could not be well represented.   Where spring discha rge flows in streams, the surfa ce water can infiltrate into the groundwa ter system and then be available for

JA_16260

Table 4-11
Initial Estimates of Conductances for Spring Drains
(Page 1 of 2)

Spring Name	DRN and SFR2 Observation Name	Initial Spring DRN Conductance ft^2/d (m^2/d)	Comment
Arnoldson Spring	SPiw07_2_01	644.0 (59.83)	---
Blue Point Spring	SDiw15_2_##	57.69 (5.360)	---
Brownie Spring	SPis09_4_01	491.2 (45.63)	---
Butterfield Spring	SPib07_10_01	1,175 (109.2)	---
Caine Spring	SPis95_3_01	NA	Small spring represented by ET DRN
Campbell Ranch Springs	SPib79_5_01	NA	Small spring represented by ET DRN
Cherry Creek Hot Springs	SPr79_2_01	3.693 (0.3431)	---
Cold Spring	SPiw07_3_01	428.8 (39.84)	---
Cold Spring	SPis79_4_01	NA	Small spring represented by ET DRN
Emigrant Springs	SPib07_15_01	537.7 (49.95)	---
Flag Springs 1	SPiw07_9_01	205.5 (19.09)	Flag #1, #2, and #3 are in the same cell
Flag Springs 2	SPiw07_8_01		
Flag Springs 3	SPiw07_7_01		
Foote Res. Spring	SPib95_12_01	2,199 (204.3)	---
Four Wheel Drive Spring	SPis84_11_01	NA	Small spring represented by ET DRN
Hardy Spring NW	SPis07_12_01	627.1 (58.26)	Small spring represented by ET DRN
Hardy Springs	SPis07_11_01		
Hot Creek Spring	SPr07_1_01	2,174 (202.0)	---
Keegan Spring	SPis84_12_01	927.0 (86.12)	---
Kell Spring	SPis95_13_01	302.5 (28.10)	---
Lund Spring	SPib07_5_01	5,899 (548.0)	---
McGill Spring	SPiw79_1_01	5,386 (500.4)	---
Minerva Spring	SPis84_13_01	1,484 (137.9)	---
Monte Neva Hot Springs	SPr79_3_01	141.3 (13.13)	---
Moon River Spring	SPr07_14_01	380.0 (35.30)	---
Moorman Spring	SPr07_6_01	206.0 (19.14)	---
Nicholas Spring	SPiw07_13_01	463.3 (43.04)	---
North Millick Spring	SPis84_3_01	1,069 (99.28)	---
North Spring	SPiw84_8_01	NA	Small spring represented by ET DRN
Osborne Springs	SPis84_10_01	NA	Small spring represented by ET DRN
Panaca Spring	SPr03_1_01	511.7 (47.54)	---
Preston Big Spring	SDr07_4_##	1,218 (113.2)	---
Rogers Spring	SDiw15_1_##	120.9 (11.23)	---
South Bastian Spring	SPis84_5_01	NA	Small spring represented by ET DRN
South Bastian Spring 2	SPis84_6_01	NA	Small spring represented by ET DRN
South Millick Spring	SPib84_4_01	1,114 (103.5)	---
Stonehouse Spring	SPis84_14_01	NA	Small spring represented by ET DRN

Spring Name	DRN and SFR2 Observation Name	Initial Spring DRN Conductance ft^2/d (m^2/d)	Comment
The Seep	SPiw84_15_01	NA	Small spring represented by ET DRN
Twin Spring	SPib95_15_01	3,514 (326.5)	---
Unnamed 5 Spring	SPis84_16_01	NA	Small spring represented by ET DRN
Unnamed Spring	SPis95_14_01	NA	Small spring represented by ET DRN
Gandy Warm Springs near Gandy, UT	SPiw95_2_##	2,947 (273.8)	---
Gandy Warm Springs near Gandy, UT	SPiw95_2_01	2,947 (273.8)	---
Willard Springs	SPis84_2_01	NA	Small spring represented by ET DRN
Willow Spring	SPiw84_1_01	6.958 (0.6464)	---

Note: NA = Not applicable
indicates two-digit number corresponding to stress period.

discharge by ET. In such cases, use of the SFR2 package is more applicable. SFR2 allows springs to discharge to streams and stream water to infiltrate into the flow system downstream from the spring orifice. The spring systems in the Muddy River Springs Area, Pahranagat Valley, and the Big Springs area in Snake Valley are represented with SFR2.

4.4.4.2.1   *General Representation of Springs*

The SFR2 package simulates the discharge of gr oundwater from a spring and the flow of   this discharged water in a stream channel.   SFR2 typically acc ounts for surficial stream-aquifer interactions. Springs in the numerical model, however, are conceptualized to discharge from geologic units at depths beyond surficial and alluvial layers.

To represent springs within the framework of the SFR2 package, SFR2 cells are defined at depth. The only appar ent restriction on t he reach cells is that the stream stage or, in this case, aquifer hydraulic head have a g radient downstream. Downstream is specified by the order of the SFR2 reaches (model cells) and river segments (collections of reaches).

For springs, a stream segment is defined to represent the spring structure extending from the ground surface to the top or bottom of the carbonate, depending on the spring type. To monitor spring flow, gages (Table 4-12) are added at the surface reach of t he SFR2 segments. These gages allow the spring flow discha rge to be monitored. Whe re SFR2 cells at the spring reach the surface, SFR2 segments are connected to conventional stream segments to allow flow downstream.

Once the spring flow reaches the ground surface, flow is confined to stream segments in the top active model layer. Water in the c hannel can flow downstream, evaporate, be removed by diversion (ditch or pipe), or reinfiltrate into the aquifer (a losing channel). Water from the aquifer can also seep into the river (gaining channel). Because of the small surface area of the channels relative to the model

Table 4-12
Spring Flow Gages Modeled Using SFR2 Package

Spring Name	Observation Name	Spring Type[a]
Big Springs Area		
Big Springs	GdBIG_SPR_61	INT
End of Lake Creek	GdLKCK_END_##	RIV
Muddy River Springs Area		
Muddy River near Moapa	GdmrMOAPA_##	RIV
Muddy River near Glendale	GdmrGLEND_##	RIV
Muddy River at Overton	GdOVERTON_61	RIV
Muddy River at Lake Mead	GdLK_MEAD_01	RIV
Pahranagat Valley Area		
Hiko Spring	GdHIKO_01	REG
Crystal Springs	GdXTL_61	REG
Ash Springs	GdASH_61	REG
End of Pahranagat Wash	GdPW_7_##	RIV

[a]REG: Regional flow system designation; INT: Intermediate flow system designation;
 RIV: Surface-water flow
indicates two-digit number corresponding to stress period.

cell size, recharge is not applied to the river (recharge is applied to the entire cell via the RCH module).

In most parts of the model, evaporation accounted for by the SFR2 module is relatively small, as it is a function of the surface area of the open water channel. The rate of ET is defined as the open-water ET rate for the area of the model (Table 4-13). Evaporation due to riparian vegetation is not accounted for using SFR2. For the water to be evapotranspired, it must leak back into the aquifer, where it can then be discharged in ET DRN cells. Note that the SFR2 and ET DRN cell may be the same cell.

Table 4-13
Open-Water ET Rates for SFR2 Streams

SFR2 Stream	ET Rate ft/yr (m/d)
Big Springs Creek/Lake Creek	5.63 (0.004699)
Muddy River	6.71 (0.0056)
Pahranagat Wash	6.12 (0.005105)

Flow to springs simulated using the SFR2 package was controlled by riverbed hydraulic conductivities. Table 4-14 lists the spring names and their corresponding parameter name and initial estimates of riverbed hydraulic conductivities.

Table 4-14
Parameter Names and Initial Estimates for Springs
Simulated Using SFR2 Package

Spring Name	Parameter Name	Hydraulic-Conductivity Estimate ft/d (m/d)
Big Springs Area		
Big Springs	SFR_COND3	0.328 (0.1)
Muddy River Springs Area		
Baldwin Spring	SFR_COND19	0.328 (0.1)
Jones Spring	SFRaCOND19	0.328 (0.1)
M-10	SFR_COND19	0.328 (0.1)
M-11	SFRaCOND19	0.328 (0.1)
M-12	SFRaCOND19	0.328 (0.1)
M-13	SFRaCOND19	0.328 (0.1)
M-15	SFRaCOND19	0.328 (0.1)
M-16	SFRaCOND19	0.328 (0.1)
M-19	SFRaCOND19	0.328 (0.1)
M-20	SFRaCOND19	0.328 (0.1)
Muddy Spring	SFR_COND19	0.328 (0.1)
Pederson East Spring	SFRaCOND19	0.328 (0.1)
Pederson Spring	SFRaCOND19	0.328 (0.1)
Warm Springs East	SFRaCOND19	0.328 (0.1)
Pahranagat Valley Area		
Ash Springs	SFR_COND17	0.328 (0.1)
Crystal Springs	SFR_COND16	0.328 (0.1)
Hiko Spring	SFR_COND15	0.328 (0.1)

4.4.4.2.2   *Detailed Descriptions of Springs/Streams Simulated with SFR2 Package*

Detailed descriptions of the SFR2 package representation of the Muddy River Springs, Pahranagat Valley, and the Big Springs areas in Snake Valley are provided in this section.

Muddy River Springs Area

The Muddy River Springs Area is the largest spring discharge area in the model area. Predevelopment conditions for spring discharge from 14 significant springs, groundwater ET, and Muddy River stream flow measured at the Muddy River near Moapa, Nevada (09416000), gage are estimated at 26,315 afy (88,870 m^3/d), 5,988 afy (20,224 m^3/d), and 34,000 afy (114,821 m^3/d), respectively. Additional unmeasured springs and seeps occur in this area and account for the difference between the measured spring discharge and the groundwater ET and Muddy River stream flow, a difference of about 14,000 afy (47,279 m^3/d). Because only a small portion of the spring discharge in this area is consumed by ET, the remainder enters the Muddy River, where it is measured at the Muddy River near Moapa, Nevada, gage (approximately 1 mi downstream), and flows

downstream through the hydrographic areas of California Wash, Lower Meadow Valley Wash, and Lower Moapa Valley.

The spring discharge in the Muddy River Springs Area could have been removed from the model at the spring locations, but by the time the Muddy River reaches Overton, Nevada, stream flow was about 7,100 afy (24,000 m^3/d) during predevelopment conditions, assuming about half of the stream flow measured from Water Year 1914 to Water Year 1916 was groundwater discharge (Wells, 1954). This suggests that about 27,000 afy (91,000 m^3/d) seeped back into the aquifer or was consumed by riparian vegetation simulated as Wetland ET. This volume of water accounts for more than half the ET estimated in California Wash, southern Lower Meadow Valley Wash, and Lower Moapa Valley. The stream and aquifer interactions of the Muddy River were approximated using the SFR2 package as follows:

- The Muddy River channel was subdivided into 18 stream segments and 87 reach cells. Figure 4-26 illustrates the SFR2 cells defining the Muddy River (Table 4-15).

- The Open Water ET rate for the Muddy River Springs Area from SNWA (2009a) was used for the surface SFR2 channels. For stream segments representing connections to deep springs, zero ET was specified.

- Stream channel elevations were approximated from 2-ft contour data of the Muddy River channel area. Riverbed spring channel elevations for segments were based on the minimum and maximum spring pool elevations in an SFR2 cell.

- Surface channel widths were approximated, ranging from 10 ft (3 m) to 75 ft (23 m). Subsurface channel widths were assumed to be 328 ft (100 m). Surface channel segment lengths were based on the mapped river channel length in each model cell. Model layer thicknesses were used to represent the channel length for subsurface springs.

Three gages were used in the model calibration (see Figure 4-26). An additional seven gages were defined to monitor trends in the total stream flow. These gages are defined in Table 4-16 and shown in Figure 4-27.

Pahranagat Valley

Three regional springs discharge at the northwest part of Pahranagat Valley. Down-gradient of these springs is a significant extent of wetland phreatophyte along Pahranagat Wash, which flows south along the axis of the valley. SNWA (2009a) explains that these wetlands are maintained by the groundwater discharge from these regional springs. In other words, groundwater is made available to wetland phreatophyte communities supported by a shallow alluvial aquifer that is recharged by groundwater discharge from the regional springs.

The representation of groundwater discharge in Pahranagat Valley is complex, in part, because the conceptual model predicts that 93 percent of the water that evapotranspires from Pahranagat Valley first flows out of Ash, Brownie, Crystal, and Hiko springs. This prediction implies that there is relatively little other groundwater discharge in Pahranagat Valley. From a practical standpoint, discharging 26,735 afy (90,287 m^3/d) out of four springs and having relatively little other
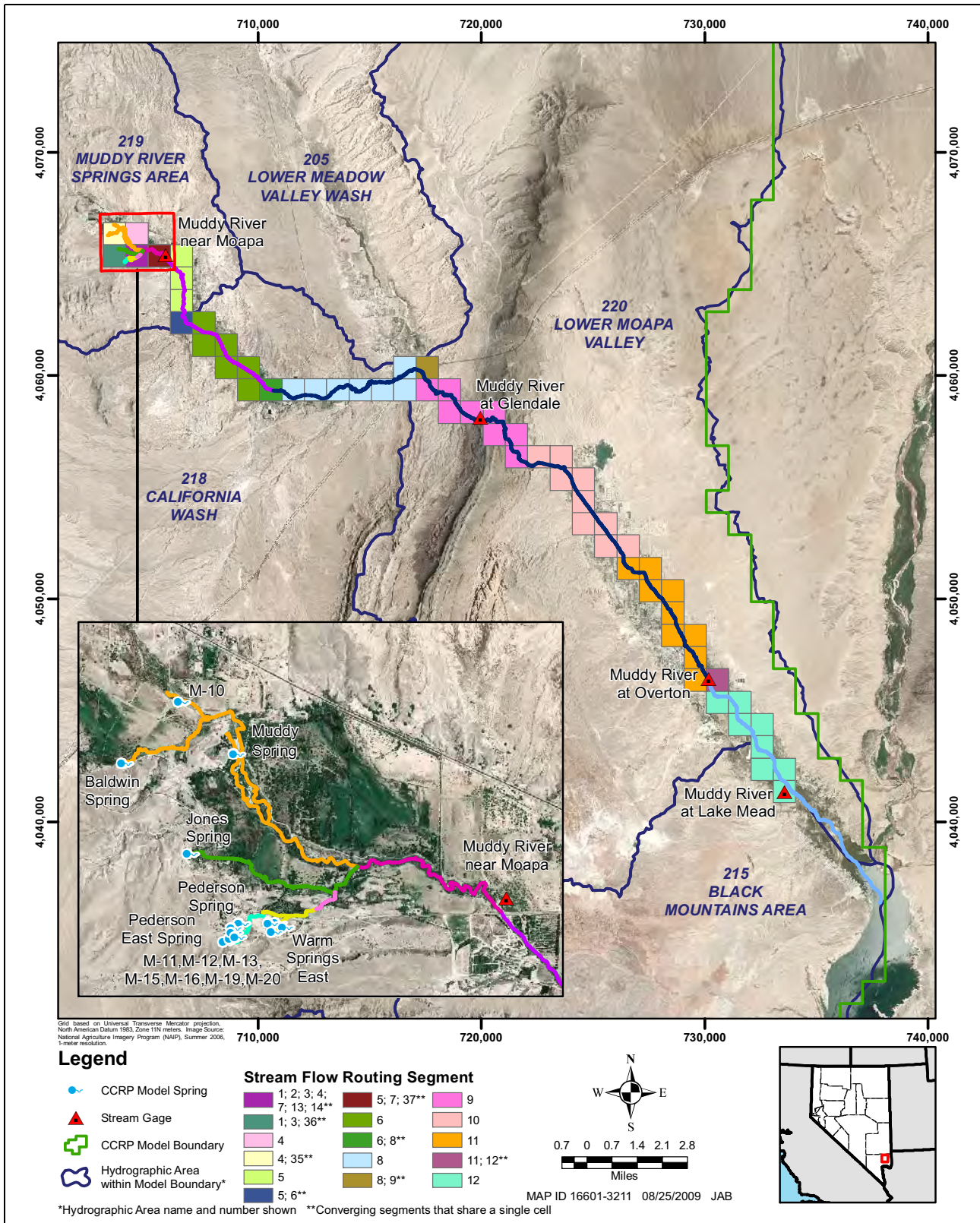
Figure 4-26
Representation of the Muddy River Springs and Muddy River
in the Numerical Model Using the SFR2 Package

Section 4.0

SE ROA 50865

JA_16266

Table 4-15
Characteristics of Muddy River Stream Flow Routing Segments

Segment	Number of Reaches	Downstream Segment ID	Segment Length ft (m)	Conductance Parameter	Riverbed Elevation Upstream ft amsl (m amsl)	Riverbed Elevation Downstream ft amsl (m amsl)	Channel Width ft (m)	ET Rate ft/yr (m/d)	Reynolds Number	Description
1	2	2	1,867 (569)	SFR_COND1	1,800 (548.64)	1,775 (541)	10 (3)	6.71 (0.0056)	0.041	Warm Springs West Channel
2	1	13	2,438 (743)	SFR_COND1	1,775 (541)	1,745 (532)	10 (3)	6.71 (0.0056)	0.041	Iverson Flume Channel
3	2	14	3,931 (1,198)	SFR_COND1	1,784 (543.76)	1,729 (527)	10 (3)	6.71 (0.0056)	0.041	Jones Spring Channel
4	2	7	13,482 (4,109)	SFR_COND1	1,777 (541.54)	1,719 (524)	10 to 23 (3 to 7)	6.71 (0.0056)	0.041	Muddy Springs Channel
5	5	6	13,879 (4,230)	SFR_COND24	1,709 (521)	1,663 (507)	49 to 75 (15 to 23)	6.71 (0.0056)	0.030	Moapa to California Wash HA
6	8	8	16,792 (5,118)	SFR_COND25	1,663 (507)	1,591 (485)	49 to 75 (15 to 23)	6.71 (0.0056)	0.030	California Wash HA to Glendale
7	2	5	5,033 (1,534)	SFR_COND1	1,719 (524)	1,709 (521)	23 to 49 (7 to 15)	6.71 (0.0056)	0.035	Moapa Channel
8	9	9	29,539 (9,003)	SFR_COND2	1,591 (485)	1,512 (461)	36 to 75 (11 to 23)	6.71 (0.0056)	0.035	Glendale to Lower Moapa HA
9	9	10	29,358 (8,948)	SFR_COND20	1,512 (461)	1,458 (444.5)	36 to 75 (11 to 23)	6.71 (0.0056)	0.035	Lower Moapa HA toward Overton
10	9	11	22,885 (6,975)	SFR_COND21	1,458 (444.5)	1,322 (403)	36 to 75 (11 to 23)	6.71 (0.0056)	0.035	Mid #1 Overton to mid #2 Overton
11	10	12	25,159 (7,668)	SFR_COND22	1,322 (403)	1,243 (379)	36 to 75 (11 to 23)	6.71 (0.0056)	0.035	Mid #2 Overton to mid #3 Overton
12	9	Lake Mead	24,221 (7,383)	SFR_COND23	1,243 (379)	1,169 (356.4)	36 to 75 (11 to 23)	6.71 (0.0056)	0.025	Overton to Lake Mead
13	1	14	705 (215)	SFR_COND1	1,745 (532)	1,729 (527)	10 (3)	6.71 (0.0056)	0.041	Below Iverson Flume
14	1	7	912 (278)	SFR_COND1	1,729 (527)	1,719 (524)	10 to 23 (3 to 7)	6.71 (0.0056)	0.041	Below Jones Spring and Iverson Flume
15	5	4	10,794 (3,290)	SFR_COND19	1,798 (548.03)	1,777 (541.54)	328 (100)	0	0.050	Baldwin, Muddy, and M-10 springs
16	1	3	3,281 (1,000)	SFR_COND19	1,788 (545)	1,785 (544)	328 (100)	0	0.050	Jones Spring Channel
17	5	1	10,815 (3,296)	SFR_COND19	1,811 (551.99)	1,800 (548.46)	328 (100)	0	0.050	Pederson, Pederson East, M-12, M-13, and M-19 springs
18	5	2	10,804 (3,293)	SPR_COND19	1,800 (548.64)	1,775 (541)	328 (100)	0	0.050	M-11, M-15, M-16, M-20, and Warm Springs East springs

Table 4-16
Muddy River Gages

Gage Name	Segment	Reach
Warm Springs West	2	1
Iverson Flume	13	1
Muddy River near Moapa	5	2
Muddy River at California Wash HA Boundary	5	6
California Wash	8	1
Muddy River near Glendale	8	9
Muddy River at mid #1 to mid #2 Overton Segment	10	1
Muddy River at mid #2 to mid #3 Overton Segment	11	1
Muddy River at Lewis Avenue at Overton	12	1
Muddy River at Lake Mead	12	9
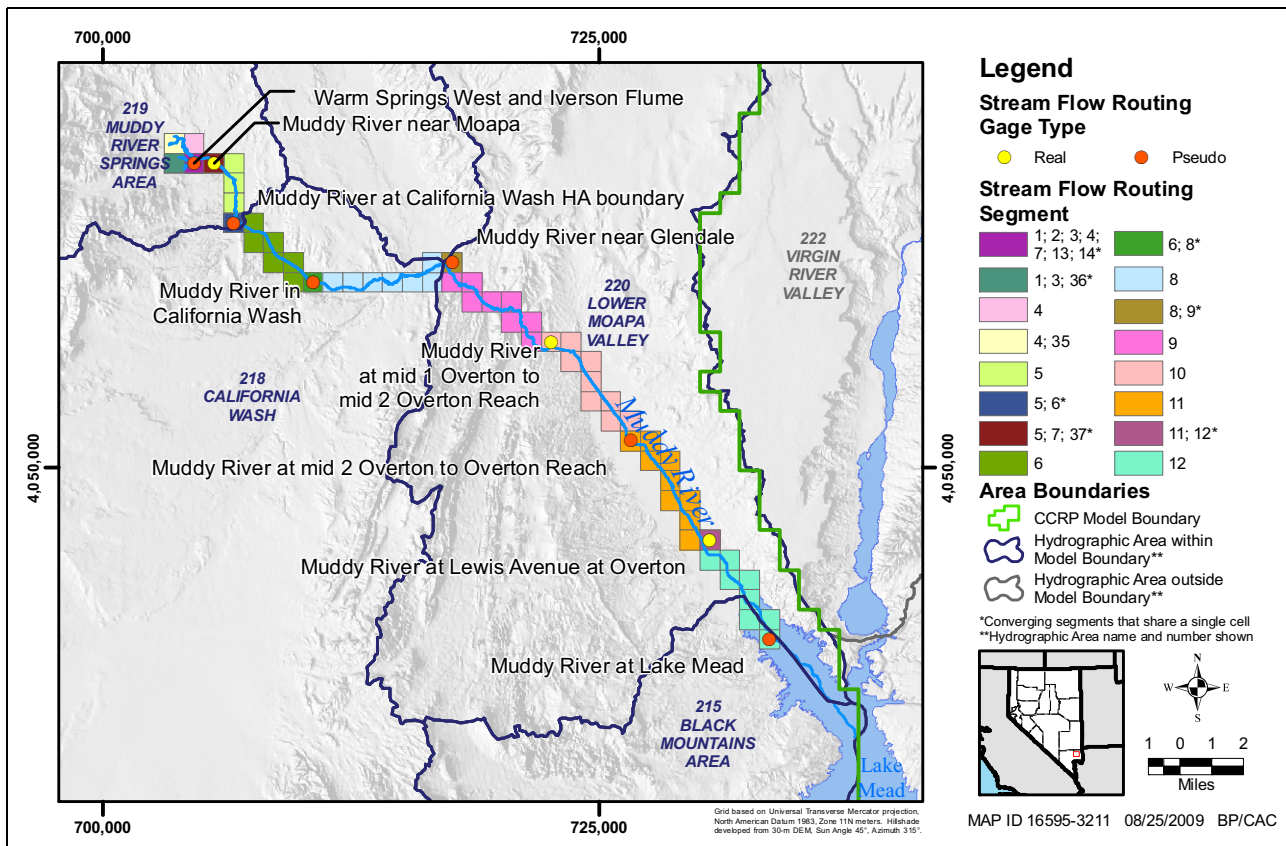
Figure 4-27
Gages Along the Muddy River

SE ROA 50867

JA_16268

regional/intermediate aquifer water discharging 1,785 afy (6,029 m³/d) from neighboring model cells requires special treatment and/or adjustments to the conceptual model.

To approximate the discharges estimated in the conceptual model, the following assumptions were made for Pahranagat Wash:

1. The Wash channel floor and phreatophyte (ET DRN ce lls) from Hiko to Ash springs is essentially impermeable. This allows significa nt artesian pressures (head above ground surface) to build in the area of the springs, providing sufficient flow out the springs and into Pahranagat Wash, without allowing any other groundwater seepage. In the numerical model, the SFR2 channel conductances and ET DRN cell conductances were set to zero or near zero.

2. From Ash Spring south to the Pahranagat Shear Zone, Pahranagat Wash, and we lls drilled near the wash, and the riparian vegetation along the river sides are drawing water largely from a perched or semiperched, stream-channel aquifer sustained by Pahranagat Wash. The numerical model was not configured to mana ge perched conditions, but the net result can be approximated. Along the entire le ngth of the wash, the channel width is def ined to be between 492 ft (150 m) and 984 ft (300 m) wide. The actual channel width is closer to 15 to 33 ft (5 to 10 m). These e xcessively wide channel widths are meant to reflect the open water area as well as the r iparian areas supported by Pahranagat Wash. This appr oach allowed sufficient discharge as ET without maintaining higher hydraulic heads in the aquifer necessary to achieve groundwater-derived ET rates.

The SFR2 package represents the regional springs and Pahranagat Wash to a pproximate these processes, which are similar to what is occurring at Muddy River Springs Area and along the Muddy River. A vertical segment was defined below each spring pool to the bottom of the carbonate RMU. Additional segments were added to carry flows southeast into the Pahranagat Shear Zone. In addition to matching spring flows in P ahranagat Wash, flows in Pahranagat Wash should be zero at the point where Pahranagat Wash reaches Coyote Spring Valley.

Pahranagat Wash was defined using 10 stream segments and 92 reach cells (see Figure 4-28). The description of each segment is presented in Table 4-17.

Spring SFR2 cells at depth for Hiko and Crystal springs were shifted one cell west so that the springs would be dr awing water from the lar ger-*K* large-displacement and moderate-displacement fault zones. They were originally located in carbonate-mountain-block materials. Prior to this adjustment, expected flows were impossible to obtain.

SFR2 package specifications for Pahranagat Wash included the following:

1. The Open Water ET rate for the Pahranagat Valley hydrographic area from SNWA (2009a) was used for the surface SFR2 channels. For spring channel segments, zero ET was defined.

2. Riverbed stream channel elevations were estimated from the USGS 30-m DEM. R iverbed spring channel elevations were based on the spring po ol elevation and the 30-m DEM
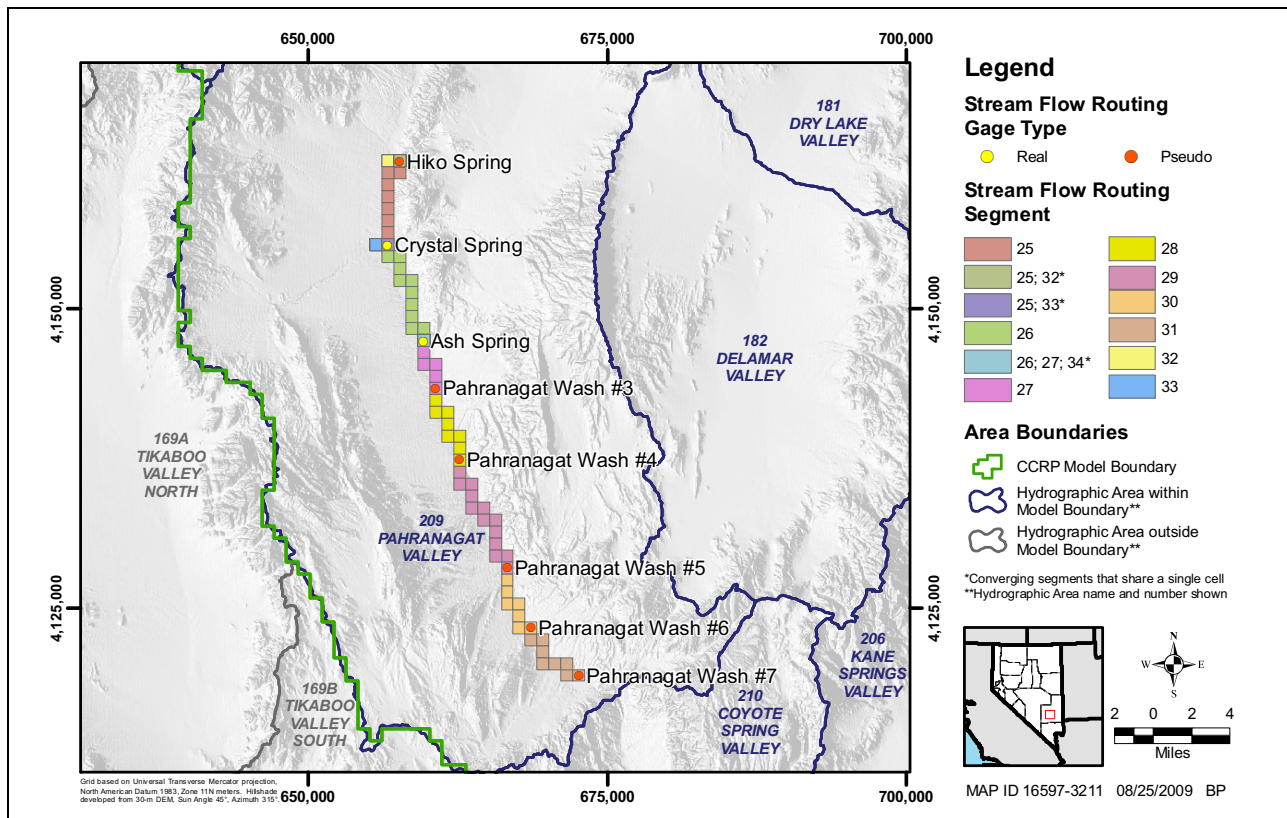
Figure 4-28
Pahranagat Wash Stream Flow Routing Segments

elevation where the spring tributary left the model cell or at its confluence with Pahranagat Wash.

3. Surface channel widths were assumed to be 10 ft (3 m). Subsurface channel widths were assumed to be 328 ft (100 m).

4. Surface channel segment lengths w ere based on the mapped river channel length in each model cell. Channel lengths for spring segme nts occurring at depth were based on model layer thicknesses.

5. The Pahranagat Wash is assumed and required to dry up before the last SRF2 reach.

Four flow observations were specified as gages and used as mode l constraints. An additional six gages were defined to monitor tre nds in the total stream flow. These are defined in Table 4-18 and shown in Figure 4-28.

Big Springs Area

In southern Snake Valley, Big Springs is a large intermediate-class spring that supplies water to Big Springs Creek, Lake Creek, and Pruess Lake. Significant Wetland ET occurs along the length of the creek. The S FR2 package was used to represent the process of supplying Big Springs discharge to Wetland ET areas along the creek.

SE ROA 50869

JA_16270

Table 4-17
Characteristics of Pahranagat Wash Stream Flow Routing Segments

Segment	Number of Reaches	Downstream Segment ID	Segment Length ft (m)	Conductance Parameter	Riverbed Elevation Upstream ft amsl (m amsl)	Riverbed Elevation Downstream ft amsl (m amsl)	Channel Width ft (m)	ET Rate ft/yr (m/d)	Reynolds Number	Description
25	9	26	26,540 (8,089)	SPR_COND8	3,853 (1,174.4)	3,803 (1,159.1)	984 (300)	6.12 (0.0051)	0.035	Hiko Spring to Crystal Springs
26	11	27	28,315 (8,630)	SPR_COND9	3,803 (1,159.1)	3,600 (1,097.0)	984 (300)	6.12 (0.0051)	0.035	Crystal Springs to Ash Springs
27	6	28	18,139 (5,529)	SPR_COND10	3,600 (1,097.0)	3,533 (1,076.9)	492 (150)	6.12 (0.0051)	0.035	Stream Segment #3
28	8	29	22,390 (6,825)	SPR_COND11	3,533 (1,076.9)	3,468 (1,056.9)	492 (150)	6.12 (0.0051)	0.035	Stream Segment #4
29	13	30	33,615 (10,246)	SPR_COND12	3,468 (1,056.9)	3,349 (1,020.7)	492 (150)	6.12 (0.0051)	0.035	Stream Segment #5
30	7	31	18,821 (5,737)	SPR_COND13	3,349 (1,020.7)	3,221 (981.8 m)	492 (150)	6.12 (0.0051)	0.035	Stream Segment #6
31	12	End of River	29,679 (9,046)	SPR_COND14	3,221 (981.8)	3,110 (947.8)	492 (150)	6.12 (0.0051)	0.035	End of Stream
32	8	25	13,820 (4,212)	SPR_COND15	3,875 (1,181.1)	3,853 (1,174.4)	328 (100)	0	0.05	Hiko Spring
33	9	26	16,058 (4,894)	SPR_COND16	3,803 (1,159.2)	3,803 (1,159.1)	328 (100)	0	0.05	Crystal Springs
34	9	27	15,849 (4,831)	SPR_COND17	3,622 (1,104.0)	3,600 (1,097.0)	328 (100)	0	0.05	Ash Springs

Table 4-18
Pahranagat Wash Gages

Gage Name	Segment	Reach
Pahranagat Wash at Crystal Springs	25	9
Pahranagat Wash at Ash Springs	26	11
Pahranagat Wash #3	27	6
Pahranagat Wash #4	28	8
Pahranagat Wash #5	29	13
Pahranagat Wash #6	30	7
End of Wash	31	8
Hiko Spring	32	8
Crystal Springs	33	8
Ash Springs	34	8

Similar to the Muddy River Springs Area, a vertical stream segment was defined below the spring pool. Additional stream segments carry flows northeast to Pruess Lake and slightly beyond toward Baker. Big Springs discharge was used as a model observation. Stream flows at the final reach should be approximately zero.

Big Springs Creek and Lake Creek were defined using 6 stream segments and 50 reach cells (Figure 4-29). The description of each segment is presented in Table 4-19.

SFR2 package specifications for Big Springs included the following:

1. The Open Water ET rate for the Snake Valley hydrographic area from SNWA (2009a) was used for the surface SFR2 channels. For spring channel segments, zero ET was defined.

2. Riverbed stream channel elevations were estimated from the USGS 30-m DEM. Riverbed spring channel elevations were based on the spring pool elevation and the 30-m DEM elevation where the spring tributary left the model cell or at its confluence with Big Springs Creek.

3. Surface channel widths were assumed to be 10 ft (3 m). Subsurface channel widths were assumed to be 328 ft (100 m).

4. Surface channel segment lengths were based on the mapped river channel length in each model cell. Channel lengths for spring segments occurring at depth were based on model layer thicknesses.

5. Lake Creek is assumed and required to dry up north of Pruess Lake and before the final SRF2 reach.
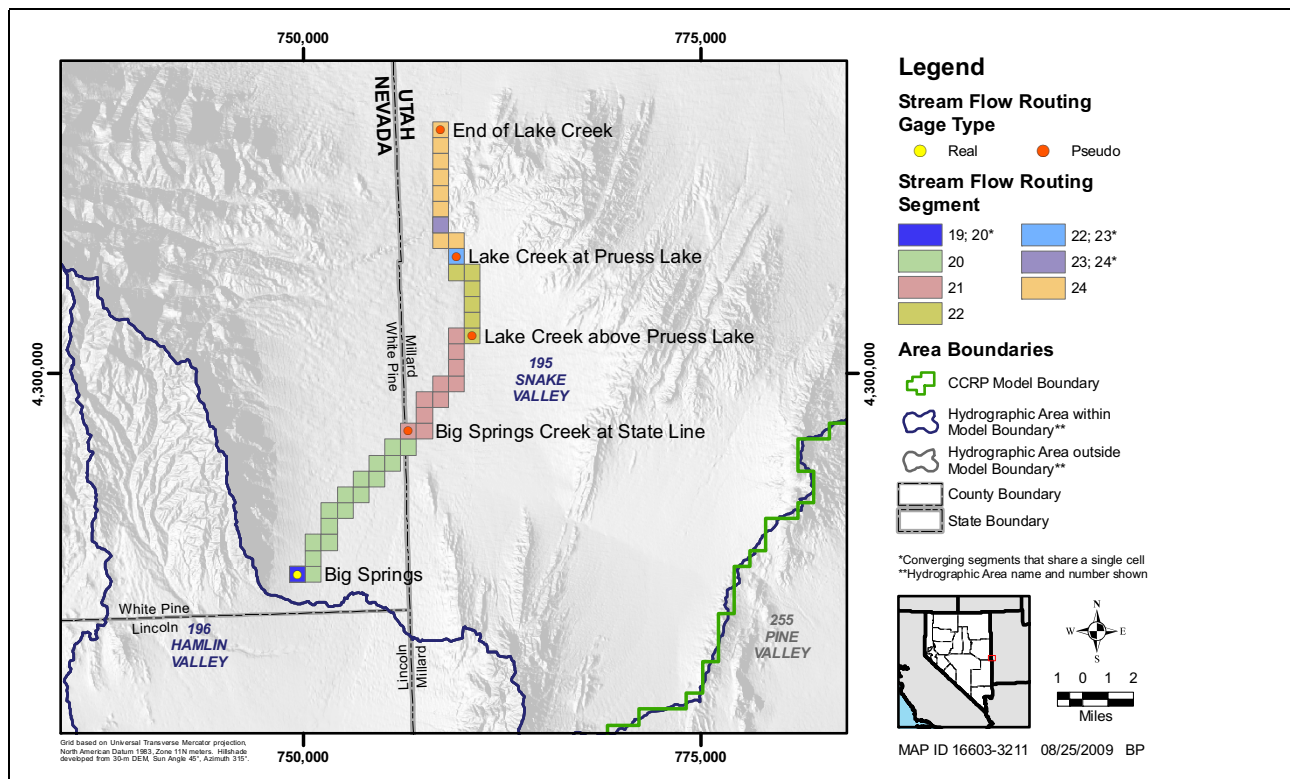
Figure 4-29
Big Springs Creek and Lake Creek Stream Flow Routing Segments and Gages

Table 4-19
Characteristics of Big Springs Area Stream Flow Routing Segments

Segment	Number of Reaches	Downstream Segment ID	Segment Length ft (m)	Conductance Parameter	Riverbed Elevation		Channel Width ft (m)	ET Rate ft/yr (m/d)	Reynolds Number	Description
					Upstream ft amsl (m amsl)	Downstream ft amsl (m amsl)				
19	6	20	5,404 (1,647)	SFR_COND3	5,568 (1,697.1)	5,528 (1,685.0)	328 (100)	0 (0.00)	0.05	Big Springs
20	16	21	40,753 (12,421)	SFR_COND4	5,528 (1,685.0)	5,430 (1,655)	32.8 (10)	5.63 (0.0047)	0.035	Utah Border
21	10	22	26,753 (8,154)	SFR_COND5	5,430 (1,655)	5,361 (1,634)	32.8 (10)	5.63 (0.0047)	0.035	Stream Segment #2
22	7	23	18,925 (5,768)	SFR_COND6	5,361 (1,634)	5,358 (1,633)	32.8 (10)	5.63 (0.0047)	0.035	Stream Segment #3
23	4	24	7,041 (2,146)	SFR_COND7	5,358 (1,633)	5,355 (1,632)	1,969 (600)	5.63 (0.0047)	0.035	Pruess Lake
24	7	End of Creek	20,756 (6,326)	SFR_COND18	5,355 (1,632)	5,227 (1,593)	32.8 (10)	6.11 (0.0051)	0.035	End of Lake Creek

Two flow observations were specified as gages and used as model constraints along Big Springs and Lake creeks. An additional three gages were defined to monitor trend s in the tot al stream flow. These gages are defined in Table 4-20 and shown in Figure 4-29.

Table 4-20
Big Springs Area Gages

Gage Name	Segment	Reach
Big Springs	20	1
Big Springs Creek at State Line	21	1
Lake Creek above Pruess Lake	22	1
Lake Creek at Pruess Lake	23	1
End of Lake Creek	24	7

4.5   Precipitation Recharge

Groundwater recharge was represented in the numerical model using the MODFLOW-2000 recharge (RCH) package (McDonald and H arbaugh, 1988). A brief description of the RCH pac kage is presented, followed by the methodology us ed to generate the input recharge grid and its implementation in the numerical model.

4.5.1   RCH Package

The RCH package simulates areally distributed recharge to the flow system represented in the model flow domain. In general, the sole source of the simulated areal recharge is precipitation (McDonald and Harbaugh, 1988).

The recharge distribution is input to the model in the form of a grid of recharge rate values (in units of length per unit time). The recharge flow rate applied to the model through the top face of each model cell is calculated by the RCH package as the input recharge rate times the area of the top face of the model cell. The resulting recharge flow rate is applied to the top model layer (McDonald and Harbaugh, 1988). The R CH package could be used to simulate areal recharge from other sourc es, such as artificial recharge or secondary recharge from irrigation.

A limitation of the RCH package allows the input of recharge rates only as a distributed recharge-rate grid. If recharge needs to be varied during model calibration, the recharge rates themselves must be treated as parameters. A methodology was developed to a llow more flexi bility in the parameterization of the recharge distribution.

4.5.2   Methodology

The methodology described in this section uses the potential-recharge-estimation process described in SNWA (2009a), distributes the recharge to appropriate locations, and integrates the generation of the input recharge grid in the model-calibration process. The int egration of this methodology into the

model calibration is a complex process that requires numerous operations prior to the execution of MODFLOW-2000. Some operations are done once; others must be repeated with each change to a recharge-related parameter. Because of the complexity of the problem, the recharge distribution cannot be calculated inside MODFLOW-2000. Therefore, UCODE_2005 was used to manage these tasks.

The methodology was developed to use precipitation as the starting point for estimating the input recharge distribution for the model and to allow recharge rates to vary during the numerical-model calibration process, where necessary. This methodology also resolves issues associated with the limitations stemming from the use of a groundwater-balance method to derive the initial distribution of recharge from precipitation.

Groundwater-balance recharge methods, such as the Maxey-Eakin method (Maxey and Eakin, 1949) and that used by SNWA (2009a) for the numerical model, only provide an estimate of the distribution of potential recharge. Potential recharge is defined as the sum of the in-place recharge and the undistributed portion of runoff recharge. In these groundwater-balance methods, the precipitation distribution and estimated annual discharge volumes are used to derive a spatial distribution of RE (SNWA, 2009a). Limitations of this method are that (1) the hydrogeology of the rocks located above the water table through which in-place recharge infiltrates is ignored; (2) as a result, the in-place and runoff recharge components are lumped; and (3) the runoff recharge component is not distributed along the runoff pathways where it infiltrates.

The methodology was developed and implemented in a preprocessing step to MODFLOW-2000 to separate the two components of potential recharge and distribute the runoff recharge along likely pathways (Figure 4-30). The following describes each step of the process:

- Step 1: The process is initiated by discretizing precipitation, RE, and potential recharge areas using the model grid and then combining the grids to obtain a grid of potential recharge.

  - The precipitation is in the form of a grid of annual mean rates.

  - The RE are specified for predefined precipitation intervals and are expressed as a fraction of the precipitation rates. The RE are also in grid form.

  - Potential recharge consists of two components: in-place recharge and recharge from runoff. For a given basin, potential recharge areas are defined as the area of the basin, excluding areas where precipitation is less than 8 in. or within an ET area. This is a masking grid where valley-bottom grid values are set to zero and all other grid values are set to 1.

  - A distribution of potential recharge is derived for the model area by multiplying the precipitation grid, the recharge efficiency grid, and the potential recharge area grid.

- Step 2: This step requires the potential recharge grid and a grid of hydrogeologic factors accounting for the type of rock receiving the precipitation. The hydrogeologic factors represent the fraction of the potential recharge that becomes in-place recharge. The remainder is runoff recharge.

```
┌─────────────────┐   ┌─────────────────┐   ┌─────────────────┐
│        A        │   │        B        │   │        C        │
│                 │   │                 │   │   Potential     │
│     PRISM       │   │    Recharge     │   │ Recharge Area   │
│ Precipitation Grid │ │ Efficiency Grid │   │      Grid       │
└────────┬────────┘   └────────┬────────┘   └────────┬────────┘
         │                     │                     │
         └──────────────┬──────▼─────────────────────┘
                        │
              ┌─────────▼───────┐   ┌─────────────────┐
              │    D=AxBxC      │   │        E        │
              │                 │   │                 │
              │   Potential     │   │ Percent In-Place │
              │  Recharge Grid  │   │  Recharge Grid  │
              └────────┬────────┘   └────────┬────────┘
                       │                     │
           ┌───────────┴──────┐    ┌─────────┴─────────┐
           │                  │    │                   │
┌──────────▼──────┐  ┌────────▼────────┐   ┌───────────▼─────┐
│      F=DxE       │  │   G=Dx(1-E)     │   │        H        │
│                  │  │  Undistributed  │   │ Runoff Recharge │
│ In-place Recharge│  │ Runoff Recharge │   │  Distribution   │
│      Grid        │  │      Grid       │   │    Network      │
└──────────┬──────┘  └────────┬────────┘   └────────┬────────┘
           │                  └──────────┬──────────┘
           │                             │
           │                   ┌─────────▼───────┐
           │                   │        I        │
           │                   │                 │
           │                   │ Runoff Recharge │
           │                   │  Distribution   │
           │                   └─────────┬───────┘
           │                             │
           └──────────────┬──────────────┘
                          │
                ┌─────────▼───────┐
                │      J=F+I       │
                │                  │
                │  CCRP Recharge   │
                │   Distribution   │
                └─────────────────┘
```
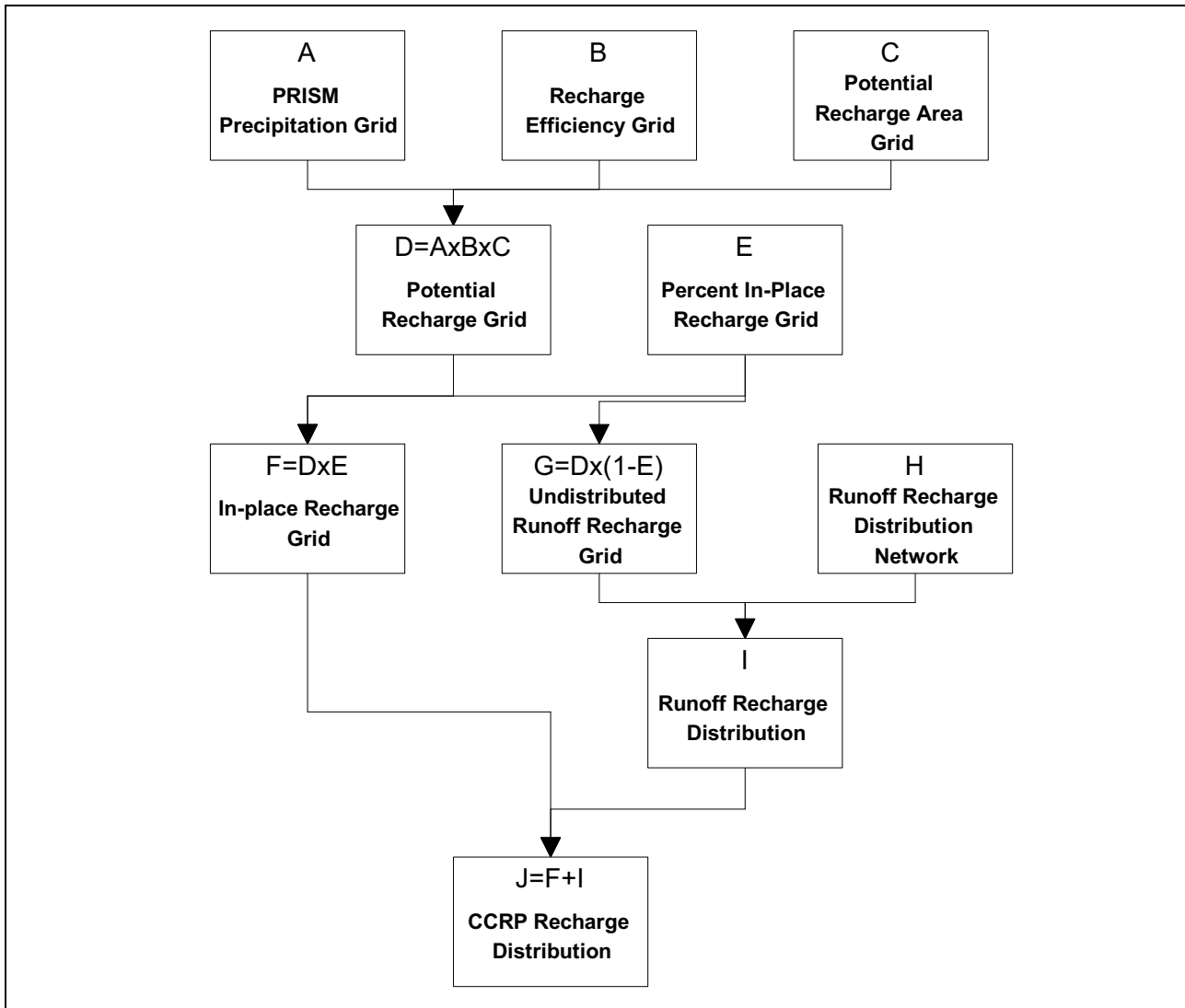
Figure 4-30
Process to Develop Recharge Distribution

- Step 3: This step requires the portion of potential recharge that constitutes runoff recharge calculated in the previous step and a grid of runoff pathways derived from watershed analysis. The volume of runoff recharge calculated for each watershed is distributed along the system of runoff pathways.

- Step 4: This step consists of adding the two grids representing the in-place recharge and the distributed runoff recharge to derive a recharge grid for MODFLOW-2000.

4.5.3   Methodology Application

The methodology described above was implemented in a preprocessing step to MODFLOW-2000 to separate the two components of potential recharge and distribute the runoff recharge along likely pathways. Specific details about the methodology steps are provided in this section.

4.5.3.1   *Potential Recharge (Step 1)*

This section describes the potential recharge distribution generated for the num erical model are a following Step 1 of the methodology outlined previously. Descriptions of the precipitation, RE, and potential recharge area grids are provided first.

The precipitation distribution used in the conc   eptual model (SNWA, 2009a) is the Parameter-elevation Regressions on I ndependent Slopes Model (PRISM) (800-m 1971 to 2000 normal, version 2) precipitation grid. This grid was resampled to the numerical model grid (i.e., the grid was converted from its 6,888,903 ft^2 [640,000 m^2] grid to the numerical model's 10,763,910 ft^2 [1-km^2] grid). These data estim ate the amount of annual precipitation for eve ry model grid cell (Figure 4-31).

As discussed in SNWA (2009a), RE were estimated for the four interpreted major flow systems in the model area (Table 4-21): the White River, Goshute Valley, Great Salt La ke Desert, and Meadow Valley flow systems. Dur ing modeling, several subregions were also divi ded out (Table 4-22). Hamlin Valley, for example, is within the Great Salt Lake Desert, but its surficial geology is similar, over most of the basin, to that of the MVFS. As a result, RE from the two flow systems were applied to the appropriate portions of Hamlin Valley (Figure 4-32). The RE were assumed to be the same as for the WRFS. As discussed in Section 3.0, to facilitate model calibration using the limited data available for the northernmost portion of the WRFS, Long Valley and a portion of Jakes Valley were reclassified as being part of the Newark Flow System. The initial RE for the Newark Flow System were assumed to be the same as for the WRFS. Several parameters were defined to vary the RE (Table 4-21). The recharge efficiency distribution for the numerical model is represented by a grid and is illustrated in Figure 4-32.

Areas of potential recharge are defined in SNWA (2009a) as a reas where most of the in-place recharge occurs and m ountain-front runoff is generated. This are a of potential rec harge is used to estimate the recharge distribution. Potential recharge is assumed to occur in all areas of a given basin except in (1) groundwater-discharge areas and (2) areas where the precipitation is less than 8 in. The valley bottom of each basin was delineated using the USGS 30-m DEM. The potential recharge areas and valley bottoms were represented in grid form by values of 1 and 0.

The distribution of potential recharge to the aqui fer system is a f unction of local pr ecipitation and recharge efficiency. Additionally, zero recharge is assumed to occur where precipitation is less than 8 in. and in ET areas. Thus, t he distribution of potential recharge in the numerical model area was calculated as the product of the three grids and is illustrated in Figure 4-33.

4.5.3.2   *In-Place Recharge and Runoff Recharge (Step 2)*

The potential recharge from precipitation for a given area is portioned into in-plac e and runoff recharge components based on the hydraulic conductivity of t he material present between the land surface and t he water table (unsaturated zone). Because the model used in this project was not designed to simulate the detailed processes of recharge, a simplification was made to partition the potential recharge using hydrogeologic factors.
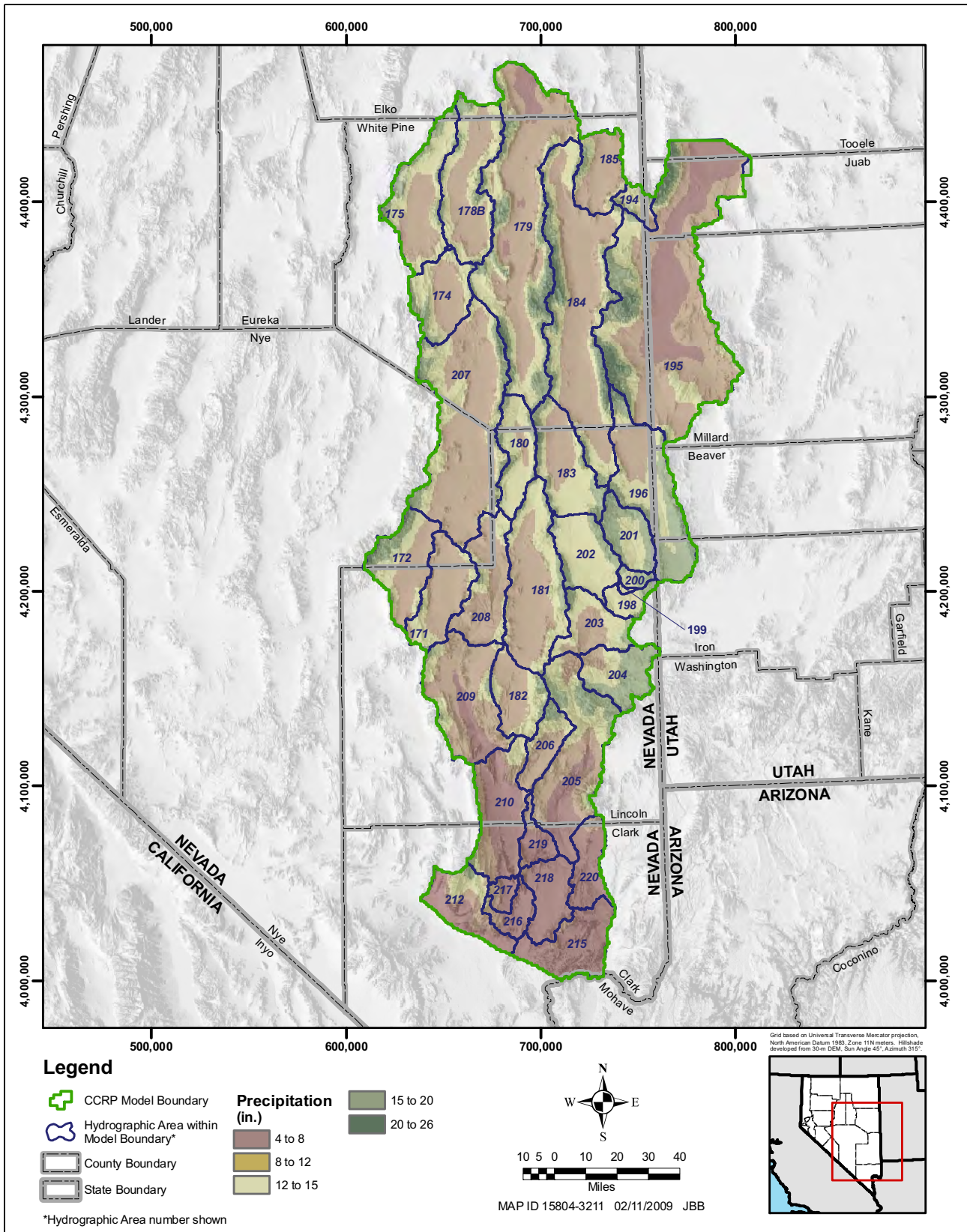
Figure 4-31
Distribution of PRISM Precipitation

SE ROA 50877

JA_16278

Table 4-21
Recharge Efficiencies as Fraction of Precipitation and
MODFLOW-2000 and UCODE_2005 Parameter Names

Precipitation Zone (in./yr)	Recharge Efficiency (fraction of precipitation)	MODFLOW-2000 Parameter Name	UCODE_2005 Parameter Name
Goshute Valley Flow System			**RSC_ME_GV**
<8	0	---	---
8 to 12	0.0141	R_ME2_GV_R	RtME2_GV_R
12 to 15	0.0530	R_ME3_GV_R	RtME3_GV_R
15 to 20	0.1266	R_ME4_GV_R	RtME4_GV_R
>20	0.3165	R_ME5_GV_R	RtME5_GV_R
Great Salt Lake Desert Flow System			**RSC_ME_GSL**
<8	0	---	---
8 to 12	0.0091	R_ME2_GSLD	RtME2_GSLD
12 to 15	0.0455	R_ME3_GSLD	RtME3_GSLD
15 to 20	0.1136	R_ME4_GSLD	RtME4_GSLD
>20	0.3059	R_ME5_GSLD	RtME5_GSLD
Las Vegas			
<8	0	---	---
8 to 12	0.0061	R_ME2_LV_R	---
12 to 15	0.0347	R_ME3_LV_R	---
15 to 20	0.1186	R_ME4_LV_R	---
>20	0.3728	R_ME5_LV_R	---
Meadow Valley Flow System			**RSC_ME_MVW**
<8	0	---	---
8 to 12	0.0006	R_ME2_MVW_	RtME2_MVW_
12 to 15	0.0108	R_ME3_MVW_	RtME3_MVW_
15 to 20	0.0625	R_ME4_MVW_	RtME4_MVW_
>20	0.2304	R_ME5_MVW_	RtME5_MVW_
Newark Flow System			
<8	0	---	---
8 to 12	0.0061	R_ME2_NE_R	RtME2_NE_R
12 to 15	0.0347	R_ME3_NE_R	RtME3_NE_R
15 to 20	0.1186	R_ME4_NE_R	RtME4_NE_R
>20	0.3728	R_ME5_NE_R	RtME5_NE_R
White River Flow System			**RSC_ME_WR**
<8	0	---	---
8 to 12	0.0061	R_ME2_WR_R	RtME2_WR_R
12 to 15	0.0347	R_ME3_WR_R	RtME3_WR_R
15 to 20	0.1186	R_ME4_WR_R	RtME4_WR_R
>20	0.3728	R_ME5_WR_R	RtME5_WR_R

Table 4-22
Recharge Efficiencies of Flow System Subregions

Precipitation Zone (in./yr)	Recharge Efficiency (fraction of precipitation)	UCODE-Derived Parameter Name
Great Salt Lake Desert Flow System (Fish Springs)		
<8	0	---
8 to 12	R_ME2_GSLD	R_ME2_GSFS
12 to 15	R_ME3_GSLD	R_ME3_GSFS
15 to 20	R_ME4_GSLD	R_ME4_GSFS
>20	R_ME5_GSLD	R_ME5_GSFS
Great Salt Lake Desert Flow System (Gandy Area Watershed)		
<8	0	---
8 to 12	R_ME2_GSLD * 1.25	R_ME2_GSGY
12 to 15	R_ME3_GSLD * 1.25	R_ME3_GSGY
15 to 20	R_ME4_GSLD * 1.25	R_ME4_GSGY
>20	R_ME5_GSLD * 1.25	R_ME5_GSGY
Great Salt Lake Desert Flow System (Garden Valley)		
<8	0	---
8 to 12	R_ME2_WR_R	R_ME2_GSGD
12 to 15	R_ME3_WR_R	R_ME3_GSGD
15 to 20	R_ME4_WR_R	R_ME4_GSGD
>20	R_ME5_WR_R	R_ME5_GSGD
Great Salt Lake Desert Flow System (Hamlin Valley - North)		
<8	0	---
8 to 12	R_ME2_GSLD * 0.50	R_ME2_GSHM
12 to 15	R_ME3_GSLD * 0.50	R_ME3_GSHM
15 to 20	R_ME4_GSLD * 0.50	R_ME4_GSHM
>20	R_ME5_GSLD * 0.50	R_ME5_GSHM
Meadow Valley Flow System (Hamlin Valley - South)		
<8	0	---
8 to 12	R_ME2_MVW_ * 0.50	R_ME2_MVHM
12 to 15	R_ME3_MVW_ * 0.50	R_ME3_MVHM
15 to 20	R_ME4_MVW_ * 0.50	R_ME4_MVHM
>20	R_ME5_MVW_ * 0.50	R_ME5_MVHM
White River Flow System (Dry Lake)		
<8	0	---
8 to 12	R_ME2_WR_R	R_ME2_WRDL
12 to 15	R_ME3_WR_R	R_ME3_WRDL
15 to 20	R_ME4_WR_R	R_ME4_WRDL
>20	R_ME5_WR_R	R_ME5_WRDL

SE ROA 50879

JA_16280
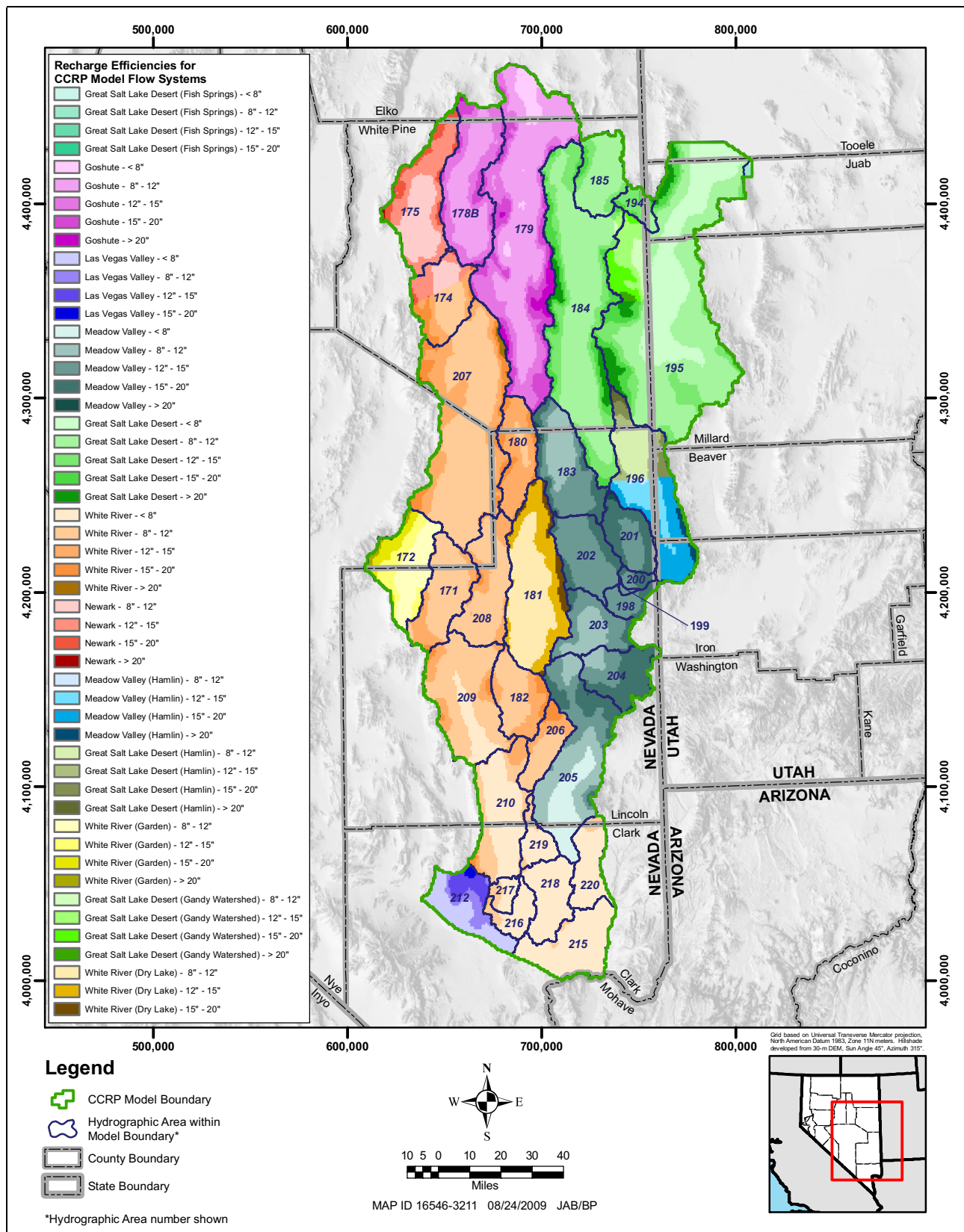
Figure 4-32
Distribution of Recharge Efficiencies
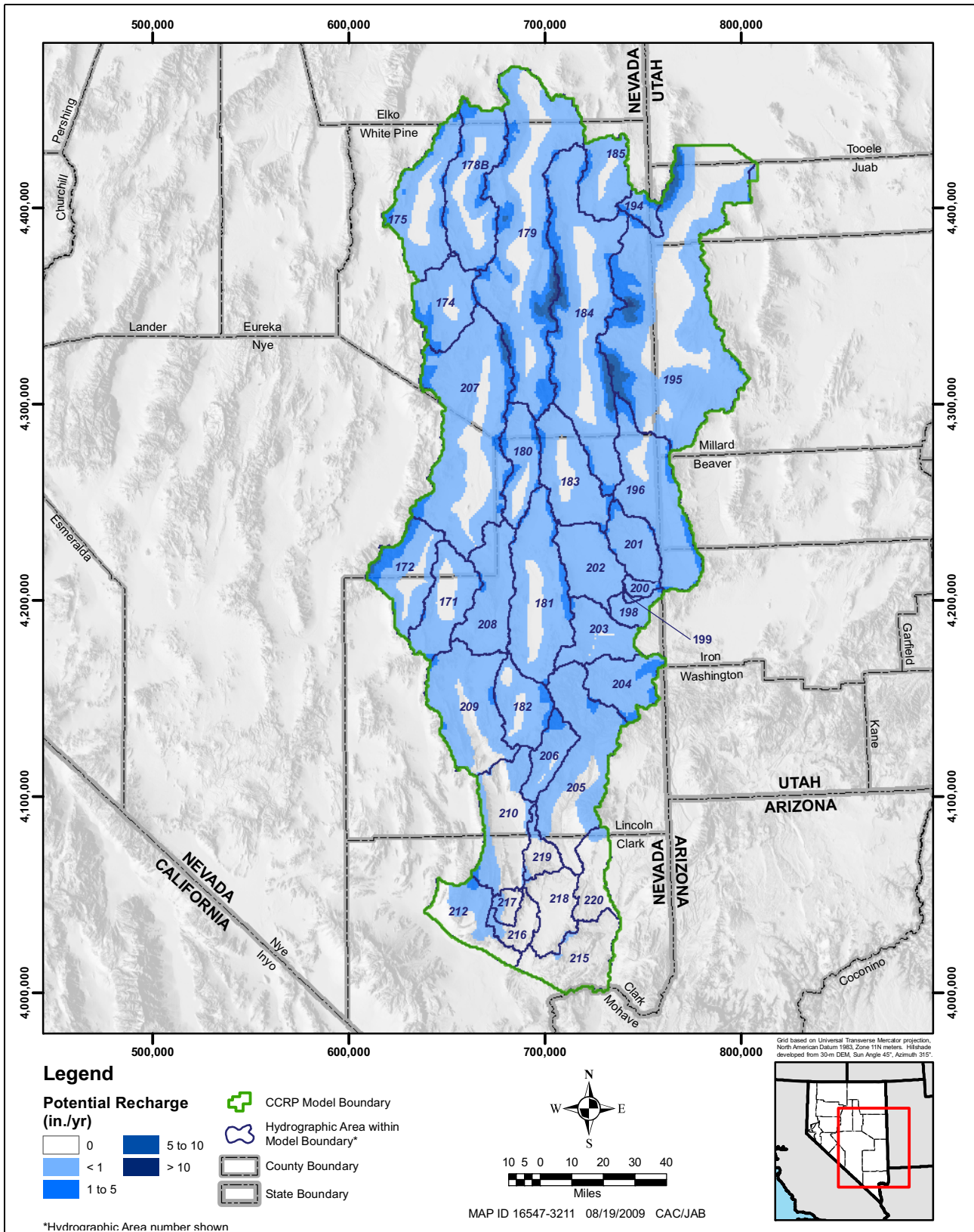
**Figure 4-33
Distribution of Potential Recharge**

SE ROA 50881

JA_16282

The hydrogeologic factor represents the portion of potential recharge that becomes in-place recharge. This factor takes into account the type of material present at and above the water table. Table 4-23 lists the hydrogeologic factors or fractions of potential recharge allowed to infiltrate in-place by RMU or group of RMUs. These factors are indicative of the hydraulic conductivity of the materials present. In high-*K* (highly-permeable) materials, 100 percent in -place infiltration is possibl e. I n low-*K* materials such as t he BASE RMU, a s little as 2 percent is assumed to infiltra te in-place, with 98 percent running off. F or example, little infiltration occurs in low-*K* plutonic or base ment rock, resulting in a small in-place–to–runoff recharge ratio and runoff of most of the potential recharge to more permeable materials along alluvial fans or valley bottoms. The hydrogeologic factors were treated as pa rameters during model ca libration. The pa rameter names a re listed in Table 4-23. Figure 4-34 illustrates the distribution of geologically controlled infiltration zones. T he amount of runoff recharge is then distributed along runoff pathways and infiltration area s discussed in the next section.

Table 4-23
Rock-Type Relationship to Runoff and In-Place
Recharge in the Calibrated Steady-State Model

Hydrogeologic Factor (In-Place Recharge as Fraction of Potential Recharge)	Rock Type Present[a]	UCODE_2005 Parameter Name
0.6	Carbonate at Water Table	R_ROCARB_W
0.3	Carbonate at Water Table, below LVF	R_ROCARB_L
1.0	Carbonate at Water Table, below UVF	R_ROCARB_U
1.0	UVF at Water Table	R_ROUVF_WT
0.35	LVF at Water Table	R_ROLVF_WT
1.0	LVF at Water Table, below UVF	R_ROLVF_UU
0.02	BASE, PLUT, UA, Kps at Water Table	R_ROLOWK_W

[a]General infiltration categories based on RMU between land surface and the estimated regional water table.

4.5.3.3 Runoff Pathways (Step 3)

To distribute the runof f recharge, it was necessary to identify t he likely runoff pathways and infiltration areas.

To accomplish this task, a watershed analysis was conducted using the USGS 30-m DEM resampled to the model grid. The purpose of the watershed analysis is to define small, local watersheds along mountain fronts. Watersheds define ar eas of runoff and catchment points, a nd distribution paths define where the runof f infiltrates into the cor responding model layer. The identified features can only be changed prior to t he execution of UCODE_2005 and MODF LOW-2000. These features cannot be programmatically adjusted during a model run (or during parameter-estimation runs).

Approximately 7,000 catchment points were defined. From these catchment points, the watersheds were delineated. Conceptually, recharge above a catchment point ca n infiltrate in-place in the cell
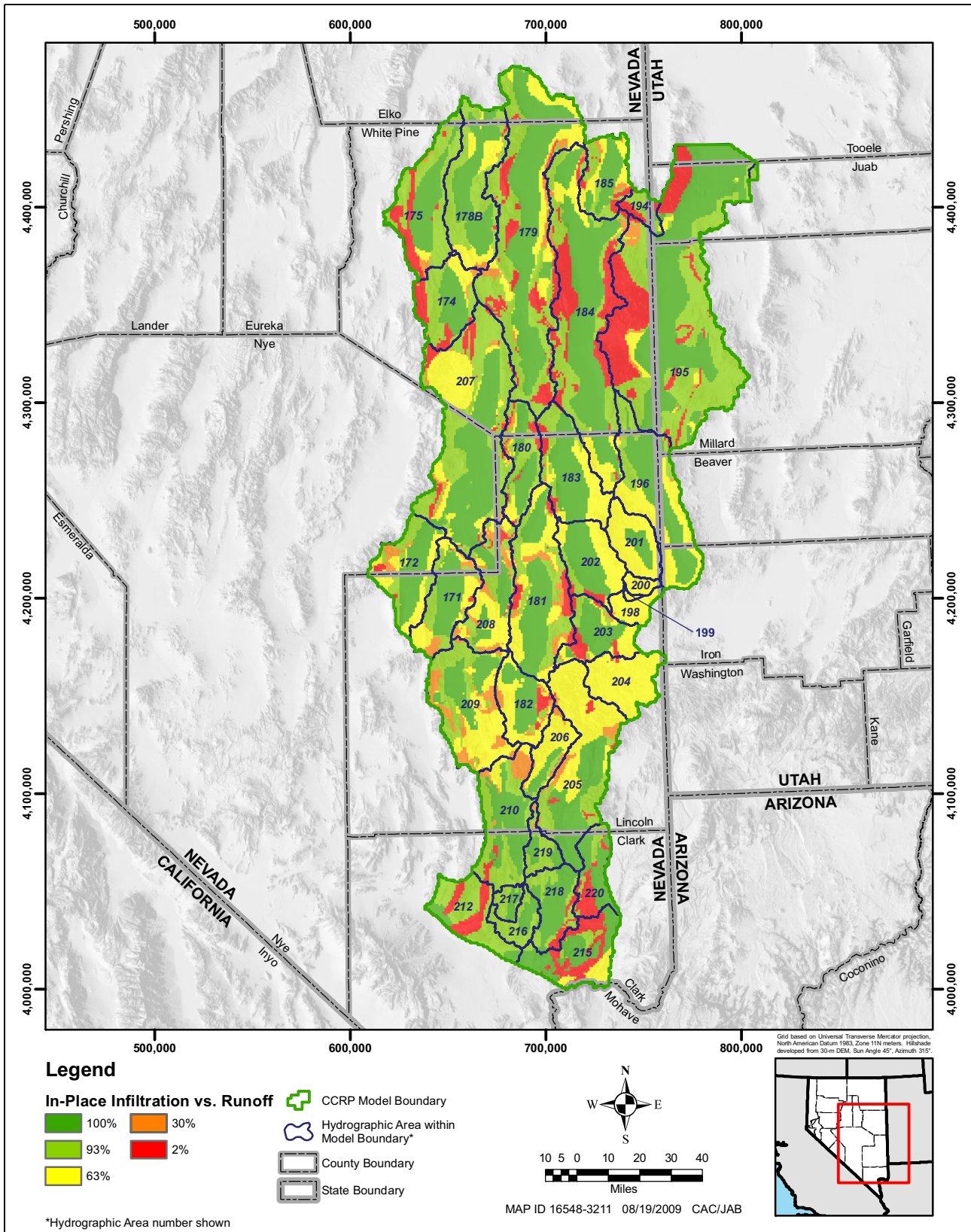
Figure 4-34
Distribution of Geologically Controlled Infiltration Zones

JA_16284

where the precipitation falls or can runoff to lower ground. Above a catchme nt point, though, no runoff water is allowed to infiltrate into another cell. In other words, all runoff in a watershed will accumulate at the catchment point.

From each catchment point, a distribution path is defined. Typically, the distribution path extends from the valley bottom where at least four cells extend into the UVF. This distribution path could be 4 cells long or as long as 40 cells. If the distribution path overlies non-UVF material, no infiltration occurs along the segment. A distribution path can contain multiple infiltration segments. Figure 4-35 shows a set of catchment points and redistribution routes in the south Snake Valley area. A linear algorithm was used to distribute the runoff volume in the catchment along the distribution path. In other words, the total runof f volume a t a c atchment point wa s equally allocated to ce lls along the distribution path. Figure 4-36 shows the redistributed runoff recharge.

4.5.3.4 Recharge Distribution (Step 4)

The recharge distribution grid us ed as the input to MODFLOW-2000 is obtained by adding the in-place recharge grid and the distributed runoff recharge grid (Figure 4-37). The grid and associated parameters are described in this section.

The total recharge in a grid cell is the sum of in-place and runof f recharge. In-place recharge is dependent on the RE and hydrogeologic factors described earlier, which are treated as UCODE_2005 parameters. Before MODFLOW-2000 is started by UCODE_2005, a new MODFLOW-2000 cell-by-cell recharge rate array (RCH) is calculated. This approach allows UCODE_2005 to estimate sensitivities and optimal values for these parameters.

Some constraints are placed on these parameters. The hydrogeologic fa ctors (in-place recharge as percent of potential recharge) were set to range between 0 and 100 percent. RE were set to increase with precipitation following a step-function. Specifically, RE for lower precipitation zones wer e required to be less than or equal to RE for higher precipitation zones.

4.5.4 Transient Recharge

Because of the lack of accurat e time-variant data, recharge was based on average annual rates, and those rates were held constant during t he entire modeling period. As a r esult, while se asonal fluctuations, drought, and wet periods were observed in some areas, such as Steptoe Valley, the model was not set up to represent those fluctuations.

4.6 Anthropogenic Stresses

Two types of anthropogenic stresses wer e applied to the numerical model: well pumping and stream diversions. The influences of Lake Mead were considered as a predevelopment condition. Predevelopment conditions were assumed to prevail before 1945. Under predevelopment conditions, while there was some groundwate r use by humans wi thin the model area, it was assumed to be minimal. Pre-1945 conditions were modeled a s steady state with no pumping and no stre am diversions. As discussed in Appendix C, groundwater was used consumptively for irrigation, mining,
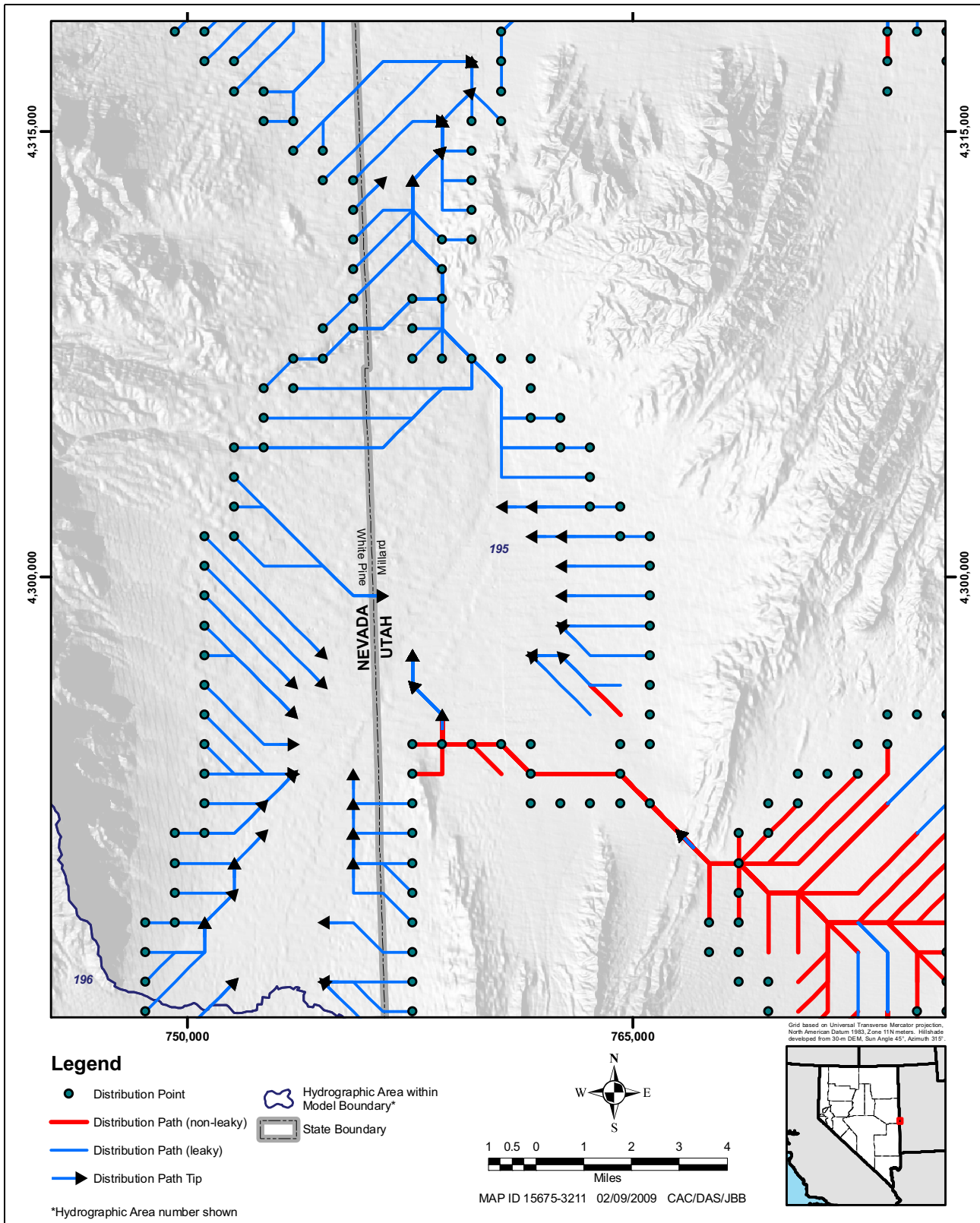
Figure 4-35
Redistributed Recharge, In-Place Recharge, and
Total Recharge in the Snake Valley and Vicinity

JA_16286
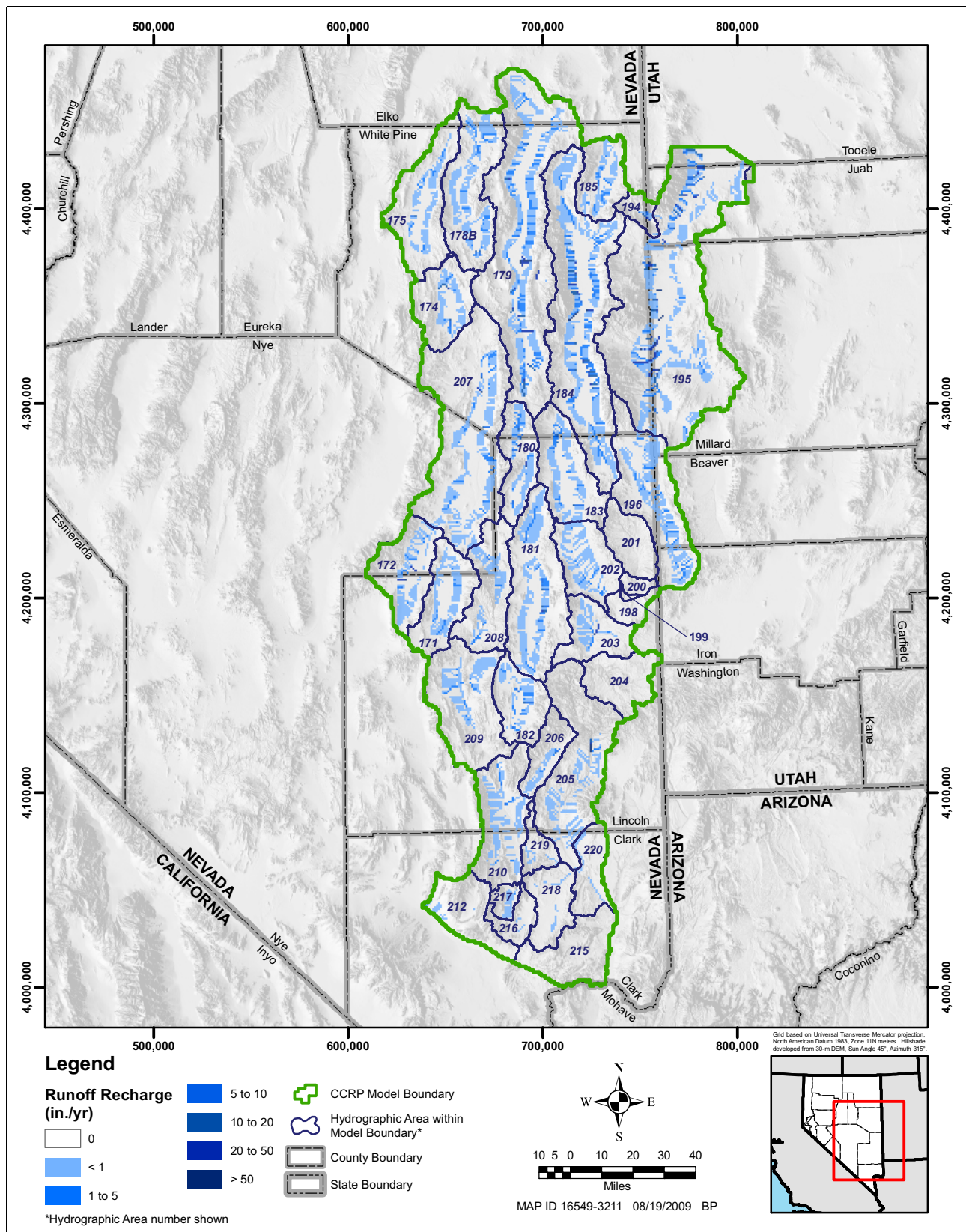
Figure 4-36
Redistributed Runoff Recharge
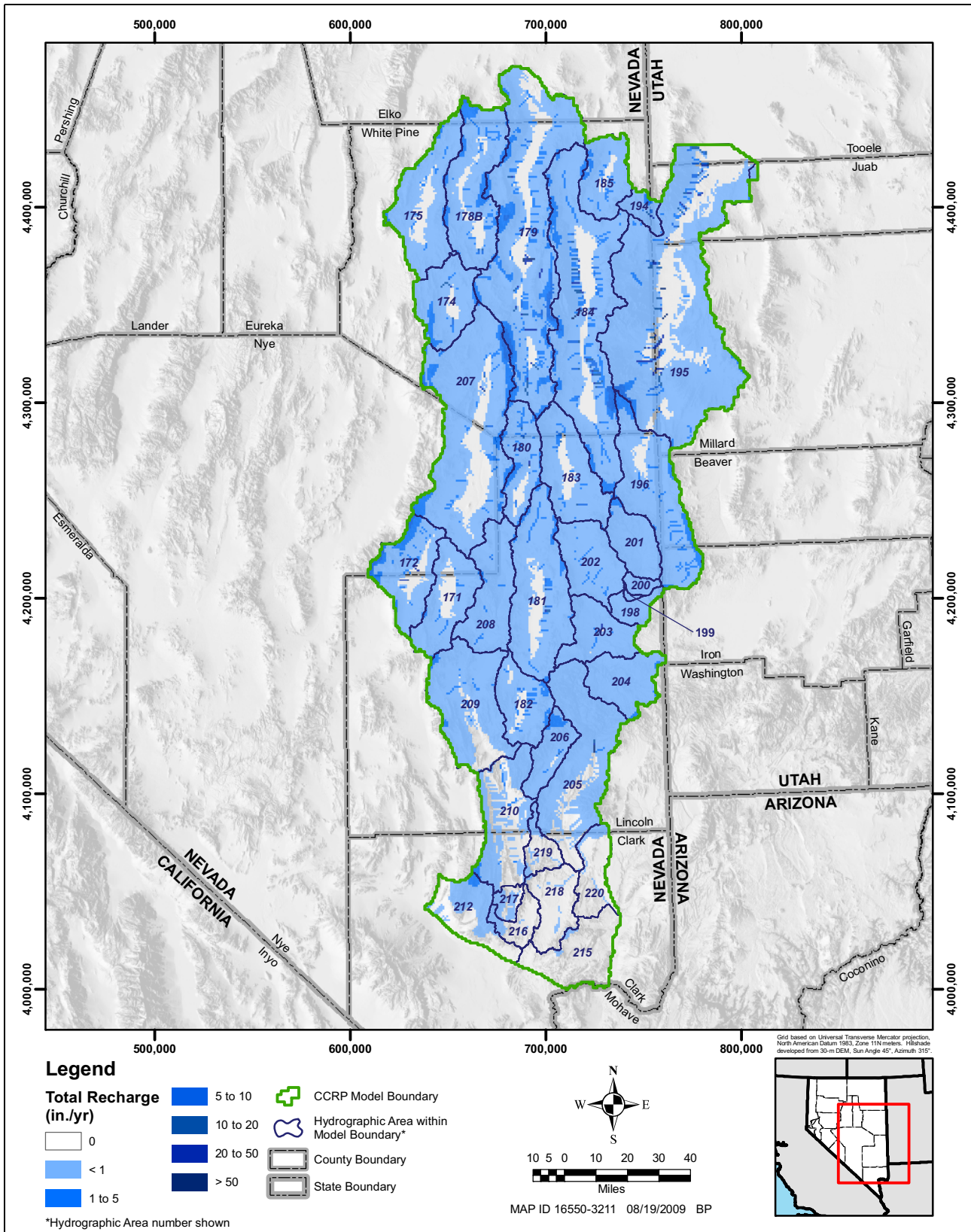
Figure 4-37
Distribution of Total Recharge (Input to MODFLOW-2000)

SE ROA 50887

JA_16288

municipal, and industrial purposes. These uses are all tied either to a point of diversion (POD) permitted by NDWR or UDWR or known well or diversion locations. The minimum stress period is one year.

4.6.1   Well Pumping

The MODFLOW Multi-Node Well (MNW) (Halford and Hanson, 2 002) module was used to simulate all pumping wells. The MNW module was used because pumping from a single well could be distributed over multiple model layers, and the MNW module would properly apportion pumping to each model layer based on the layer material properties and relative saturated thickness. The pumping rates were as defined in Appendix C and are provided in the MNW input file on the DVD. The estimation of the screened intervals and identification of perched wells are discussed below.

4.6.1.1   Estimation of Screened Intervals

For many of the wells assigned as PODs, the ground- surface elevation and the screened interval(s) were described in driller's logs. This information was required to define the model layers from which water should be extracted. For some wells, either the ground-surface elevation was missing or the screened interval information was not available. In these cases, the screened interval elevations were estimated using one of the following rules:

- Rule 1: If the well elevation was unknown, the elevation was approximated based on 98.4 ft (30 m) USGS DEM data.

- Rule 2: Where available, screen top and screen bottom were based on original driller's logs. In cases where the vertical spacing between multiple interval records was insignificant, the multiple screened intervals were merged into a single screened interval.

- Rule 3: For wells with missing screened interval information, the nearest well screened in a similar unit (UC, LC, etc.), with kn own screen-depth information was found. If a well with known screen-depth information was within 3.1 mi (5 km) and within the same hydrographic basin, screen-depth information from a nei ghboring well was used t o calculate screen elevations.

- Rule 4: For w ells not meeting rules 1, 2, or 3, the screen top was assumed to be at ground-surface elevation. The sc reen bottom was assumed to be at ground-surface elevation minus the maximum screen depth from wells within its hydrographic basin.

A saturated screen thickness was calculated as a check to ensure that the assumptions described above yielded an estimated screen interval with sufficient saturated thickness. The screen bottom elevation was subtracted from the simulated steady-state stress period water table to e stimate the saturated screen thickness. Figure 4-38 shows the distribution of saturated screen thicknesses estimated by the method described above. Figure 4-39 illustrates each POD and the rule used to estimate the screen interval information for the well.
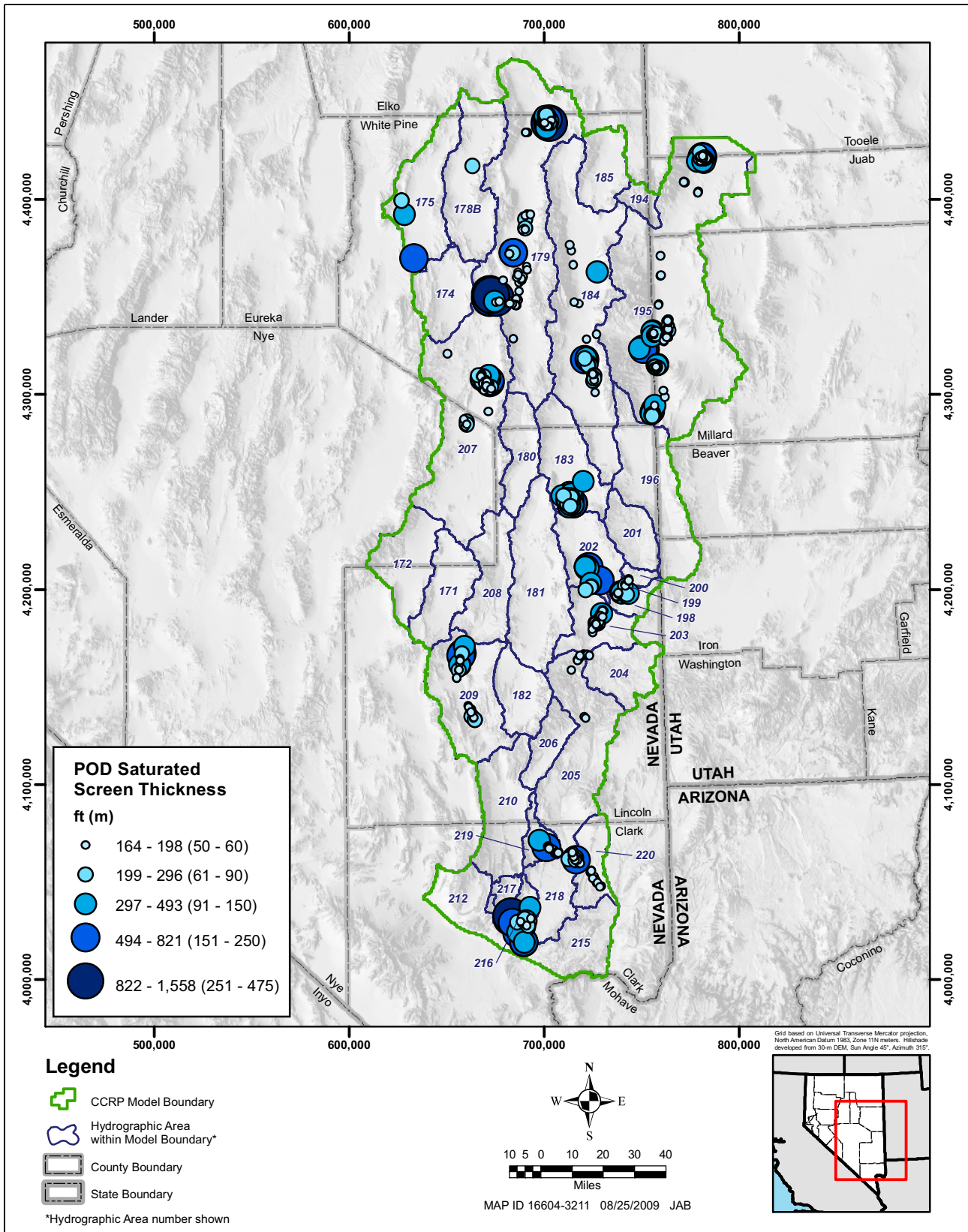
Figure 4-38
Pumping Well Saturated Screen Thickness

Section 4.0

SE ROA 50889

JA_16290
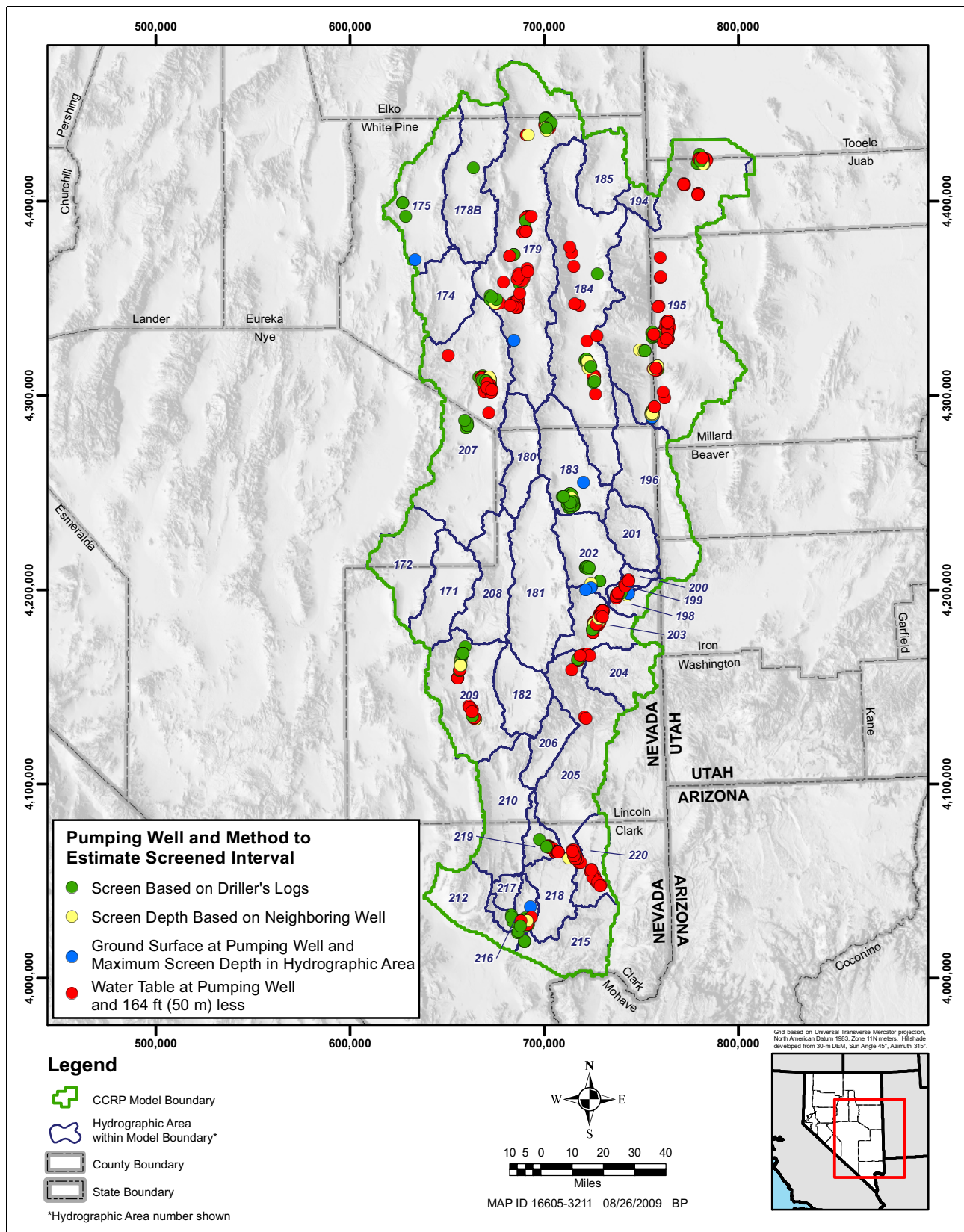
Figure 4-39
Method Used to Estimate Pumping Well Screened Interval

4.6.1.2 Perched Wells

Several pumping wells (Table 4-24) in the study a rea were not included in the numerical model. These wells were removed because they appeared to be in perched aquifer systems, typically located within unconsolidated materials not represented in the framework model.

Table 4-24
Pumping Wells Not Included in the Numerical Model

Eliminated Pumping Well	HA	Reason
WU_179_MM_1	179 (Steptoe Valley)	Groundwater diversion in Duck Creek for mine related operations.
WU194_IRR_1	194 (Pleasant Valley)	Well in perched, unconsolidated deposits not represented in model.
WU194_IRR_2		
WU204_IRR_6	204 (Clover Valley)	
WU204_IRR_8		
WU207_IRR_12	207 (White River Valley)	
WU207_IRR_16		
WU207_IRR_17		
WU207_IRR_19		

4.6.2 Stream Diversions

While there are a number of ditch and pipe diversions from springs and streams in the model area, only three stream PODs were evaluated. These were along the Muddy Ri ver near Pipeline Jones Spring, Baldwin Spring, and just upstream of the Muddy River near Moapa gage. The diverted flows were as large as 3,468.5 afy (11,713 m^3/d).

These diversions were represented in th e numerical model using the SFR2 module (Table 4-14). When water was diverted, if date available, the diversion amount was removed from the channel and removed from the model.

4.7 Observation Data

Several types of observations, including external boundary flows, hydraulic hea ds, groundwater ET, spring discharge, stream flow gages, and ground-sur face elevations, were used in the numerical model. These obser vations and their corresponding weights were used by M ODFLOW-2000 and UCODE_2005 during parameter estimation to provide values to define the objective function for the model simulation. Observation weights in MODFLOW-2000 and UCODE_2005 were derived from measures of uncertainty specified either as the variance, standard deviation, or COV. The observation data set for boundary flows, hydraulic heads, gr oundwater discharges (ET and spring flows), and stream discharges are described below.

4.7.1   Steady-State and Transient Observations

Observation wells were divided into steady-state and transient observations. Table 4-25 summarizes the observation types used for calibration statistics. External boundary flows, groundwater ET, and most small-spring observations were treated as steady-state observations. An observation was treated as a steady-state target if there was no specific time reference associated with the data, the data was pre-1945, or the estimate was specifically estimated as a predevelopment target.

Table 4-25
Observation Types Used for Calibration
and SoSWR Statistics

Observation Type	Observations	
	Steady-State	Transient
External Boundary Flux	X	---
ET Discharge	X	---
Ground-Surface Mounding	X	---
Hydraulic Heads	X	X
Spring Flows	X	X
Spring Heads	---	---
Stream Gage Flows	X	X

4.7.2   External Boundary Flow Observations

Estimates of flow across external model boundaries are presented in SNWA (2009a). These estimates represent flow-observation calibration targets for the steady-state stress period. These boundary flows are computed using the CHOB module.

At model cells assigned constant-head values, such as cells along constant-head boundaries, MODFLOW-2000 calculates the amount of flow to and from the cell required to keep the hydraulic head at that cell constant. Flow across a given face of a grid cell i s calculated as the conductance times the hydraulic-head difference. These are the conductances of the material between the center of the constant-head cell and the center of the adjacent cell within the model domain. The hydraulic-head difference is also calculated between these two points.

In the numerical model, the external boundaries represented by constant hydraulic heads were used as groundwater-flow observations. The flow rates across these boundaries were constrained within an estimated range of va lues derived by SNW A (2009a). The cell conduc tances were treated as parameters during m odel calibration. The exter nal boundary flow t argets, errors, and obs ervation names are listed in Table 4-26.

SE ROA 50892

JA_16293

Table 4-26
External Boundaries, Observation Names,
Estimated Flow Targets, and Estimated Errors

Boundary Name	Observation Name	Estimated Boundary Flow into (+) out of (-) Model Domain afy (m³/d)	Standard Deviation afy (m³/d)
Goshute Flow System			
Butte South to Butte North	B_BUTTE_001	-1,000 (-3,377)	1,750 (5,910)
Steptoe to Goshute	B_STEPTO_001	-2,000 (-6,754)	2,000 (6,754)
Great Salt Lake Desert Flow System			
Snake to Tule	B_CONFUS_001	-15,000 (-50,656)	5,000 (16,885)
Snake to Fish Springs Flat	B_FISH_001	0 (0)	1,000 (3,377)
Snake to Great Salt Lake Desert (Carbonate)	B_NSNAKE_001	-9,375 (-31,660)	7,250 (24,484)
Snake to Wah Wah	B_SNAKEE_001	0 (0)	2,500 (8,443)
Snake to Pine	B_SNAKEW_001	0 (0)	2,500 (8,443)
Tippett to Antelope Valley (South) and Deep Creek Valley	B_TIPPET_001	-3,874 (-13,083)	6,500 (21,951)
White River Flow System			
Tikaboo to Coyote Spring Valley	B_COYOTE_001	5,000 (16,886)	2,750 (9,287)
Northwest Garden to Penoyer	B_GARDEN_001	0 (0)	1,000 (3,377)
Las Vegas Valley to Three Lakes Valley South	B_LASVEG_001	0 (0)	1,497 (5,057)
Black Mountains to Lake Mead	B_LM_BM_001	0 (0)	250 (844)
North Long to Ruby	B_LONGNW_001	-2,000 (-6,754)	2,000 (6,754)
North Long to Newark	B_LONGSW_001	-12,000 (-40,525)	3,000 (10,131)
Lower Moapa to Lake Mead	B_MOAPA_001	-11,000 (-37,148)	4,250 (14,353)
Pahranagat to Tikaboo Valley South	B_PAHRAN_001	-4,000 (-13,508)	3,000 (10,131)

4.7.3   Hydraulic-Head Observations

Appendix B presents the data set of hydraulic-head observations and variances that were used in calibrating the transient model. The distribution of hydraulic-head observation wells by aquifer material is presented in Figure 4-40.

Hydraulic-head observations were treated as both steady-state and transient observations. Only wells with pre-1945 observations, though, were defined as steady-state observations. For wells with multiple hydraulic-head observations, usually only the first observation was treated as a hydraulic-head observation. Generally, any following observation was treated as a drawdown observation. This was done because for many wells, there is much less measurement uncertainty in the change in hydraulic head over time than in the actual elevation of the well or the static water surface (many wells are only located to the nearest 1/4-1/4 section). In some wells, particularly in Steptoe Valley, multiple hydraulic-head observations were assigned for all of the water-level

SE ROA 50893

JA_16294
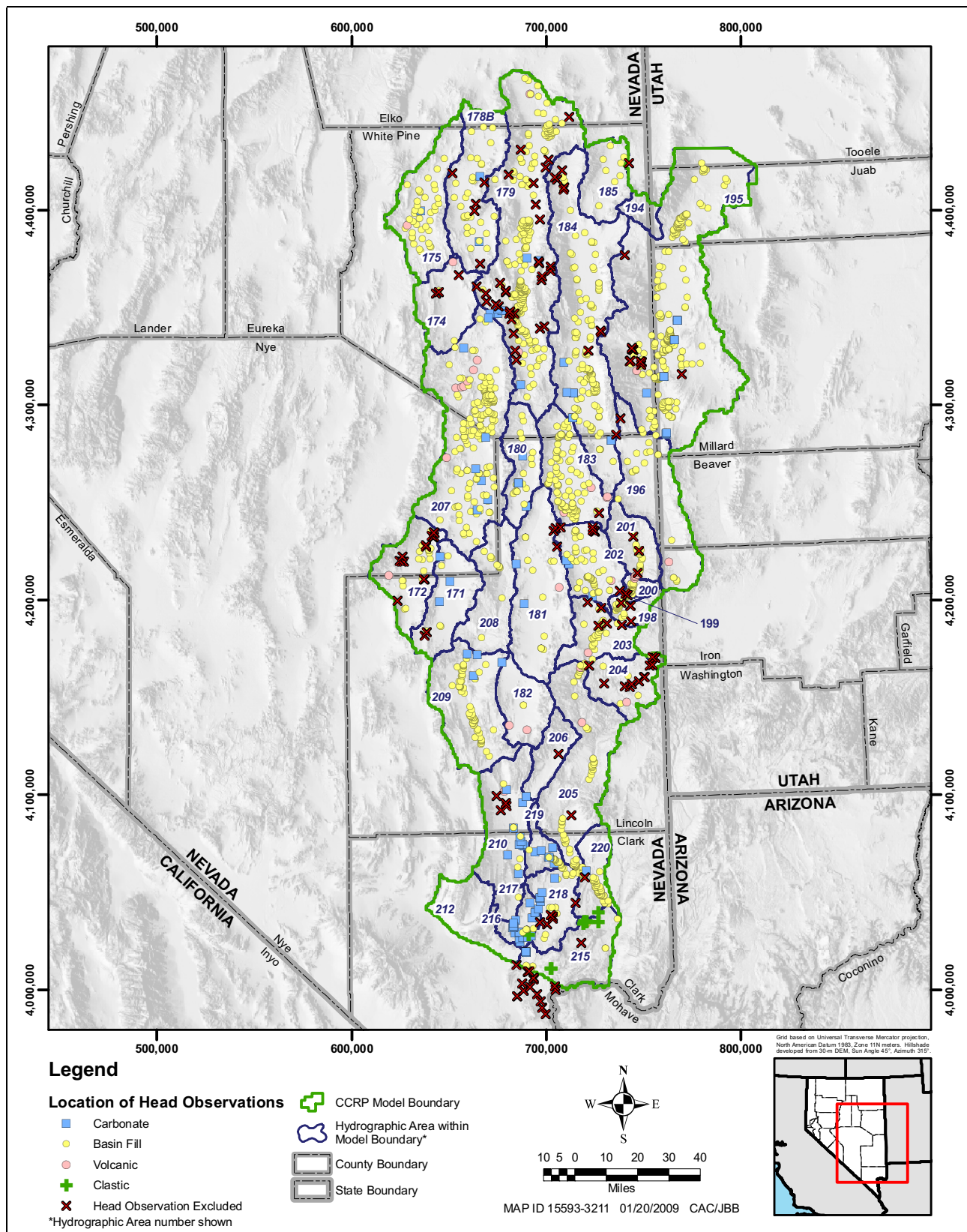
Figure 4-40
Distribution of Hydraulic-Head Observation Wells by Aquifer-Material Type

measurements at a well. This was done be cause the seasonal or longer-term climatic oscillations were more significant than the apparent drawdowns.

Appendix B provides a detailed li sting of observation locations, target hydraulic he ads, variances, rationale for variance calculations, and rationale for excluding the observation. Two variance adjustments were performed in addition to those described in Appendix B:

- Where more than one hydraulic-head observation exists in a single cell, data declustering was performed. Each observation was retained; however, the variance of each observation was multiplied by the number of observations in the cell.

- Where a hydraulic-head observation is in an ET cell, the variance was set equal to the range of 30m DEM elevation within the 1 km^2 cell.

Throughout the calibration process, the observations with large weighted residuals were scrutinized. If reasons, as described above, existed in dicating the observation was suspect, t he variance was increased or the observation was removed. Figure 4-41 illustrates the spatial distribution of declustered observations. Figure 4-42 illustrates the spatial distribution of re sulting variances assigned to hydraulic-head observations.

4.7.4 Evapotranspiration Flow Observations

SNWA (2009a) presents an uncertainty analysis of groundwater ET estimates using a Monte Carlo simulation approach. Table 4-27 lists the r esulting ET observation targets, uncertainty, and model observation names repr esented in the numerical model. The MODFLOW-2000 DRN and SFR2 packages simulate ET discharge. The DROB package was used to extract ET discharge values from the DRN package. ET from Open Water (open water represented as streams) was extracted from the SFR2 package and added to Wetland ET components in corresponding hydrographic areas.

In larger basins, ET obser vation targets were developed at a sub-basin scale. These larger basins consist of two to five sub-basins. In the calibrated model, sub-basin divisions were applied to Lower Meadow Valley Wash and S teptoe, Snake, Spring (HA 184), and White R iver valleys. These sub-basins were beneficial in the accounting of groundwater discharge by ET. Observations in the Pahranagat sub-basins were aggregated to a single value for each ET type to simplify implementation and calibration related to the SFR2 package at Pahranagat Wash. S imilarly, sub-basins 3 and 4 in Snake Valley were aggregated to simplify stream flow routing calibration at Big Springs. Sub-basin designations are presented in Table 4-27.

Thus, simulated ET rates for these ET types may be e levated. However, with the uncertainty in the ET area, type, and rate information, this simplification is reasonable. W ith the int egration of UCODE_2005, each cell's conductance could be modified to balanc e the different ET rates by coverage area. However, given the data uncertainties, this additional complexity was determined to be inappropriate for this regional-scale model.
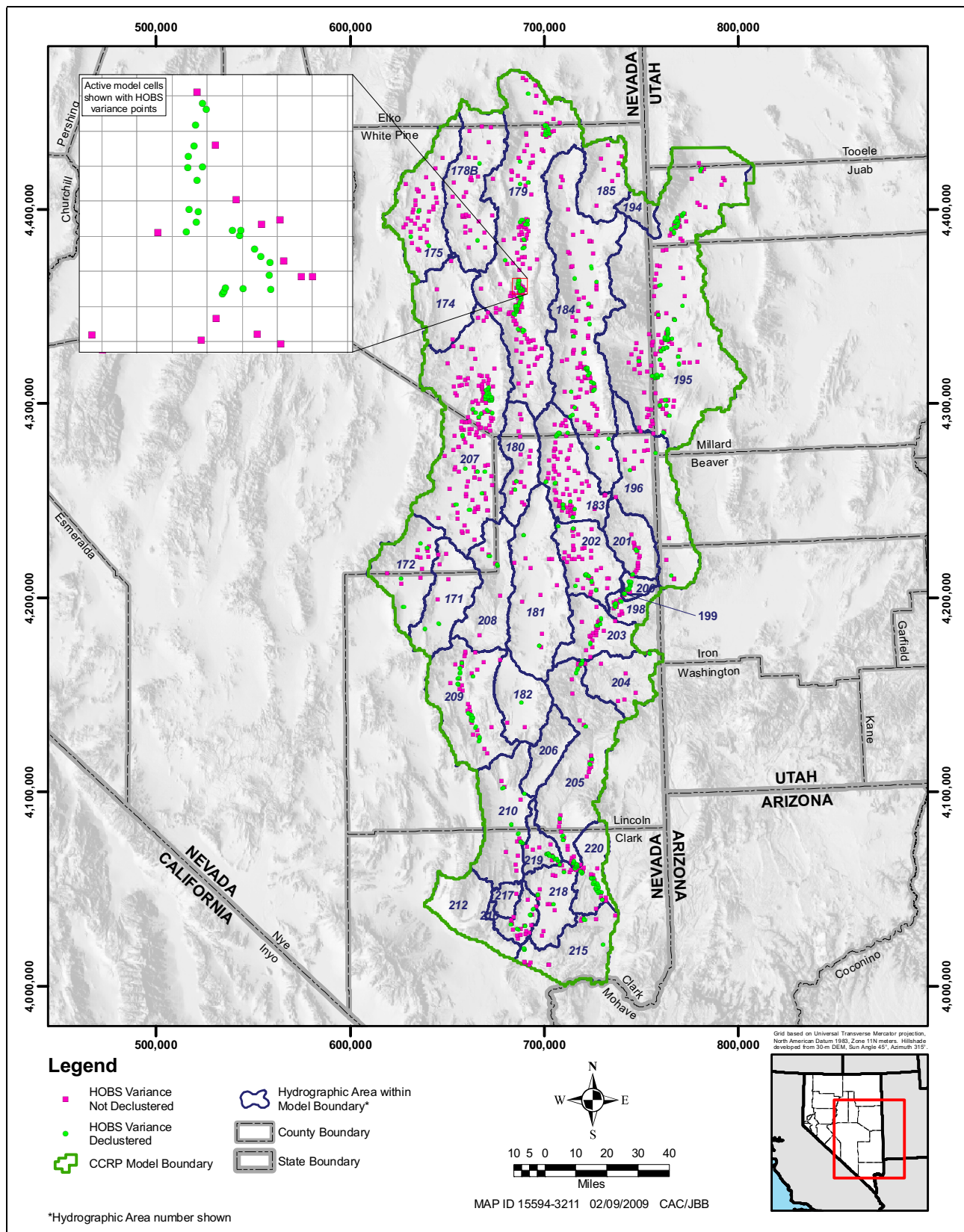
Figure 4-41
Distribution of Declustered Hydraulic-Head Observation Wells

JA_16297
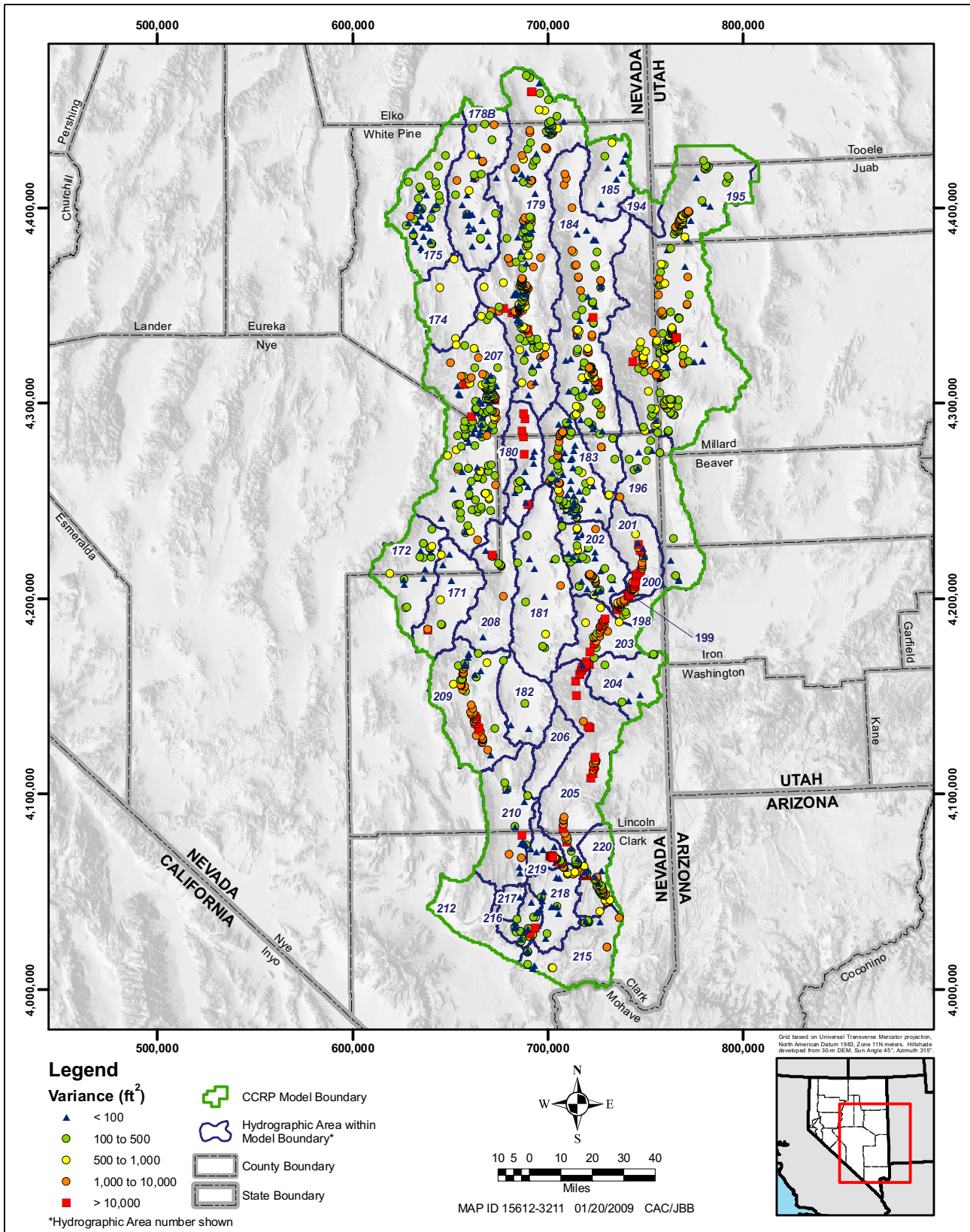
Figure 4-42
Distribution of Hydraulic-Head Observation Variances

Table 4-27
ET Observation Targets, Uncertainty, and Observation Names
(Page 1 of 3)

HA Name	HA Number	Sub-Basin	ET Observation Name[a]	Observation	Standard Deviation
				afy (m^3/d)	
Goshute Flow System					
Butte Valley (South)	178B	178B_1	ER78B_S_01	-10,185 (-34,395)	10,097 (34,099)
			ER78B_W_01	-1,559 (-5,266)	Deviation[b]
Steptoe Valley	179	179_1	ER79a_P_01	-692 (-2,338)	441 (1,490)
			ER79a_S_01	-58,115 (-196,258)	25,380 (85,711)
			ER79a_W_01	-26,521 (-89,563)	4,708 (15,899)
		179_2	EI79b_S_01	-128 (-433)	296 (1,000)
			ER79b_H_01	-1,238 (-4,182)	296 (1,000)
			ER79b_W_01	-6,743 (-22,771)	1,325 (4,475)
			ER79b_S_01	-2,815 (-9,507)	1,534 (5,181)
Meadow Valley Flow System					
Clover Valley	204	204_1	ER04_S_01	-225 (-759)	296 (1,000)
			ER04_W_01	-674 (-2,275)	296 (1,000)
Dry Valley	198	198_1	ER98_W_01	-1,394 (-4,706)	560 (1,890)
			ER98_S_01	-2,133 (-7,204)	826 (2,791)
Eagle Valley	200	200_1	ER00_S_01	-253 (-856)	296 (1,000)
			ER00_W_01	-780 (-2,635)	346 (1,170)
Lake Valley	183	183_1	ER83_S_01	-1,094 (-3,696)	1,207 (4,075)
			ER83_W_01	-4,743 (-16,018)	1,270 (4,289)
Lower Meadow Valley Wash	205	205_1	ER05a_S_01	-318 (-1,074)	296 (1,000)
			ER05a_W_01	-975 (-3,292)	757 (2,556)
		205_2	ER05b_S_01	-151 (-510)	296 (1,000)
			ER05b_W_01	-808 (-2,728)	721 (2,435)
		205_3	ER05c_S_01	-175 (-590)	296 (1,000)
			ER05c_W_01	-3,020 (-10,198)	2,194 (7,409)
		205_4	ER05d_W_01	-1,161 (-3,920)	761 (2,570)
			ER05d_S_01	-55 (-185)	296 (1,000)
		205_5	ER05e_W_01	-1,899 (-6,414)	1,228 (4,147)
			ER05e_S_01	-1,107 (3,737)	675 (2,280)
Panaca Valley	203	203_1	ER03_W_01	-11,226 (-37,912)	3,996 (13,496)
			ER03_S_01	-7,669 (-25,898)	2,627 (8,870)
Patterson Valley	202	202_1	ER02_S_01	-1,346 (-4,546)	523 (1,766)
Rose Valley	199	199_1	ER99_W_01	-441 (-1,491)	296 (1,000)
			ER99_S_01	-153 (-517)	296 (1,000)

HA Name	HA Number	Sub-Basin	ET Observation Name[a]	Observation	Standard Deviation
				afy (m³/d)	
Spring Valley	201	201_1	El01_W_01	-82 (-278)	296 (1,000)
			ER01_H_01	-266 (-900)	296 (1,000)
			ER01_S_01	-955 (-3,225)	398 (1,346)
			ER01_W_01	-2,441 (-8,245)	1,064 (3,592)
Great Salt Lake Desert Flow System					
Hamlin Valley	196	196_1	EI96_S_01	-206 (-695)	296 (1,000)
			ER96_S_01	-1,744 (-5,888)	705[c] (2,381)
Snake Valley	195	195_1	EI95a_S_01	-215 (-727)	296 (1,000)
			ER95a_P_01	-4,205 (-14,200)	4,400 (14,858)
			ER95a_W_01	-2,852 (-9,631)	419 (1,416)
			ER95a_S_01	-4,968 (-16,777)	2,343 (7,912)
		195_2	ER95b_W_01	-3,188 (-10,765)	480 (1,622)
			ER95b_S_01	-11,566 (-39,060)	3,735 (12,613)
		195_3	ER95c_P_01	-1,314 (-4,438)	884 (2,987)
			ER95c_S_01	-69,431 (-234,475)	25,638[c] (86,581)
			EI95c_S_01	-248 (-836)	296 (1,000)
			ER95c_W_01	-8,787 (-29,675)	1,526 (5,155)
			EI95c_W_01	-558 (-1,883)	296 (1,000)
			ER95d_H-01	-1,344 (-4,539)	296 (1,000)
			ER95d_S_01	-11,613 (-39,217)	4,780 (16,143)
			ER95d_W_01	-6,643 (-22,433)	1,105 (3,732)
Spring Valley	184	184_1	ER84a_S_01	-994 (-3,356)	458 (1,546)
			EI84a_S_01	-96 (-324)	296 (1,000)
			ER84a_W_01	-1,608 (-5,431)	296 (1,000)
		184_2	ER84b_P_01	-5,500 (-18,575)	2,613 (8,825)
			ER84b_S_01	-19,612 (-66,230)	8,654 (29,227)
			ER84b_W_01	-13,056 (-44,092)	2,156 (7,282)
		184_3	ER84c_S_01	-7,527 (-25,418)	3,817 (12,889)
		184_4	ER84d_S_01	-19,297 (-65,168)	10,207 (34,469)
			ER84d_W_01	-6,695 (-22,609)	1,127 (3,807)
Tippett Valley	185	185_1	ER85_S_01	-1,617 (-5,462)	1,186 (4,006)
White River Flow System					
Black Mountains Area	215	215_1	ER15_W_01	-567 (-1,915)	296 (1,000)
			ER15_S_01	-865 (-2,923)	296 (1,000)

SE ROA 50899

JA_16300

Table 4-27
ET Observation Targets, Uncertainty, and Observation Names
(Page 3 of 3)

HA Name	HA Number	Sub-Basin	ET Observation Name[a]	Observation	Standard Deviation
				afy (m³/d)	
California Wash	218	218_1	ER18_S_01	-517 (-1,746)	296 (1,000)
			ER18_W_01	-3,988 (-13,468)	1,119 (3,778)
Cave Valley	180	180_1	ER80_W_01	-1,135 (-3,831)	361 (1,218)
			ER80_S_01	-56 (-188)	296 (1,000)
			EI80_S_01	-395 (-1,334)	458 (1,548)
Garden Valley	172	172_1	ER72_S_01	-907 (-3,062)	333 (1,124)
			ER72_W_01	-226 (-764)	296 (1,000)
Long Valley	175	175_1	EI75_S_01	-71 (-240)	296 (1,000)
			ER75_S_01	-2,236 (-7,550)	2073 (7,001)
Lower Moapa Valley	220	220_1	ER20_H_01	-1,182 (-3,993)	296 (1,000)
			ER20_S_01	-3,410 (-11,515)	907 (3,065)
			ER20_W_01	-20,719 (-69,972)	5,833 (19,698)
Muddy River Springs Area	219	219_1	ER19_S_01	-795 (-2,686)	296 (1,000)
			ER19_W_01	-5,193 (-17,538)	1,477 (4,987)
Pahranagat Valley	209	209_1	ER09a_H_01	-2,693 (-9,095)	375 (1,266)[c]
			ER09a_S_01	-722 (-2,437)	296 (1,000)[c]
			ER09a_W_01	-2,268 (-7,660)	715 (2,415)[c]
			ER09b_S_01	-816 (-2,756)	296 (1,000)[c]
			ER09b_W_01	-7,885 (-26,628)	2398 (8,098)[c]
			ER09c_H_01	-3,302 (-11,151)	449 (1,517)[c]
			ER09c_W_01	-2,308 (-7,795)	691 (2,333)[c]
			ER09d_H_01	-527 (-1,780)	296 (1,000)[c]
			ER09d_S_01	-184 (-620)	296 (1,000)[c]
			ER09d_W_01	-,2492 (-8,415)	735 (2,482)[c]
			ER09e_H_01	-2,686 (-9,072)	358 (1,208)[c]
			ER09e_S_01	-321 (-1,083)	296 (1,000)[c]
			ER09e_W_01	-2063 (-6,966)	606 (2,046)[c]
White River Valley	207	207_1	EI07a_S_01	-806 (-2,721)	562 (1,898)
			EI07a_W_01	-807 (-2,726)	296 (1,000)
			ER07a_S_01	-30,749 (-103,841)	21,444 (72,419)
			ER07a_W_01	-8,914 (-30,104)	2,467 (8,331)
		207_2	ER07b_S_01	-19,455 (-65,701)	13,707 (46,290)
			ER07b_W_01	-11,528 (-38,931)	1,928 (6,511)

[a]H = water; S = shrubs; W = wet
[b]For ET less than 1,000 afy, the standard deviation was set to 296.1 afy (1,000 m³/d).
[c]Statistics calculated using coefficient of variation estimate described in the Conceptual Model Report (SNWA, 2009a).

A minimum 1,000-afy standard deviation was used, so relatively large errors for small ET discharge areas would not dominate the parameter estimation objective function or the Sum of Squared Weighted Residual (SoSWR).

4.7.5   Spring Flow Observations

Spring discharge targets were represented in the numerical model as ET observa tions and as spring discharge from a se lected set of springs.   Table 4-28 defines how the spring discha rge targets were represented in the numerical model. The two types are as follows:

- Spring flow r epresented as ET indi cates spring di scharge is aggregated with Wetland ET; spring flow was not used as an observation target.

- Spring flow represented as deep DRN cell indicates spring discharge target is aggregated with Wetland ET; spring discharge was used as an observation target. Springs represented as deep DRN cells are shown in Figure 4-25 as regional or intermediate springs.

Most of the springs in the model have limited observation data. These springs were generally represented as steady-state targets. For the springs with transient data, the model attempted to match the target flows in tim e and i gnored any estimated steady-state obs ervation target. F or transient springs with more than one annual average measurement, the first observation was a flow estimate. Subsequent observations were evaluated based on the change in f low. Note that for the springs modeled, none showed a disce rnable reduction in flow; hence, any significant change in flow simulated during model calibration was penalized by the calibration statistics. The Muddy River near Moapa gage was used to estimate flow out of the Muddy Spring Area. Representation of the Muddy River in the numerical model is discussed in Section 4.7.6.

In addition to the spring discharge targets, spring pool elevations were specified as hydr aulic-head observations to monitor head potential at ea ch spring in t he model. Specified errors for these observations were large, which effectively eliminated the observation from the objective function. In other words, pool hydraulic-head errors did not affect the model calibration or parameter-sensitivity calculations. For convenience, spring hydraulic-head observation names and targets are provided in Table 4-28. Spring observa tion names in Table 4-28 have embedded codes de fining the following spring characteristics:

- r - Hot springs and warm regional springs
- iw - Intermediate warm springs
- ib - Large intermediate springs with > 1 cfs
- is - Small intermediate springs with < 1 cfs

These spring types and name characteristics determined how springs were represented in the model. The representation of springs in the model was as follows:

- Hot spring model cells (DRN or SFR2) extend from the ground surface to the bottom of the model

Table 4-28
CCRP Spring Types and Hydraulic-Head Observation Names and Targets
(Page 1 of 2)

Spring Name	Model Type[a]	Target Type[b]	Spring Type[c]	Head Observation Name[d]	Observation ft amsl (m amsl)
Deadman Spring	CHD	---	---	---	---
North Springs	CHD	---	---	---	---
Walter Spring	CHD	---	---	---	---
Wilson Hot Spring 1	CHD	---	---	---	---
Wilson Hot Spring 2	CHD	---	---	---	---
Wilson Hot Spring 3	CHD	---	---	---	---
Wilson Hot Spring 5	CHD	---	---	---	---
(C-11-14)4bbb-S1	DRN	1	---	Sis195_11	4,298.1 (1,310.0)
Arnoldson Spring	DRN	1	---	Siw207_2	5,625.3 (1,714.5)
Blind Spring	DRN	1	---	Sis184_9	5,773.2 (1,759.6)
Blue Point Spring	DRN	2	INT	Siw215_2	1,549.9 (472.4)
Brownie Spring	DRN	1	---	Sis209_4	3,695.1 (1,126.2)
Butterfield Spring	DRN	1	---	Sib207_10	5,320.1 (1,621.5)
Caine Spring	DRN	1	---	Sis195_3	5,028.1 (1,532.5)
Cherry Creek Hot Springs	DRN	1	---	Sr179_2	6,250.6 (1,905.1)
Cold Spring	DRN	1	---	Siw207_3	5,653.2 (1,723.0)
Cold Spring	DRN	1	---	Sis195_10	4,310.2 (1,313.7)
Cold Spring	DRN	1	---	Sis179_4	5,958.0 (1,815.9)
Emigrant Springs	DRN	1	---	Sib207_15	5,480.3 (1,670.3)
Flag Springs 1	DRN	---	---	Siw207_9	5,290.3 (1,612.4)
Flag Springs 2	DRN	---	---	Siw207_8	5,280.1 (1,609.3)
Flag Springs 3	DRN	1	---	Siw207_7	5,290.3 (1,612.4)
Foote Res. Spring	DRN	1	---	Sib195_12	4,825.4 (1,470.7)
Four Wheel Drive Spring	DRN	1	---	Sis184_11	5,754.2 (1,753.8)
Hardy Spring NW	DRN	---	---	Sis207_12	5,345.4 (1,629.2)
Hardy Springs	DRN	1	---	Sis207_11	5,354.3 (1,631.9)
Hot Creek Spring	DRN	2	REG	Sr207_1	5,225.3 (1,592.6)
Keegan Spring	DRN	1	---	Sis184_12	5,617.4 (1,712.1)
Kell Spring	DRN	1	---	Sis195_13	4,910.3 (1,496.6)
Knoll Spring	DRN	1	---	Sis195_4	4,869.3 (1,484.1)
Layton Spring	DRN	1	---	Sis184_7	5,698.4 (1,736.8)
Lund Spring	DRN	2	INT	Sib207_5	5,608.2 (1,709.3)
McGill Spring	DRN	2	INT	Siw179_1	6,104.3 (1,860.5)
Minerva Spring	DRN	1	---	Sis184_13	5,825.4 (1,775.5)
Monte Neva Hot Springs	DRN	1	---	Sr179_3	6,011.4 (1,832.2)
Moon River Spring	DRN	2	REG	Sr207_14	5,223.4 (1,592.0)
Moorman Spring	DRN	2	REG	Sr207_6	5,299.1 (1,615.1)
Nicholas Spring	DRN	1	---	Siw207_13	5,635.4 (1,717.6)
North Millick Spring	DRN	1	---	Sis184_3	5,590.2 (1,703.8)

Table 4-28
CCRP Spring Types and Hydraulic-Head Observation Names and Targets
(Page 2 of 2)

Spring Name	Model Type[a]	Target Type[b]	Spring Type[c]	Head Observation Name[d]	Observation ft amsl (m amsl)
North Spring	DRN	1	---	Siw184_8	5,763.4 (1,756.6)
Osborne Springs	DRN	1	---	Sis184_10	6,127.0 (1,867.5)
Panaca Spring	DRN	2	REG	Sr203_1	4,799.0 (1,462.7)
Preston Big Spring	DRN	2	REG	Sr207_4	5,732.0 (1,747.1)
Rogers Spring	DRN	2	INT	Siw215_1	1,594.2 (485.9)
South Bastian Spring	DRN	1	---	Sis184_5	5,660.4 (1,725.2)
South Bastian Spring 2	DRN	1	---	Sis184_6	5,669.0 (1,727.9)
South Millick Spring	DRN	1	---	Sib184_4	5,592.0 (1,704.4)
Stonehouse Spring	DRN	1	---	Sis184_14	6,256.2 (1,906.8)
The Seep	DRN	1	---	Siw184_15	5,764.4 (1,756.9)
Twin Spring	DRN	1	---	Sib195_15	4,826.6 (1,471.1)
Unnamed 5 Spring	DRN	1	---	Sis184_16	5,645.3 (1,720.6)
Unnamed Spring	DRN	1	---	Sis195_14	4,853.3 (1,479.2)
Warm Creek near Gandy, UT	DRN	2	INT	Siw195_2	5,156.4 (1,571.6)
Willard Springs	DRN	1	---	Sis184_2	5,755.2 (1,754.1)
Willow Spring	DRN	1	---	Siw184_1	5,982.2 (1,823.3)
Ash Springs	SFR2	2	REG	Sr209_3	3,622.2 (1,104.0)
Baldwin Spring	SFR2	2	REG	Sr219_4	1,798.0 (548.0)
Big Springs	SFR2	2	INT	Sib195_1	5,568.2 (1,697.1)
Crystal Springs	SFR2	2	REG	Sr209_2	3,803.3 (1,159.2)
Hiko Spring	SFR2	2	REG	Sr209_1	3,875.2 (1,181.1)
Jones Spring	SFR2	2	REG	Sr219_3	1,784.2 (543.8)
M-10	SFR2	2	REG	Sr219_14	1,722.2 (524.9)
M-11	SFR2	2	REG	Sr219_6	1,800.0 (548.6)
M-12	SFR2	2	REG	Sr219_7	1,800.0 (548.6)
M-13	SFR2	2	REG	Sr219_8	1,800.0 (548.6)
M-15	SFR2	2	REG	Sr219_9	1,780.0 (542.5)
M-16	SFR2	2	REG	Sr219_10	1,780.0 (542.5)
M-19	SFR2	2	REG	Sr219_11	1,800.0 (548.6)
M-20	SFR2	2	REG	Sr219_12	1,778.0 (541.9)
Muddy Spring	SFR2	2	REG	Sr219_5	1,747.0 (532.5)
Pederson East Spring	SFR2	2	REG	Sr219_1	1,800.0 (548.6)
Pederson Spring	SFR2	2	REG	Sr219_2	1,811.0 (552.0)
Warm Springs East	SFR2	2	REG	Sr219_13	1,790.0 (545.6)

[a]DRN: MODFLOW-2000 Drain package; SFR2: MODFLOW-2000 Streamflow-Routing package; CHD: MODFLOW-2000 Constant-Head package.
[b]1: Spring flow represented as ET; 2: Spring represented as deep DRN cell. Deep spring flow aggregated with ET observation.
[c]REG: Regional flow system designation; INT: Intermediate flow system designation.
[d]Spring head observation names. Head observations used for monitoring purposes only.

SE ROA 50903

JA_16304

- Regional, intermediate warm and large intermediate spring model cells extend from the ground surface to the bottom of the deepest layer containing a carbonate RMU

- Small intermediate spring model cells are defined in the uppermost model layers.

Table 4-29 also identifies key regional and intermediate springs, represented by DRN cells, that were used as f low observation targets to provide additional constraints on the model. The MODFLOW-2000 DROB module was used to extract spring discharges from springs modeled using the DRN module.

4.7.6   Stream Discharge Flow Observations

The SFR2 package added additional flexibility to the m odel, allowing groundwater to leave the aquifer system as spring discharge but still interact with the aquifer and the ET areas. Diversions directly from the river are also supported. Four types of observations were of interest: (1) spring discharge, (2) surface water remaining at the end of the stream, (3) gaining and losing river sections, and (4) gaining and losing river sections.

The SFR2 package calibration targets, errors, and observation names are listed in Tables 4-30, 4-31, and 4-32 for Muddy R iver, Pahranagat Wash, and Big Springs stre am reaches, respectively. As discussed in Section 4.4.4.2.1, springs modeled using the SFR2 package incorporate a vertical stream segment to represent a spring. A gage is defined at the surface of the vertical reach. These gages monitor spring discharge before entering the main stream channel.

Fourteen springs in the Muddy River Springs Area were represented in the SF R2 module. The G_MR_MOAPA gage was used a s the flow observa tion for these up-gradient springs. This simplification was necessary because of the model grid size and c lose proximity of springs in t his area.

Zero flow rates were specified as targets at the end stream reaches in Lake Creek (G_LKCK_END) and Pahranagat Wash (G_PAHW_7). Target flow at the final Muddy River reach is unknown. The USGS gage at Overton, Nevada, has flowed an average of approximately 9,900 afy (33,445 m^3/d) since year 2000. Extensive irrigation in Lower Moapa Valley above the gage, however, makes this a questionable target for predevelopment conditions. The St. Thomas ga ge, located outside of the model domain near the confluence of the Muddy and Virgin rivers, operated before Lake Mead was filled. The groundwater component of the flows at the St. Thomas gage were estimated at 7,000 afy (24,000 m^3/d) assuming about half of the stre am flow in Water Years 1914-1916 were surface-water runoff. To constrain flows out of the Muddy River, a target of 7,403 afy (25,000 m^3/d) was estimated. A large error, 5,000 afy (16,885 m^3/d), was assigned to this observation (G_LK_MEAD) to account for the significant uncertainty.

Table 4-29
**Regional and Intermediate Springs Represented
by DRN Cells and Observation Targets**

Spring Name	DRN Observation Name	Date	Time	Spring Type[a]	Observation Type	Observation Target afy (m³/d)	Observation Standard Deviation afy (m³/d)
Blue Point Spring	SPiw15_2_01	12/31/1944	0:00	INT	Flow	-399 (-1,347)	60 (202)
Blue Point Spring	SDiw15_2_58	6/15/2001	6:00	INT	Flow	0 (0)	31 (104)
Blue Point Spring	SDiw15_2_59	6/15/2002	12:00	INT	Flow	0 (0)	25 (84)
Blue Point Spring	SDiw15_2_60	6/15/2003	18:00	INT	Flow	0 (0)	7 (23)
Blue Point Spring	SDiw15_2_61	6/15/2004	0:00	INT	Flow	0 (0)	11 (39)
Hot Creek Spring	SPr07_1_01	12/31/1944	0:00	REG	Flow	-10,184 (-34,392)	2,552 (8,618)
Lund Spring	SPib07_5_01	12/31/1944	0:00	INT	Flow	-5,675 (-19,165)	1,405 (4,746)
McGill Spring	SPiw79_1_01	12/31/1944	0:00	INT	Flow	-7,641 (-25,806)	1,185 (4,000)
Moon River Spring	SPr07_14_01	12/31/1944	0:00	REG	Flow	-2706 (-9,137)	927 (3,131)
Moorman Spring	SPr07_6_01	12/31/1944	0:00	REG	Flow	-843 (-2,848)	1,523 (5,144)
Panaca Spring	SPr03_1_01	12/31/1944	0:00	REG	Flow	-2,348 (-7,930)	2,707 (9,143)
Preston Big Spring	SPr07_4_01	12/31/1944	0:00	REG	Flow	-5,681 (-19,185)	852 (2,878)
Preston Big Spring	SDr07_4_41	6/14/1984	6:00	REG	Flow Change	0 (0)	349 (1,180)
Preston Big Spring	SDr07_4_58	6/15/2001	0:00	REG	Flow Change	0 (0)	129 (434)
Preston Big Spring	SDr07_4_59	6/15/2002	6:00	REG	Flow Change	0 (0)	194 (653)
Preston Big Spring	SDr07_4_60	6/15/2003	12:00	REG	Flow Change	0 (0)	231 (779)
Preston Big Spring	SDr07_4_61	6/14/2004	18:00	REG	Flow Change	0 (0)	361 (1,220)
Rogers Spring	SPiw15_1_01	12/31/1944	0:00	INT	Flow	-1,205 (-4,068)	181 (610)
Rogers Spring	SDiw15_1_44	6/15/1987	6:00	INT	Flow Change	0 (0)	137 (463)
Rogers Spring	SDiw15_1_45	6/14/1988	12:00	INT	Flow Change	0 (0)	60 (203)
Rogers Spring	SDiw15_1_46	6/14/1989	18:00	INT	Flow Change	0 (0)	115 (388)
Rogers Spring	SDiw15_1_47	6/15/1990	0:00	INT	Flow Change	0 (0)	122 (412)
Rogers Spring	SDiw15_1_48	6/15/1991	6:00	INT	Flow Change	0 (0)	68 (228)
Rogers Spring	SDiw15_1_49	6/14/1992	12:00	INT	Flow Change	0 (0)	152 (512)
Rogers Spring	SDiw15_1_50	6/14/1993	18:00	INT	Flow Change	0 (0)	170 (575)
Rogers Spring	SDiw15_1_51	6/15/1994	0:00	INT	Flow Change	0 (0)	50 (168)
Rogers Spring	SDiw15_1_52	6/15/1995	6:00	INT	Flow Change	0 (0)	85 (286)
Rogers Spring	SDiw15_1_53	6/14/1996	12:00	INT	Flow Change	0 (0)	65 (219)
Rogers Spring	SDiw15_1_54	6/14/1997	18:00	INT	Flow Change	0 (0)	94 (316)
Rogers Spring	SDiw15_1_55	6/15/1998	0:00	INT	Flow Change	0 (0)	31 (104)
Rogers Spring	SDiw15_1_56	6/15/1999	6:00	INT	Flow Change	0 (0)	55 (185)
Rogers Spring	SDiw15_1_57	6/14/2000	12:00	INT	Flow Change	0 (0)	49 (167)
Rogers Spring	SDiw15_1_58	6/14/2001	18:00	INT	Flow Change	0 (0)	44 (149)
Rogers Spring	SDiw15_1_59	6/15/2002	0:00	INT	Flow Change	0 (0)	8 (28)
Rogers Spring	SDiw15_1_60	6/15/2003	6:00	INT	Flow Change	0 (0)	22 (73)
Rogers Spring	SDiw15_1_61	6/14/2004	12:00	INT	Flow Change	0 (0)	36 (122)
Warm Creek near Gandy, UT	SPiw95_2_01	12/31/1944	0:00	INT	Flow	-12,027 (-40,616)	1,804 (6,092)

[a]REG: Regional flow system designation; INT: Intermediate flow system designation

Table 4-30
Muddy River Gages, Discharge Targets, Errors, and Observation Names
(Page 1 of 3)

Gage Name	Observation Name	Date	Observation Type	Segment	Reach	Calibration Target afy (m^3/d)	Standard Deviation afy (m^3/d)
Warm Springs West	G_WARM_SW_01	12/31/1944	Flow	2	1	NA	NA
Iverson Flume	G_IVERSON_01	12/31/1944	Flow	13	1	NA	NA
Muddy River near Moapa	GdmrMOAPA_02	6/15/1945	Flow	5	2	33,386 (112,747)	5,008 (16,912)
Muddy River near Moapa	GdmrMOAPA_03	6/15/1946	Flow	5	2	33,928 (114,577)	5,089 (17,186)
Muddy River near Moapa	GdmrMOAPA_04	6/15/1947	Flow	5	2	34,223 (115,575)	5,134 (17,336)
Muddy River near Moapa	GdmrMOAPA_05	6/15/1948	Flow	5	2	33,513 (113,176)	5,027 (16,976)
Muddy River near Moapa	GdmrMOAPA_06	6/15/1949	Flow	5	2	34,092 (115,133)	5,114 (17,270)
Muddy River near Moapa	GdmrMOAPA_07	6/15/1950	Flow	5	2	33,314 (112,506)	4,997 (16,876)
Muddy River near Moapa	GdmrMOAPA_08	6/15/1951	Flow	5	2	34,108 (115,187)	5,116 (17,278)
Muddy River near Moapa	GdmrMOAPA_09	6/15/1952	Flow	5	2	34,001 (114,825)	5,100 (17,224)
Muddy River near Moapa	GdmrMOAPA_10	6/15/1953	Flow	5	2	33,207 (112,144)	4,981 (16,822)
Muddy River near Moapa	GdmrMOAPA_11	6/15/1954	Flow	5	2	33,173 (112,030)	4,976 (16,804)
Muddy River near Moapa	GdmrMOAPA_12	6/15/1955	Flow	5	2	33,756 (113,997)	5,063 (17,100)
Muddy River near Moapa	GdmrMOAPA_13	6/15/1956	Flow	5	2	33,179 (112,050)	4,977 (16,807)
Muddy River near Moapa	GdmrMOAPA_14	6/15/1957	Flow	5	2	35,122 (118,612)	5,268 (17,792)
Muddy River near Moapa	GdmrMOAPA_15	6/15/1958	Flow	5	2	34,809 (117,553)	5,221 (17,633)
Muddy River near Moapa	GdmrMOAPA_16	6/15/1959	Flow	5	2	35,672 (120,468)	5,351 (18,070)
Muddy River near Moapa	GdmrMOAPA_17	6/15/1960	Flow	5	2	34,255 (115,683)	5,138 (17,352)
Muddy River near Moapa	GdmrMOAPA_18	6/15/1961	Flow	5	2	32,014 (108,115)	4,802 (16,217)
Muddy River near Moapa	GdmrMOAPA_19	6/15/1962	Flow	5	2	31,963 (107,941)	4,794 (16,191)
Muddy River near Moapa	GdmrMOAPA_20	6/15/1963	Flow	5	2	32,782 (110,709)	4,917 (16,606)
Muddy River near Moapa	GdmrMOAPA_21	6/15/1964	Flow	5	2	31,667 (106,942)	4,750 (16,041)
Muddy River near Moapa	GdmrMOAPA_22	6/15/1965	Flow	5	2	31,258 (105,561)	4,689 (15,834)
Muddy River near Moapa	GdmrMOAPA_23	6/15/1966	Flow	5	2	30,196 (101,976)	4,529 (15,296)
Muddy River near Moapa	GdmrMOAPA_24	6/15/1967	Flow	5	2	30,225 (102,073)	4,534 (15,311)
Muddy River near Moapa	GdmrMOAPA_25	6/15/1968	Flow	5	2	29,617 (100,018)	4,443 (15,003)
Muddy River near Moapa	GdmrMOAPA_26	6/15/1969	Flow	5	2	30,422 (102,736)	4,563 (15,410)
Muddy River near Moapa	GdmrMOAPA_27	6/15/1970	Flow	5	2	28,855 (97,444)	4,328 (14,617)
Muddy River near Moapa	GdmrMOAPA_28	6/15/1971	Flow	5	2	28,295 (95,554)	4,244 (14,333)
Muddy River near Moapa	GdmrMOAPA_29	6/15/1972	Flow	5	2	30,548 (103,162)	4,582 (15,474)
Muddy River near Moapa	GdmrMOAPA_30	6/15/1973	Flow	5	2	31,425 (106,124)	4,714 (15,919)
Muddy River near Moapa	GdmrMOAPA_31	6/15/1974	Flow	5	2	29,071 (98,175)	4,361 (14,726)
Muddy River near Moapa	GdmrMOAPA_32	6/15/1975	Flow	5	2	28,281 (95,507)	4,242 (14,326)
Muddy River near Moapa	GdmrMOAPA_33	6/15/1976	Flow	5	2	28,305 (95,588)	4,246 (14,338)
Muddy River near Moapa	GdmrMOAPA_34	6/15/1977	Flow	5	2	25,699 (86,787)	3,855 (13,018)
Muddy River near Moapa	GdmrMOAPA_35	6/15/1978	Flow	5	2	26,234 (88,593)	3,935 (13,289)
Muddy River near Moapa	GdmrMOAPA_36	6/15/1979	Flow	5	2	27,404 (92,545)	4,111 (13,882)
Muddy River near Moapa	GdmrMOAPA_37	6/15/1980	Flow	5	2	28,346 (95,729)	4,252 (14,359)
Muddy River near Moapa	GdmrMOAPA_38	6/15/1981	Flow	5	2	27,239 (91,988)	4,086 (13,798)

Gage Name	Observation Name	Date	Observation Type	Segment	Reach	Calibration Target afy (m^3/d)	Standard Deviation afy (m^3/d)
Muddy River near Moapa	GdmrMOAPA_39	6/15/1982	Flow	5	2	26,989 (91,144)	4,048 (13,672)
Muddy River near Moapa	GdmrMOAPA_40	6/15/1983	Flow	5	2	28,424 (95,990)	4,264 (14,398)
Muddy River near Moapa	GdmrMOAPA_41	6/15/1984	Flow	5	2	26,187 (88,436)	3,928 (13,265)
Muddy River near Moapa	GdmrMOAPA_42	6/15/1985	Flow	5	2	27,332 (92,303)	4,100 (13,846)
Muddy River near Moapa	GdmrMOAPA_43	6/15/1986	Flow	5	2	26,473 (89,401)	3,971 (13,410)
Muddy River near Moapa	GdmrMOAPA_44	6/15/1987	Flow	5	2	27,877 (94,143)	4,182 (14,121)
Muddy River near Moapa	GdmrMOAPA_45	6/15/1988	Flow	5	2	27,193 (91,834)	4,079 (13,775)
Muddy River near Moapa	GdmrMOAPA_46	6/15/1989	Flow	5	2	24,002 (81,056)	3,600 (12,158)
Muddy River near Moapa	GdmrMOAPA_47	6/15/1990	Flow	5	2	24,835 (83,871)	3,725 (12,581)
Muddy River near Moapa	GdmrMOAPA_48	6/15/1991	Flow	5	2	25,780 (87,062)	3,867 (13,059)
Muddy River near Moapa	GdmrMOAPA_49	6/15/1992	Flow	5	2	26,830 (90,608)	4,025 (13,591)
Muddy River near Moapa	GdmrMOAPA_50	6/15/1993	Flow	5	2	28,255 (95,420)	4,238 (14,313)
Muddy River near Moapa	GdmrMOAPA_51	6/15/1994	Flow	5	2	28,422 (95,983)	4,263 (14,397)
Muddy River near Moapa	GdmrMOAPA_52	6/15/1995	Flow	5	2	24,091 (81,358)	3,614 (12,204)
Muddy River near Moapa	GdmrMOAPA_53	6/15/1996	Flow	5	2	23,879 (80,641)	3,582 (12,096)
Muddy River near Moapa	GdmrMOAPA_54	6/15/1997	Flow	5	2	25,060 (84,629)	3,759 (12,694)
Muddy River near Moapa	GdmrMOAPA_55	6/15/1998	Flow	5	2	24,605 (83,094)	3,691 (12,464)
Muddy River near Moapa	GdmrMOAPA_56	6/15/1999	Flow	5	2	24,556 (82,926)	3,683 (12,439)
Muddy River near Moapa	GdmrMOAPA_57	6/15/2000	Flow	5	2	24,479 (82,668)	3,672 (12,400)
Muddy River near Moapa	GdmrMOAPA_58	6/15/2001	Flow	5	2	22,716 (76,713)	3,407 (11,507)
Muddy River near Moapa	GdmrMOAPA_59	6/15/2002	Flow	5	2	23,510 (79,394)	3,526 (11,909)
Muddy River near Moapa	GdmrMOAPA_60	6/15/2003	Flow	5	2	22,011 (74,333)	3,302 (11,150)
Muddy River near Moapa	GdmrMOAPA_61	6/15/2004	Flow	5	2	22,761 (76,867)	3,414 (11,530)
Muddy River near Glendale	GdmrGLEND_08	6/15/1951	Flow	8	9	32,086 (108,359)	4,813 (16,254)
Muddy River near Glendale	GdmrGLEND_09	6/15/1952	Flow	8	9	34,522 (116,584)	5,178 (17,488)
Muddy River near Glendale	GdmrGLEND_10	6/15/1953	Flow	8	9	32,378 (109,344)	4,857 (16,402)
Muddy River near Glendale	GdmrGLEND_11	6/15/1954	Flow	8	9	31,757 (107,246)	4,764 (16,087)
Muddy River near Glendale	GdmrGLEND_12	6/15/1955	Flow	8	9	34,383 (116,116)	5,157 (17,417)
Muddy River near Glendale	GdmrGLEND_13	6/15/1956	Flow	8	9	31,193 (105,342)	4,679 (15,801)
Muddy River near Glendale	GdmrGLEND_14	6/15/1957	Flow	8	9	34,818 (117,583)	5,223 (17,637)
Muddy River near Glendale	GdmrGLEND_15	6/15/1958	Flow	8	9	32,442 (109,558)	4,866 (16,434)
Muddy River near Glendale	GdmrGLEND_16	6/15/1959	Flow	8	9	32,461 (109,625)	4,869 (16,444)
Muddy River near Glendale	GdmrGLEND_17	6/15/1960	Flow	8	9	33,278 (112,382)	4,992 (16,857)
Muddy River near Glendale	GdmrGLEND_18	6/15/1961	Flow	8	9	32,854 (110,950)	4,928 (16,642)
Muddy River near Glendale	GdmrGLEND_19	6/15/1962	Flow	8	9	30,322 (102,400)	4,548 (15,360)
Muddy River near Glendale	GdmrGLEND_20	6/15/1963	Flow	8	9	28,453 (96,090)	4,268 (14,413)
Muddy River near Glendale	GdmrGLEND_21	6/15/1964	Flow	8	9	29,279 (98,879)	4,392 (14,832)
Muddy River near Glendale	GdmrGLEND_22	6/15/1965	Flow	8	9	31,302 (105,711)	4,695 (15,857)
Muddy River near Glendale	GdmrGLEND_23	6/15/1966	Flow	8	9	27,573 (93,117)	4,136 (13,968)

Table 4-30
Muddy River Gages, Discharge Targets, Errors, and Observation Names
(Page 3 of 3)

Gage Name	Observation Name	Date	Observation Type	Segment	Reach	Calibration Target afy (m^3/d)	Standard Deviation afy (m^3/d)
Muddy River near Glendale	GdmrGLEND_24	6/15/1967	Flow	8	9	29,826 (100,723)	4,474 (15,109)
Muddy River near Glendale	GdmrGLEND_25	6/15/1968	Flow	8	9	30,767 (103,904)	4,615 (15,586)
Muddy River near Glendale	GdmrGLEND_26	6/15/1969	Flow	8	9	30,927 (104,443)	4,639 (15,666)
Muddy River near Glendale	GdmrGLEND_27	6/15/1970	Flow	8	9	31,192 (105,337)	4,679 (15,801)
Muddy River near Glendale	GdmrGLEND_28	6/15/1971	Flow	8	9	29,614 (100,011)	4,442 (15,002)
Muddy River near Glendale	GdmrGLEND_29	6/15/1972	Flow	8	9	28,886 (97,552)	4,333 (14633)
Muddy River near Glendale	GdmrGLEND_30	6/15/1973	Flow	8	9	29228 (98705)	4384 (14,806)
Muddy River near Glendale	GdmrGLEND_31	6/15/1974	Flow	8	9	28,356 (95,762)	4,253 (14,364)
Muddy River near Glendale	GdmrGLEND_32	6/15/1975	Flow	8	9	27,873 (94,129)	4,181 (14,119)
Muddy River near Glendale	GdmrGLEND_33	6/15/1976	Flow	8	9	28,806 (97,279)	4,321 (14,592)
Muddy River near Glendale	GdmrGLEND_34	6/15/1977	Flow	8	9	24,872 (83,995)	3,731 (12,599)
Muddy River near Glendale	GdmrGLEND_35	6/15/1978	Flow	8	9	28,729 (97,019)	4,309 (14,553)
Muddy River near Glendale	GdmrGLEND_36	6/15/1979	Flow	8	9	26,945 (90,996)	4,042 (13,649)
Muddy River near Glendale	GdmrGLEND_37	6/15/1980	Flow	8	9	27,368 (92,425)	4,105 (13,864)
Muddy River near Glendale	GdmrGLEND_38	6/15/1981	Flow	8	9	25,642 (86,596)	3,846 (12,989)
Muddy River near Glendale	GdmrGLEND_39	6/15/1982	Flow	8	9	26,642 (89,971)	3,996 (13,496)
Muddy River near Glendale	GdmrGLEND_42	6/15/1985	Flow	8	9	25,995 (87,786)	3,899 (13,168)
Muddy River near Glendale	GdmrGLEND_43	6/15/1986	Flow	8	9	26,934 (90,958)	4,040 (13,644)
Muddy River near Glendale	GdmrGLEND_44	6/15/1987	Flow	8	9	27,098 (91,512)	4,065 (13,727)
Muddy River near Glendale	GdmrGLEND_45	6/15/1988	Flow	8	9	25,865 (87,350)	3,880 (13,103)
Muddy River near Glendale	GdmrGLEND_46	6/15/1989	Flow	8	9	21,886 (73,911)	3,283 (11,087)
Muddy River near Glendale	GdmrGLEND_47	6/15/1990	Flow	8	9	23,395 (79,006)	3,509 (11,851)
Muddy River near Glendale	GdmrGLEND_48	6/15/1991	Flow	8	9	24,855 (83,937)	3,728 (12,591)
Muddy River near Glendale	GdmrGLEND_49	6/15/1992	Flow	8	9	26,368 (89,048)	3,955 (13,357)
Muddy River near Glendale	GdmrGLEND_50	6/15/1993	Flow	8	9	28,760 (97,124)	4,314 (14,569)
Muddy River near Glendale	GdmrGLEND_51	6/15/1994	Flow	8	9	24,369 (82,296)	3,655 (12,344)
Muddy River near Glendale	GdmrGLEND_52	6/15/1995	Flow	8	9	23,192 (78,322)	3,479 (11,748)
Muddy River near Glendale	GdmrGLEND_53	6/15/1996	Flow	8	9	22,130 (74,736)	3,320 (11,210)
Muddy River near Glendale	GdmrGLEND_54	6/15/1997	Flow	8	9	23,104 (78,024)	3,466 (11,704)
Muddy River near Glendale	GdmrGLEND_55	6/15/1998	Flow	8	9	27,674 (93,456)	4,151 (14,018)
Muddy River near Glendale	GdmrGLEND_56	6/15/1999	Flow	8	9	26,061 (88,011)	3,909 (13,202)
Muddy River near Glendale	GdmrGLEND_57	6/15/2000	Flow	8	9	24,211 (81,764)	3,632 (12,265)
Muddy River near Glendale	GdmrGLEND_58	6/15/2001	Flow	8	9	23,160 (78,212)	3,474 (11,732)
Muddy River near Glendale	GdmrGLEND_59	6/15/2002	Flow	8	9	23,077 (77,933)	3,462 (11,690)
Muddy River near Glendale	GdmrGLEND_60	6/15/2003	Flow	8	9	22,781 (76,934)	3,417 (11,540)
Muddy River near Glendale	GdmrGLEND_61	6/15/2004	Flow	8	9	23,482 (79,302)	3,522 (11,895)
Muddy River at Overton	GdOVERTON_61	6/15/2004	Flow	12	1	9,903 (33,445)	5,000 (16,885)
Muddy River at Lake Mead	GdLK_MEAD_01	12/31/1944	Flow	12	9	7,403 (25,000)	5,000 (16,885)

Note: NA = Not applicable

Gage Name	Observation Name	Date	Observation Type	Segment	Reach	Calibration Target afy (m³/d)	Standard Deviation afy (m³/d)
Hiko Spring	GdHIKO_01	12/31/1944	Flow	32	8	4,170 (14,082)	643 (2,173)
Crystal Springs	GdXTL_61	6/15/2004	Flow	33	8	9,205 (31,086)	5,713 (19,293)
Pahranagat Wash at Crystal Spring	G_PW_XTL_01	12/31/1944	Flow	25	9	NA	NA
Ash Springs	GdASH_61	6/15/2004	Flow	34	8	13,027 (43,992)	1,418 (4,788)
Pahranagat Wash at Ash Spring	G_PW_ASH_01	12/31/1944	Flow	26	11	NA	NA
Pahranagat Wash #3	G_PW_3_01	12/31/1944	Flow	27	6	NA	NA
Pahranagat Wash #4	G_PW_4_01	12/31/1944	Flow	28	8	NA	NA
Pahranagat Wash #5	G_PW_5_01	12/31/1944	Flow	29	13	NA	NA
Pahranagat Wash #6	G_PW_6_01	12/31/1944	Flow	39	7	NA	NA
End of Pahranagat Wash	GdPW_7_01	12/31/1944	Flow	31	8	0 (0)	1,000 (3,377)
End of Pahranagat Wash	GdPW_7_06	6/15/1949	Flow	31	8	0 (0)	1,000 (3,377)
End of Pahranagat Wash	GdPW_7_11	6/15/1954	Flow	31	8	0 (0)	1,000 (3,377)
End of Pahranagat Wash	GdPW_7_16	6/15/1959	Flow	31	8	0 (0)	1,000 (3,377)
End of Pahranagat Wash	GdPW_7_21	6/15/1964	Flow	31	8	0 (0)	1,000 (3,377)
End of Pahranagat Wash	GdPW_7_26	6/15/1969	Flow	31	8	0 (0)	1,000 (3,377)
End of Pahranagat Wash	GdPW_7_31	6/15/1974	Flow	31	8	0 (0)	1,000 (3,377)
End of Pahranagat Wash	GdPW_7_36	6/15/1979	Flow	31	8	0 (0)	1,000 (3,377)
End of Pahranagat Wash	GdPW_7_41	6/15/1984	Flow	31	8	0 (0)	1,000 (3,377)
End of Pahranagat Wash	GdPW_7_46	6/15/1989	Flow	31	8	0 (0)	1,000 (3,377)
End of Pahranagat Wash	GdPW_7_51	6/15/1994	Flow	31	8	0 (0)	1,000 (3,377)
End of Pahranagat Wash	GdPW_7_56	6/15/1999	Flow	31	8	0 (0)	1,000 (3,377)
End of Pahranagat Wash	GdPW_7_61	6/15/2004	Flow	31	8	0 (0)	1,000 (3,377)

Note: NA = Not available

4.7.7   Ground-Surface-Elevation Observations

Large parts of the numerical model have limited hydraulic-head observations, particularly in the mountain blocks. The elevations of the ground surface were used as observations in the numerical model to provide additional constraints on the simulated hydraulic heads in these areas. The intent of these observations was to limit unrealistic groundwater mounding above the ground surface. Note that these observations were made only during the steady-state stress period. Hydraulic heads should only decline from steady-state conditions as pumping during the transient-state stress periods occur.

Table 4-32
Big Springs Gages, Discharge Targets, Errors, and Observation Names

Gage Name	Observation Name	Date	Time	Observation Type	Segment	Reach	Calibration Target afy (m³/d)	Standard Deviation afy (m³/d)
Big Springs	GdBIG_SPR_61	6/15/2004	0:00	Flow	20	1	7,431 (25,094)	411 (1,387)
Utah/Nevada State Line	G_ST_LIN_01	12/31/1944	0:00	Flow	21	1	NA	NA
Above Pruess Lake	GaLKPRUES_01	12/31/1944	0:00	Flow	22	1	NA	NA
Pruess Lake	G_LKPRUES_01	12/31/1944	0:00	Flow	23	1	NA	NA
End of Lake Creek	GdLKCK_END_01	12/31/1944	0:00	Flow	24	7	0 (0)	1,000 (3,377)
End of Lake Creek	GdLKCK_END_06	6/15/1949	6:00	Flow	24	7	0 (0)	1,000 (3,377)
End of Lake Creek	GdLKCK_END_11	6/15/1954	12:00	Flow	24	7	0 (0)	1,000 (3,377)
End of Lake Creek	GdLKCK_END_16	6/15/1959	18:00	Flow	24	7	0 (0)	1,000 (3,377)
End of Lake Creek	GdLKCK_END_21	6/15/1964	0:00	Flow	24	7	0 (0)	1,000 (3,377)
End of Lake Creek	GdLKCK_END_26	6/15/1969	6:00	Flow	24	7	0 (0)	1,000 (3,377)
End of Lake Creek	GdLKCK_END_31	6/15/1974	12:00	Flow	24	7	0 (0)	1,000 (3,377)
End of Lake Creek	GdLKCK_END_36	6/15/1979	18:00	Flow	24	7	0 (0)	1,000 (3,377)
End of Lake Creek	GdLKCK_END_41	6/15/1984	0:00	Flow	24	7	0 (0)	1,000 (3,377)
End of Lake Creek	GdLKCK_END_46	6/15/1989	6:00	Flow	24	7	0 (0)	1,000 (3,377)
End of Lake Creek	GdLKCK_END_51	6/15/1994	12:00	Flow	24	7	0 (0)	1,000 (3,377)
End of Lake Creek	GdLKCK_END_56	6/15/1999	18:00	Flow	24	7	0 (0)	1,000 (3,377)
End of Lake Creek	GdLKCK_END_61	6/15/2004	0:00	Flow	24	7	0 (0)	1,000 (3,377)

NA = Not available

It is necessary to understand that in groundwater ET areas, groundwater occurs at or near the ground surface. Thus, simulated hydraulic head is expected to be near the ground surface in discharge areas. Moreover, it is possible for a model cell on the surface to have a hydraulic head higher than the ground surface. In fact, for water to flow out of an artesian spring, the hydraulic head must be higher than the ground-surface elevation at the spring. Therefore, ground-surface observation targets were used to minimize substantial mounding above ground surface without overconstraining the model. To accomplish this goal, the maximum estimate of the ground-surface elevation within a grid cell was used as a target and was calculated as follows:

$$T = ME + 2SD \qquad \text{(Eq. 4-5)}$$

where,

T = Target not to exceed elevation
ME = Mean 30-m DEM elevation in the 247.1 acre (1 km²) grid cell
SD = Standard deviation of 30-m DEM elevations in the 247.1 acre (1 km²) grid cell

SE ROA 50910

JA_16311

The resulting ground-surface observations minimize mounding in valley bottoms but give flexibility in steep topographic ar eas. Ground-surface observations were configured in UCODE_2005 as follows:

- If the s imulated hydraulic-head was below the target ground-surface elevation, the residual was set to zero.

- If the simulated hydraulic head was above the target ground-surface elevation, the a ctual residual was calculated.

Initially, a ground-surface target was used for every model grid cell, resulting in 53,581 observations. This large number of observations significantly extended the model run time. Consequently, this number was reduced by using every twenty-fifth cell (one on every fifth row and fifth column). This reduced the number to 2,145 ground-sur face observations in the final model conf iguration, as depicted in Figure 4-43.
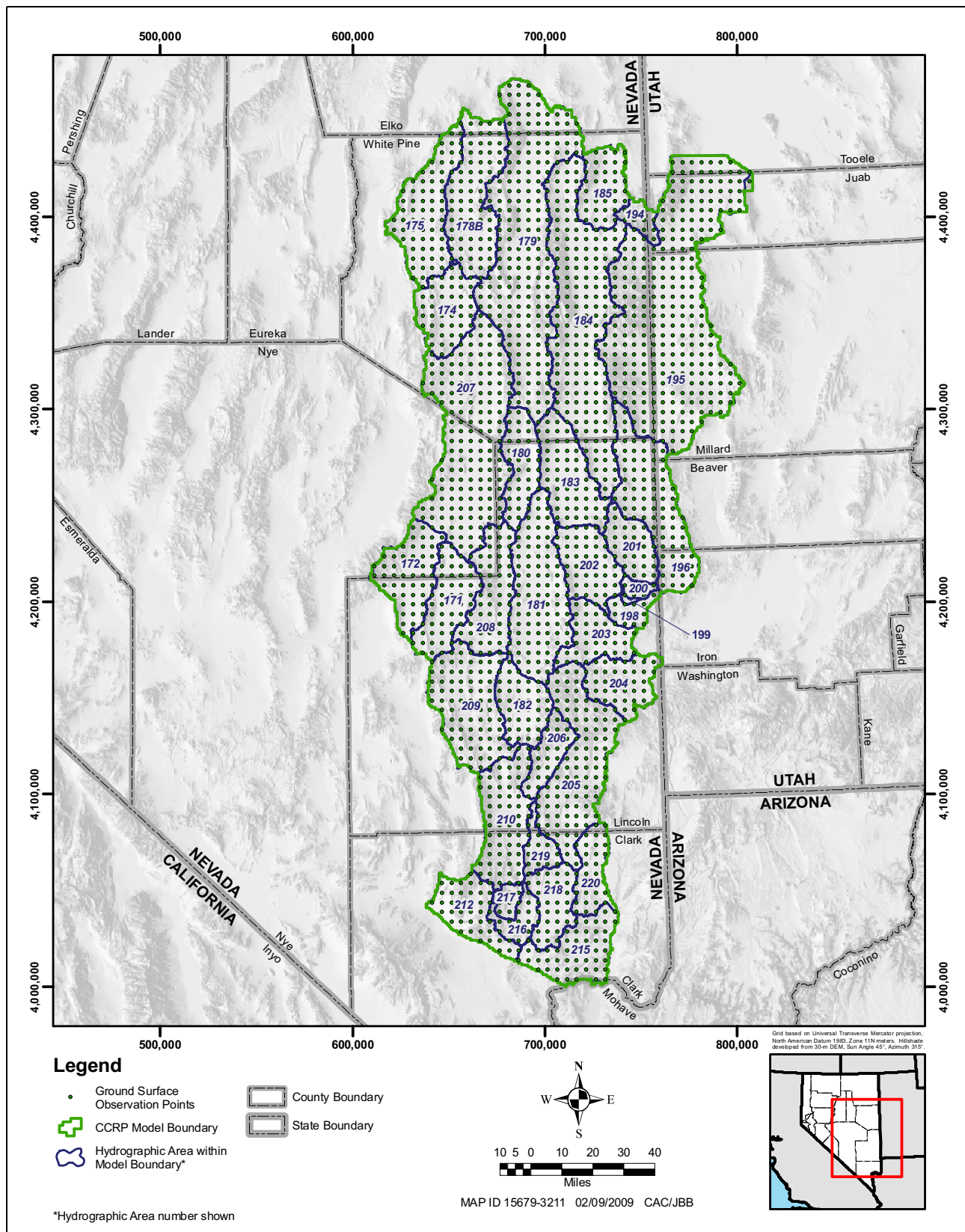
Figure 4-43
Location of Ground-Surface Observations Used to Constrain Potentiometric Surface

JA_16313

This Page Intentionally Left Blank

JA_16314

5.0 NUMERICAL MODEL CALIBRATION PROCESS AND CONCEPTUAL MODEL TESTING

The process followed to calibrate the numerical model is described in this section, followed by a presentation of calibration activities designed to test and adjust the conceptual model represented in the numerical model. These calibration activities consisted of reweighting the observations and testing and adjusting the various components of the conceptual model. Additional adjustments made to the western portion of the model domain, which coincided mostly with the WRFS as defined in the Conceptual Model Report (SNWA, 2009a), are presented separately at the end of this section. Model parameters were also refined during these calibration activities, but the final parameter-estimation simulations are discussed in Section 6.0 along with the evaluation of the calibrated numerical model.

5.1 Calibration Process

Although automated-regression techniques may constitute more efficient and accurate tools for model calibration, manual trial-and-error calibration is often necessary to develop a reasonable representation of a complex hydrogeologic system with sparse data and significant uncertainties. In fact, combining the two methods provided greater flexibility in testing the representation of various features of the flow system in the numerical model.

5.1.1 Model Calibration Guides

The parameter-estimation and testing-analysis capabilities of UCODE_2005 provided valuable insights, which were used to guide the calibration of the numerical model. Useful model-calibration guides consisted of indicators of data quality, the relative importance of each parameter in the parameter-estimation process, and indicators of calibration improvement. Particularly useful were the dimensionless sensitivities, the CSS, the SoSWR, and the weighted residuals.

- The dimensionless sensitivities quantify the influence of a single observation on a single parameter estimate. They are not only used internally by UCODE_2005 to seek a solution, but they were also used externally by the modelers to evaluate the importance of observations to the parameter estimation.

- CSS were used during calibration to decide which parameters to include and exclude from the parameter-optimization process. In general, parameters with relatively high CSS values were typically included in the estimation process, while parameters with relatively low CSS values were not. In the case of two correlated parameters (as determined from parameter-correlation coefficients), the parameter with the lower sensitivity typically was not optimized directly.

- As the SoSWR is a reflection of the f it of the simul ated values to the observed values, it represents an indicator of overall model fit. A decrease in the SoSWR was used as a general measure of improvement in model fit. Being dimensionless, the SoSWR is also useful for comparing observation errors of different types, such as flows and hydraulic heads.

- Weighted residuals, while indicative of model fit, are dimensionless and can be less intuitive compared to unweighted residuals. A weighted residual is the product of the residual and the square root of its weight. In UCODE_2005, the weight is the inverse of the va riance. Considering that the variance is the square of the standa rd deviation, the we ighted residual may be calculated as the ratio of the unweighted value to the standard deviation. Therefore, if the unweighted residual is twice as large as the standard deviation, the value of the weighted residual is 2.0 (Hill , 1998; Hill and Tiedeman, 2007). Decr easing weighted residuals of individual observations indicate a better match to weighted observations and therefore an improvement of model fit to those observations.

- Another indicator of model-c alibration improvement is more realistic calibrated parameter values (Hill, 1998; Hill and Tiedeman, 2007).

5.1.2   Conceptual Model Testing and Adjustment Process

The representation of the conce ptual model in the numerical model was iteratively refined using a combination of trial and error and the parameter-estimation methods of UCODE_2005.

An iteration generally consisted of (1) modify ing a given component of the c onceptual model representation (observation weight or model construc tion element), (2) adjusting the component by trial and error (UCODE_2005 run with si ngle MODFLOW-2000 simulation), and (3) per forming a UCODE_2005 optimization run (UCODE_2005 run with multiple MODFLOW-2000 simulations), when the results of the trial-and-error simulations were judged reasonable.

The results of the UCODE_2005 testing analyses we re used throughout the proc ess to evaluate the state of the calibration and to make decisions about subsequent adjustments. These results were used to reevaluate observation weights and to make changes to the model construction, both regionally and locally, by adjusting defined parameters or modifying aspects of model construction.

5.1.3   Final Parameter Estimation

During the model simulations described in this se ction, the conce ptual model representation in the numerical model was refined to yield a better fit of the model to the observations. At the same time, parameter estimates were improved but were not considered to all be final calibrated values. At the end of the calibration process, attempts were made to refine these estimates using the optimization capabilities of UCODE_2005. The details of these activities are provided in Section 6.1.

SE ROA 50915

JA_16316

5.2   Observation Data Review and Reweighting

Weighted residuals simplify the evaluation of overall model fit by lumping observed data of different types into a single observation data set. The weights were initially assigned based on the uncertainty associated with each of the observations. During the model-calibration process, hydraulic-head and drawdown, spring flow, stream flow, and groundwater-flow observations and corresponding weights were evaluated to determine if they appropriately constrained the flow model.

The DVD included with this report provides a detailed listing of observation locations, target heads, variances, rationale of varia   nce calculations, and rationale for   excluding the obs ervation. Section 4.7.3 introduces variance adjustments performed in addition to t hose reported on the D VD. As described in Section 4.0, several types of observations were used in the numerical model and these are listed again in Table 5-1. During calibration of t he numerical model, observa tions were given equal consideration, regardless of type. In other words, a well observation with a COV of 10 percent carried equal weight as a spring flow observation or an ET observation with a C OV of 10 perc ent. This approach gave hydraulic-head observations more overall importance in the model calibration because of the significant number of hydraulic-head observations (see Table 5-1). A large number of ground-surface observations were also used. However, ground-surface observations have small individual weights.

Table 5-1
Number of Calibration Observations by Type

Observation Type	Count	Comment
Hydraulic-Head Observations	2,707	---
Hydraulic-Drawdown Observations	4,301	---
Spring Hydraulic-Head Observations	0	---
Groundwater ET Discharge	126	Includes spring flows.
Steady-State Spring Flows	44	---
Transient Spring Flow Change	27	---
CHD Boundary Flow	16	---
Interbasin Flow	0	---
SFR2 Spring/Stream Gage	144	---
Ground Surface	2,145	Selected where surface ponding occurred but fell between the regular ground-surface observations. Mounding could occur between the 5 x 5 cell ground-surface-observation grid locations. These targeted specific problem locations.
Total	**9,510**	

The bias toward hydraulic-head observations was apparent during parameter-estimation simulations. For example, an optimization simulation would converge (TOLPAR = 0.01). However, flow errors from the major springs in Pahranagat Valley and Muddy River exceeded one st andard deviation. While the total SoS WR was reduced, the model fit at these key features was unacceptable. A s a result, the standard deviation of key spring and gage observations was adjusted (Table 5-2) by a factor of 10, increasing the influence of these observations.

Table 5-2
Selected Observations and Revised Standard Deviations

| Observation | Standard Deviation | | Rationale for Revising Observation Weight |
	Original afy (m^3/d)	Deviation afy (m^3/d)	
GdBIG_SPR_61	---	---	Intermediate spring (Big Springs; 2004)
GdLKCK_END_##	1,000 (3,377)	100 (337.7)	End of Big Springs Creek/Lake Creek. Channel should be dry.
GdASH_61	---	---	Regional spring (Ash Springs; 2004)
GdHIKO_01	---	---	Regional spring (Hiko Spring; 1944)
GdXTL_61	---	---	Regional spring (Crystal Springs; 2004)
GdPW_7_##	1,000 (3,377)	100 (337.7)	End of Pahranagat Wash. Channel should be dry.
GdmrGLEND_08	4,813 (16,254)	481 (1,625.4)	Muddy River near Glendale gage measurement (1951)
GdmrGLEND_##	various	various/10	Muddy River near Glendale gage measurement (1952 to 2004)
GdmrMOAPA_02	5,008 (16,912)	501 (1,691.2)	Muddy River near Moapa gage measurement (1945).
GdmrMOAPA_##	various	various/10	Muddy River near Moapa gage measurement (1946 to 2004)
GdOVERTON_61	5,000 (16,885)	500 (1,688.5)	Muddy River at Overton (2004)
GdLK_MEAD_01	5,000 (16,885)	500 (1,688.5)	Muddy River at Lake Mead shore (1944)

refers to stress-period identifier.

5.3   Conceptual Model Testing and Adjustment

As described in Section 3.0 and Section 4.0, variations of four major components of the conceptual model were evaluated to test additional features of the flow system. These variations were refinements to the simplified conceptual model. Conceptual model variations were considered for (1) hydrogeologic framework, (2) external flow boundaries, (3) definition of recharge processes, and (4) definition of discharge areas. For each change in the conceptual model, sensitivities were calculated, and parameter values were estimated. In general, conceptual model changes contributing to significant improvement in model fit, as indicated by a reduction in the SoSWR, were retained in the final calibrated model. Variations in hydrogeologic framework interpretation contribute most to improving the numerical model fit.

5.3.1   Variations in the Hydrogeologic Framework

The simplified hydrogeologic framework developed for the conceptual model (SNWA, 2009a) lacks sufficient detail to represent certain characteristics of the flow systems. Some of these detailed characteristics were obtained from SNWA (2008) or from the literature and were tested in the model but only as allowed by the size of the model grid cells. Many of the hydrogeologic framework complexities are much smaller than the size of the grid cells and cannot be represented in the model. Tested aspects consist of the spatial variations in RMUs and the representation of partial barriers to flow in the numerical model.

JA_16318

5.3.1.1 Spatial Variations in RMUs

More details were added to the representation of the RMUs in the numerical model both at the scale of the hydrographic areas and at the local scale.

At the scale of the hydrographic areas, zones wer e identified based on na tural characteristics or important processes at that scale. Zones were defined based on (1) lithologic variation, (2) regional faulting, (3) thermal alteration, and (4) regional tectonism. In some cases, the final number of zones was arrived at by evaluating dif ferent numbers of zones through multiple model sim ulations. Multiplication factors on the original zone parameters were typically used to adjust zone pr operties. The final zonation was described in Section 4.0. Parameters derived by UCODE_2005 define zones with similar properties into a smaller set of model parameters.

The resolution of the numerical model grid inhibits accurate representation of geometries. In some cases, the lack of de tail limits the ability to represent important local- or inte rmediate-scale hydrogeologic features that result in springs or ET zones.

5.3.1.1.1 Warm Springs near Gandy, Utah

At Warm Springs near Gandy, Utah (Figure 4-25), the simpli fied hydrogeologic framework model lacks sufficient detail to repre sent the in terpreted geologic structure controlling spring flow. The target flow is 12,027 afy (40,616 m^3/d), but simulating flows larger than 4,341 afy (14,662 m^3/d) has proved elusive. To improve the representation of this spring and incre ase flow, the following steps have been implemented or tested:

- In SNWA (2008), a carbonate feature is described as exte nding through the Qua ternary-Tertiary alluvium (QTa) in the UVF. This feature is not re presented in the regional hydrogeologic framework (SNWA, 2009a). An LC zone was added into the UVF R MU to incorporate this feature into the model and better approximate the interpreted hydrogeologic setting. Spring flows increased slightly (100 to 800 afy) with this change. This adjustment was kept in the numerical model.

- Mankinen and McKee (2009) identified a gravity anomaly area in the C onfusion Range. Decreasing *K* in this area increases hydraulic heads along the east side of Snake Valley. This adjustment increased flow at Warm Springs (hundreds of afy). This adjustment was kept in the numerical model.

- Two large watersheds are west of Warm Springs. Runoff from these areas have the potential to deliver significant volumes of wate r to the Warm Springs Are a. Adjust ments to runoff pathways (see Section 4.5.3.3) were made to test the ef fects on spring flow. First the runoff was arranged to occur near the spring or up-gradient of faults represented by HFBs. The result was increased hydraulic heads yielding approximately 1,000 afy (2,961 m^3/d) of additional flow. Sec ond, the r unoff pathway was adjusted to plac e all runoff at the DRN spring cells. This test yielded only 2,961 afy (10,000 m^3/d) flow at Warm Springs (up from about 1,000 afy). The first runoff pathway test was kept in the numerical model.

SE ROA 50918

JA_16319

- Numerous normal faults are mapped in the area. Some are represented in the framework model. Additional HFBs were added in an attempt to direct flow toward the spring. Slight increases in flow at Warm Springs were achieved. This adjustment was kept in the numerical model.

- The K of the BASE RMU between northern Spring Valley and Snake Valley was increased. This also had the advantage of moving some excess water out of Spring Valley. While this did increase flows somewhat at Warm Springs, the total flow from Spring Valley to Snake Valley was not considered reasonable, and the K of the BASE RMU was returned to its starting value.

- Recharge efficiencies were increased by 25 percent over the initial GSLDFS efficiencies along the east side of the Snake Range in Snake Valley. This adjustment yielded 4,341 afy (14,662 m^3/day). This adjustment was kept in the numerical model.

While flow at Warm Springs is 36 percent of the target, total discharge in Snake Valley is within 4 percent (Figure 6-18). Thus, discharges to ET zones on the basin floor account for the deficit of spring flows.

5.3.1.1.2   Patterson Valley to Panaca Valley

Southern Patterson Valley and Panaca Valley had opposite problems, more or less, through most of the model development. In southern Patterson Valley, the simulated water table was more than 82 ft (25 m) above ground surface, while Panaca Spring flows were undersimulated at 296 afy (1,000 m^3/day), and the target was 2,348 afy (7,930 m^3/day). The framework model, however, provided no means to move the excess water from Patterson Valley to Panaca Spring. Zonation testing in the area was ineffective. Review of faulting mapped in the area (SNWA, 2008) indicates northwest-southwest trending faults, which could provide preferential flow through the mountain block separating these valleys. A fault zone was added to the BASE, LC, and LVF RMUs to test the possible connection from Patterson Valley to Panaca Spring. The result was decreased hydraulic heads in southern Patterson Valley and increased flow at Panaca Spring. This adjustment to the framework was kept in the numerical model.

5.3.1.1.3   Upper Meadow Valley Wash

The transient calibration process revealed shortcomings of the hydrogeologic framework in northern Panaca Valley and the northern part of Meadow Valley Wash. For example, irrigation pumping from surficial materials in these areas resulted in drawdowns of 1,640 ft (500 m). Expected drawdowns are generally less than 5 m.

Comparison of the hydrogeologic framework model to the geologic maps indicates that oversimulated drawdown occurs in areas where the framework model has been oversimplified. Specifically, unconsolidated deposits (UVF) are not represented in these areas. As a result, pumping was simulated from the less permeable LVF. Zones (for K and S) along Meadow Valley Wash were applied to these areas in the LVF and LC. Simulated drawdowns decreased to approximately 262 ft

(80 m). The faulting applied to the mountain block between Patterson Valley and Panaca Spring (described above) also reduced oversimulated drawdowns.

Significant improvements were achieved by the adjustments described above; however, drawdowns in two observation wells remained significantly oversimulated. Errors from these wells (Z03_4_## and Z03_6_##) accounted for over 40 percent of the objective function SoSWR. As a result, parameter-estimation simulations were biased by these observations. To resolve this issue, the initial hydraulic-head observation from each well was kept as an observation. The remaining drawdown observations were not included as observations. This area is expected to continue reporting larger than expected drawdowns during model prediction.

5.3.1.2   Horizontal Flow Barriers

The representation of some faults as partial barriers to groundwater flow was evaluated by considering alternative conceptual models that would also result in reasonable simulated hydraulic-head or spring flow distributions. During the initial stages of model development, two basic conceptual models were considered. In the first one, rocks in the mountain blocks were assigned significantly low hydraulic conductivities. In the second one, rocks in the mountain blocks were assigned moderately low hydraulic conductivities associated with faults containing small cross-fault transmissivity. During model calibration, focus shifted from the first to the second conceptual model, which was implemented using the HFB package as described in Section 4.0. The adoption of the second conceptual model was influenced by three major factors, which support the explicit inclusion of faults in the model using the HFB package. These three factors are discussed in the following text, followed by the final list of HFBs included in the model and their parameters.

5.3.1.2.1   Mountain-Block Hydraulic Heads, Recharge, and Runoff

Early in the model calibration, it was noted that mountain blocks with significantly low K created very large groundwater recharge mounds (water modeled above the ground surface). To maintain effective recharge rates under this conceptual model, it was necessary to increase recharge runoff.

Aspects of this increase of recharge that are of particular note include:

- For UA, BASE, and PLUT materials, because of their perceived competence, 98 percent of the recharge applied to mountain blocks containing these units had to be moved to the valley bottoms. Given the limited capacity of small-K mountain blocks to absorb water, matching hydraulic-head elevations in these mountain blocks was very difficult. Small changes in the recharge rate, the percent of in-place recharge, or the host rock K could all cause large changes in hydraulic head.

- For carbonate (LC and UC) and LVF units, more evidence existed to suggest that more infiltration was possible in these areas. Carbonates in the model area are known to act as good aquifers. LVF materials, in many cases, were more transmissive than UA, BASE, and PLUT units. Carbonate and LVF units required larger K to prevent mounding.

- The hydraulic prope rties of the UVF unit also needed to be ade quately large to allow infiltration of this water at the base of m ountain fronts. It was generally assumed that most redistributed-runoff recharge occurred not more than 2 to 5 mi from the m ountain-front transitional areas. If too much runoff was generated, the model would predict large mounds in these transitional areas, particularly in places where the UVF RMU was quite thin. To prevent this, the following measures were taken:

  - The *K* of the UVF unit was increased within reasonable limits.

  - Runoff from the mountains was reduced. This lead to increasing *K* in the mountain block, which sometimes resulted in a significant decrease in hydraulic heads in the mountain block.

  - Recharge was reduced; however, in many areas, recharge rates needed to be maintained in order to maintain spring and ET flows.

5.3.1.2.2   Hydraulic-Head Changes across Faults

Regional water levels suggest that fa ults act as barriers to groundwater flow. Although well-documented examples are scarce, water levels occurring in several key areas close to, or on both sides, of faults display significant hydraulic-head drops. One example of this occ urs between Dry Lake Valley and Patterson Valley (Figure 5-1). Hydraulic heads in Patterson Valley are fairly flat at about 5,650 ft. There are additional hydraulic-head observations on the Dry Lake Valley side of the carbonate mountain block, where hydraulic heads have dropped to 5,450 ft. The lar ge drop in hydraulic head occ urs across two normal faults represented by HFBs. Hydraulic hea ds drop an additional 1,100 ft down to about 4,300 ft in central Dry Lake Valley. Even with low *K* flow barriers, the numerical model had trouble in t his area matching the large hydraulic-head drop across the fault zone on the Dry Lake Valley side of the mountain block (Bristol Range). From these and ot her observations in Dry Lake Valley, the large hydraulic-head drop appears to be controlled by faulting rather than by mountain-block material.

5.3.1.2.3   Spring Flows at Faults

The occurrence of springs in areas immediately up-gradient of faults is another i ndicator of faults acting as hydraulic barriers to groundwater flow. Examples include Lund Spring (in White River Valley) and Muddy Springs (in the Muddy River Springs Area). In many cases where springs are associated with fa ults, sufficient flow was not simulated from these springs unti l a horizontal-flow barrier was incorporated into the hydrogeologic framework and numerical model.

In most cases, model fit improved more dramatically when HFBs were used in these hydrogeologic settings. HFBs were much more effective than using hydraulic-conductivity changes from small *K* mountain-block units to larger *K* valley-fill units. Beca use HFBs were added in plac es where data were present to indicate a dra matic hydraulic gra dient change, it is quit e possible that ther e are locations in the model domain where faults act as flow barriers, but the data were not available to indicate their presence. Thus, the model may actually underrepresent HFBs model-wide.

Dry Lake Valley to Patterson Valley Head Observations

Figure 5-1
Evaluation of Hydraulic-Head Changes
across Faults between Patterson and Dry Lake Valleys
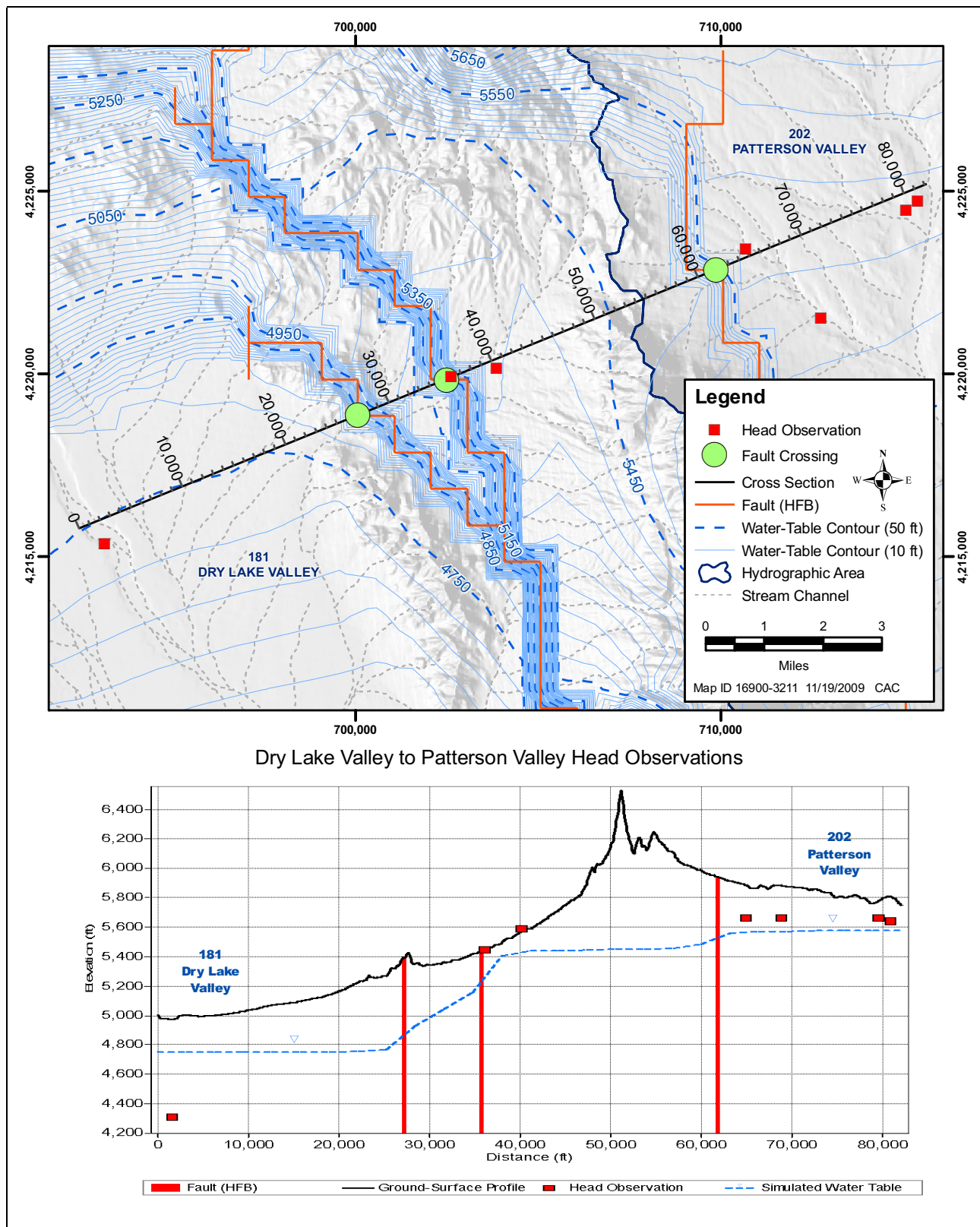
5.3.1.2.4   Final HFB Configuration

The evidence described above demonst rates that barriers to groundwater flow were necessary in many cases to better control simulated hydraulic heads and improve gradients and flows. Therefore, the second conceptual model was adopted with barriers to groundwater flow explicitly represented in the model using HFBs . Initially, HFBs were assigned to lateral and normal faults of r egional significance and were tested during model calibration. This testing resulted in the removal of many faults as potential horizontal flow barriers. Table 5-3 lists all t ested HFBs including the ones that were removed during testing. Normal faults identified as potential barriers to flow ar e listed in Table 5-3 and are illustrated in Figure 4-11. The selected normal and lateral faults were represented both as high-transmissivity zones and HFBs (Section 4.0).

5.3.2   Location and Nature of Flow Boundaries

External boundary flows were estimated from sparse water-level data, interpretive hydrogeologic framework information, and estimates from previous studies. Because of limited data, external boundary flow obs ervations are difficult to characterize. The model-calibration process includes modification of external boundaries to test the adequacy of their representation. A djustments to external boundaries include the following:

- Northern Steptoe Valley at the boundar y with Goshute Valley (Figure 4-14) – This boundary was shifted from the structural basin into a mountain-block area. Observed hydraulic heads (W179_280 and W179_283) in the mountain-block area were 160 to 200 ft (50 to 60 m) lower than surrounding water levels in northern S teptoe Valley. Water levels in S teptoe Valley appear to be influenced by faults near these two observations.

- Tippett Valley (Figure 4-15) – An additional constant-head boundary was added to the northeastern side of the hydrographic area near Deep Creek Valley. This was done because hydraulic-head observations along the Ante lope and D eep Creek boundaries indicate a relatively flat gradient, while hydr aulic heads in central Tippett Valley show elevated heads. The flatter gradient suggests some poss ible leakage through t he mountain block t o Deep Creek Valley.

- Long Valley (Figure 4-17) – The target flow to Newark Valley was increased from 0 to 12,000 afy (40,525 m^3/d). As discussed in Section 4.3.2.2, it was not possible to simulate large quantities of groundwa ter flow from Long Valley to Jakes Valley, as sug gested in the simplified conceptual model (SNWA, 2009a). To help ba lance the gr oundwater budget in Long Valley, some of the excess water was allowed to flow out of the valley southwest into Newark Valley and northwest into R uby Valley. Although the re vised target for flow to Newark Valley is consistent with other interpretations (e.g., Prudic et al., 1995), it is highly uncertain because of the lack of data in that area. The ta rget flow for the additional flow-boundary segment adde d to the model to help remove the r est of the exc ess water simulated in Long Valley was set to 2,000 afy (6,754 m^3/d). The location of t his flow-boundary segment is also c onsistent with Prudic et al. (1995). However, Prudic et al. (1995) show, in their upper model layer for the nor thwestern boundary of Long Valley, that flow moves into Long Valley.

Table 5-3
Normal and Lateral Faults Identified as Flow Barriers
(Page 1 of 2)

Fault Description	Subdivision	Fault Type	Extends Through All RMUs	Added and Tested During Calibration	Tested and Eliminated	Parameter Name	Modeled Conductance (1/d)
Caliente Caldera Area	---	Lateral	Yes	---	---	HFB_GROUP	9.014E-07
California Wash	East	Normal	Yes	X	X	HFB_CALIFE	9.014E-07
	West	Normal	Yes	X	---	HFB_CALIFW	9.014E-07
Cave Valley	North	Lateral	Yes	---	---	HFB_CAVE_N	9.014E-07
	Northeast	Normal	Yes	X	---	HFB_CAVENE	9.014E-07
	Southwest	Normal	Yes	X	---	HFB_CAVESW	9.014E-07
Coal Valley	North	Normal	Yes	X	---	HFB_COAL_N	2.704E-06
	West	Normal	Yes	X	---	HFB_COAL_W	2.323E-06
Dry Lake Area	North	Lateral	Yes	---	---	HFB_GROUP	9.014E-07
	North	Normal	Yes	X	---	HFB_DRYL_N	9.014E-07
	South	Lateral	Yes	---	---	HFB_GROUP	9.014E-07
	East	Normal	Yes	X	---	HFB_DRYL_E	9.014E-07
	West	Normal	Yes	X	---	HFB_DRYL_W	9.014E-07
Garden Valley	Central	Normal	Yes	X	X	HFB_GARD_C	9.014E-05
	East	Normal	Yes	X	X	HFB_GARD_E	9.014E-05
	North	Normal	Yes	X	---	HFB_GARD_N	9.014E-07
	West	Normal	Yes	X	---	HFB_GARD_W	2.704E-06
Hamlin Valley	---	Normal	Yes	X	X	HFB_HAMLIN	9.014E-07
Kane Springs Area	---	Lateral	Yes	---	---	HFB_KANE	9.014E-07
Lake Mead	Black Mountain	Lateral	Yes	---	---	HFB_LAKEMD	9.014E-08
Long Valley	East	Normal	Yes	X	---	HFB_LONG_E	9.014E-07
Muddy River Springs Area	East of Muddy Springs	Normal	Yes	X	---	HFB_MUDDYR	9.014E-04
Pahranagat Shear Zone	Eastern	Lateral	Yes	---	---	HFB_PAHR_E	1.426E-05
	Northwestern	Lateral	Yes	---	---	HFB_PAHRnW	2.704E-05
	Southwestern	Lateral	Yes	---	---	HFB_PAHRsW	2.704E-06
Pahranagat Valley	East Side of Wash South to Ash Spring	Normal	Yes	X	---	HFB_PAHR_1	9.014E-07
	Sixmile Flat - East	Normal	Yes	X	---	HFB_6MILEE	9.014E-07
	Sixmile Flat - West	Normal	Yes	X	X	HFB_6MILEW	9.014E-07
Pahroc Valley	North Pahroc to Delamar	Normal	Yes	X	X	HFB_PROCDM	9.014E-07
	Central to Delamar	Normal	Yes	X	---	HFB_PROCD2	9.014E-07
	Cross Valley	Normal	Yes	X	---	HFB_PROC_X	9.014E-06
	North	Normal	Yes	X	---	HFB_PROC_N	2.704E-06
	South	Normal	Yes	X	---	HFB_PROC_S	9.014E-07

SE ROA 50924

JA_16325

Fault Description	Subdivision	Fault Type	Extends Through All RMUs	Added and Tested During Calibration	Tested and Eliminated	Parameter Name	Modeled Conductance (1/d)
Panaca Valley	Below Panaca Spring	Normal	Yes	X	---	HFB_PANACA	9.014E-07
	Further South in Central Valley	Normal	Yes	X	---	HFB_PANAC2	9.014E-07
Patterson Valley	Central Valley	Normal	Yes	X	---	HFB_PATV_1	9.014E-07
	Southeast	Normal	Yes	X	---	HFB_PATTSE	9.014E-07
Snake Range and Snake Valley	At Warm Springs near Gandy, UT	---	Yes	---	---	HFB_GANDY	9.014E-08
	Eastern Flank, Southern Section	Normal	Yes	X	---	HFB_SNRS_E	1.532E-06
	Eastern Flank, Central Section, West of Warm Springs	Normal	Yes	X	---	HFB_SNRCwE	9.014E-07
	Eastern Flank, Central Section, East of Warm Springs	Normal	Yes	X	---	HFB_SNRCeE	4.507E-05
	Eastern Flank, Northern Section	Normal	Yes	X	---	HFB_SNRN_E	9.014E-05
	West of Baker	Lateral	Yes	---	---	HFB_GROUP	9.014E-07
	Near Confusion	Normal	Yes	X	---	HFB_SNKCON	9.014E-07
Spring Valley	Northeast	Normal	Yes	X	---	HFB_SPR_CE	9.014E-07
	Central-east	Normal	Yes	X	---	HFB_SPR_NE	9.014E-07
Steptoe Valley	To Cave Valley	Normal	Yes	X	X	HFB_SwSTEP	9.014E-07
	Near McGill Spring	Normal	Yes	X	---	HFB_MCGILL	9.014E-07
	East Model Boundary	Normal	Yes	X	---	HFB_STEPBE	9.014E-07
	South Model Boundary	Normal	Yes	X	---	HFB_STEPBS	9.014E-07
	West Model Boundary	Normal	Yes	X	---	HFB_STEPBW	9.014E-07
Tippett Valley	East	Normal	Yes	X	---	HFB_TIPP_E	9.014E-07
	West	Normal	Yes	X	---	HFB_TIPP_W	9.014E-07
White River Valley	Caldera	Lateral	Yes	---	---	HFB_WRCALD	9.014E-07
	Cross Valley, Near Moorman Spring	Normal	Not UVF	X	---	HFB_WR_X_C	9.014E-07
	East Side of Valley, North Near Lund	Normal	Yes	X	---	HFB_WR_E_N	9.014E-07
	Hot Creek Springs Area	Normal	Yes	X	---	HFB_WR_HCS	9.014E-07
	Near Pahroc Valley	Normal	Not UVF	X	---	HFB_WR_PRC	9.014E-07
	West of Hot Creek Springs Area, Along Mountain Block	Normal	Yes	X	---	HFB_WR_WHC	9.014E-07
	East Side of Valley, Southern End	Normal	Yes	X	X	HFB_WR_E_S	9.014E-07

- Pahranagat Valley (Figure 4-19) – During model calibration, discharge by groundwater ET from Pahranagat Valley tended to be larger than expected. A constant-head boundary was added to southwestern Pahranagat Valley to allow some of the discharge to flow out of the model area through the Pahranagat Shear Zone, thereby decreasing discharge by groundwater ET to more reasonable levels. This is consistent with some previous studies (Winograd and Friedman, 1972; Dettinger, 1989; Kirk and Campana, 1990; Thomas et al., 1996), and models (D'Agnese et al., 1997) have suggested that groundwater flow from Pahranagat Valley toward the DVFS is possible. However, Thomas et al. (2001) and Thomas and Mihevc (2007) balanced a deuterium-mass-balance model of the WRFS based on updated deuterium measurements without any subsurface outflow from the western boundary of Pahranagat Valley. San Juan et al. (2004) found that the most reasonable estimate of boundary flow between Tikaboo Valley and Pahranagat Valley is 800 afy of inflow to Pahranagat Valley. While the calibrated groundwater ET rates are still high, opening the Pahranagat Shear Zone boundary allows some of the excess water to exit. At the same time, adequate flow is delivered to Coyote Spring Valley and the Muddy River through the Pahranagat Shear Zone.

- Confusion Range (Figure 4-16) – The constant-head boundary at the Confusion Range in southeastern Snake Valley was tested to evaluate its extent along the range. A reduced boundary length along the Confusion Range resulted in a better representation of hydraulic heads in Snake and Hamlin valleys and discharges through ET and springs. In the conceptual model, the Confusion Range boundary extended about 28 mi (45 km) north of that shown in Figure 4-13. Simulated hydraulic heads were predicted to decline to the north. During model calibration, this tended to reduce flows at Twin Springs and Foote Reservoir Spring and to lower hydraulic heads in the mountain block, often to levels lower than those seen on the floor of Snake Valley. Analysis of recent data collection (Mankinen, pers. comm., 2008) suggests a significant gravity anomaly in this northern section of the Confusion Range. This indicates a change in material type from the southern boundary area. The *K* could be higher or lower, but given the behavior of the model in the area, a low *K* zone appears more reasonable, making representing this section with a constant-head boundary less reasonable. During early testing, hydraulic heads were raised along this boundary to improve flow at Twin Springs and surrounding hydraulic-head observations. However, hydraulic heads were raised 650 ft (200 m) along the northern boundary before good matches were attained. Given that no source existed for this water, the approach was abandoned and a reduction in boundary length was used.

- Fish Springs Range/Fish Springs Area (Figure 4-16) – The source of water at Fish Springs was evaluated throughout the model-calibration process. Initial calibration efforts assigned no flow conditions along the Fish Springs Range between Snake Valley and Fish Springs Flat. The volume of discharge at Fish Springs suggests that the origin of water occurs outside of Fish Springs Flat (Bolke and Sumsion, 1978; Gates and Kruer, 1981; Carlton, 1985; Harrill et al., 1988). The calibrated model suggests 718 afy (2,425 m^3/d) is flowing into Snake Valley from Fish Springs Flat. In general, small flows (<1,000 afy) across this boundary alternated between, into, and out of the model domain. Flows predicted at this boundary appear to be small, but whether flow is really into or out of the model domain is unclear.

The flow-boundary segments and their re presentation in the model are only interpretations. Their actual locations and fl ow rates may differ from simulated flow because of unce rtainties in the recharge estimates and because the hydraulic properties of the rocks are unknown over most of the model domain.

5.3.3   Definition of Recharge Processes

Section 4.5 describes the development of recharge input to the CCRP model. Recharge was based on five basic processes, including:

- PRISM precipitation distribution
- Runoff watershed areas and catchment points
- Runoff distribution pathways
- Recharge efficiencies
- In-place versus runoff recharge percentages for potential recharge

Of the five processes, PRISM precipitation distribution and watershed areas and catchment points were not modified during calibration. Runoff pathways, efficiencies, and in-place percentages were adjusted during ca libration. The following sections describe the calibration of these recharge processes.

5.3.3.1   Runoff Distribution Paths

The runoff distribution paths we re the r esult of an a utomated topographic-based geographic information system (GIS) algorithm described in Section 4.0. The paths were not modified programmatically during model calibration. Instead, they we re adjusted manually prior to model execution. The refore, runoff distribution paths were not manipulated by UCODE _2005 for sensitivity calculations or parameter estimation. As part of the calibration process, adjustments to runoff pathways refined the runoff recharge component. For example, the r echarge process could produce runoff to model cells with a very small thickness of permeable rock type. This could result in unrealistic mounding. In addit ion, converging distribution paths could also result in un realistic simulated mounds in the water table. In short, manual modifications to runoff pathways resolved unrealistic mounding. Exte nding a distribution path typically resolved unrealistic water-table mounding.

5.3.3.2   Recharge Efficiencies

SNWA (2009a) provides initial estimates RE for the flow systems within the model domain. For each flow system, four e fficiency intervals were defined in the model, a nd the following rules desc ribe their implementation:

- RE for lar ger precipitation rates were equal to or larger than the efficiency for smaller precipitation rates (i.e., $RE4 \geq RE3 \geq RE2 \geq RE1 \geq 0.0$).

JA_16328

- RE were grouped with a multiplication factor by flow system. When the factor was modified, all the efficiencies for the flow system were raised or lowered by an equal percentage.

- RE multiplication factors were limited to a range of 0.1 to 2.0 in UCODE_2005. A factor of 1.0 implies the initial RE were unchanged. A factor of 2 would imply twice the expected recharge enters the flow system, a nd 0.1 would i mply only 10 percent of the expected recharge enters the flow system. The bound on the multiplication factor was found to stabilize the recharge-efficiency parameters during the estimation process.

Convergence issues were encountered with t he RE during parameter estimation. Therefore, manual adjustment was the primary calibration method for these parameters.

During the calibration, the RE were some of the most sensitive model param eters, second to the constant-head boundary parameters. Early in the calibration when using parameter estimation to estimate parameter values, the initial values for RE were often unr easonable. In some c ases, rates could exceed 100 pe rcent of precipitation or trend toward zero. In the calibrated model, the RE estimates were very similar to those defined in the conceptual model, with the exception of the Goshute Valley Flow System (GVFS) efficiencies. These were raised by 25 perc ent because simulated heads and ET rates in Steptoe Valley were typically low and because the recharge rate used in the conceptual model was at the low end of the literature for Steptoe Valley (discussed more in Section 6.0).

5.3.3.3   In-Place and Runoff Recharge Efficiencies

The range of possible values of in-pla ce recharge efficiency is 0.0 to 1.0 in UCODE_2005. Two parameters, R_ROCARB_W and R_ROLVF_WT, are commonly sensitive parameters. The final model calibration estimates these parameters. The R_ROLVF_WT parameter controls volcanic areas and had significant influence on hydraulic-head observations in Clover Valley and the Caliente Caldera Complex.

Convergence issues were encountered with the in -place and runoff efficiencies during parameter estimation. Therefore, manual adjustment was the primary calibration method for these parameters.

5.3.3.4   Additional Recharge Zonations

In the original conceptual model, there were four primary recharge efficiency regions. The se represented the Gre at Salt Lake Desert, Goshute Valley, Meadow Valley, and White River flow systems. During model calibration, all the flow systems other than Goshute Valley were subdivided. Because some of these flow systems cover extensive regions, it is not sur prising that there would be local variations.

Hamlin Valley is an example where the hydrogeologic conditions do not match the rechar ge efficiencies established for the flow system. While Hamlin Valley is part of the GS LDFS (see Figure 4-32), the climate and rock types in the sou thern half of the basin are more similar to those

seen in the MVFS. As a result, Hamlin Valley was divided approximately in half for recharge purposes, with the southern half being reassigned to the MVFS.

Long Valley was originally modeled as being part of the WRFS. As a result of the calibration process, Long Valley and the northern half of Jakes Valley appear to be part of the Newark Valley Flow System (see Figure 4-32). RE were originally equal to the WRFS efficiencies. However, RE were decreased by 50 percent to minimize groundwater mounding simulated in the area.

An additional subzone was defined in the GSLDFS. This subzone occurs in Snake Valley in the northern Snake Range south of the Kern Mountains (see Figure 4-32). This subzone was created in an effort to increase spring flows at Warm Springs, west of Gandy, Utah (see Section 5.3.1.1.1). This predominantly north- and east-facing area of the Snake Range was assumed to have a 25 percent higher recharge efficiency.

In tests to reduce ET discharge in some areas, RE in Dry Lake and Garden Valley (Figure 4-32) were defined. The final numerical model left the efficiencies in these areas unchanged (same as WRFS).

5.3.4 Definition of Discharge Areas

The two basic types of groundwater-discharge parameters defined in the numerical model are (1) ET and spring flow discharge, which are simulated using the DRN package and associated parameters, and (2) spring-fed stream flows, which are simulated using the SFR2 package and associated parameters. Groundwater ET and spring flows are grouped because the water that discharges from springs may be derived from greater depths in the flow system and supplies the wetlands, shrublands, playas, and open water bodies. Spring-fed stream flow is routed to ET areas that are somewhat distant from immediate groundwater-discharge locations. Groundwater ET was represented with the DRN package using four conductance modifiers treated as parameters and representing wetland, shrubland, playa, and open water for both regional and intermediate discharge areas (Table 5-4).

Table 5-4
ET Regions and Conductance Modifier Parameters

ET Regions	Parameter Name
Wetland	ETrWET and ETiWET
Shrubland	ETrSHR and ETiSHR
Playa/Wet Soil	ETrPLY
Open Water	ETrWAT
HA 209 Wetland	ETr209WET
HA 209 Open Water	ETr209WAT

Note: There are no intermediate Playa and Open Water ET areas.

5.3.4.1   ET Sub-Basins

To better constrain the distribution of ET across large valley bottoms, larger valleys were subdivided into ET sub-basins. ET estimates for each of the ET sub-basins were provided in SNWA (2009a). This more detailed constraint on the spatial distribution of ET facilitated a more even distribution of simulated ET along the lar ge valley bottom s. H owever, considering the unc ertainty in t he ET estimates, matching these targets by hydrographic area remained the primary goal.

5.3.4.2   ET-Extinction Depth

The elevation of drains representing ET areas was initially defined to equal the minimum elevation of the USGS 30-m DE M cell occurring within the 247.1-acre (1 km^2) model grid ce ll, minus 33 ft (10 m). This drain e levation approximates the elevation in the m odel domain below which groundwater ET ceases (corresponds to extinction depth). As model calibration improved, some ET areas required an adjustment to better approximate extinction depth. In the se areas, simulated hydraulic heads were consistently low. To evaluate the ET-extinction depth, the depth subtrac ted from the minimum DEM elevation was adjusted. In the calibrated model, one of two drain depths was used: (1) the mean USGS 30-m DEM elevation within the 247.1-acre (1 km^2) model grid cell, minus 33 ft (10 m) or (2) the minimum USGS 30-m DEM elevation within the 247.1-acre (1 km^2) model grid cell, minus 16.4 ft (5 m). In a given m odel cell with an ET drain, the lower of these two values was used.

5.3.4.3   Spring Depth

Different types of springs we re conceptualized to draw water from different model layers (depths). Regional springs were initially assigned to the uppermost model layer containing the LC RMU. Spring flows at these regional springs improved when the springs w ere assigned to model layers containing the LC RMU. Intermediate springs were initially assigned to the upper one or two model layers to represent shallow groundwater flow features. Spring flows improved when these springs were assigned to shallow and deep model layers, suggesting that these features have a mixture of deep and shallow groundwater sources.

5.3.4.4   Spring Conductances

Drain conductance was adjusted during calibration to better simulate spring discharge. Table 5-5 lists initial conductance estimates and the calibrated conductance. The largest modification (factor of 10) to drain conductance occurs at Hot Creek Spring.

5.3.4.5   Spring (Riverbed) Hydraulic Conductivities

Springs simulated using the SFR2 package were assigned riverbed hydraulic conduc tivities. For these springs, the riverbed hydraulic conductivities were adjusted manually to improve matches with the spring flow obse rvations.   Table 5-6 lists initial estimates and the c alibrated hydraulic conductivities.

Table 5-5
Conductances for Springs Modeled with DRNs

Spring Name	Observation Name	Original Conductance Estimate ft²/d (m²/d)	Updated Conductance Estimate ft²/d (m²/d)
Arnoldson Spring	SPiw07_2_##	644.0 (59.83)	No Change
Blue Point Spring	SPiw15_2_##	57.70 (5.360)	173.1 (16.08)
Brownie Spring	SPis09_4_##	491.2 (45.63)	No Change
Butterfield Spring	SPib07_10_##	1,175 (109.2)	587.6 (54.59)
Cherry Creek Hot Springs	SPr79_2_##	3.693 (0.3431)	No Change
Cold Spring	SPiw07_3_##	428.8 (39.84)	No Change
Emigrant Springs	SPib07_15_##	537.7 (49.95)	No Change
Flag Springs 1	SPiw07_7_##	205.5 (19.09)	821.8 (76.35)
Flag Springs 2			
Flag Springs 3			
Foote Res. Spring	SPib95_12_##	2,199 (204.3)	No Change
Hardy Spring NW	SPis07_11_##	627.1 (58.26)	No Change
Hardy Springs			
Hot Creek Spring	SPr07_1_##	2,174 (202.0)	21,740 (2,020)
Keegan Spring	SPis84_12_##	927.0 (86.12)	No Change
Kell Spring	SPis95_13_##	302.5 (28.10)	No Change
Lund Spring	SPib07_5_##	5,899 (548.0)	973.4 (90.42)
McGill Spring	SPiw79_1_##	5,386 (500.4)	No Change
Minerva Spring	SPis84_13_##	1,484 (137.9)	No Change
Monte Neva Hot Springs	SPr17_3_##	141.3 (13.13)	No Change
Moon River Spring	SPr07_14_##	380.0 (35.30)	759.9 (70.60)
Moorman Spring	SPr07_6_##	206.0 (19.14)	No Change
Nicolas Spring	SPiw07_13_##	463.3 (43.04)	No Change
North Millick Spring	SPis84_3_##	1,069 (99.28)	No Change
Panaca Spring	SPr03_1_##	511.7 (47.54)	No Change
Preston Big Spring	SPr07_4_##	1,218 (113.2)	3,655 (339.6)
Rogers Spring	SPiw15_1_##	120.9 (11.23)	241.6 (22.45)
South Millick Spring	SPib84_4_##	1,114 (103.5)	No Change
Twin Spring	SPib95_15_##	3,514 (326.5)	No Change
Warm Creek near Gandy, UT	SPiw95_2_##	2,947 (273.8)	No Change
Willow Spring	SPRiw184_1_##	6.958 (0.6464)	No Change

refers to stress-period identifier.

Table 5-6
Hydraulic Conductivities for Springs Modeled with SFR2 Package

Spring Name	Observation Name	Parameter Name	Hydraulic Conductivity Estimate ft/d (m/d)	Updated Hydraulic Conductivity Estimate ft/d (m/d)
Ash Springs	G_ASH_SPR	SFR_COND17	0.328 (0.1)	No Change
Baldwin Spring	G_MR_MOAPA	SFR_COND19	0.328 (0.1)	0.131 (0.04)
Big Springs	G_BIG_SPR	SFR_COND3	0.328 (0.1)	3.28 (1.0)
Crystal Springs	G_XTL_SPR	SFR_COND16	0.328 (0.1)	0.0197 (0.006)
Hiko Spring	G_HIKO_SPR	SFR_COND15	0.328 (0.1)	0.0098 (0.003)
Jones Spring	G_MR_MOAPA	SFR_COND19	0.328 (0.1)	0.0328 (0.01)
M-10	G_MR_MOAPA	SFR_COND19	0.328 (0.1)	0.131 (0.04)
M-11	G_WARM_SW	SFR_COND19	0.328 (0.1)	0.0328 (0.01)
M-12	G_WARM_SW	SFR_COND19	0.328 (0.1)	0.0328 (0.01)
M-13	G_WARM_SW	SFR_COND19	0.328 (0.1)	0.0328 (0.01)
M-15	G_IVERSON	SFR_COND19	0.328 (0.1)	0.0328 (0.01)
M-16	G_IVERSON	SFR_COND19	0.328 (0.1)	0.0328 (0.01)
M-19	G_WARM_SW	SFR_COND19	0.328 (0.1)	0.0328 (0.01)
M-20	G_IVERSON	SFR_COND19	0.328 (0.1)	0.0328 (0.01)
Muddy Spring	G_MR_MOAPA	SFR_COND19	0.328 (0.1)	0.131 (0.04)
Pederson East Spring	G_WARM_SW	SFR_COND19	0.328 (0.1)	0.0328 (0.01)
Pederson Spring	G_WARM_SW	SFR_COND19	0.328 (0.1)	0.0328 (0.01)
Warm Springs East	G_IVERSON	SFR_COND19	0.328 (0.1)	0.0328 (0.01)

5.3.5   Storage Parameters

Many aquifer st orage parameters were gener ally found to be insensitive (see Section 6.0). T he exception is UVF_SYTP. The sensitivity of the UVF storage parameter is reasonable because most pumping occurs in the shallow unconsolidated UVF deposits. Relatively few fe atures are in the system to stress the other parameters.

The initial S_y estimate for UVF_SYTP was 10 percent. This wa s a conservative value for unconsolidated deposits and within literature ranges. Dur ing initial modeling, though, drawdowns across the model generally significantly exceeded observed drawdowns. Early parameter-estimation runs predicted UVF S_y values in excess of 30 perc ent regionally. This was considered unreasonably large. During conversations with the USGS, and based on S NWA work (see Appendix A), UVF S_y values in the Snake Valley and Bake r, Nevada, area were estimated in the 12 to 28 percent range. Based on this work, the UVF_SYTP was increased to 18 percent. Drawdown in some areas remains overpredicted (e.g., 183 N06 E66 35C 1 USBLM - Pony Springs Well). However, this value appears to be reasonable.

SE ROA 50932

JA_16333

5.4 Adjustments in Western Model Area

The western side of the numerical model study area was particularly difficult to calibrate and required additional efforts. The difficulties stem from two major issues within the WRFS (1) groundwater flow in the Long Valley area and (2) groundwater flow in the Pahranagat Valley area.

5.4.1 Groundwater Flow in Long Valley

Originally, the RE for Long Valley were assumed to be the same as the rest of the WRFS. Considering the relatively high elevation of Long Valley, relative to other nearby valleys (with lower elevation), recharge was expected to be significant (i.e., nonzero). Based on the simplified conceptual model used to derive the initial recharge distribution (SNWA, 2009a), 20,000 afy of precipitation recharge and additional groundwater was estimated to flow from Long Valley to Jakes Valley and, ultimately, to White River Valley.

The hydrogeologic framework model in the Long Valley area contains a significant thickness of the UA RMU. The presence of such a thickness of UA in conjunction with the initial recharge rates caused extreme groundwater mounding in Long Valley. The UA prevented vertical flow from the upper unconsolidated UVF deposits to the lower carbonate (LC3). The UA acted more or less as an effective confining unit at various tested thicknesses and/or hydraulic conductivities for the unit.

The northwestern portion of the model area, including Long and Jakes valleys, lacks well information to accurately assess the thickness of the UA in this area. Faulting from Long Valley through Jakes Valley and into White River Valley has been mapped from satellite imagery and aerial photography. Tests were initially performed to identify appropriate adjustments to the hydrogeologic framework model to allow approximately 37,000 afy of groundwater to flow from Long and Jakes Valley into White River Valley. It was found that even with a zone of LC extending from Long Valley to White River Valley, between the major normal faults through Jakes Valley, with *K's* as high as 33 ft/d, large fluxes through Jakes Valley were still not possible. This finding is consistent with the potential presence of a groundwater divide in central Jakes Valley, with flow from northern Jakes Valley to Long Valley to Newark Valley (Prudic et al., 1995). Because simulating large flows through Jakes Valley was not possible, it was concluded that (1) either the initial recharge in Long and Jakes valleys was too high (2) or the groundwater resulting from recharge had to be moving through areas other than Jakes Valley. After review of earlier work in the area, it was found that Prudic et al. (1995) simulated 12,700 afy of groundwater from Long Valley to Newark Valley. It was assumed that an additional 4,000 afy of flow might be moving from Butte Valley and Long Valley northwest to Rose Valley**.**

5.4.2 Groundwater Flow in Pahranagat Valley

The aquifer system of Pahranagat Valley was difficult to represent in the numerical model. This difficulty is due to the large uncertainties associated with the hydrogeologic conceptualization of this basin and vicinity. This basin occurs at the confluence of groundwater flow from many of the WRFS valleys. The Pahranagat Shear Zone, which is located at the southern end of Pahranagat Valley, constitutes a major structural feature, controlling groundwater flow into Coyote Spring Valley and

ultimately Muddy River Springs and Muddy River. Groundwater may also flow along the Pahranagat Shear Zone to the southwest into Tikaboo Valley and on toward the Amargosa Desert (Prudic et al., 1995). Further complicating the conceptual model of groundwater flow in Pahranagat Valley, nearly 90 percent of the ET discharging from this valley is reported to be a result of groundwater discharge from Ash, Hiko, and Crystal springs. These springs discharge to the Pahranagat Wash and probably feed the local riparian vegetation. Although no data are available to confirm it, Pahranagat Wash may be interpreted to be perched or semiperched.

Given the representation of the simplified hydrogeology of the Pahranagat Valley region represented in the model, it was not possible to simulate approximately 30,000 afy of groundwater discharge only from Ash, Crystal, and Hiko springs. Simulating these large volumes of groundwater discharge from the springs in the north end of the valley, while maintaining hydraulic heads well below land surface in the southern part of the valley, was not feasible by reasonable means. To reduce the excess groundwater flow in Pahranagat Valley a reduction in potential recharge in and around this basin was tested. However, this reduction as a reduction in in-place recharge and/or an increase in runoff recharge in basins up-gradient of Pahranagat Valley, resulted in undersimulated flow at many of the important regional springs throughout the WRFS. This same issue occurred when recharge was reduced in Garden and Coal valleys. Therefore, the excess groundwater in Pahranagat Valley must be removed from the basin by other processes: (1) groundwater flow through the Pahranagat Shear Zone to Coyote Spring Valley (2) discharge into Pahranagat Wash and ET, and/or (3) groundwater flow by another route.

Allowing more groundwater to flow though the Pahranagat Shear Zone results in anomalously high water levels in Coyote Spring Valley. The water could be sent farther south, but the hydraulic properties required to transmit water through faults and fractured carbonate rocks to Muddy River Springs and Muddy River would need to be unreasonably large. Thus, the first route was deemed unreasonable. Prudic et al. (1995) suggested that an additional 10,000 afy of ET may discharge from a shallow water table south of the spring along Pahranagat Wash. A similar feature was included in the numerical model but was insufficient to significantly reduce the excess groundwater simulated in Pahranagat Valley to acceptable levels. Previous investigators (Winograd and Thordarson, 1975) suggested that water from Pahranagat Valley may also flow southwest to the Ash Meadows groundwater basin. This interpretation corresponds to the third route and was incorporated in the final version of the numerical model. In summary, given the current framework model, the best solution was a combination of two processes: (1) allow more ET to discharge from Pahranagat Wash as suggested by Kirk and Campana (1990) and (2) allow some groundwater to flow out to Tikaboo Valley toward Amargosa Desert, as suggested by other researchers (Winograd and Thordarson, 1975).

This Page Intentionally Left Blank

SE ROA 50935

JA_16336

6.0 FINAL PARAMETER ESTIMATION AND MODEL EVALUATION

This section presents the evaluation of the tra nsient numerical model c alibration and describes the final parameter-estimation simulations. The calibration process and conceptual model refinements were presented in Section 5.0. The nonlinear regression method discussed in Section 5.0 provides a better understanding of model strengths and weaknesses, and has a built-in protocol to help evaluate how well simulated hydraulic heads and groundwater discharge match the observed values. It also provides a means f or assessing the relative sensitivity of e stimated parameter values and other measures of parameter and prediction uncertainty.

The evaluation of the numerical model calibration includes (1) reviewing the model fit and simulated hydraulic heads and flows, (2) evaluating parameter sensitivities and parame ter-estimation results, and (3) evaluating the modeling pa rameter values. Finally, an evalua tion of the flow sys tems as simulated by the model is provided. This evaluation includes detailed descriptions of interbasin flow, groundwater-flow regions, and groundwater budgets. The details are based on the optimized solution obtained through model calibration using spar se data, which is only one of many other potential reasonable solutions.

6.1 Evaluation of Model Fit

This section provides an e valuation of model fit, including a discussi on of ove rall model fit, simulated hydraulic heads and drawdowns, simulated flows, distribution of weighted residuals versus unweighted simulated values, and normality of weighted residuals and model linearity.

6.1.1 Overall Model Fit

The contributions of each type of observation to the objective function are listed in Table 6-1. The SoSWR for the hydraulic-head observations constitute the largest portion of the objective function (64.4 percent), followed by hydraulic-head drawdown observations (24.8 percent). SFR2 spring and stream flow observations account for 7.5 percent of the objective function, but this percentage is only this large because the standard deviations of the regional springs and Muddy Ri ver gage flow targets were divided by 10.0. The standar d deviations for these observations were decreased because (1) they were felt to be some of the most important observations in the study area, and (2) without the modification, the parameter-estimation routine did not honor these obse rvations adequately. ET-discharge observations constitute 2.35 percen t of the tot al SoSWR, and the remaining observations contribute less than 1 percent of the objective function. More details on the model fit by observation type are provided in the following sections.

Table 6-1
Calibrated Model - Summary of Observation Statistics

Observation Type	Observation Type Code	Count	Average Positive Weighted Residuals	Average Negative Weighted Residuals	SoSWR	Percent of Objective Function
Hydraulic-Head Observations	W	2,707	1.1	-1.52	19,804.3	64.36%
Hydraulic-Drawdown Observations	Z	4,301	0.68	-1	7,625.0	24.78%
Spring Head Observations	S	0	---	---	0.0	0.00%
Groundwater ET	E	126	2	-1.53	723.9	2.35%
Spring Flow	SP	44	1.26	-1.67	251.4	0.82%
Spring Flow Change	SD	27	0.28	---	13.3	0.04%
CHD Boundary Flow	BND	16	0.79	-1.09	21.2	0.07%
Interbasin Flow	IBF	0	---	---	0.0	0.00%
SFR2 Spring/Stream Gage	G	144	2.65	-3.38	2,312.6	7.52%
Ground Surface	GS	2,145	---	-0.84	19.7	0.06%
Total	---	9,510	---	---	30,771.4	100.00%

As listed in Table 6-1, the SoSWR is 19,804 for hydraulic heads, 7,625 for hydraulic drawdowns, 724 for ET discharge, 265 for spring flow and spring flow change, 21 for CHD boundary flows, 2,313 for spring and/or stream gage flows, and 20 for ground-surface observations. The standard error of the regression equals 1.7994, which indicates that overall model fit is consistent with hydraulic-head standard deviations that are 1.7994 times the assigned values. For flow out of groundwater ET cells, overall model fit is consistent with 1.7994 times the assigned COVs of 10 to 120 per cent. Thus, effective model fit for groundwater ET is between approximately 18 and 216 percent.

The observations represented in the numerical model and listed in Table 6-1 fall into one of the following categories:

- Observations used in the objective function for parameter-optimization purposes.

- Observations used to derive observations used in the objective function for parameter-optimization purposes (i.e., spring head observations).

- Observations not used by the objective function. These observations were for informational or monitoring purposes only and did not affect model statistics.

Observations, such as hydraulic heads, hydraulic drawdowns, ET-discharge rates, spring flows, spring flow changes, CHD boundary flow, and stream gage flow, were assigned realistic variances. The uncertainty of these observations could be quantified. It was therefore reasonable to include them when optimizing the parameters to minimize the objective function. In some cases, the variances were reduced in order to increase the influence of some observations over others.

Additional observations, such as estimated regional potential hydraulic head at a spring, small spring flows, or interbasin flows, were typically flagged by using very large variances (greater than 1.0E10). In UCODE, noncalibration target types were given a Use-Code Flag of "N" (see Appendix B). This eliminated these observations from statistical consideration. These observations were treated in this manner for one of the following re asons: (1) the observations were estimated with ve ry little confidence (e.g., interbasin flow); (2) the observations were related to a feature that could not be reasonably simulated with a regional-scale model (e.g., small spring flows less than 1 c fs); or (3) the observations were being tracked for informational purposes only (hydraulic heads at spring pools).

Observations monitored during model calibration, such as spring hydraulic heads, interbasin flows, and small spring flows, w ere assigned large variances to mi nimize their weights in the objective function. In the final sensitivi ty run, these parameters were removed from the model to si mplify the output and to eliminate their small contribution to the objective function. Similarly, 2,145 ground-surface observations with a zero residual were removed from the final sensitivity run. If these zero-residual pseudo-observations were used in the statistical analyses of the results, they would create a significant statistical bias and inhibit the interpretation of model-calibration results.

6.1.2   Simulated Hydraulic Heads and Drawdowns

The simulated hydraulic he ads are shown on Plates 2 and 3. Whi le significantly more de tail is in these model results, the overall regional hydraulic-head levels and flow directions are consistent with previous models and studi es for this are a (Prudic et al., 1995). The model re sults are compared in greater detail in Section 6.4.2.

Stress period 1 in the numerical model is ste ady-state and represents predevelopment conditions. Drawdown calculated for subsequent stress periods (2 through 61) repr esents changes in simulated hydraulic head from stress period 1. Figure 6-1 shows drawdowns at the end of stress period 61 (December 31, 2004) in detail. Figure 6-2 shows the progression of drawdowns through time. Plots of simulated hydraulic heads and drawdowns for a ll wells are presented in electronic form (see DVD).

In general, simulated transient dra wdowns match observed drawdowns. S easonal and lar ger-term climatic cycles are not simulated, but the overall trends also generally match well. Wells (C-11-17) 1bdc 2 and (C-20- 20)12acc 1 are distributed across Snake Valley and re present how the numer ical model matches the general trend of hydra ulic-head observations (Figures 6-3 and 6-4). Sim ilarly, wells Behmer-MW and 219 S 14 E65 21AC 1 EH-4 illustrate the response of wel ls in the Muddy River Springs Area (Figures 6-5 and 6-6). In some instances, the numerical model may simulate one well poorly and one well adequately in the same model cell. Wells 219 S14 E65 23BB 1 and 219 S14 E65 23ABBB 1 are examples (Figures 6-7 and 6-8).

6.1.2.1   Evaluation of Weighted Residuals

Statistics for the we ighted residuals associated with the observation groups were presented in Table 6-1 and discussed i n Section 6.1. The spatial distributions of hydraulic-head and drawdown

SE ROA 50938

JA_16339
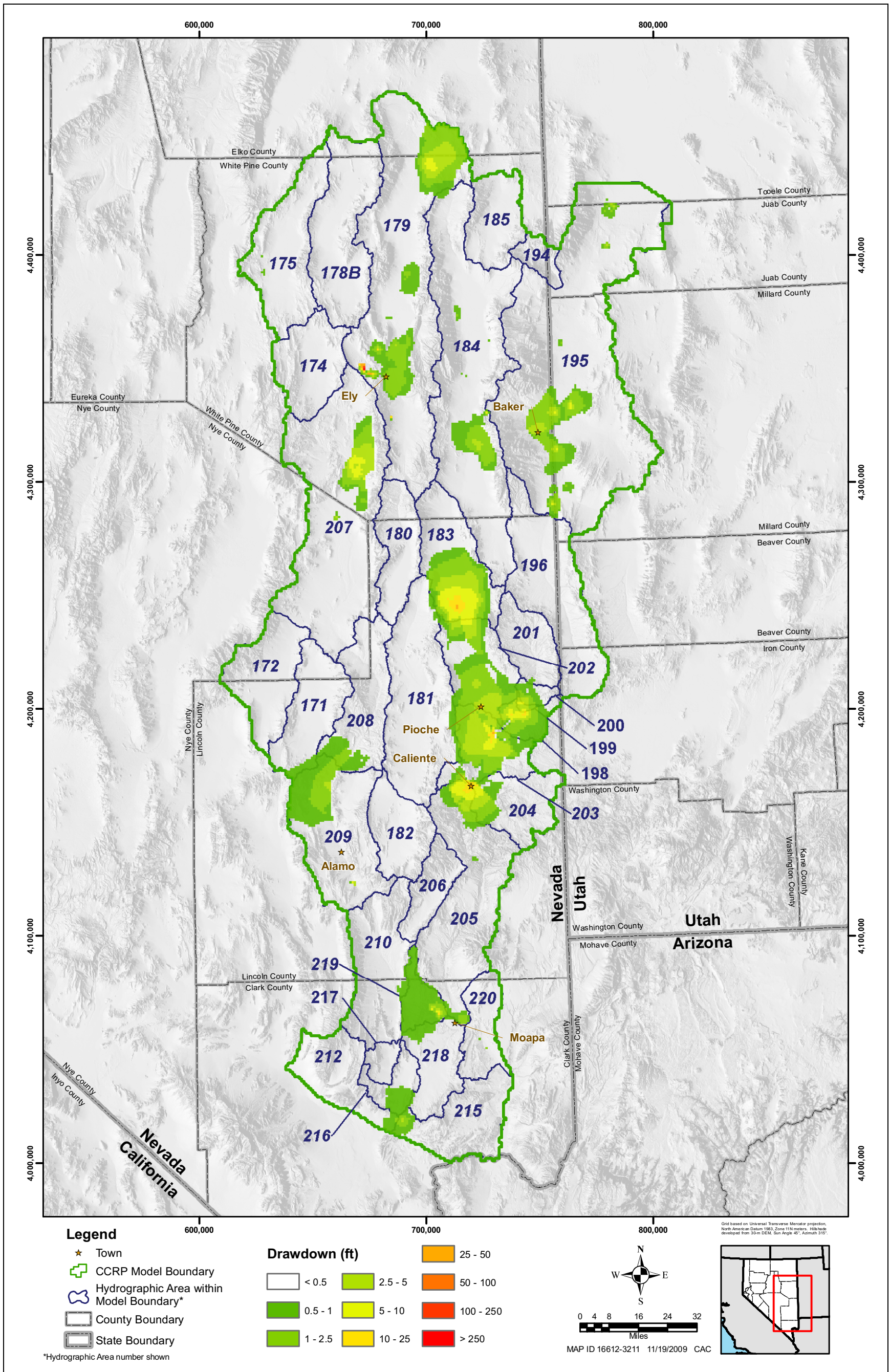
Figure 6-1
Simulated Drawdowns for End of Stress Period 61 (December 31, 2004)

JA_16340
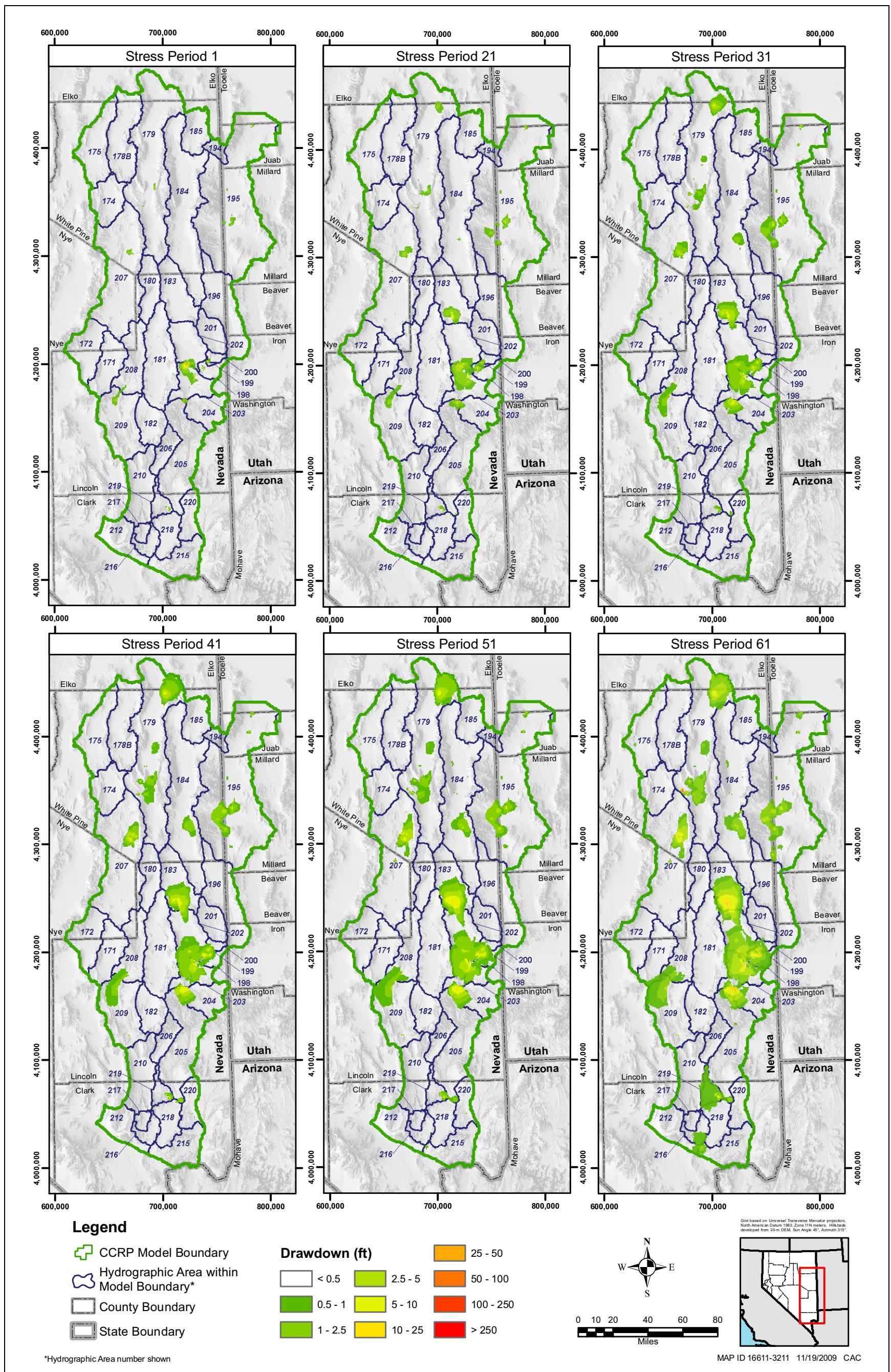
Figure 6-2
Simulated Progression of Drawdowns

Legend

CCRP Model Boundary

Hydrographic Area within Model Boundary*

County Boundary

State Boundary

*Hydrographic Area number shown

Drawdown (ft)

< 0.5	25 - 50
0.5 - 1	2.5 - 5	50 - 100
1 - 2.5	5 - 10	100 - 250
	10 - 25	> 250

0 10 20   40   60   80
Miles

Grid based on Universal Transverse Mercator projection, North American Datum 1983, Zone 11N meters. Hillshade developed from 30-m DEM. Sun Angle 45°, Azimuth 315°.

MAP ID 16611-3211   11/19/2009   CAC

SE ROA 50940

JA_16341

Figure 6-3
Simulated and Observed Drawdowns for Well (C-11-17) 1bdc 2
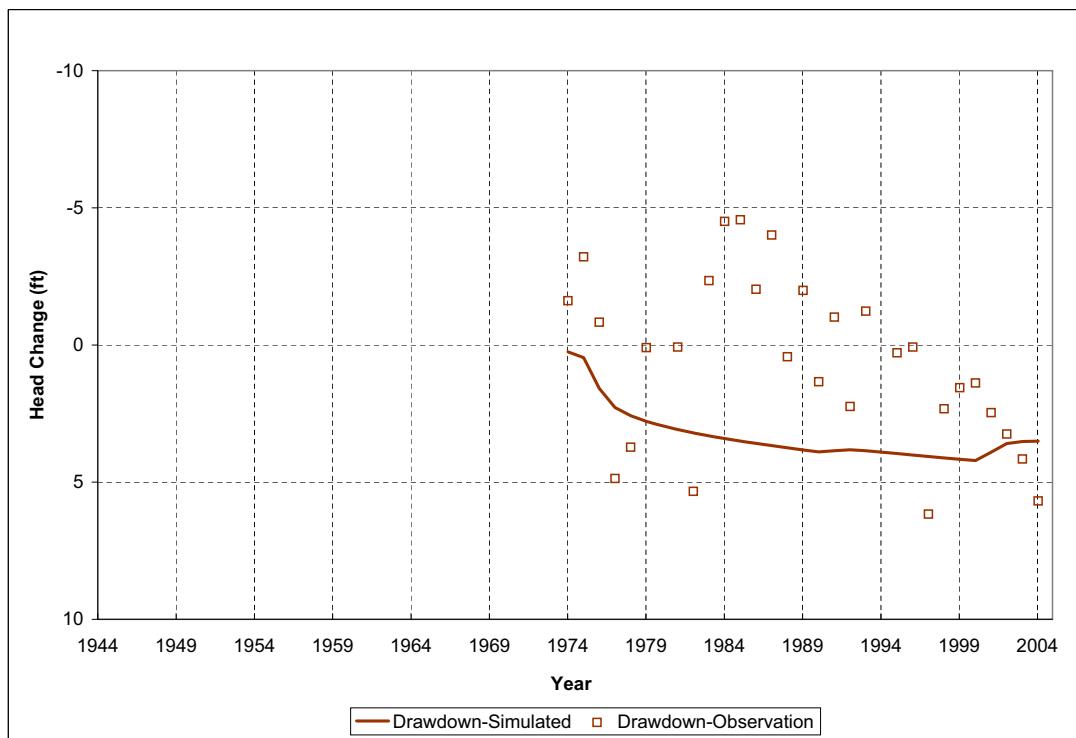
Figure 6-4
Simulated and Observed Drawdowns for Well (C-20-20) 12acc 1
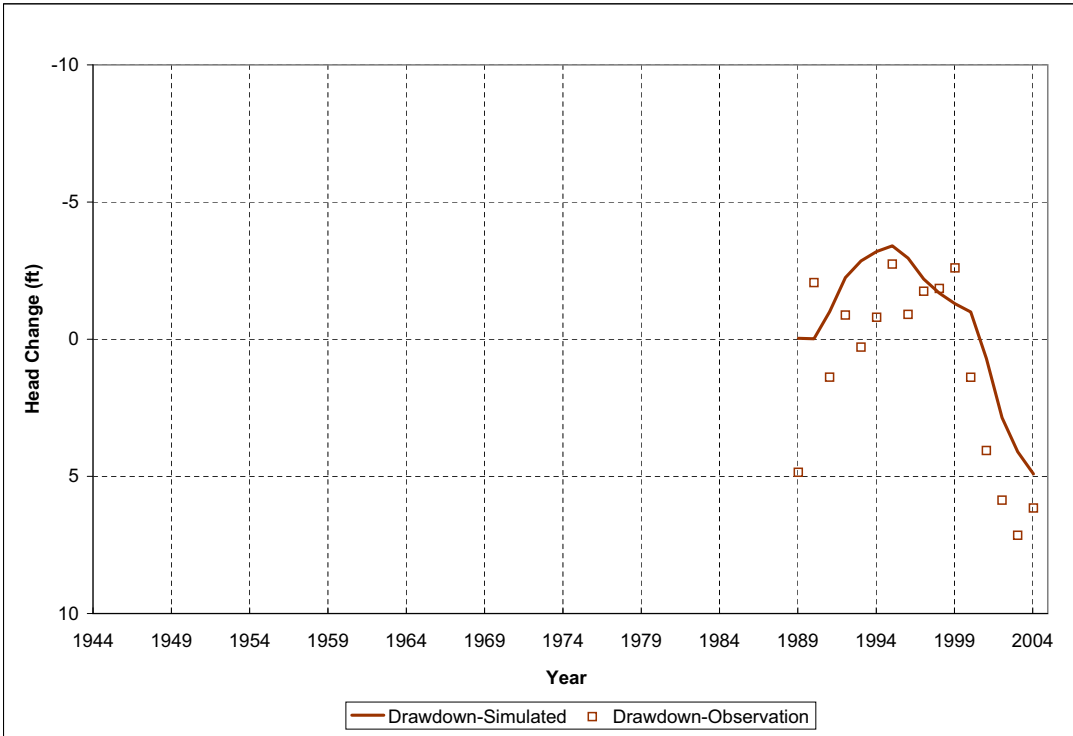
Figure 6-5
Simulated and Observed Drawdowns for Well Behmer-MW
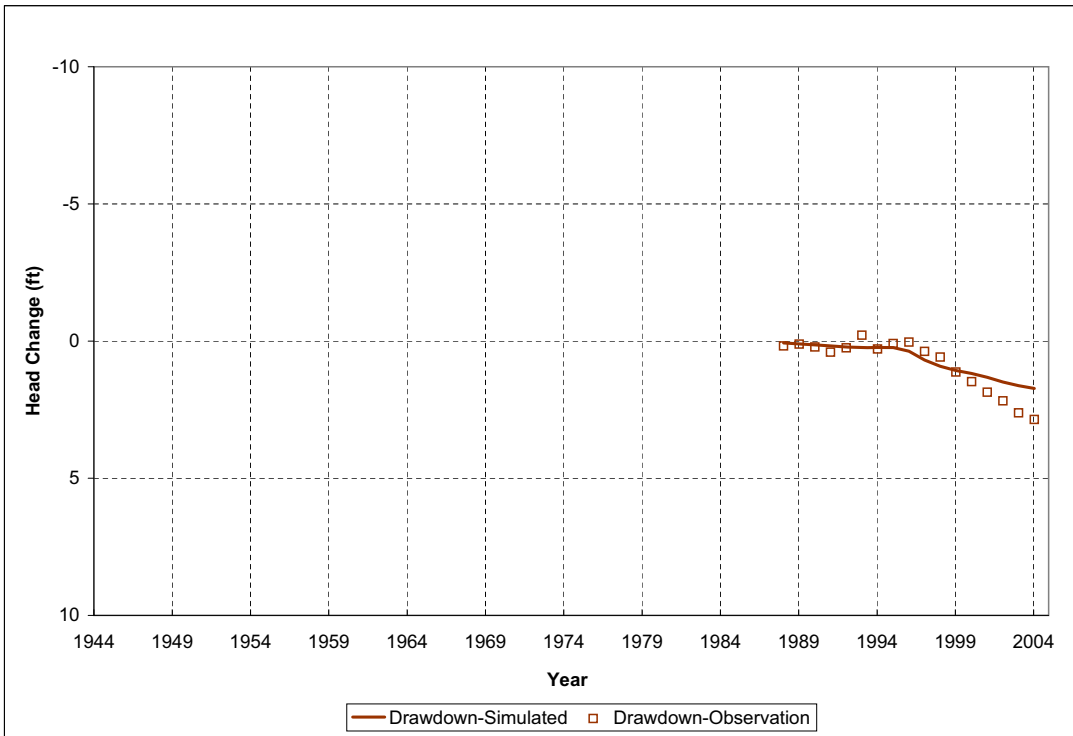
Figure 6-6
Simulated and Observed Drawdowns for Well 219 S14 E65 21AC 1 EH-4

JA_16343
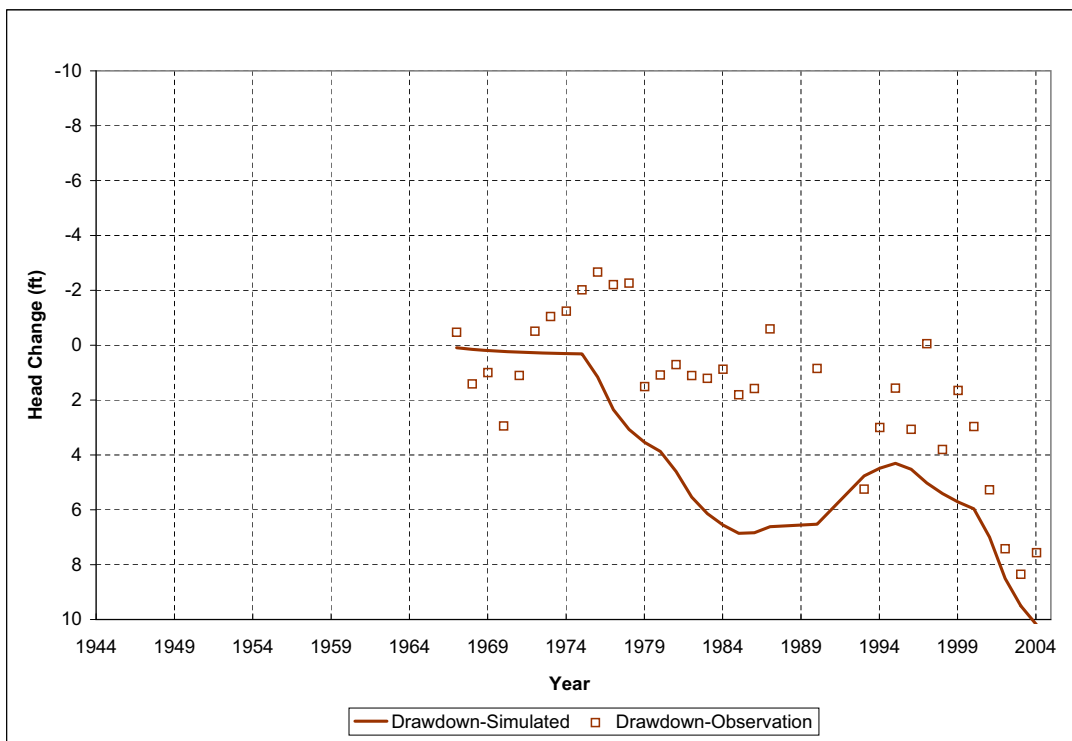
Figure 6-7
Simulated and Observed Drawdowns for Well 219 S14 E65 23BB 1
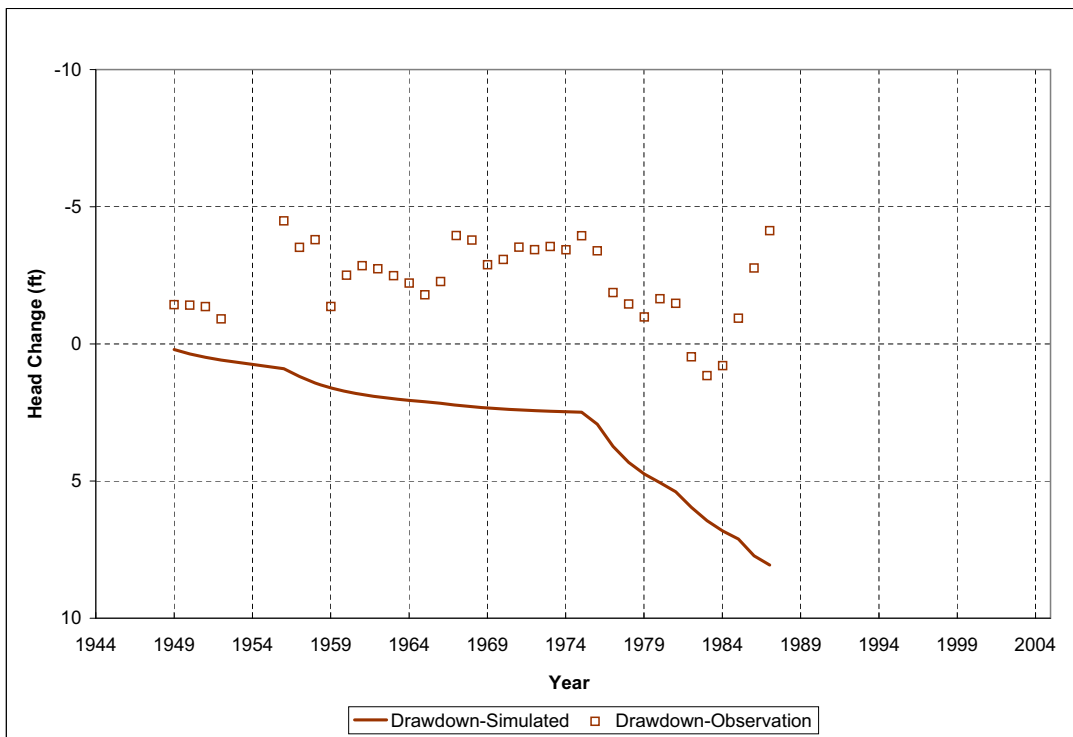
Figure 6-8
Simulated and Observed Drawdowns for Well 219 S14 E65 23ABBB 1

residuals are described and presented in figures in the following sections. More detailed versions of these figures are also included on the DVD.

6.1.2.2 Unweighted Residuals

Statistics for the unweighted residuals associated with the observations are presented in Table 6-2. Such statistics are listed for boundary flux, stream gage flow, ground-surface elevation, groundwater ET discharge, spring flow, well head, and well drawdown.

Table 6-2
Unweighted Observed versus Simulated Observation Statistics

Observation Type	Units	Number of Samples	Mean Error	Mean Absolute Error	Root Mean Square Error	Standard Deviation	Target Data Range	RMSE/ Range	Expected Error Size with Increasing Target Size[a]
Boundary Flux	afy	16	1,169	1,703	2,273	2,013	20,000	11%	Increasing
Gage Flow[b]	afy	140	255	1,211	1,687	1,674	35,672	5%	Increasing
Ground Surface[c]	ft	2,145	(0)	0	5	5	---	NA	Constant
Regional ET Discharge	afy	108	(250)	1,769	2,912	2,915	69,431	4%	Increasing
Spring Flow[d]	afy	48	(685)	816	1,666	1,534	13,027	13%	Increasing
Well Drawdown	ft	4,301	(1)	4	9	9	238	4%	Constant
Well Head	ft	2,707	15	45	91	90	6,461	1%	Constant

NA = Not Applicable
[a]The error associated with hydraulic head would be expected to be constant with elevation. The error associated with spring flow would be expected to increase with larger flows.
[b]Ash, Big, Crystal, and Hiko springs measurements removed from gage statistics.
[c]Because all ground-surface measurements were expected to be 0.0 (no mounding), the target data range is 0.0, and RMSE/Range cannot be calculated.
[d]Ash, Big, Crystal, and Hiko springs measurements added to spring statistics.

Note that for observations such as hydraulic head and drawdown, average error is a useful metric across the full range of data. The error in the model would be expected to be similar at low, intermediate, and high elevations in the model. The average error for observations such as spring or stream flow, however, may be less useful. For example, similar errors would be expected for a spring with flows of 0.01 cfs and another with 100 cfs. For some observations, the magnitude of the error should be fairly constant through the target data range (minimum to maximum observed value). For other data types, the magnitude of the error would be expected to grow with the size of the observation.

Figure 6-9 illustrates the spatial distribution of unweighted hydraulic-head residuals. Unweighted residuals were calculated as observed hydraulic head minus simulated hydraulic head. Thus, unweighted residuals provide a direct comparison of the observed to the simulated hydraulic heads. As shown in Figure 6-9, large unweighted residuals are generally distributed across the model domain, located within mountain ranges or at the mountain-block/valley bottom margin. Some spatial bias, however, is illustrated with the unweighted residuals, including overestimates of

SE ROA 50944

JA_16345

HA Number	HA Name
171	Coal Valley
172	Garden Valley
174	Jakes Valley
175	Long Valley
178B	Butte Valley (Southern Part)
179	Steptoe Valley
180	Cave Valley
181	Dry Lake Valley
182	Delamar Valley
183	Lake Valley
184	Spring Valley
185	Tippett Valley
194	Pleasant Valley
195	Snake Valley
196	Hamlin Valley
198	Dry Valley
199	Rose Valley
200	Eagle Valley
201	Spring Valley
202	Patterson Valley
203	Panaca Valley
204	Clover Valley
205	Lower Meadow Valley Wash
206	Kane Springs Valley
207	White River Valley
208	Pahroc Valley
209	Pahranagat Valley
210	Coyote Spring Valley
212	Las Vegas Valley
215	Black Mountains Area
216	Garnet Valley
217	Hidden Valley (North)
218	California Wash
219	Muddy River Springs Area
220	Lower Moapa Valley

Legend

Unweighted Hydraulic-Head Residuals (ft)

- -440 to -200
- -200 to -50
- -50 to 50
- 20 to 200
- 200 to 955

CCRP Model Boundary

Hydrographic Area within Model Boundary*

State Boundary

County Boundary

*Hydrographic Area (HA) number shown corresponds to HA number and name provided in inset table.

0   10   20   30
Miles

Projection: Universal Transverse Mercator, NAD83, Zone 11N. Hillshade developed from 30-m DEM, Sun Angle 45°, Azimuth 315°.

MAP ID 16867-3211   11/19/2009   JAB

**Figure 6-9
Spatial Distribution of Unweighted Hydraulic-Head Residuals**

SE ROA 50945

JA_16346

hydraulic head (negative residuals) in Pahroc Valley and Dry Lake V alley and underestimates (positive residuals) in northern Cave Valley and Spring Valley.

Caution should be used when evaluating unweighted residuals because observation uncertainty is not considered in the calculation of the residual. Observation uncertainty can include many factors and can be significant in some cases. Appendix B describes the rigorous process used in developing the hydraulic-head observation data set, which includes observation uncertainty. The observation uncertainty is used by UCODE_2005 in the regression process. In simple terms, observations with large uncertainty are considered less important in the regression. Thus, evalua tion of unweighted residuals without consideration of observation uncertainty can lead to misleading interpretations.

6.1.2.3 *Spatial Distribution of Weighted Residuals*

Figure 6-10 illustrates the spatial distribution of unweighted drawdown residuals. The spatial distributions of the weighted r esiduals of hydrau lic heads and dra wdowns are evaluated separately and then in combination.

Figure 6-11 illustrates the spatial distribution of weighted hydraulic-head residuals. Less spatial bias is observed with weighted residual hydraulic hea ds as compare d to unweighted residual hydraulic heads. This spatial distribution shows that wells with poorer model fit are generally scattered across the model domain or are located predominantly within mountain ra nges or a t the mountain-block/valley bottom margins. Spa tial bias, however, is sti ll observed in P ahroc and Dry Lake valleys.

Figure 6-12 illustrates the spatial distribution of weighted drawdown residuals. Overpredicted drawdown is evident in northern White River Valley, southern Lake Valley, Dry Valley, and Panaca Valley. Spatial bias is observed in Pahroc and Dry Lake valleys.

Figure 6-13 illustrates the spatial distribution of the S oSWR by well. The SoSWR by well statistic was developed to provide a single residual per well. The SoSWR by well statistic sums the squares of weighted residuals for hydra ulic heads a nd drawdowns at each well. In other wor ds, all weighted hydraulic-head and dra wdown residuals are included in the S oSWR by well. As shown in Figure 6-13, the spatial distributi on shows tha t wells with poorer model fit are generally located in isolated areas, predominantly within mountain ranges or at the mountain-block/valley bottom margin. Areas with large SoSWR include central Steptoe Valley, central Cave Valley, southern Lake Valley, northern Coal Valley, central Delamar Valley, southern Patterson Valley, and extre me southern Hamlin Valley. In many cases, these ranges may represent areas where potentially and/or locally controlled water levels were used in the model a s hydraulic-head targets to represent regional groundwater conditions.

6.1.3 *Evaluation of Simulated Flows*

Evaluation of the si mulated flows to observe d ranges using graphical methods is provided in t his section. Simulated flows include flow into and out of external boundaries, groundwater discharge by ET, discharge by springs, and discharge by stream flow routing.

SE ROA 50946

JA_16347
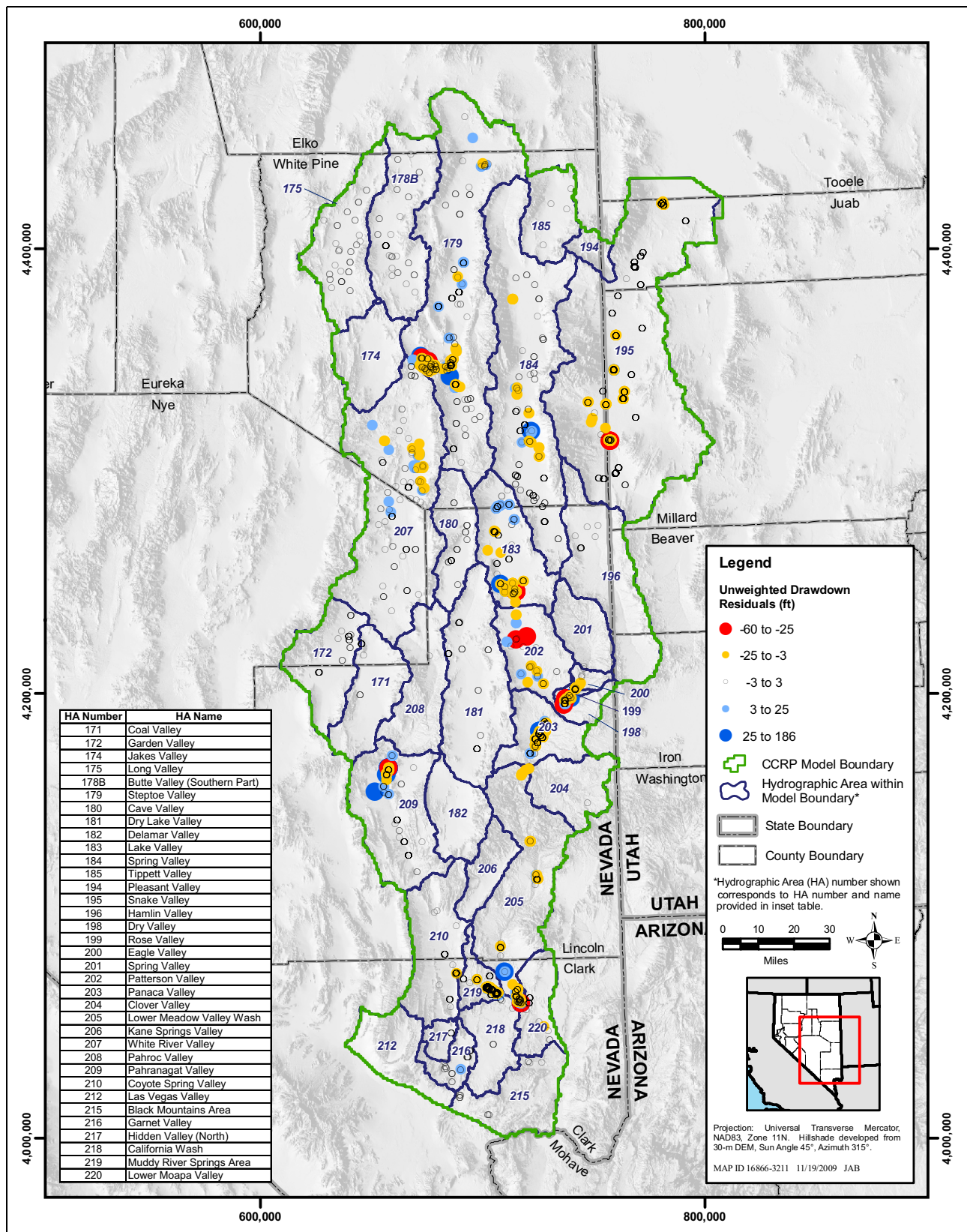
Figure 6-10
Spatial Distribution of Unweighted Drawdown Residuals

SE ROA 50947

JA_16348
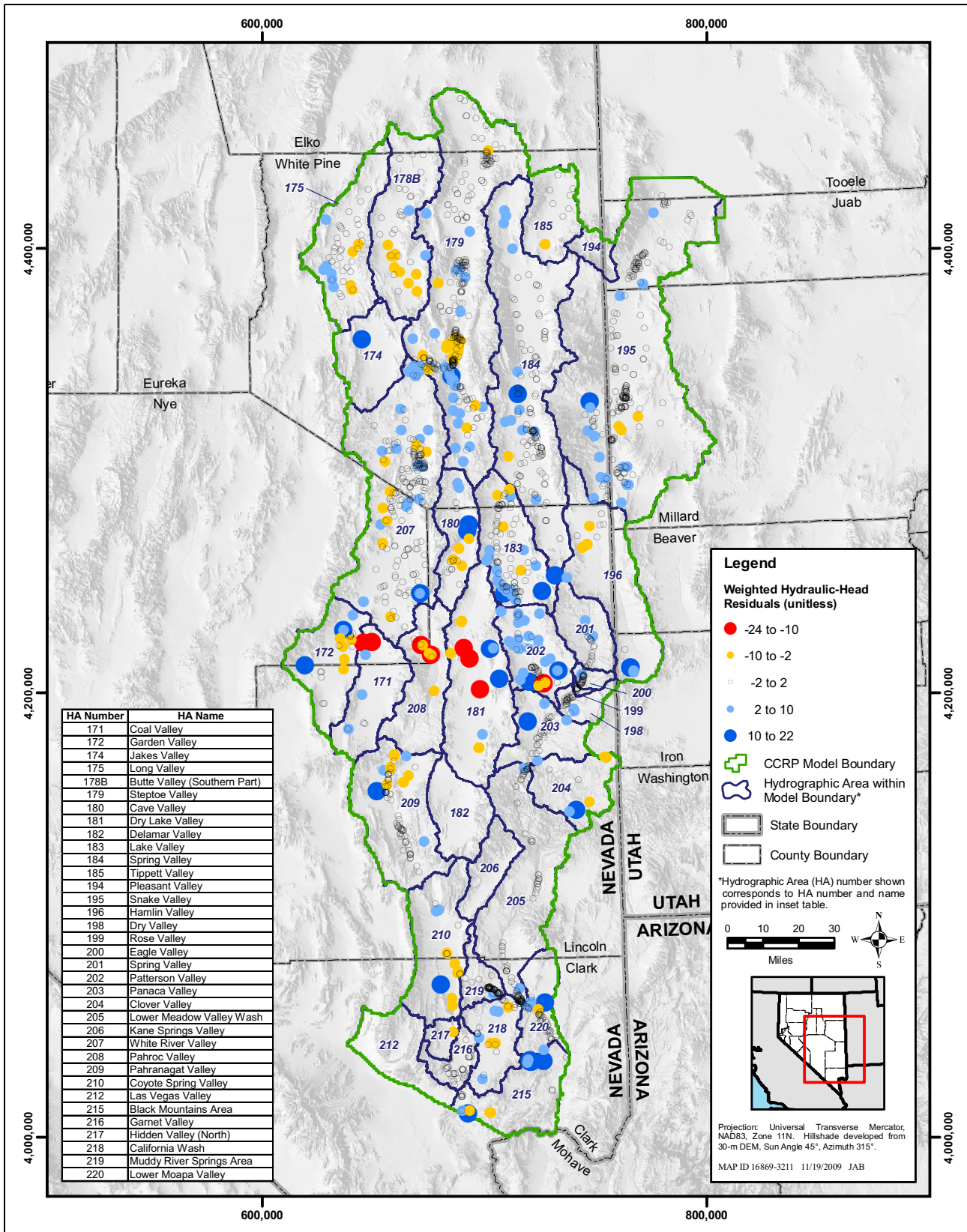
Figure 6-11
Spatial Distribution of Weighted Hydraulic-Head Residuals
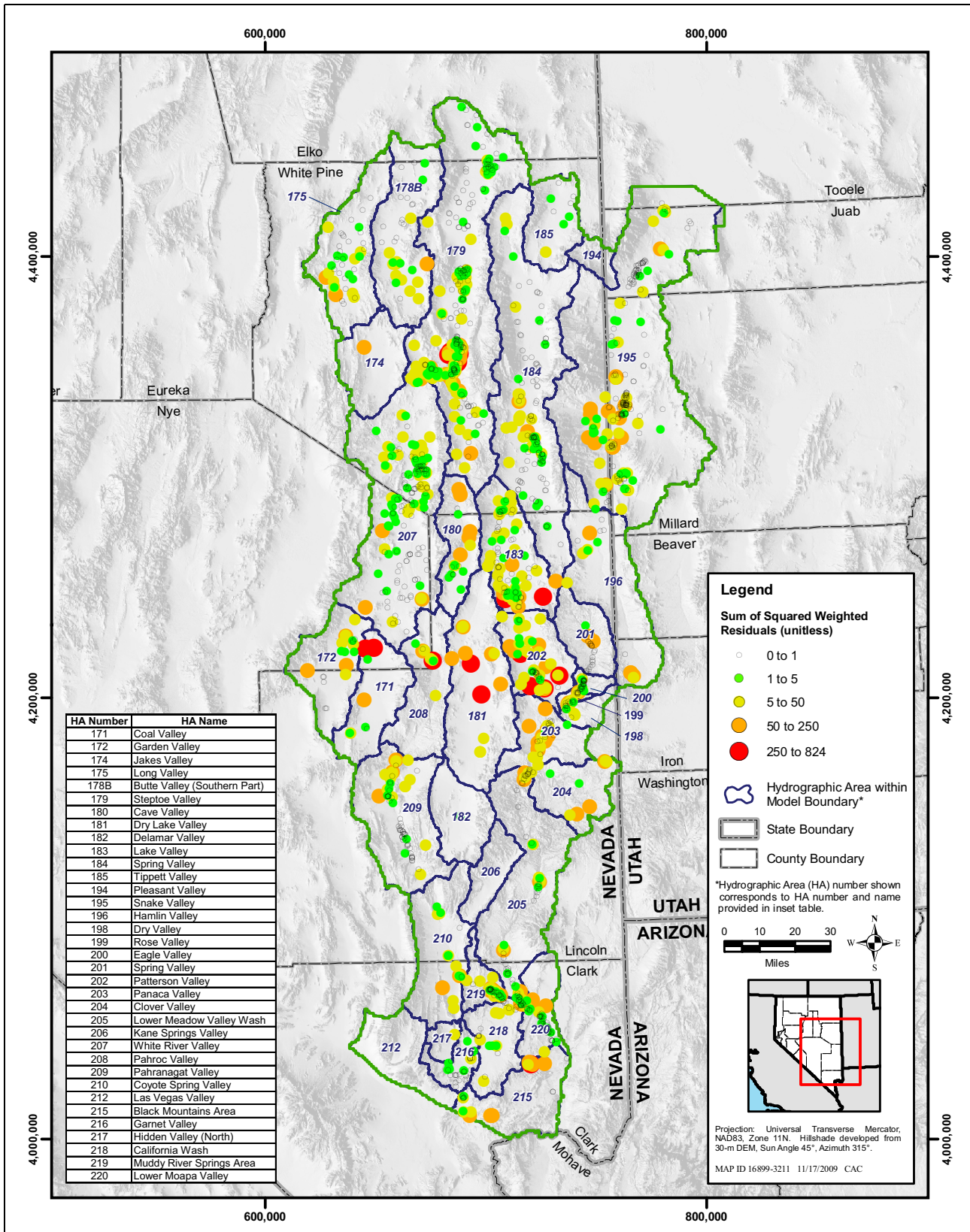
Figure 6-13
Spatial Distribution of SoSWR for Wells

SE ROA 50950

JA_16351

6.1.3.1   External Boundary Flow

This section describes the simulated steady-state groundwater flows through external boundaries in the calibrated numerical model and their comparison to estimates provided in the Conceptual Model Report (SNWA, 2009a) for predevelopment conditions.

The final CHD parameters, while being some of the most sensitive parameters in the numerical model, were not optimized. These parameters were manually calibrated. This calibration was done because the hydraulic heads were reasonably well known or because the lack of observation constraints near the boundary caused limited application of model parameter estimation. The final hydraulic heads used at each constant-head boundary are defined in Table 6-3.

Table 6-3
Final Constant-Head Boundary (CHD) Values (Manually Estimated)

Parameter Name	Flow-Boundary Segment Name	Final CHD Parameter Value[a] (-)	Calibrated Constant-Head Values ft (m)
C_BUTTE	Butte Valley	1.021	6,211 (1,893)
C_COYOTE	Coyote Spring Valley	1	2,362 (720)
C_FISH	Fish Springs Flat (Depth)	0.988	4,287 (1,307)
C_FISH_G	Fish Springs Flat (Ground Layer)	1	4,291 (1,308) – 4,335 (1,321)
C_GARDEN	Garden Valley	1	4,806 (1,465)
C_LK_MEAD	Lake Mead	1	1,169 (356.43)
C_LASVEGAS	Las Vegas Valley	1	2,329 (710)
C_LONG_NW	Long Valley (NW)	0.99	6,139 (1,871)
C_LONG_SW	Long Valley (SW)	0.97	5,789 (1,764)
C_PAHRANAG	Pahranagat Valley	0.985	3,167 (980) – 3,264 (995)
C_CONFUSON	Snake Valley (Confusion Range)	1.01	4,709 (1,435)
C_NSNAKE	Snake Valley (North; Depth)	0.983	4,266 (1,300)
C_NSNAKE_G	Snake Valley (North; Ground Layer)	1	4,267 (1,301)
C_E_SSNAKE	Snake Valley (Southern - East)	0.99	4,944 (1,507)
C_W_SSNAKE	Snake Valley (Southern - West)	1.005	5,045 (1,538)
C_NSTEPTOE	Steptoe Valley	1	5,627 (1,715)
C_TIPPETT	Tippett Valley	1	5,508 (1,679)

[a]The CHD parameters are factors used to adjust the constant heads at the boundary during calibration.

Figures 6-14 through 6-16 present the simulated and estimated target flows through external model boundaries by flow system, hydrographic area, and individual flow-boundary segment. Intervals of ±2 standard deviations are shown on these figures to illustrate the uncertainties associated with the targets. A negative sign indicates flow out of the numerical model domain; a positive sign indicates flow into the numerical model domain. Table 6-4 lists the simulated and estimated target external boundary fluxes. The boundary fluxes are within the expected flow range (Table 6-4).
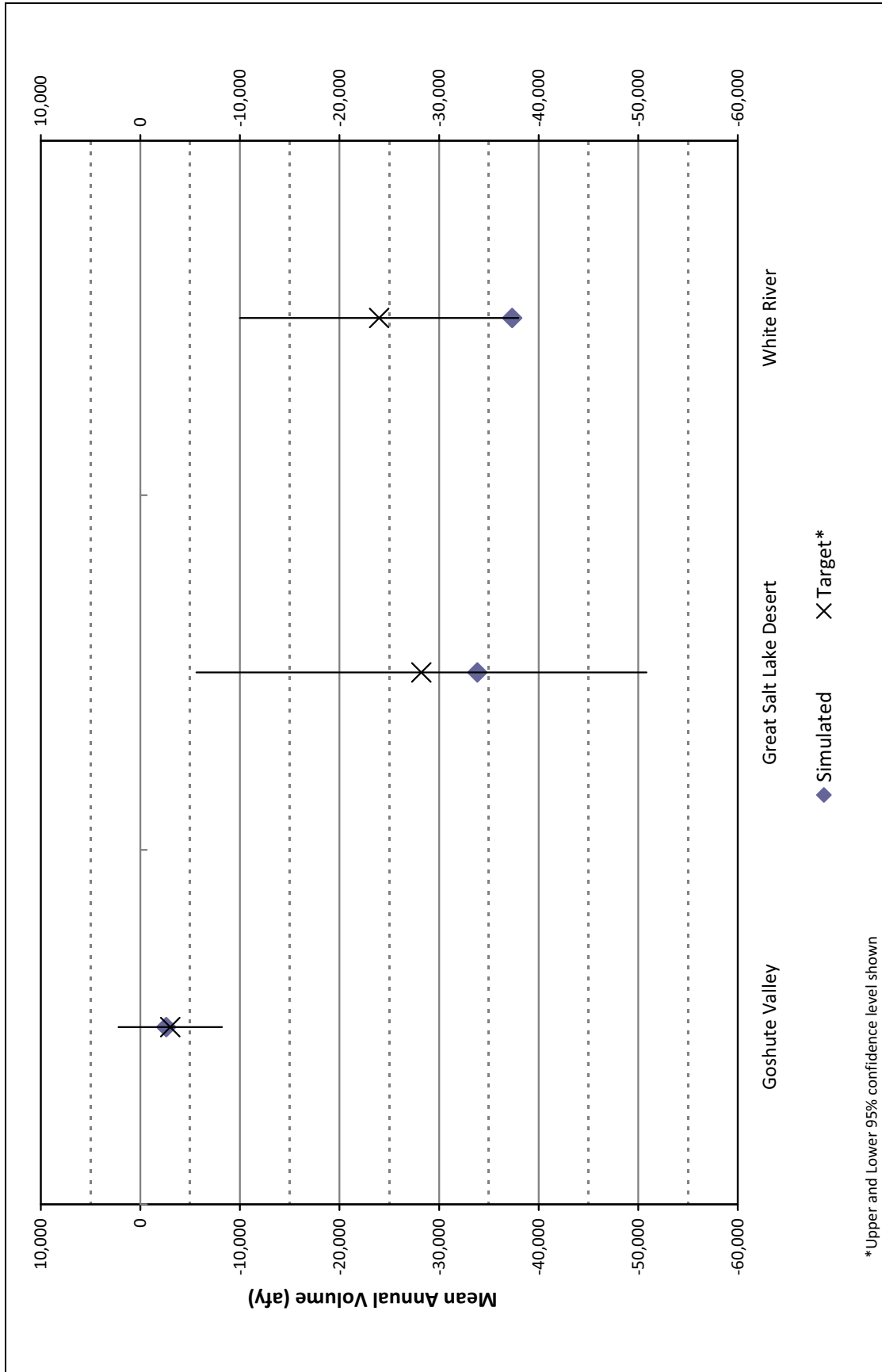
Figure 6-14
Groundwater Flow through External Boundaries for Flow Systems Simulated and Target with ±2 Standard Deviations
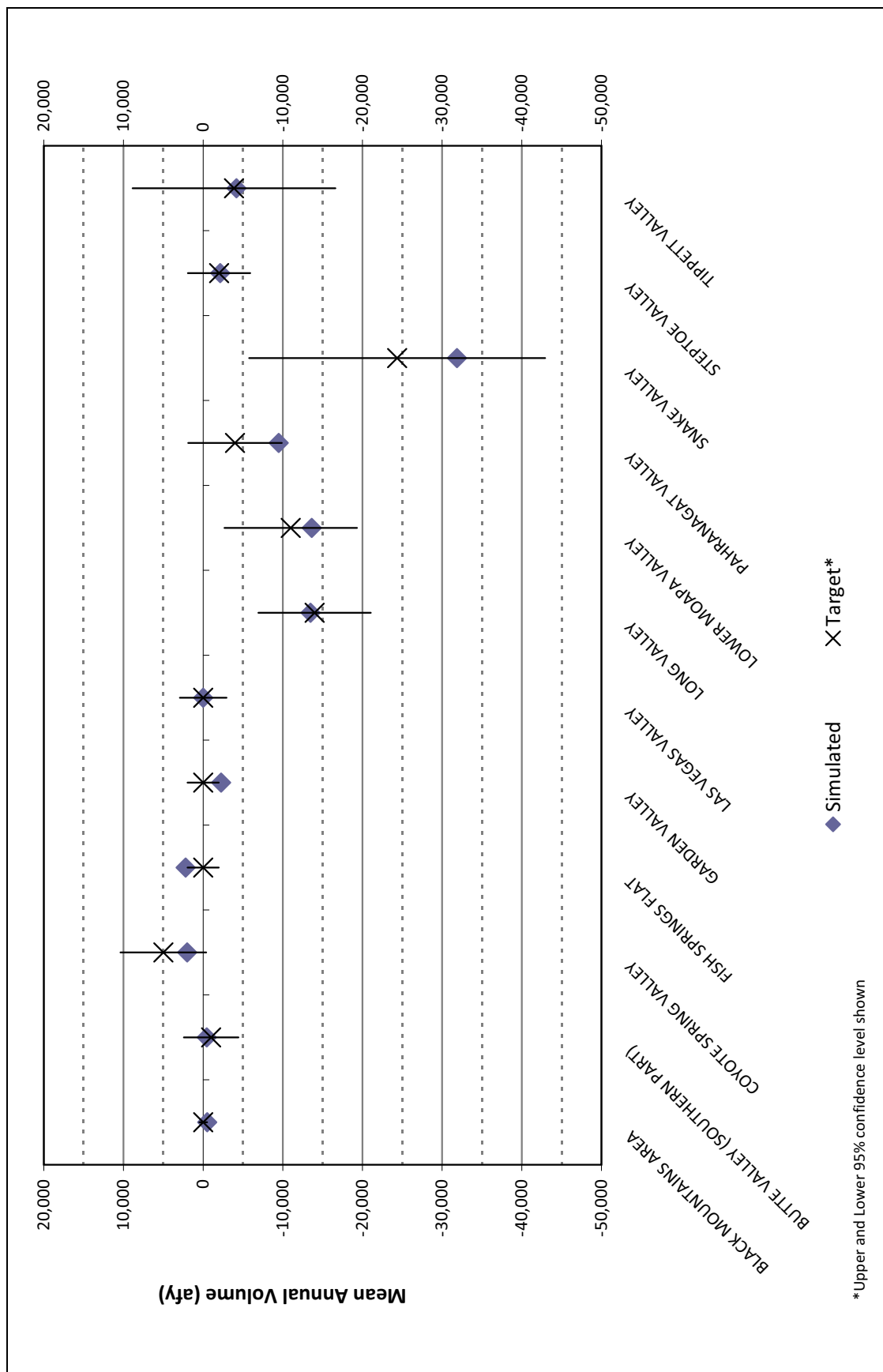
Note: Negative sign indicates flow out of model.

*Upper and Lower 95% confidence level shown

**Figure 6-15
Groundwater Flow through External Boundaries for Hydrographic Areas
Simulated and Target with ±2 Standard Deviations**

Note: Negative sign indicates flow out of model.

*Upper and Lower 95% confidence level shown

Figure 6-16
Groundwater Flow through External Boundaries for Individual Flow Boundaries Simulated and Target with ±2 Standard Deviations

Mean Annual Volume (afy)

◆ Simulated   ✕ Target*

*Upper and Lower 95% confidence level shown

Note: Negative sign indicates flow out of model.

B_BUTTE_001
B_CONFUS_001
B_COYOTE_001
B_FISH_001
B_GARDEN_001
B_LASVEG_001
B_LM_BM_001
B_MOAPA_001
B_LONGNW_001
B_LONGSW_001
B_NSNAKE_001
B_STEPTO_001
B_PAHRAN_001
B_SNAKEE_001
B_SNAKEW_001
B_TIPPET_001

SE ROA 50954

JA_16355

Table 6-4
Simulated and Target Values for Groundwater Flow
through External Boundaries

Flow System	HA Name	Observation Name	Simulated Value afy (m^3/d)	Target Value afy (m^3/d)
Goshute Valley	Butte Valley (Southern Part)	B_BUTTE_001	-472 (-1,592)	-1,000 (-3,377)
	Steptoe Valley	B_STEPTO_001	-2,145 (-7,245)	-2,000 (-6,754)
Great Salt Lake Desert	Fish Springs Flat	B_FISH_001	2,200 (7,428)	0 (0)
	Snake Valley	B_CONFUS_001	-15,127 (-51,085)	-15,000 (-50,656)
		B_NSNAKE_001	-13,354 (-45,097)	-9,375 (-31,660)
		B_SNAKEE_001	-2,053 (-6,933)	0 (0)
		B_SNAKEW_001	-1,387 (-4,684)	0 (0)
	Tippett Valley	B_TIPPET_001	-4,170 (-14,082)	-3,874 (-13,083)
White River	Black Mountains Area	B_LM_BM_001	-512 (-1,729)	0 (0)
	Coyote Spring Valley	B_COYOTE_001	2,004 (6,768)	5,000 (16,886)
	Garden Valley	B_GARDEN_001	-2,254 (-7,612)	0 (0)
	Las Vegas Valley	B_LASVEG_001	-1 (-5)	0 (0)
	Long Valley	B_LONGNW_001	-449 (-1,516)	-2,000 (-6,754)
	Lower Moapa Valley	B_MOAPA_001	-13,666 (-46,150)	-11,000 (-37,148)
	Pahranagat Valley	B_PAHRAN_001	-9,526 (-32,169)	-4,000 (-13,508)

Note: Negative sign indicates flow out of model; simulated values are as output by model and do not imply this level of accuracy, values were not rounded for tracking purposes.

It should be noted that external boundaries in Long and Pahranagat valleys differ from those described in the Conceptual Model Report (SNWA, 2009a). The numerical model simulates a regional flow divide at Jakes Valley (see Section 6.4 and Plates 2 and 3). Thus, an external boundary (Long Valley to Newark Valley Flow System) was necessary to simulate hydraulic heads in Long Valley. The Conceptual Model Report (SNWA, 2009a) describes the primary regional flowpath from Long Valley to Jakes Valley but also indicates the possibility that some flow may occur from Long Valley to Newark Valley.

The regional flowpath from Long Valley to Newark Valley is postulated in other investigations. The Carbonate-Rock Province (CRP) model (Prudic et al., 1995) simulates 12,700 afy from Long Valley to Newark Valley and simulates a regional divide in the Jakes Valley area. Regional potentiometric surfaces from Belcher (2004) and Welch et al. (2008) suggest the potential for some outflow to occur from Long Valley to Newark Valley. Others (Thomas et al., 2001; San Juan et al., 2004; and Thomas and Mihevc, 2007) interpret flow across this boundary to be zero or in the other direction. Because of the lack of data in this particular region, the flow patterns near this boundary are uncertain.

The numerical model also includes an external boundary between Pahranagat and Tikaboo valleys. This external boundary was not considered in the conceptual model, which is consistent with the interpretation of Eakin (1966). However, this boundary was necessary to simulate hydraulic head and discharge in Pahranagat Valley. The target outflow in Pahranagat Valley along the Pahranagat Shear

Zone was set to 4,000 afy. This target was based on estimates provided in S NWA (2009a). The numerical model simulates approximately 9,500 afy of outflow from Pahranagat Valley.

6.1.3.2   Groundwater Discharge by ET

This section discusses simulated steady-state groundwater discharge in ET areas in the calibrated numerical model. Simulated ET discharge and estimated ET targets include groundwater discharge to regional springs. Section 6.1.3.3 discusses simulated discharge from re gional and interme diate springs.

Figure 6-17 shows simul ated and estimated groundwater discharge in ET areas for flow systems. Intervals of ±2 standard deviations are shown to illustrate uncertainties of the targets. Simulated ET discharge in Goshute, Mea dow Valley, Great Salt Lake Desert, and White Ri ver flow sys tems are within 10 percent, 1 per cent, 2 percent, and less than 1 pe rcent of e stimated targets, respectively (Figure 6-17). Figure 6-18 through Figure 6-19 summarize groundwater ET by hydrographic area and sub-basin. For the entire numerical model domain, simulated groundwater discharge in ET areas (491,700 afy) is within 3 percent of the estimated target (506,500 afy).

As shown i n Figure 6-18, ET discharge in Steptoe Valley is undersimulated by approximately 8,000 afy. ET discharge (including spring discharge) in Snake Valley is undersimulated by 4,700 afy. Although different from the estimated targets, these results are within the uncertainty ranges associated with the ET-discharge estimates provided in SNWA (2009a).

As described in SNWA (2009a), groundwater discharge in Pahranagat Valley occurs as the result of both spring flow a nd ET from a shallow water table. Spring flow discharge occurs at three regional springs (Hiko, A sh, and Crystal). The target spring discharge is appr oximately 26,000 afy and the simulated value is approximately 23,800 afy. The target ET discharge, which includes spring discharge, in Pahranagat Valley is 28,500 afy and the simulated value is approximately 37,000 afy.

Figures 6-20 through 6-31 summarize simulated E T discharge by ET type for flow systems, hydrographic areas, and sub-basins, respectively. The se figures provide more detail on the components of si mulated discharge by ET type. In general, where discharge in S hrubland is oversimulated, discharge in Wetland is undersim ulated. Si milarly, where discharge in W etland is oversimulated, discharge in Shrubl and is undersimulated. Open Water and Playa represent a small component of the total discharge.

Simulated ET ra tes were computed for ea ch ET type, by m odel cell. Figure 6-32 illustrates the minimum, 25th percentile, m edian, maximum, and 75th percentile as box plots. Based on the area-weighted mean groundwater ET rates reported by SNWA (2009a) for each ET unit of each sub-basin, the expected ranges of groundwater ET by unit are:

- 1.34 to 3.46 ft/yr for Wetland
- 0.02 to 2.90 ft/yr for Shrubland
- 0.01 to 0.31 ft/yr for Playa
- 4.11 to 8.61 ft/yr for Open Water

SE ROA 50956

JA_16357
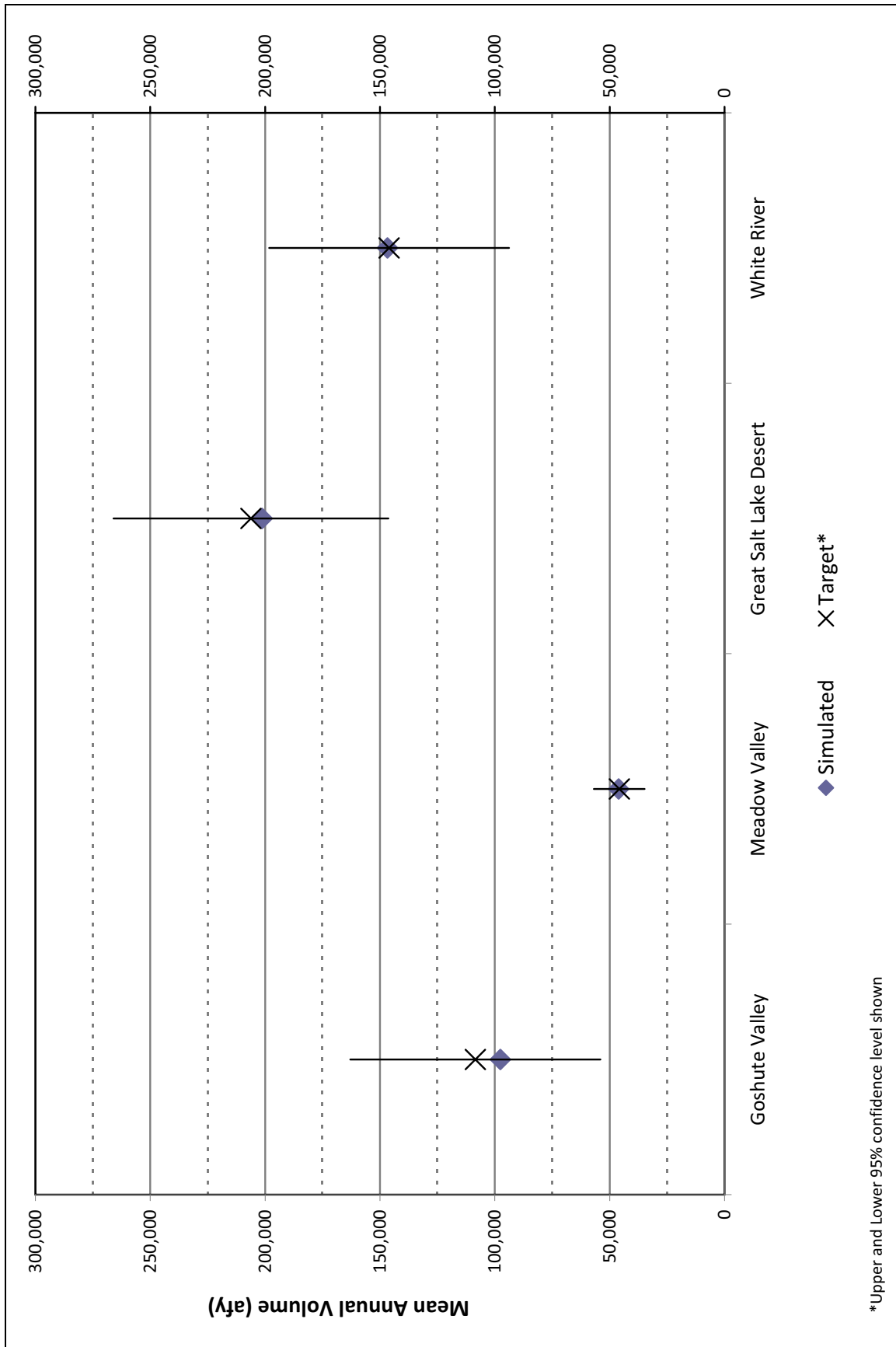
Figure 6-17
Groundwater Discharge by ET and Springs for Flow Systems
Simulated and Target with ±2 Standard Deviations
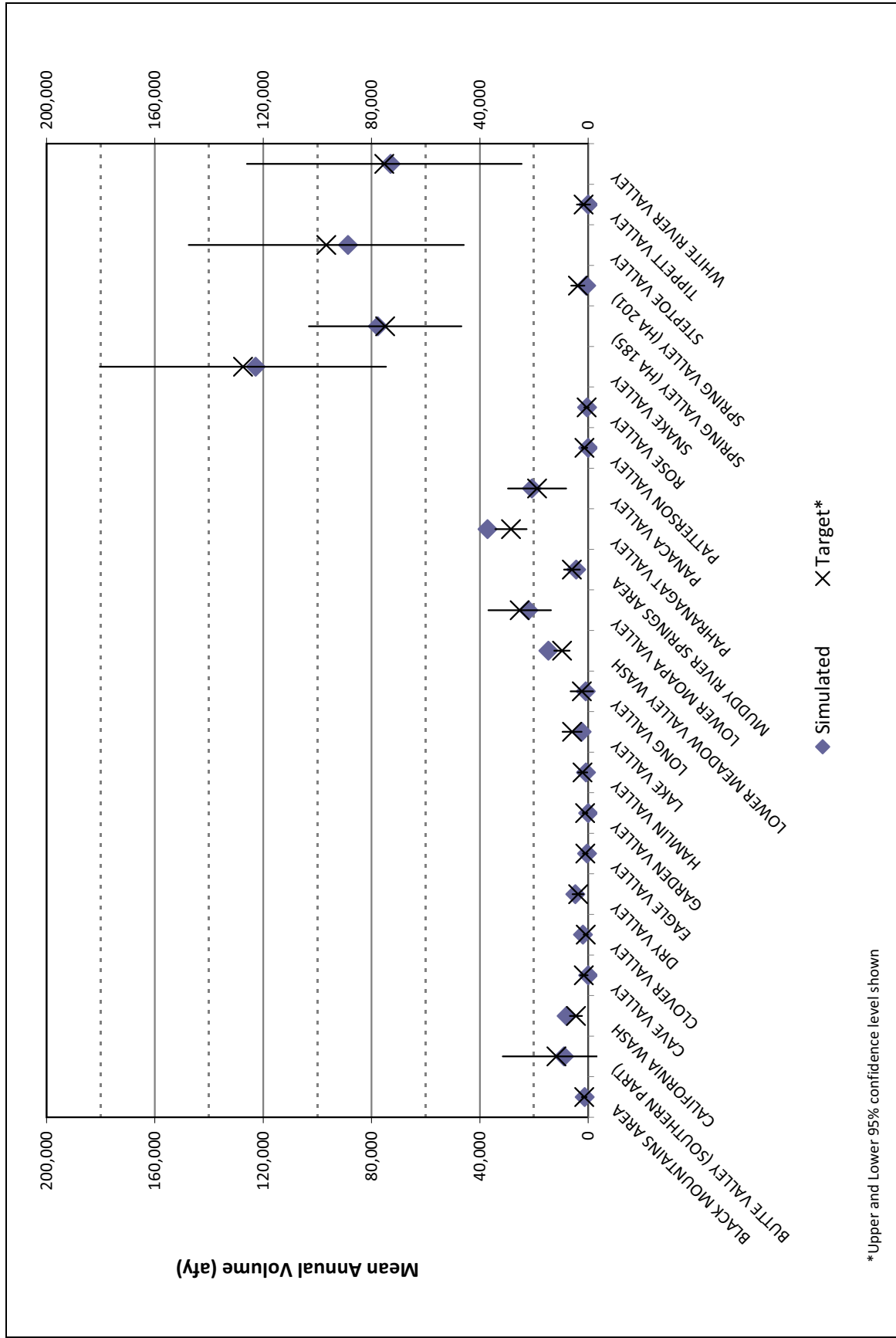
**Figure 6-18
Groundwater Discharge by ET and Springs for Hydrographic Areas
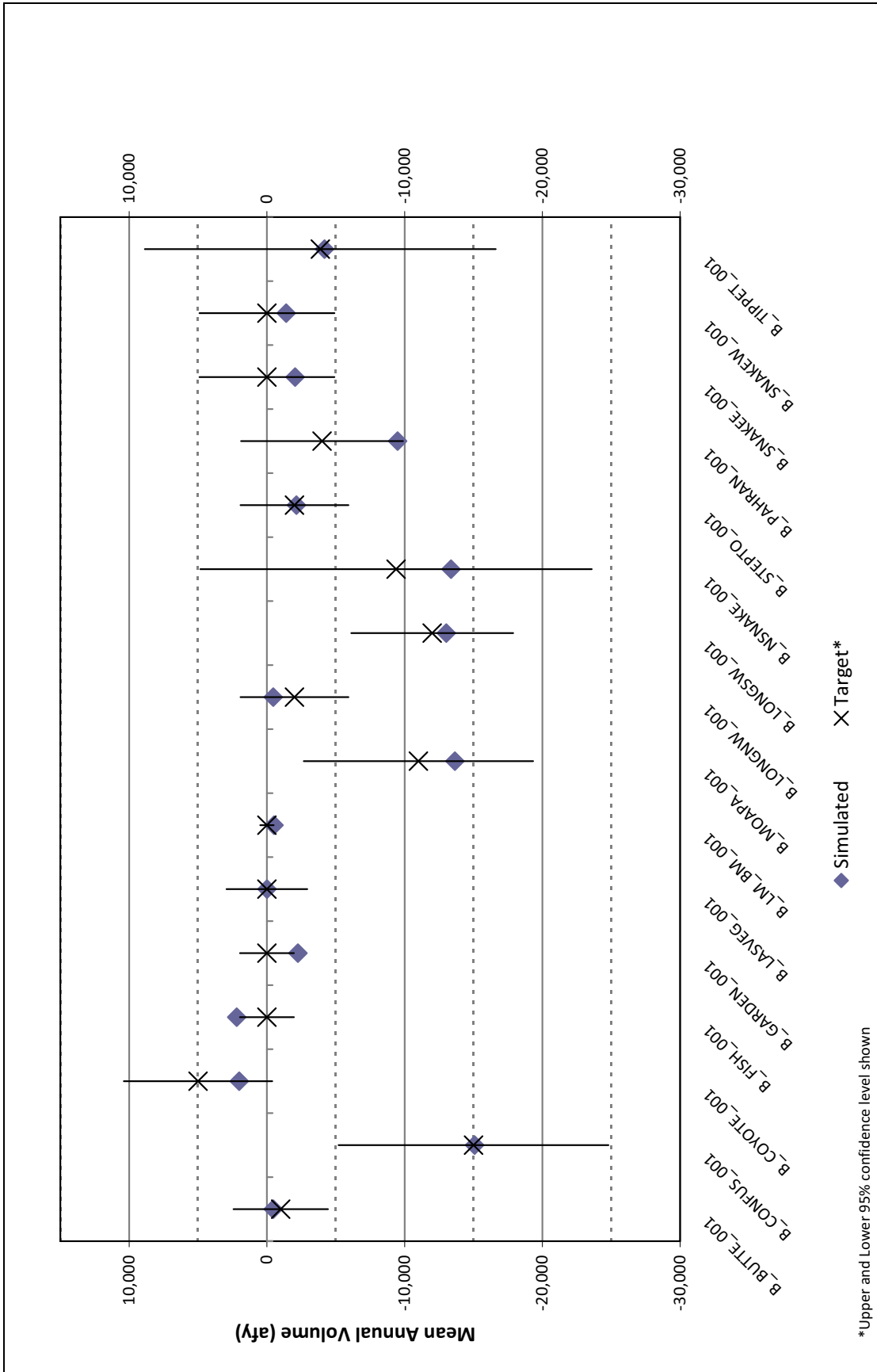Simulated and Target with ±2 Standard Deviations**

*Upper and Lower 95% confidence level shown

Section 6.0

SE ROA 50958

JA_16359
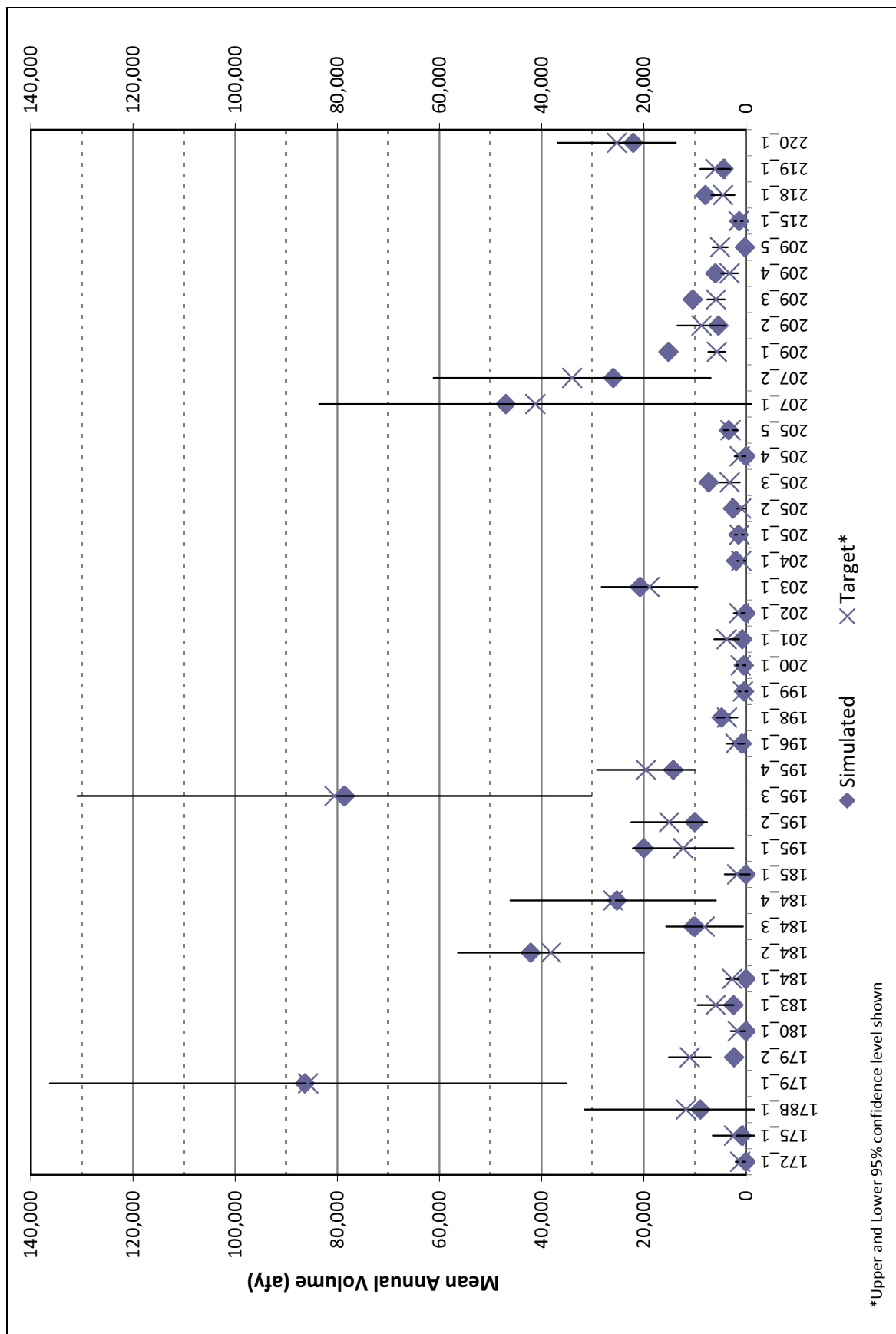
Figure 6-19
Groundwater Discharge by ET and Springs for Sub-Basins
Simulated and Target with ±2 Standard Deviations

*Upper and Lower 95% confidence level shown
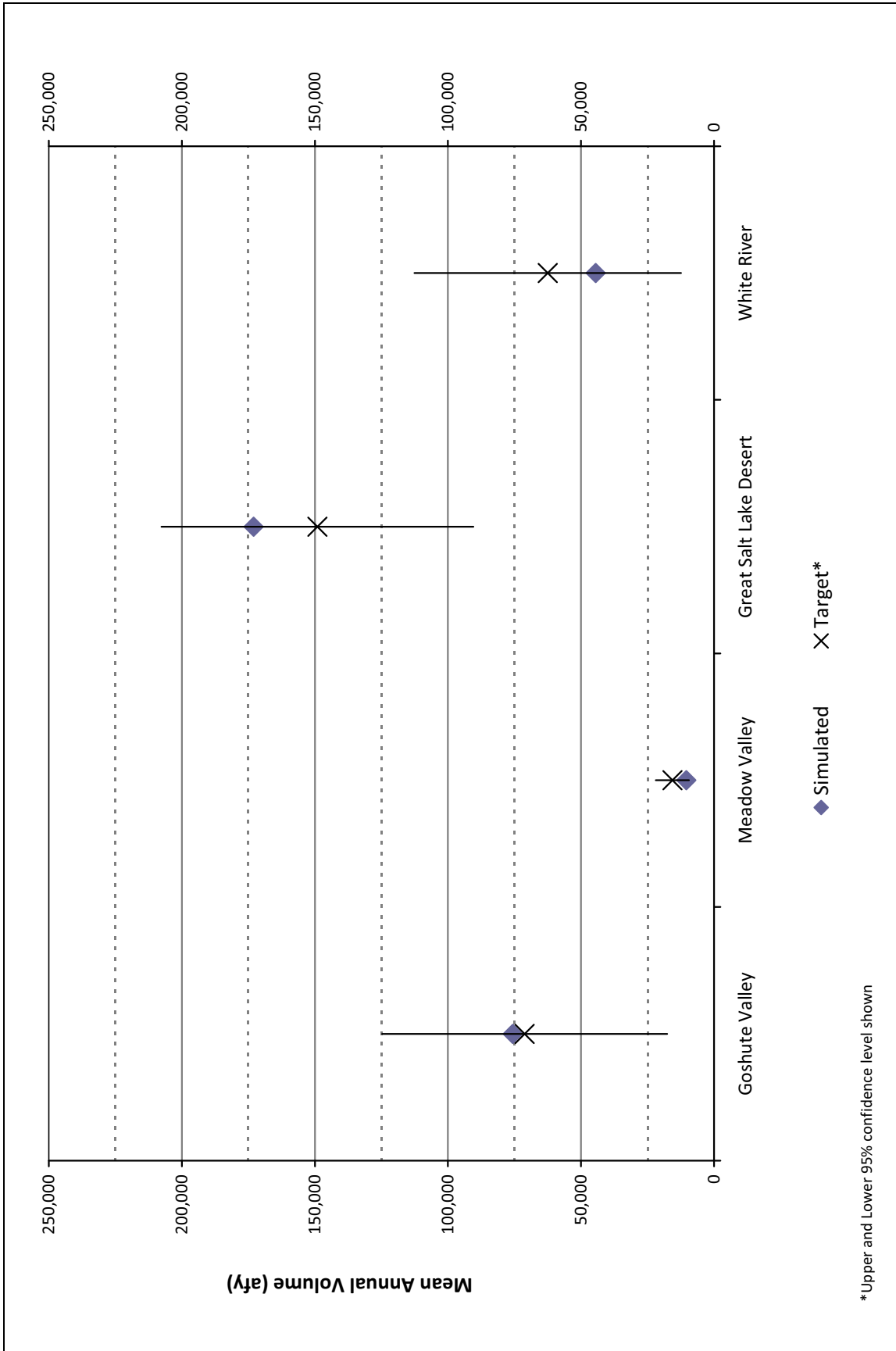
Figure 6-20
Groundwater Discharge by ET and Springs in Flow Systems for Shrubland Simulated and Target with ±2 Standard Deviations

*Upper and Lower 95% confidence level shown

JA_16361
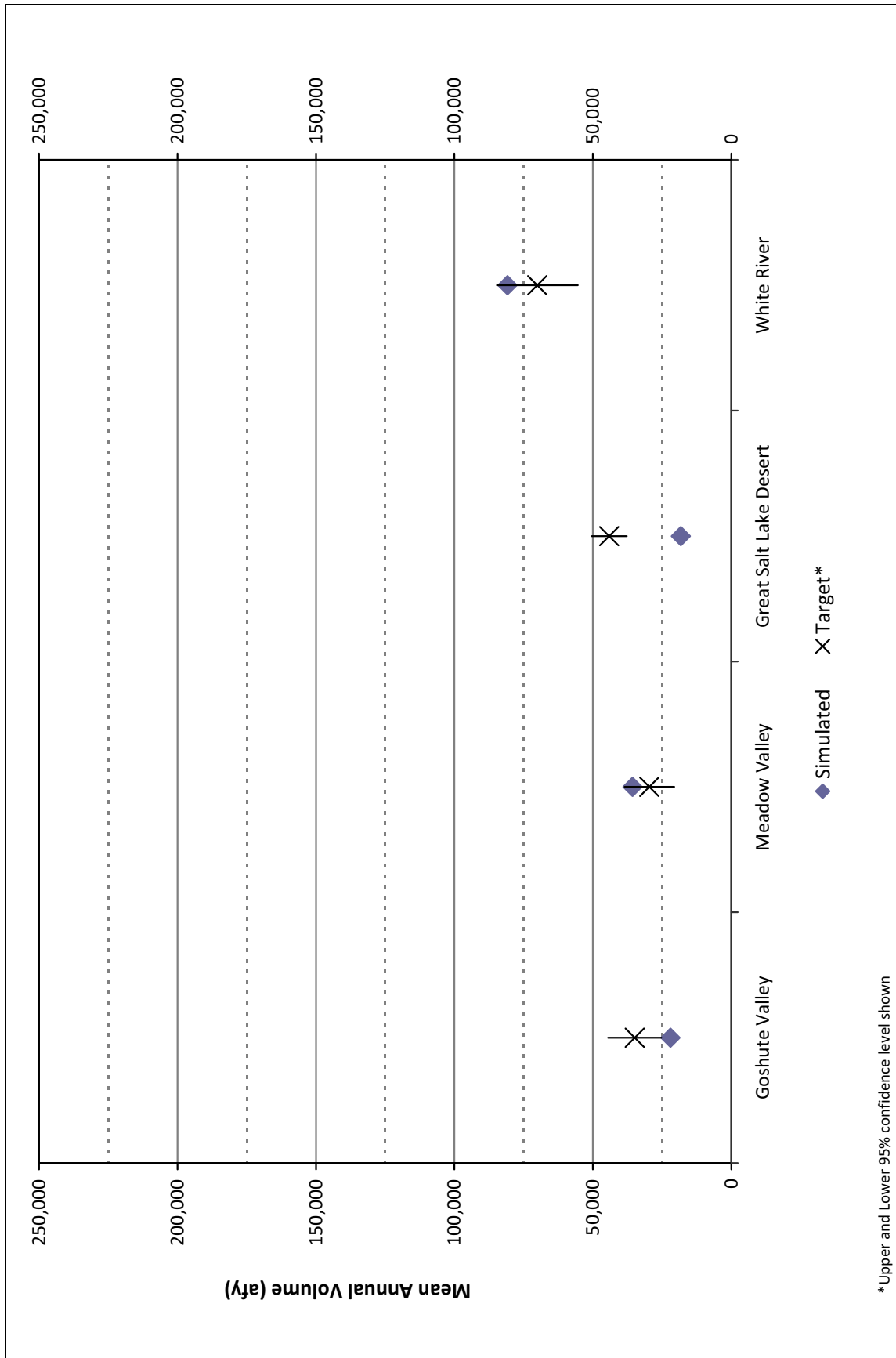
Figure 6-21
**Groundwater Discharge by ET and Springs in Flow Systems for Wetland
Simulated and Target with ±2 Standard Deviations**

*Upper and Lower 95% confidence level shown
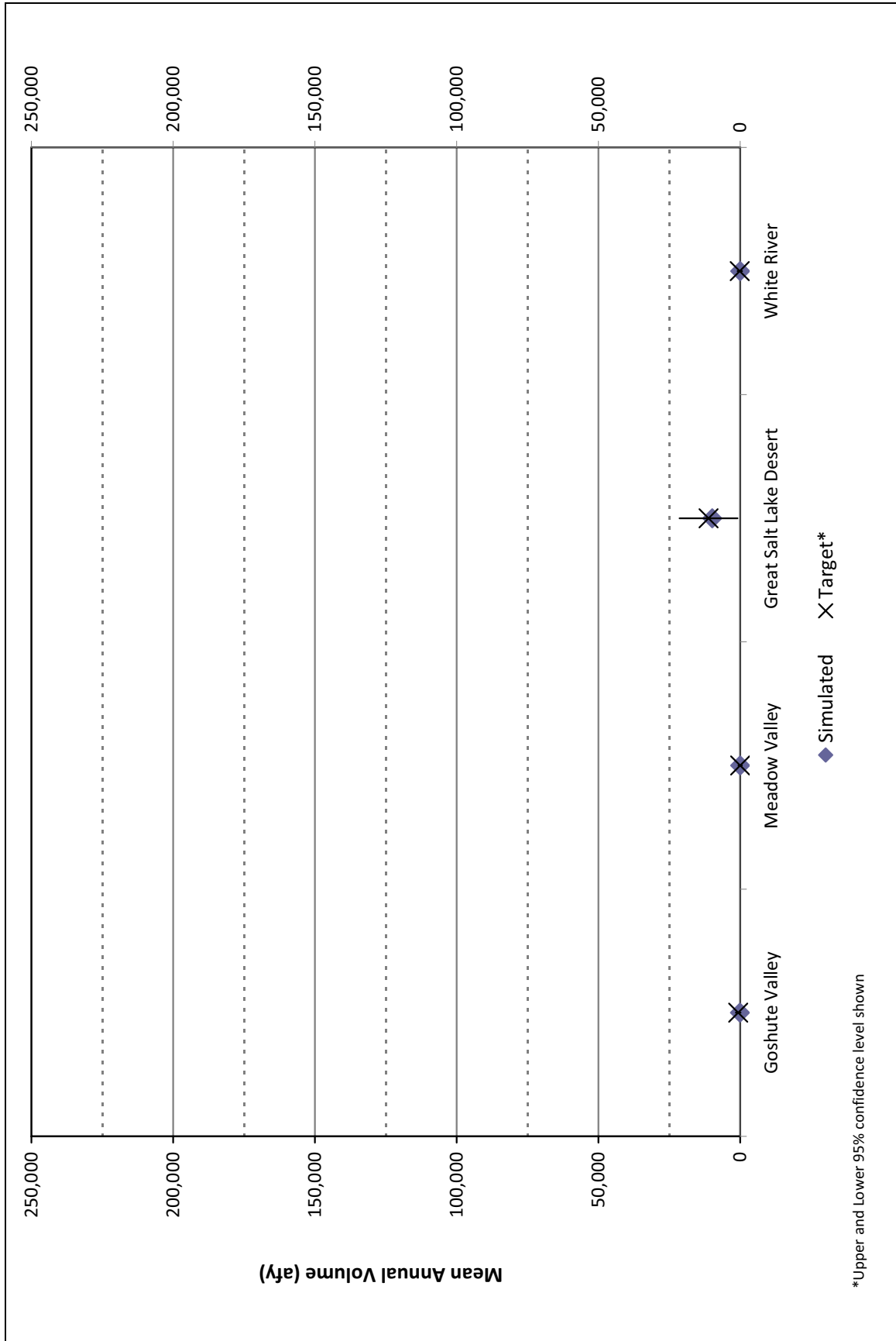
Figure 6-22
Groundwater Discharge by ET and Springs in Flow Systems for Playa Simulated and Target with ±2 Standard Deviations

◆ Simulated   ✕ Target*

*Upper and Lower 95% confidence level shown

JA_16363
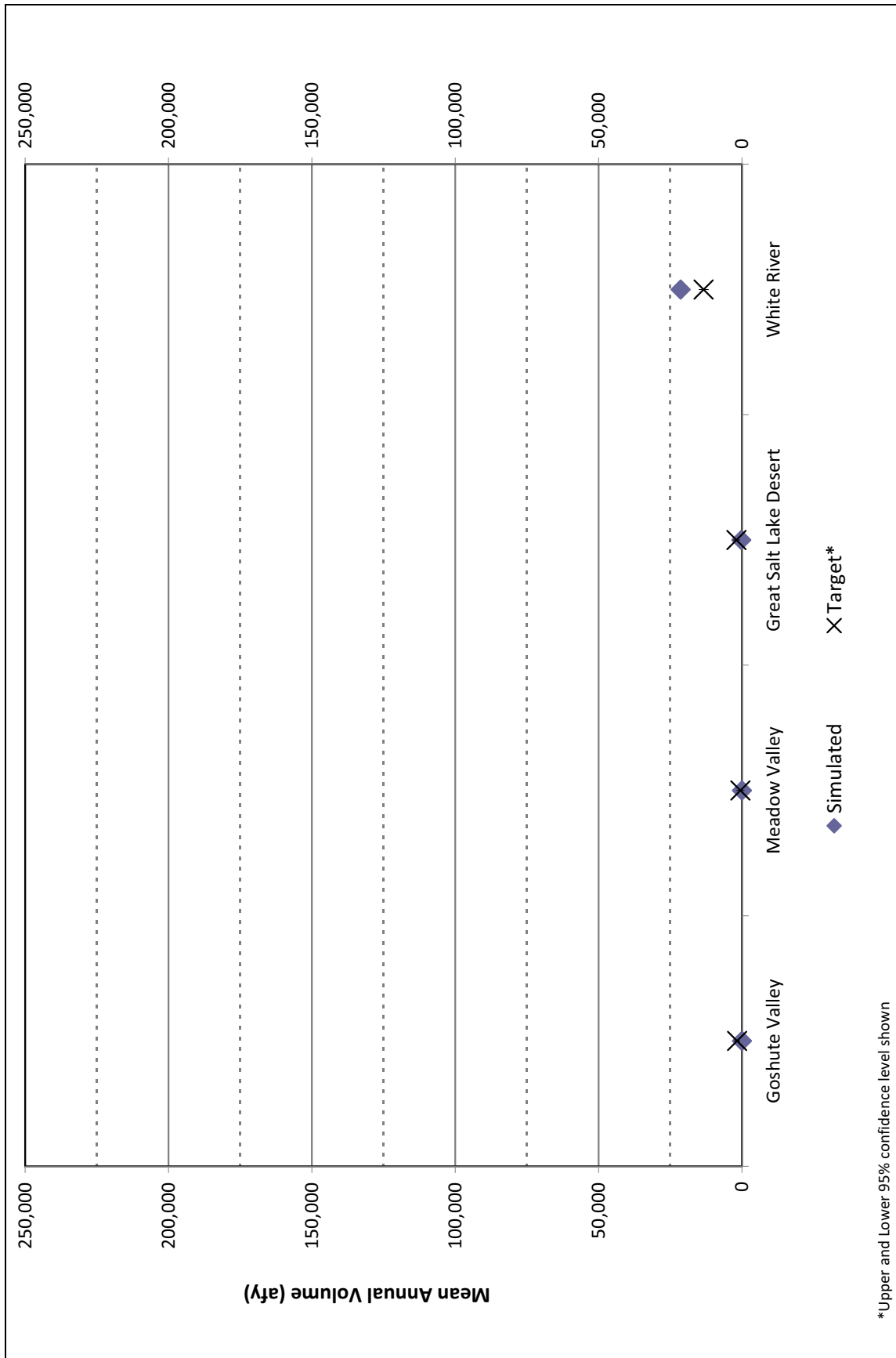
Figure 6-23
Groundwater Discharge by ET and Springs in Flow Systems for Open Water Simulated and Target with ±2 Standard Deviations

*Upper and Lower 95% confidence level shown

SE ROA 50963

JA_16364
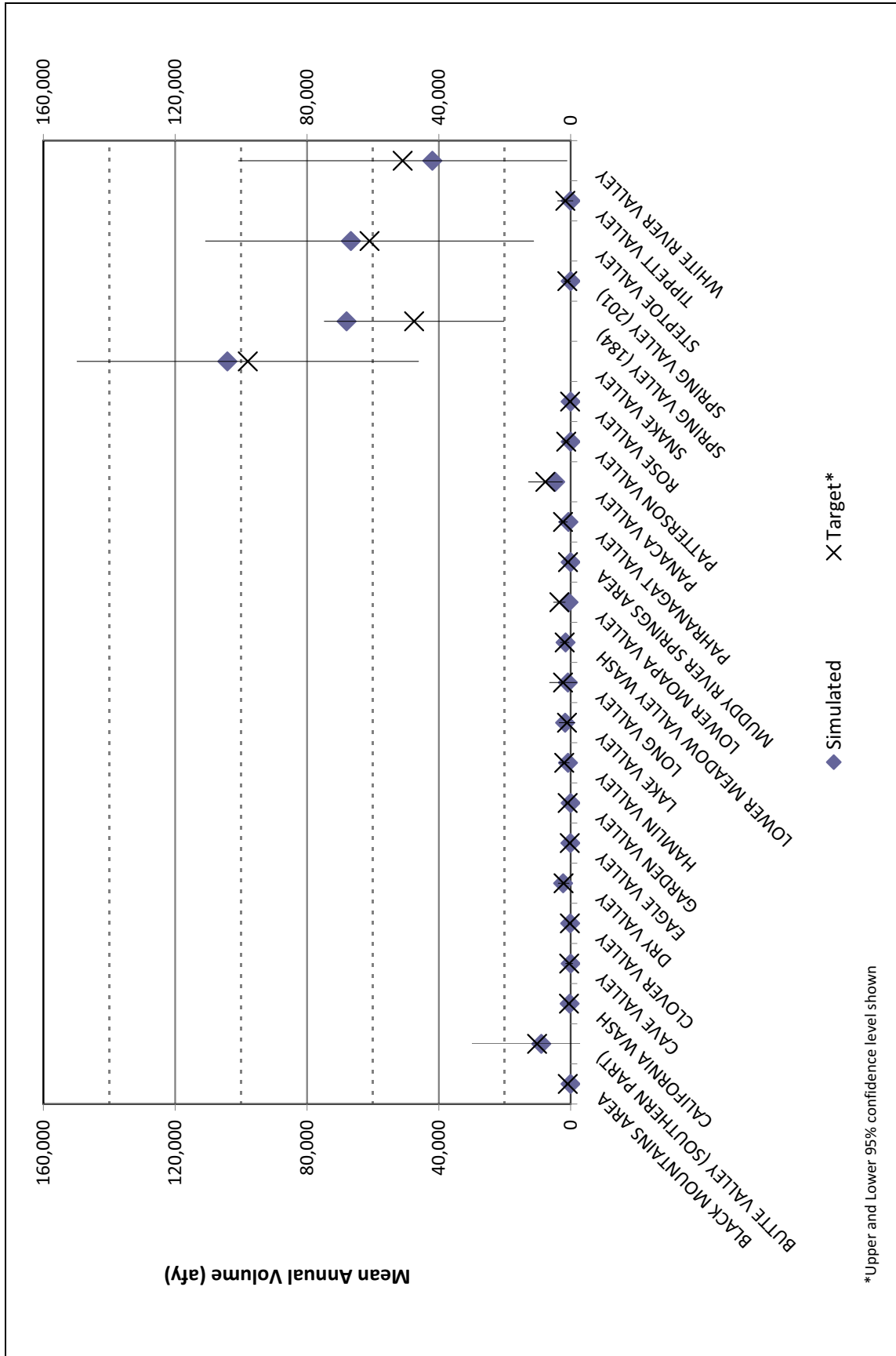
Figure 6-24
Groundwater Discharge by ET and Springs in Hydrographic Areas for Shrubland Simulated and Target with ±2 Standard Deviations

*Upper and Lower 95% confidence level shown

Section 6.0

SE ROA 50964

JA_16365
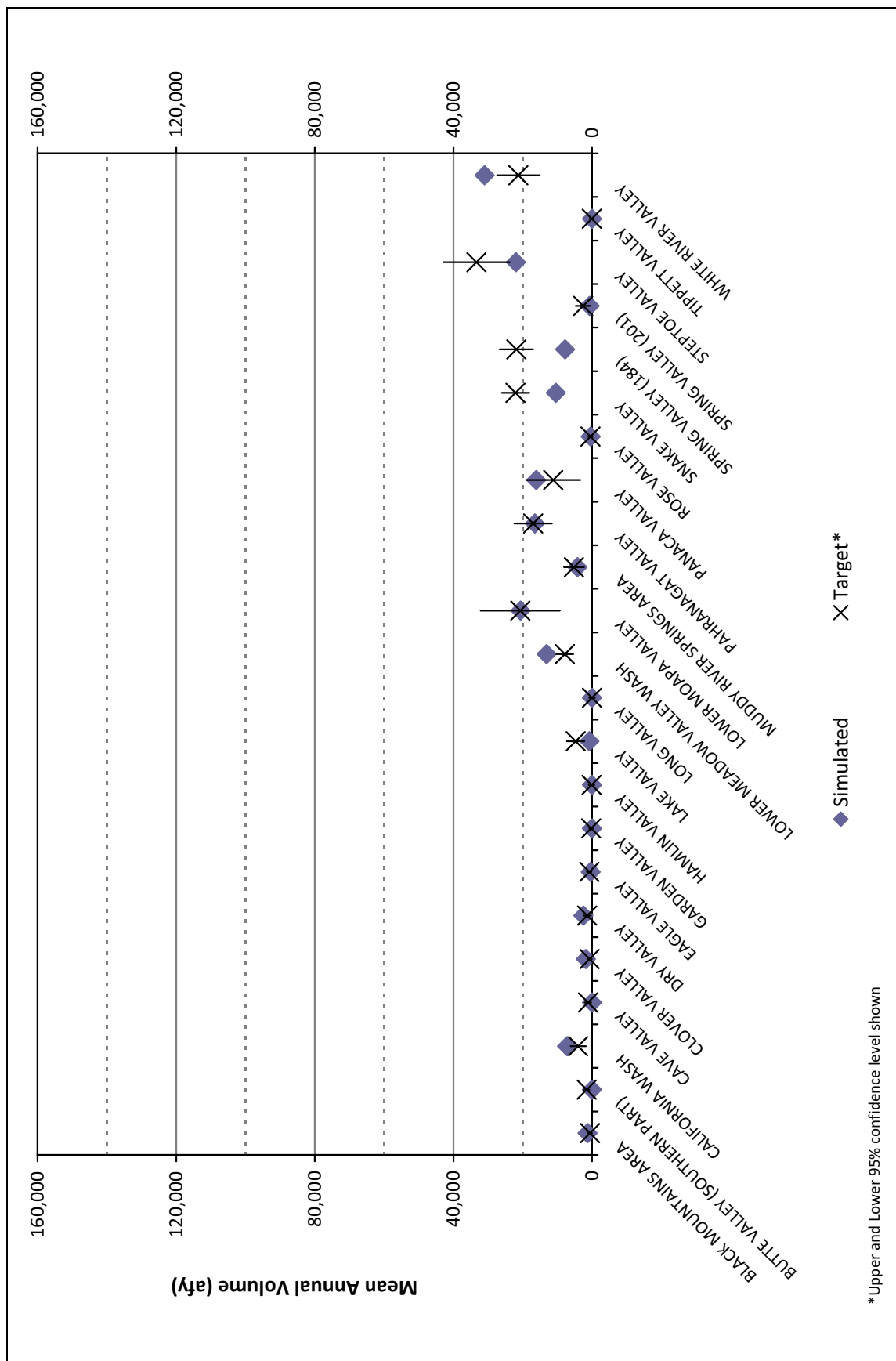
Figure 6-25
Groundwater Discharge by ET and Springs in Hydrographic Areas for Wetland Simulated and Target with ±2 Standard Deviations

*Upper and Lower 95% confidence level shown
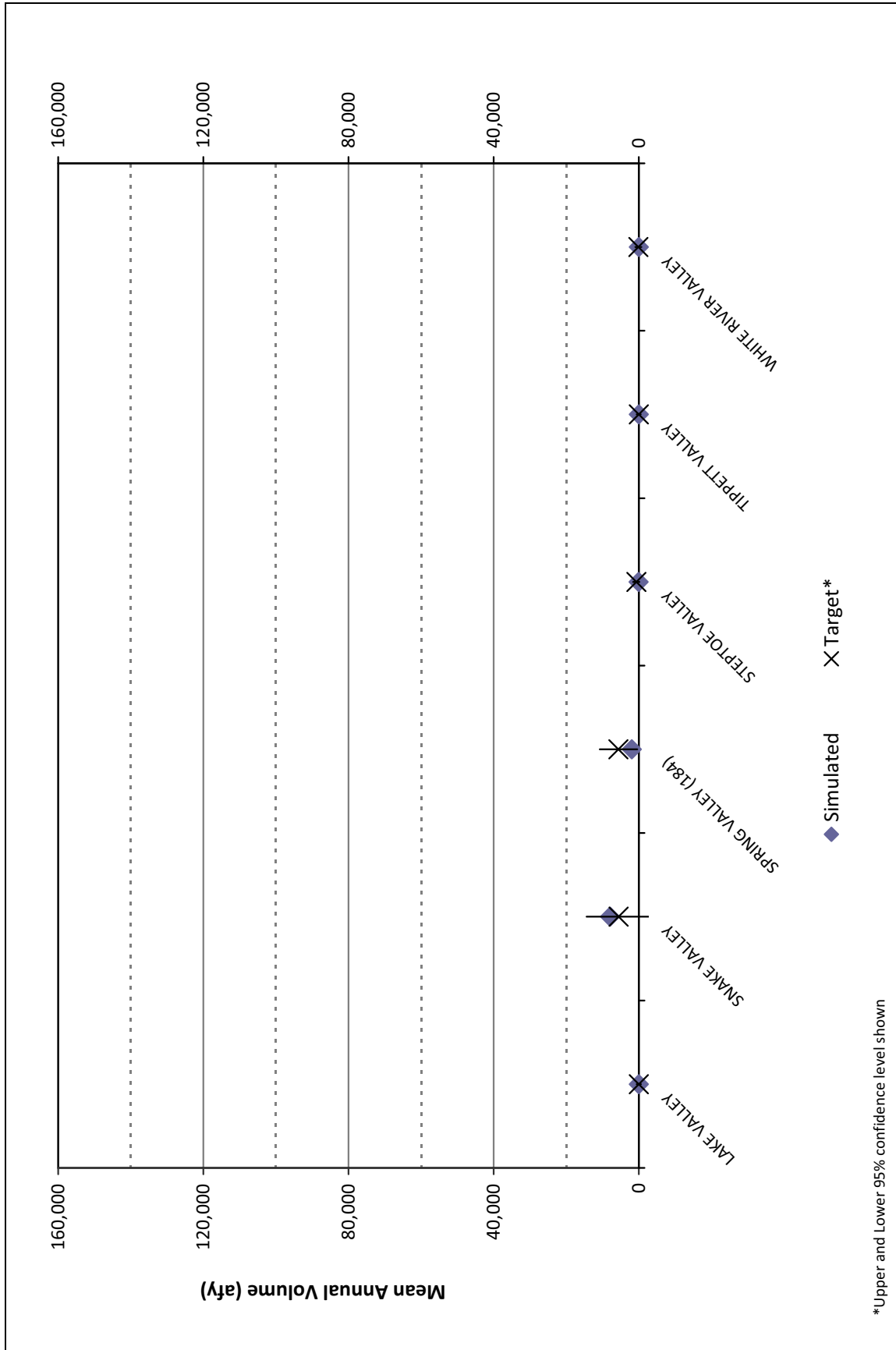
Figure 6-26
Groundwater Discharge by ET and Springs in Hydrographic Areas for Playa Simulated and Target with ±2 Standard Deviations

*Upper and Lower 95% confidence level shown

JA_16367
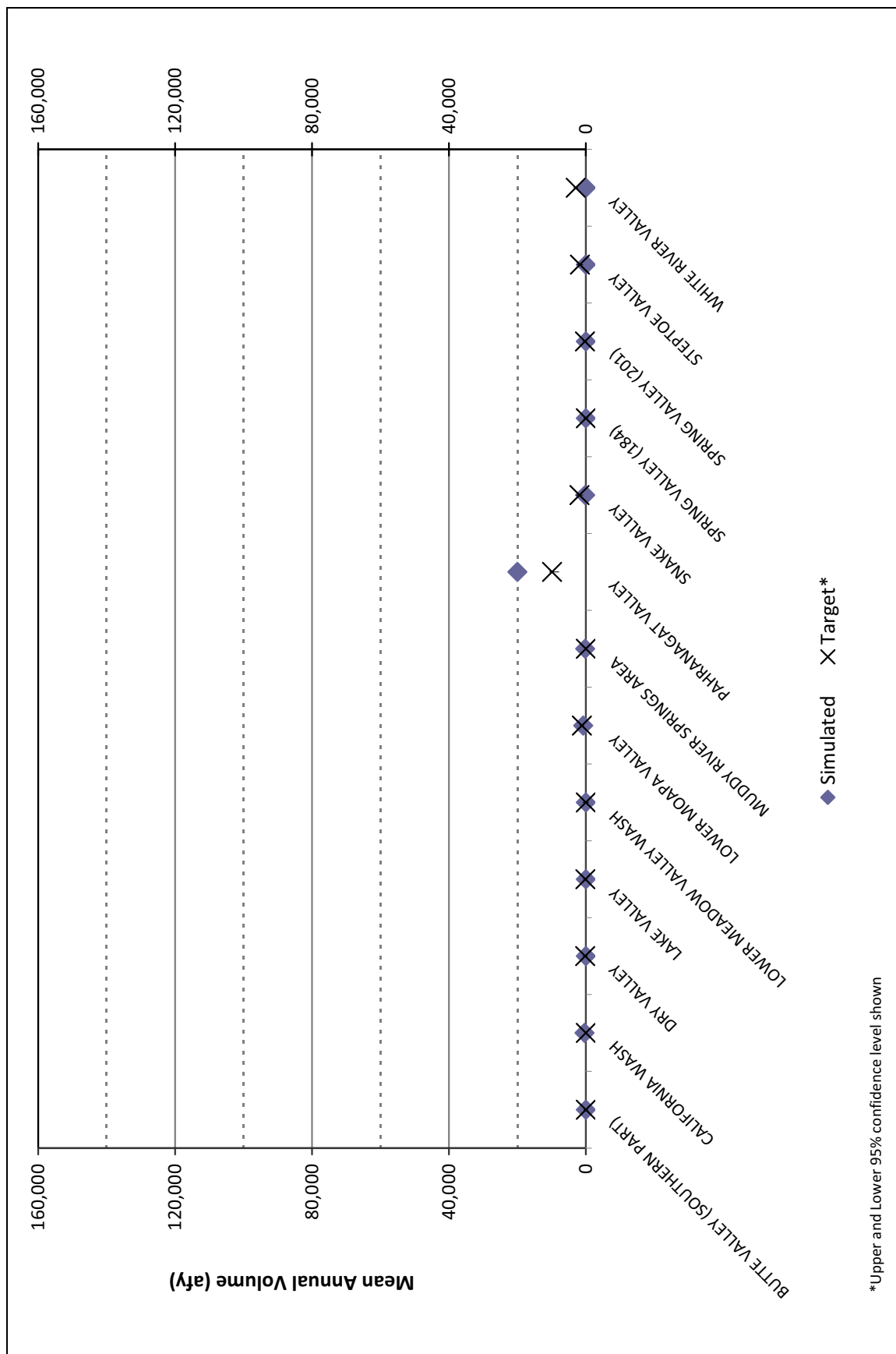
Figure 6-27
Groundwater Discharge by ET and Springs in Hydrographic Areas for Open Water Simulated and Target with ±2 Standard Deviations

◆ Simulated   ✕ Target*

*Upper and Lower 95% confidence level shown

SE ROA 50967

JA_16368
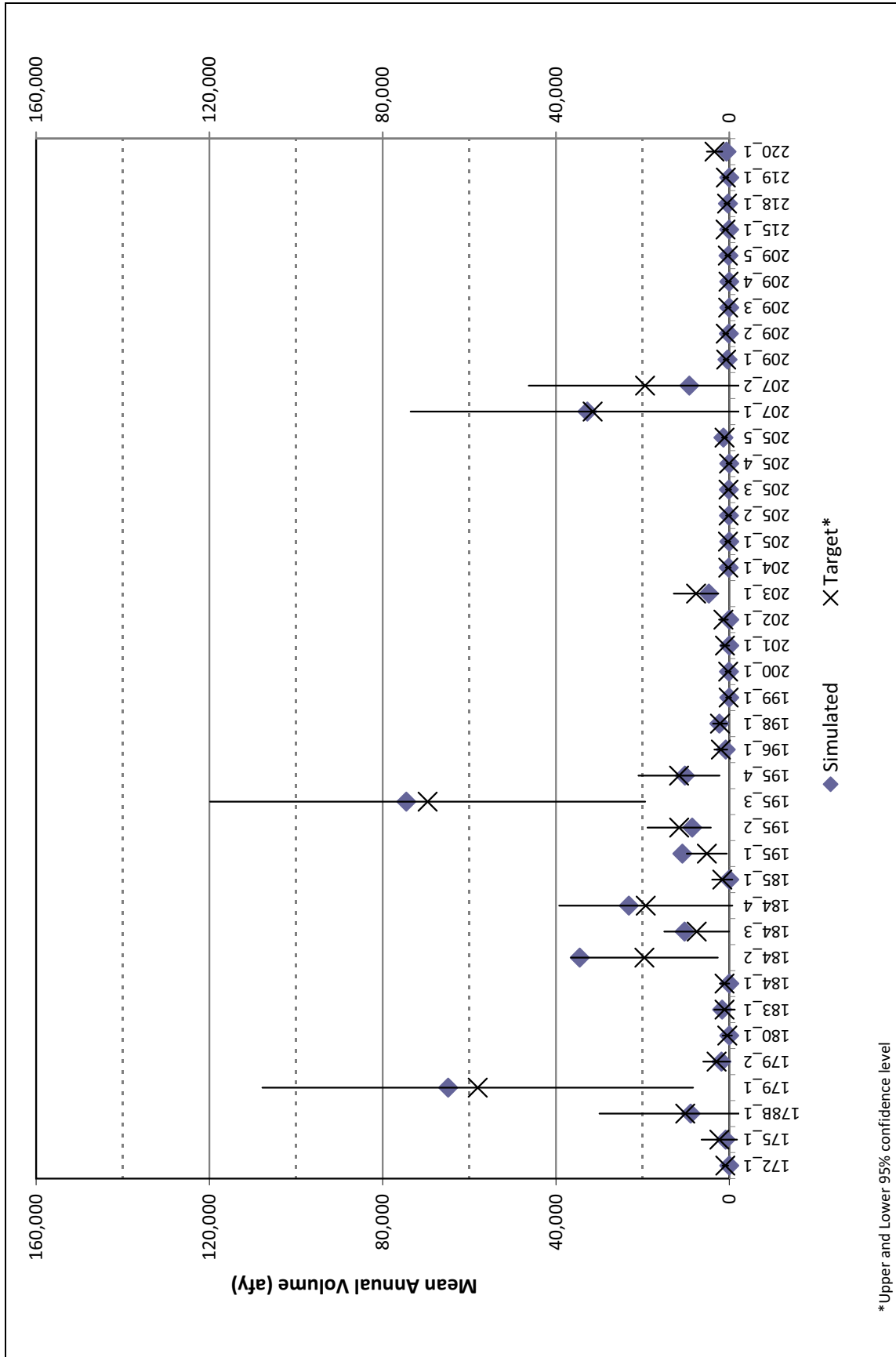
Figure 6-28
Groundwater Discharge by ET and Springs in Sub-Basins for Shrubland Simulated and Target with ±2 Standard Deviations

*Upper and Lower 95% confidence level

JA_16369
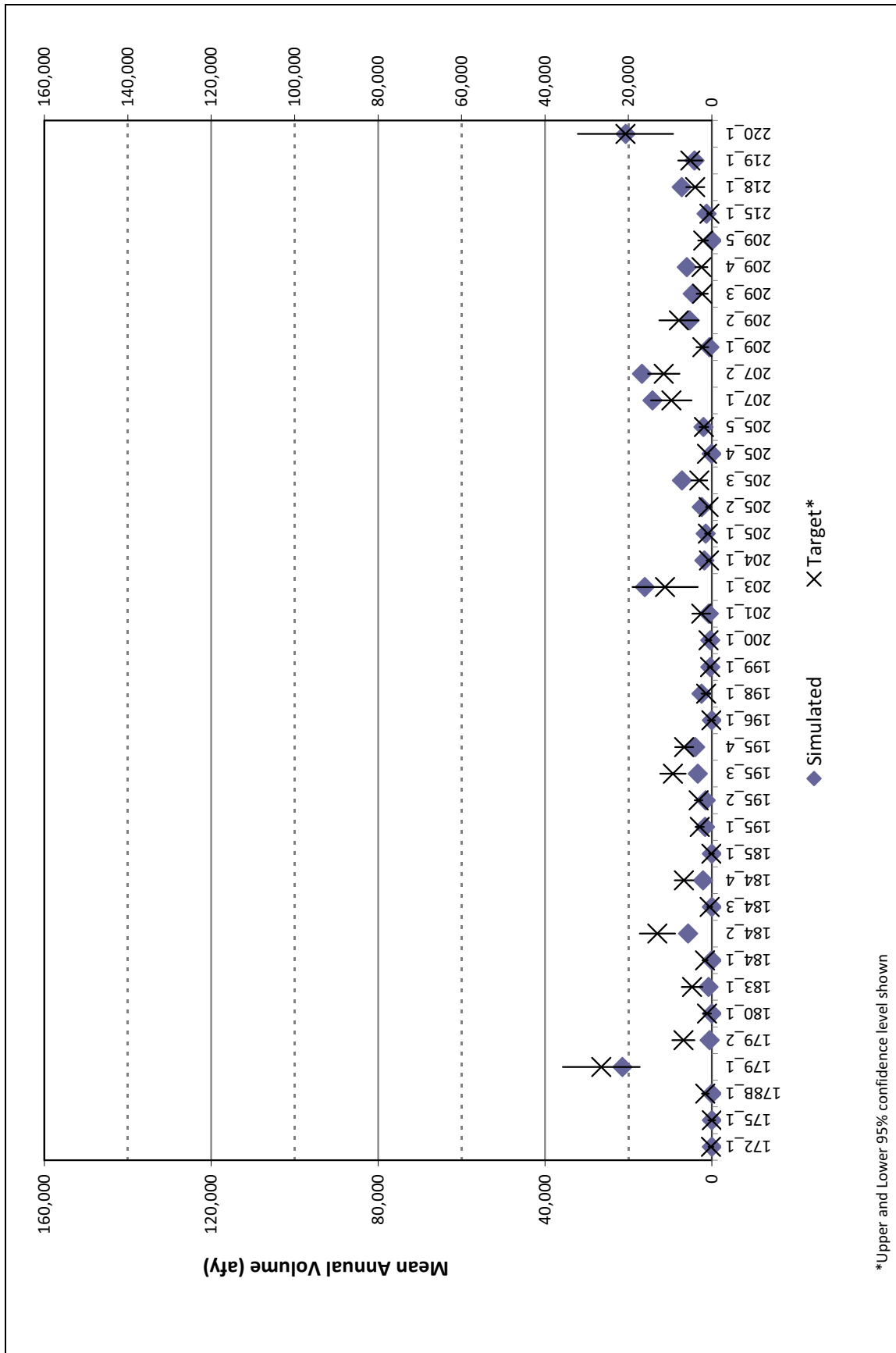
Figure 6-29

**Groundwater Discharge by ET and Springs in Sub-Basins for Wetland
Simulated and Target with ±2 Standard Deviations**

*Upper and Lower 95% confidence level shown

SE ROA 50969

JA_16370
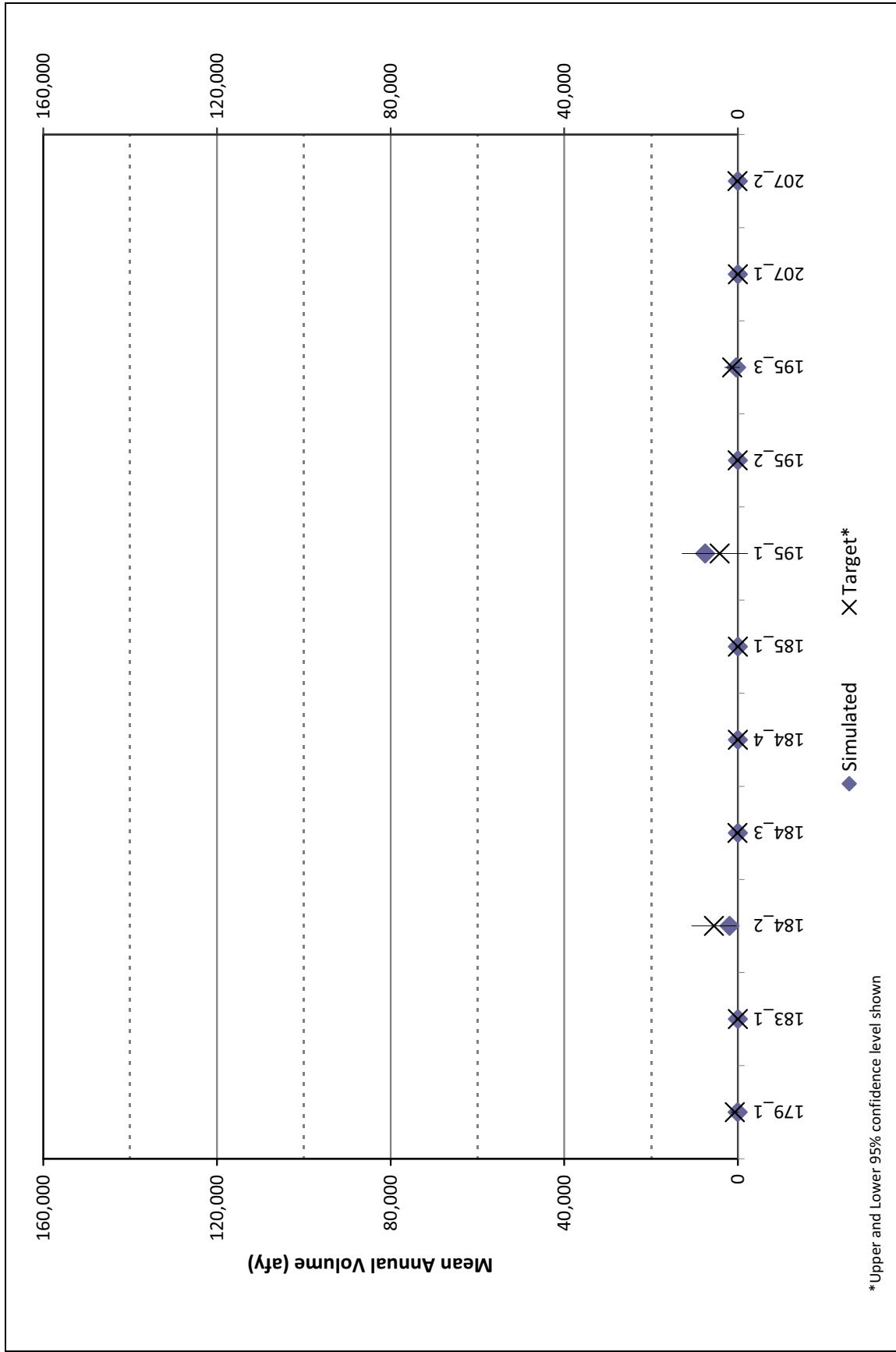
Figure 6-30
Groundwater Discharge by ET and Springs in Sub-Basins for Playa Simulated and Target with ±2 Standard Deviations

*Upper and Lower 95% confidence level shown

JA_16371
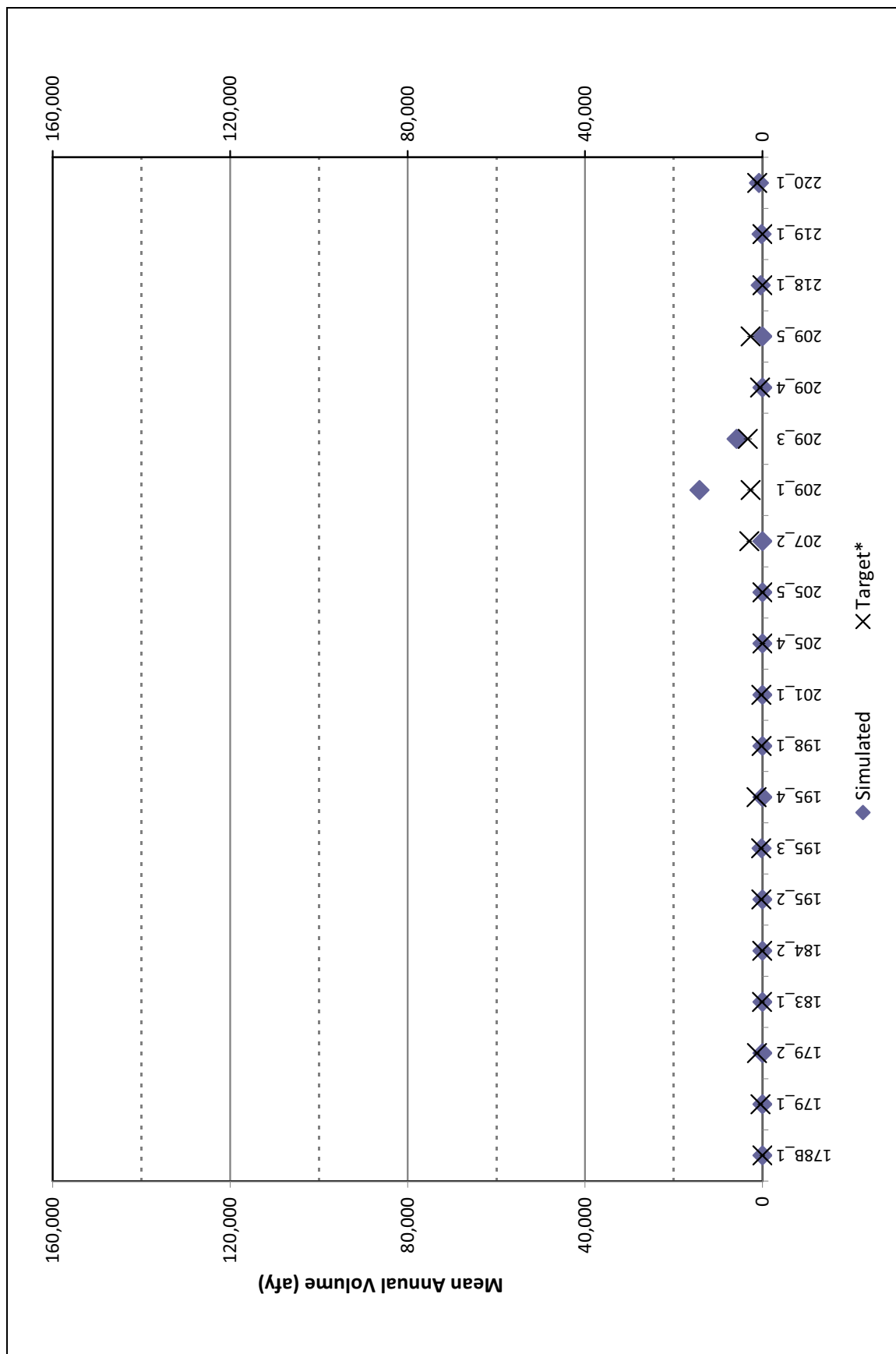
Figure 6-31
Groundwater Discharge by ET and Springs in Sub-Basins for Open Water Simulated and Target with ±2 Standard Deviations
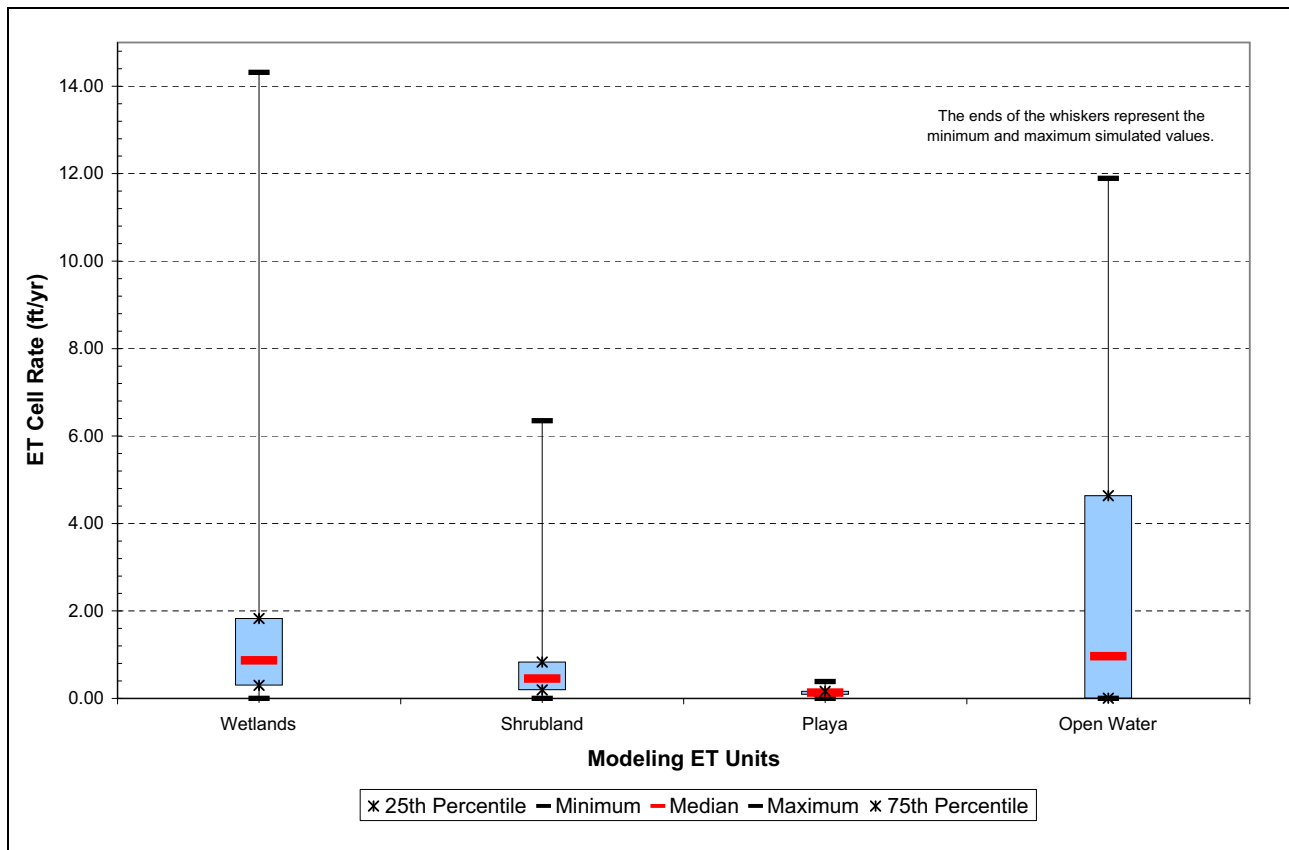
Figure 6-32
Simulated Groundwater ET Discharge Rates by ET Type

These ranges overlap with the simulated ranges and the ranges defined by the 25th and 75th percentiles presented in Figure 6-32.

6.1.3.3   Spring Discharge

This section discusses groundwater discharge to regional and intermediate springs simulated using the DRN package in the numerical model. Regional springs in Pahranagat Valley, the Muddy River Springs Area, and at the intermediate spring, Big Springs in Snake Valley, are represented using the SFR2 package and are discussed in Section 6.1.3.4.

Figure 6-33 shows simulated and observed discharge rates to springs. Intervals of ± 2 standard deviations are shown to illustrate uncertainties on the targets. Figure 6-33 summarizes spring discharge by (A) Regional Springs and (B) Intermediate Springs.

As shown on Figure 6-33, regional spring flow rates match closely to observed targets. Hot Creek Spring and Preston Big Spring flow rates are within 10 percent of the target. Spring flow for Moorman, Moon River, and Panaca springs are within 13 percent, 32 percent, and 15 percent of target observations, respectively.

JA_16373
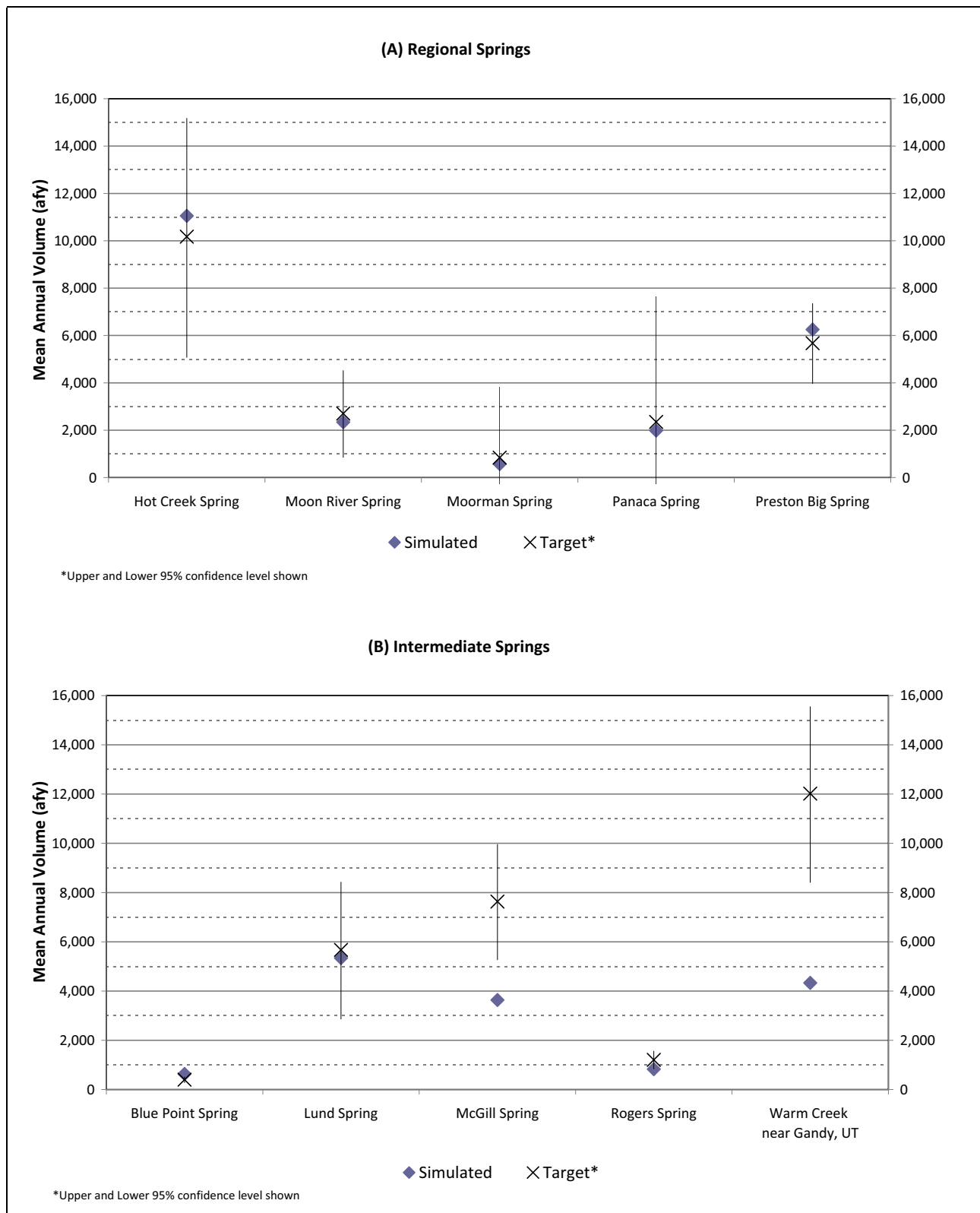
Figure 6-33
Groundwater Discharge from Regional (A) and Intermediate (B) Springs
Simulated and Target with ±2 Standard Deviations

JA_16374

Intermediate spring flow rates are not matched as closely to observed targets as compared to regional springs. McGill S pring and W arm Springs near Gandy, Utah, springs are undersimulated by 52 percent and 64 percent, respectively. Errors occurring in intermediate spring flows may be derived from inadequate representation of the c omplex hydrogeologic framework that giv es rise to t hese springs. In addition, a major component of the flow at intermediate springs may be derived from localized groundwater-flow processes that are not represented in this regional-scale model.

6.1.3.4   Stream Flow Routing Discharge

This section discusses simulated steady-state groundwater discharge to spring-fe d streams in the calibrated numerical model. Regional springs in Pahranagat Valley, the Muddy Ri ver Springs Area, and at Big Springs are represented using the SFR2 package.

Figure 6-34 shows simulated and observed discharge to streams. Intervals of ±2 standard deviations are shown to i llustrate uncertainties on the targets. As shown on Figure 6-34, regional springs and stream gages are simulated closely to observed targets.
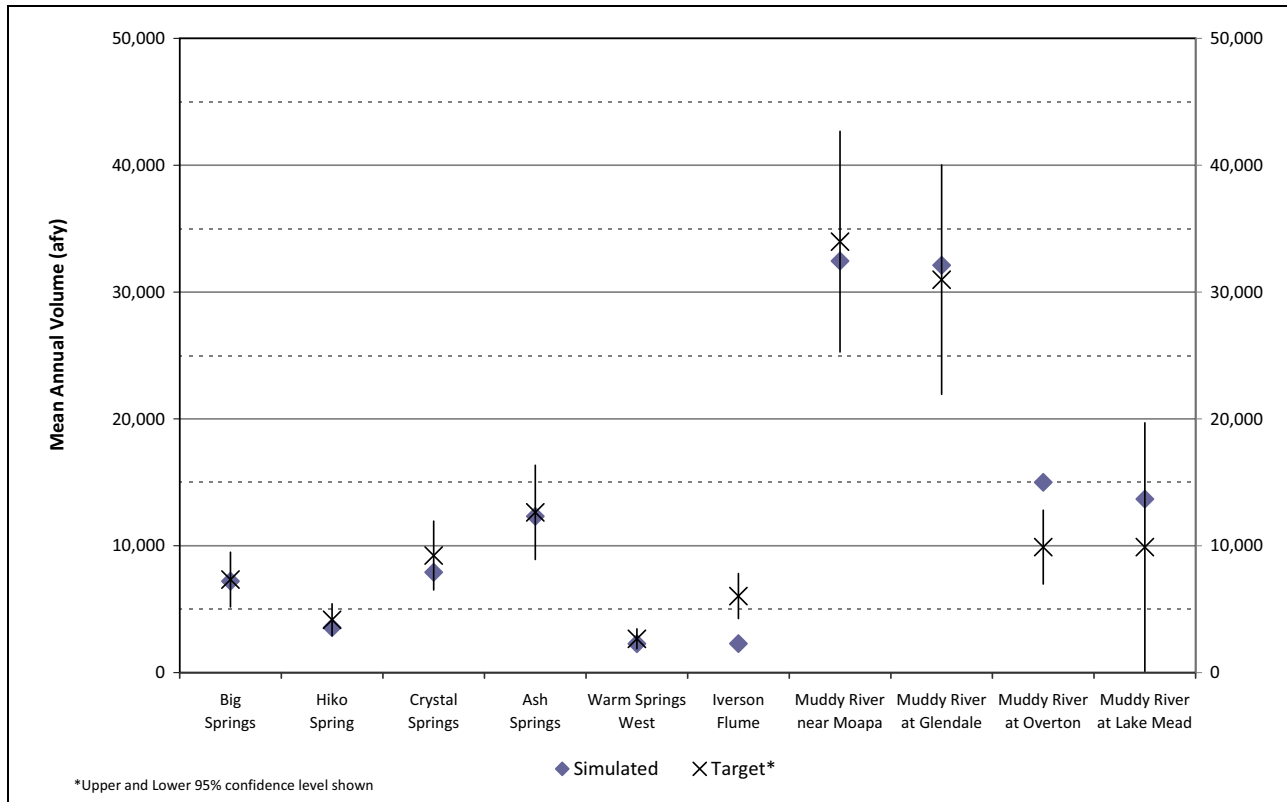
Figure 6-34
Groundwater Discharge at Stream Flow Routing Gages
Simulated and Target with ±2 Standard Deviations

Gages at the Muddy River near Moapa and the Muddy River near Glendale simulate flows within 4 percent of the targets. The Muddy River gage at Lake Mead is a surrogate gage (used for tracking purposes only). Flow at this surrogate gage represents surface-water outflow in the Muddy River out of the model domain and is simulated at 13,700 afy.

In Pahranagat Valley, gages representing Ash, Crystal, and Hiko springs simulate spring flow rates within 2 percent, 14 percent, and 15 percent of the targets, respectively.

Discharge to the intermediate Big Springs in Snake Valley is within 2 percent of the target flow observation.

ET from open water along stream channels is simulated in the SFR2 module. This ET component is added to ET simulated by the DRN package. Additions are done at the hydrographic-area scale. Figure 6-35 illustrates the ET component resulting from the SFR2 module, in the form of surface-water evaporation.
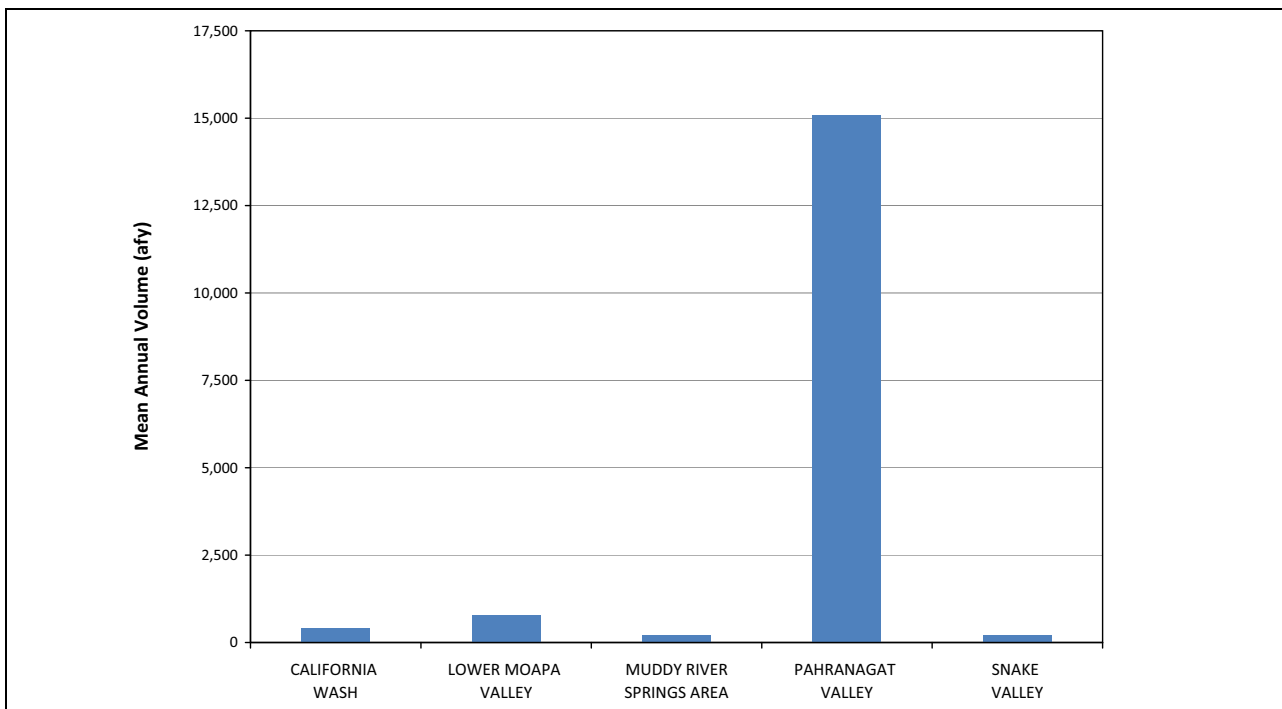
Figure 6-35
Simulated Evaporation from Surface Water in the SFR2 Package

6.1.4   *Distribution of Weighted Residuals versus Unweighted Simulated Values*

To evaluate model results for systematic model error or errors in assumptions concerning observations and weights, weighted residuals were plotted against unweighted simulated values for hydraulic-head observations. Ideally, weighted residuals will vary randomly about zero regardless of the simulated value.

Figure 6-36 shows that most of the weighted r esiduals for hydraulic he ads in the numerical model vary randomly about a value of zero. Eighty-seven values are greater than +5.3982, which is three times the regression standard error of 1.7994; 105 values are less than -5.3982. F or normally distributed sample populations, approximately 3 in 1,000, on average, would be so different from the expected value. For this samp le set of 7,007 obser vations, 21 obse rvations would be expe cted to exceed ±5.3982. Clearly, quite a few more exceed the 3 in 1,000 limit. While t his distribution is somewhat biased by large negative values, the distribution is still largely random (Figure 6-36).
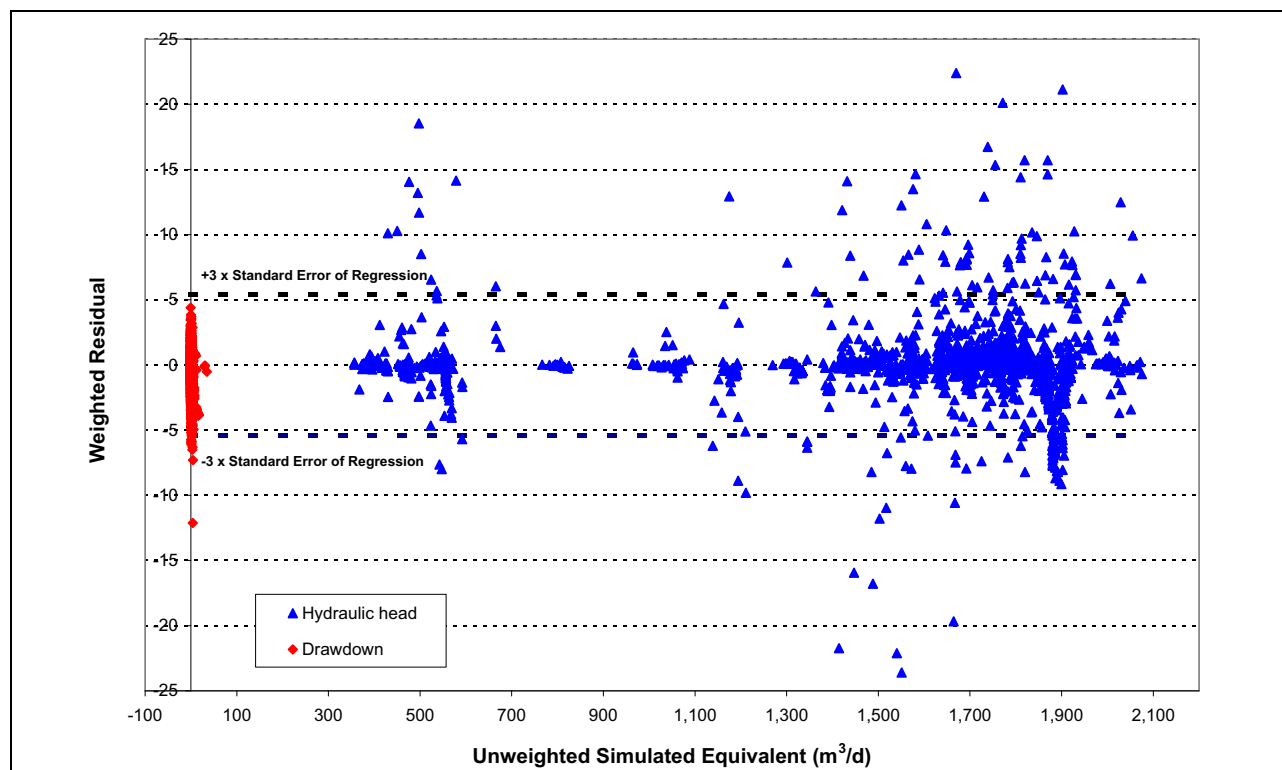
Figure 6-36
Weighted Residuals Relative to Unweighted Simulated Equivalent Hydraulic Heads

Figure 6-37 through Figure 6-40 show we ighted residuals for flow obse rvations plotted against unweighted simulated values for f low observations. These plots demonstrate that relatively fe w of the weighted residuals for flow observations exceed +/-5.3982.

6.1.5 Normality of Weighted Residuals and Model Linearity

The normality of the weighted residuals and model linearity are important to measures of parameter and prediction un certainty, such as linear confidence intervals. Specifically, the weighted residuals need to be normally distributed. In a ddition, the model must be e ffectively linear for the calculated linear confidence intervals on e stimated parameters and pr edicted hydraulic heads and flows to accurately represent simulation uncertainty. In the numerical model, confidence intervals were considered only on estimated parameter values.

JA_16377
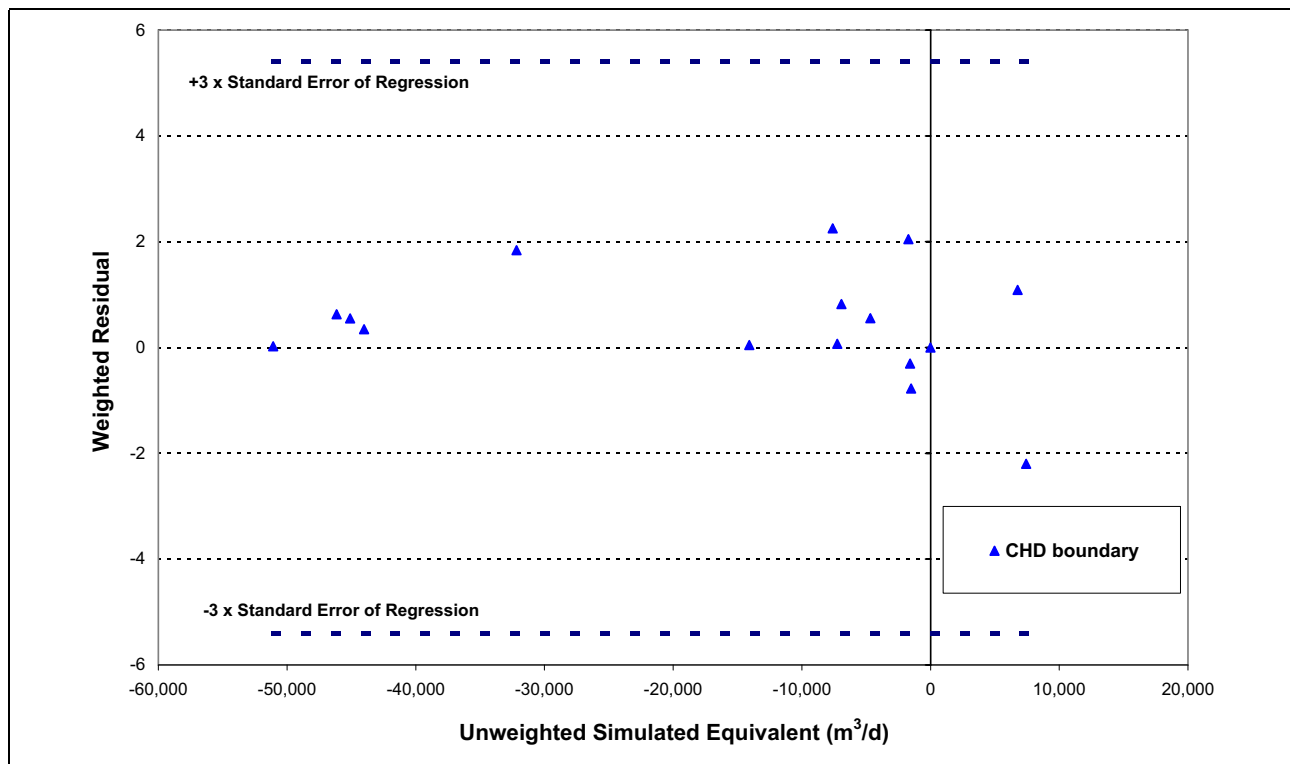
Figure 6-37
Weighted Residuals versus Unweighted Simulated Equivalents for CHD
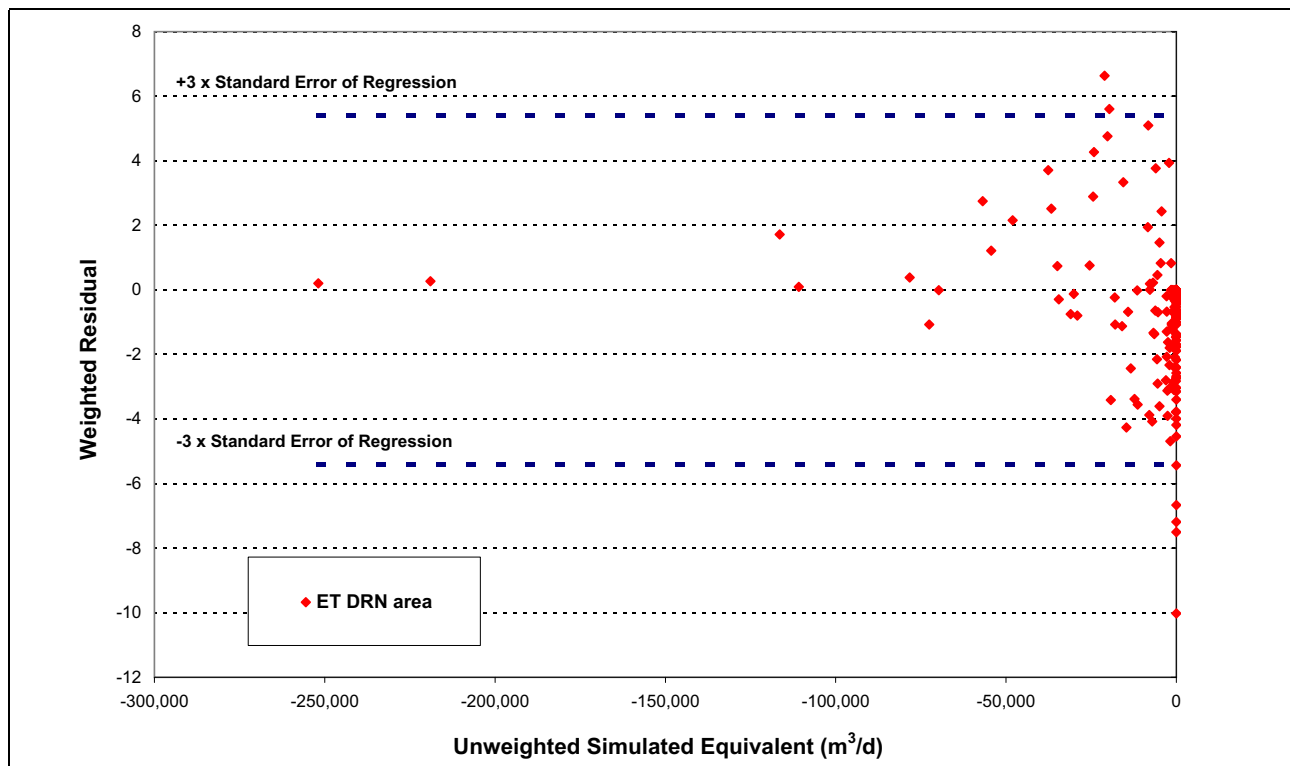
Figure 6-38
Weighted Residuals versus Unweighted Simulated Equivalents for ET Drains

SE ROA 50977

JA_16378
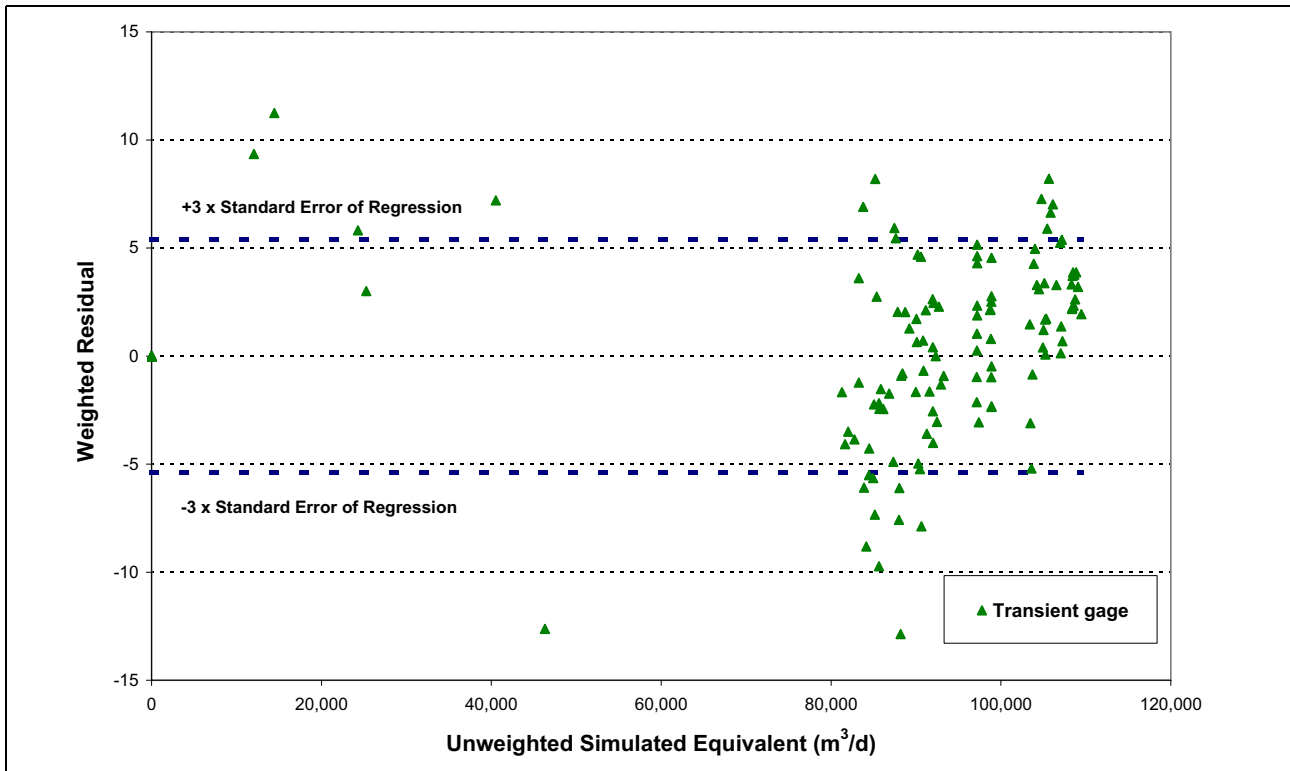
Figure 6-39
Weighted Residuals versus Unweighted Simulated Equivalents for Stream Flow
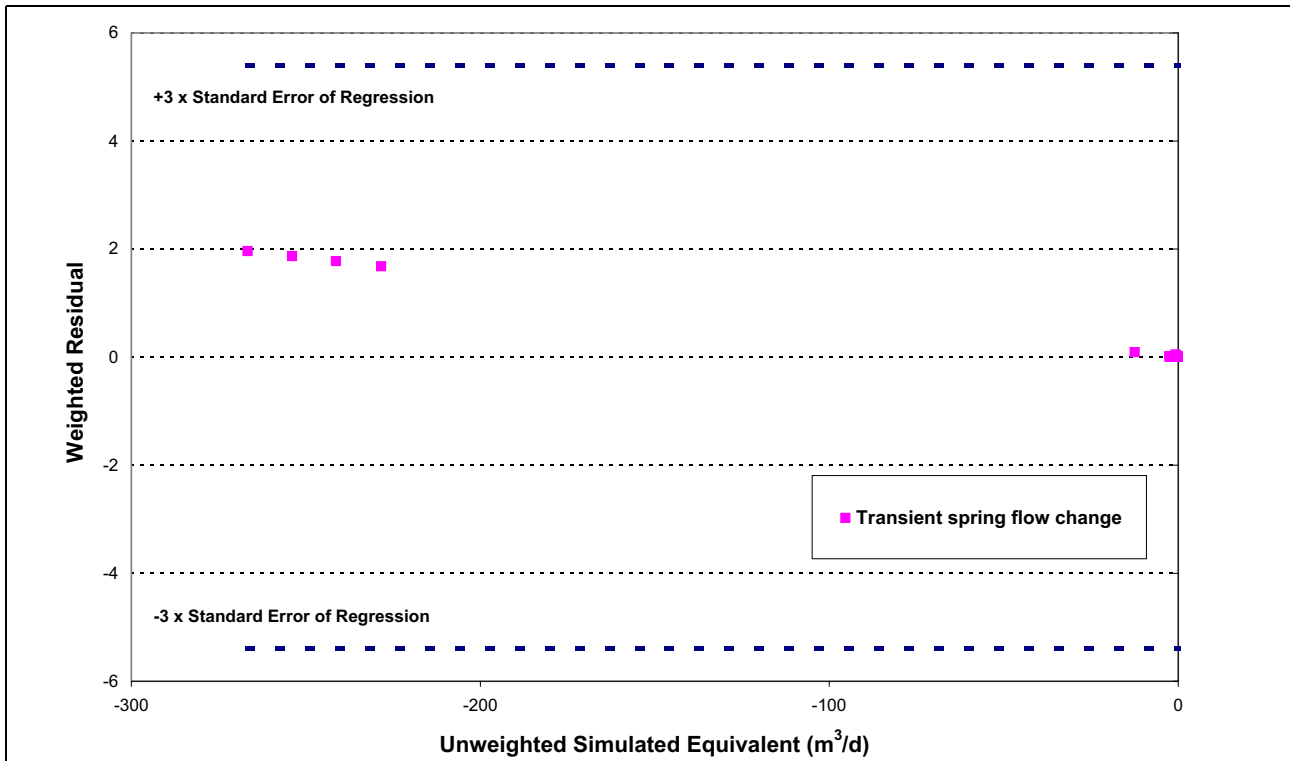
Figure 6-40
Weighted Residuals versus Unweighted Simulated Equivalents for Spring Flow

SE ROA 50978

JA_16379

The normal probability plot of the weighted residuals for the final calibrated model is shown in Figure 6-41. The points would be expected to fall along a straight line if the weighted residuals were both independent and normally distributed. Clearly, the points do not fall along a straight line. One possibility is that the residuals are normally distributed, but they are correlated instead of being independent. Correlations are derived from the fitting of the regression.
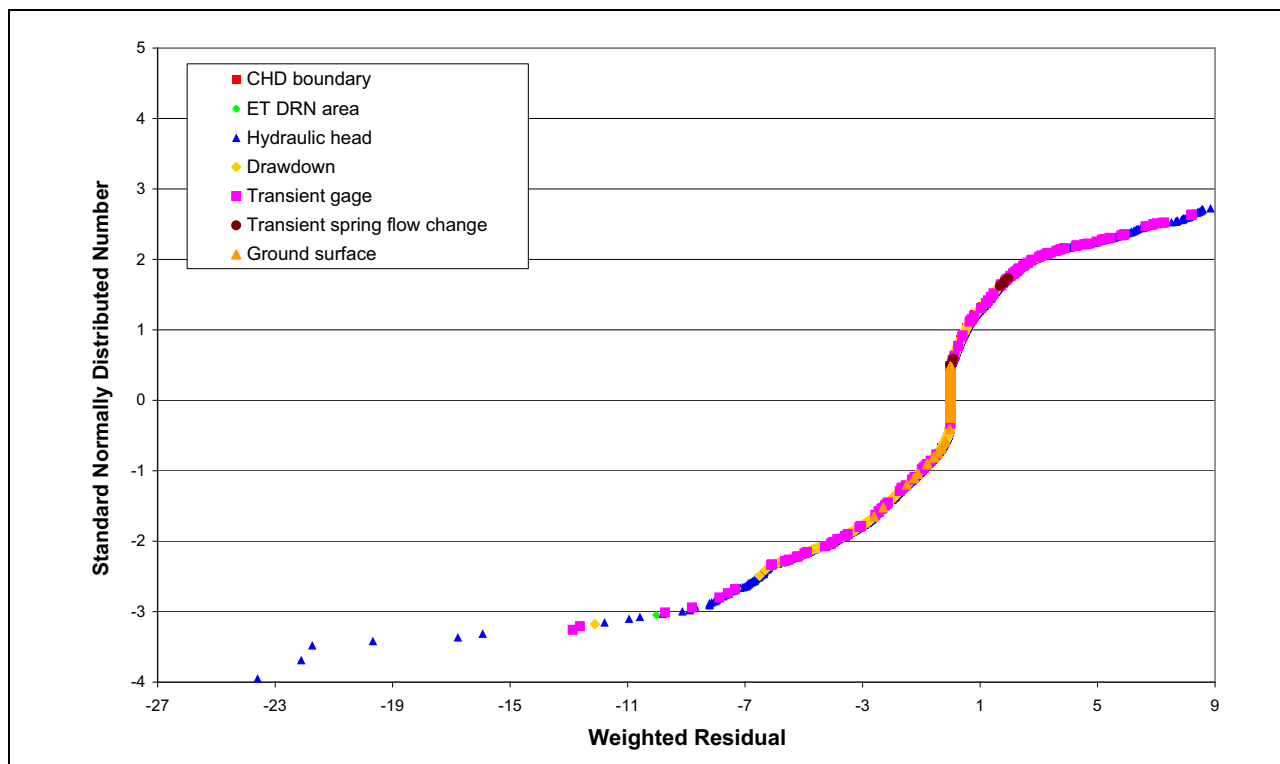
Figure 6-41
Normal Probability Plot of Weighted Residuals

The source of correlation can be investigated using the graphical procedures described by Cooley and Naff (1990). Normally distributed, random numbers generated to be consistent with the regression-derived correlations are called correlated-normal numbers and are shown in Figure 6-42. Most of the curvilinearity in Figure 6-42 cannot be attributed to regression-derived correlations. This analysis suggests that the weighted re siduals are not normally distributed and th at they are not correlated.

Model linearity was tested using a statistic referred to as the modified Beales measure (Cooley and Naff, 1990). The modified Beales measure calculated for the numerical model equals $0.972 \times 10^{+9}$. If the Beales measure is less than 0.044, the model is effectively linear. If the Beales measure is greater than 0.48, the model is highly nonlinear. Thus, the final calibrated model is highly nonlinear.

The lack of normality of the weighted residuals and the degree of nonlinearity of the numerical model indicate that linear confidence intervals may be inaccurate. Despite this problem, linear confidence intervals were used in the numerical model as rough indicators of the uncertainty in estimated parameter values in the presence of model nonlinearity. This approach is consistent with the previous work of Christensen and Cooley (1996).

SE ROA 50979

JA_16380
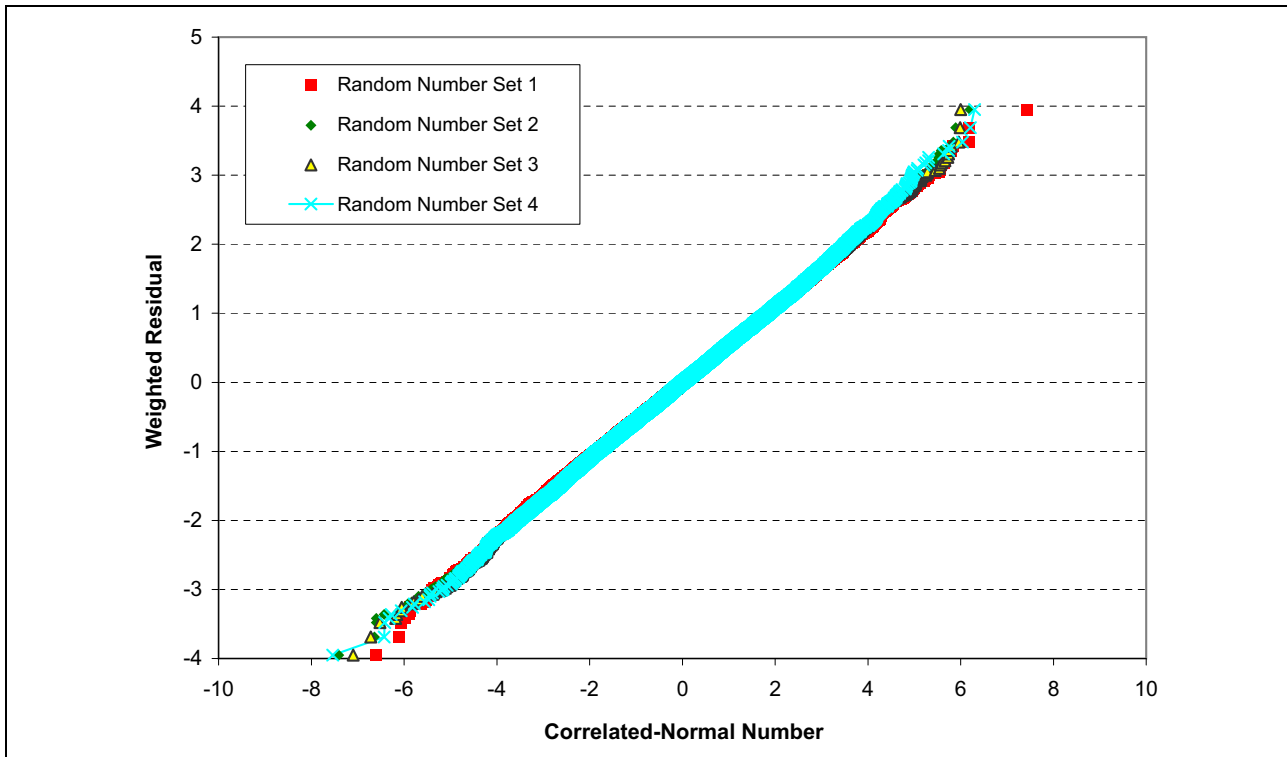
Figure 6-42
Normal Probability Plot of Weighted Residuals versus Correlated-Normal Numbers

6.2 Evaluation of Parameter Sensitivities and Parameter-Estimation Results

CSS are provided on the DVD for all parameters. The CSS of the 100 most sensitive UCODE parameters are shown in Table 6-5. These sensitivities are based on the input values to the last parameter-estimation run and were not recalculated with the final model estimates.

Given the large number of parameters in the model, and the small number of parameters that can be practically estimated, a second set of parameters was created that combined nearly all the model parameters into 10 aggregate parameters (Table 6-6). These parameters combined like materials and were used to assign a multiplication factor to raise or lower the values for the entire group. These group parameters did not capture all the individual model parameters but did account for or influence approximately 95 percent of them.

In this stage of the optimization process, two groups of parameters were excluded, constant-head boundaries (CHDs) and recharge parameters:

- CHDs were the most sensitive parameters. Because some, like Lake Mead or North Snake Valley, were well constrained, estimating them made little sense, as the actual values were well known. In other cases, such as when the boundary is in a mountain block where there is no control, an appropriate hydraulic-head selection depends on a proper estimate of the K of the host rock. In these cases, it is better to estimate the K value and manually adjust the boundary head. Except during preliminary simulations, CHD parameters were not optimized.

Table 6-5
Model Composite-Scaled Sensitivities for Final Calibrated Model (Top 100)

Position[a]		Parameter Name	Composite-Scaled Sensitivity	Parameter Type[b]		Position[a]	Parameter Name	Composite-Scaled Sensitivity	Parameter Type[b]
x	1	LC_MB_S_HK	6.110	*K*		---	51	fUV207VB_H	0.1960	Kx
---	2	fLw210LFtH	3.282	Kx		---	52	fUV196AF_H	0.1957	Kx
---	3	RSC_ME_WR	2.890	RCH-ME		---	53	UA_VA	0.1939	*K*
x	4	KDEP_LCLDF	2.654	KDEP		---	54	fHFBPAHRnW	0.1933	Kx
x	5	UVF_AF_HK	2.639	*K*		---	55	fLd219SB_H	0.1929	Kx
---	6	RSC_ME_MVW	2.341	RCH-ME		---	56	fHFBCOAL_N	0.1885	Kx
x	7	KDEP_UVF	2.089	KDEP		---	57	UC_HK	0.1826	*K*
---	8	R_ROLVF_WT	2.039	RCH-RO		---	58	fHFBMUDDYR	0.1824	Kx
---	9	FAULT_FDUC	1.672	Kx		---	59	fLw180MB_H	0.1801	Kx
---	10	ETrWET	1.656	ET		---	60	ETr209WAT	0.1789	ET
x	11	LC_MB_D_HK	1.467	*K*		---	61	fLw171SB_H	0.1737	Kx
---	12	RSC_ME_GV	1.370	RCH-ME		---	62	fLwJWRMB_H	0.1736	Kx
---	13	HFB_HK	1.358	HFB		---	63	fUV209AF_H	0.1720	Kx
---	14	tHFBPAHR_E	1.298	*K*		---	64	fUV195VB_H	0.1682	Kx
---	15	ALT_FACT	1.164	Kx		---	65	LC_MB_VA	0.1546	*K*
---	16	RSC_ME_GSL	1.126	RCH-ME		---	66	fUV195AF_H	0.1545	Kx
---	17	R_ROCARB_W	1.097	RCH-RO		---	67	fLw174SB_H	0.1545	Kx
---	18	fLPSZ_MB_H	1.085	Kx		---	68	fLdOFZ_H	0.1537	Kx
x	19	CA_SBSD_HK	1.058	*K*		---	69	fUV181AF_H	0.1529	Kx
x	20	LV_CCCMB_H	0.9017	*K*		---	70	UV_SSVAF_H	0.1490	*K*
---	21	SFR_COND19	0.8642	SFR		---	71	R_ROLOWK_W	0.1460	RCH-RO
---	22	FAULT_FPAH	0.7860	Kx		---	72	fUAa_HK	0.1424	Kx
---	23	fLw207SB_H	0.7208	Kx		---	73	fLdPW_LF_H	0.1379	Kx
---	24	UVF_VB_HK	0.5280	*K*		---	74	UV_NLVPY_H	0.1352	*K*
---	25	tHFBCOAL_W	0.4774	*K*		---	75	fLd182MB_H	0.1273	Kx
---	26	fLw209MB_H	0.4482	Kx		---	76	fUV196VB_H	0.1232	Kx
---	27	BAS_HK	0.3808	*K*		---	77	SFRaCOND19	0.1218	SFR
---	28	SFR_COND15	0.3759	SFR		---	78	UVF_VA_Spc	0.1152	*K*
---	29	LV_WRCMB_H	0.3758	*K*		---	79	fUV195VBsH	0.1130	Kx
---	30	LV_IPCMB_H	0.3606	*K*		---	80	LVF_RIV_V	0.1108	*K*
---	31	fBA_IPC_H	0.3588	Kx		---	81	fLw172MB_H	0.1083	Kx
---	32	SPR_REGION	0.3466	SPR		---	82	fUV181PY_H	0.1029	Kx
---	33	UVF_VA	0.3452	*K*		---	83	fHFBGARD_W	0.1017	Kx
---	34	KDEP_LCMDF	0.3277	KDEP		---	84	PLUT_HK	0.0982	*K*
---	35	ETr209WET	0.3250	ET		---	85	FAULT_FLVF	0.0981	Kx
---	36	LVF_RIV_H	0.3091	*K*		---	86	fLe195MB_H	0.0968	Kx
---	37	BAS_P2P_HK	0.3057	*K*		---	87	LV_QRCMB_H	0.0959	*K*
---	38	f207LF_TST	0.2908	Kx		---	88	LV_IPCSB_H	0.0951	*K*
---	39	fLw209MFtH	0.2823	Kx		---	89	LVF_VA	0.0946	*K*
---	40	UVF_SYTP	0.2822	*K*		---	90	fUV195PY_H	0.0918	Kx
---	41	LVF_HK	0.2701	*K*		---	91	fLw171LF_H	0.0910	Kx
---	42	LVF_VOL_VA	0.2592	*K*		---	92	CA_SBSD_VA	0.0898	*K*
---	43	fLw171MB_H	0.2404	Kx		---	93	fHFBPROC_N	0.0799	Kx
---	44	BAS1_HK	0.2360	*K*		---	94	UA_NW1_HK	0.0773	*K*
---	45	R_ROUVF_WT	0.2358	RCH-RO		---	95	fUV181VB_H	0.0760	Kx
---	46	SFR_COND16	0.2308	SFR		---	96	UV_SSVVB_H	0.0746	*K*
---	47	SPR_INTRMD	0.2292	SPR		---	97	SFR_COND17	0.0725	SFR
---	48	fLw219MB_H	0.2238	Kx		---	98	fUwMB_HK	0.0697	Kx
---	49	ETrSHR	0.2131	ET		---	99	UA_NW1_VA	0.0697	*K*
---	50	UA_HK	0.2111	*K*		---	100	fLw218MB_H	0.0693	Kx

[a]x indicates parameter optimized using UCODE_2005
  parameter estimation
[b]HFB = Horizontal flow barrier conductance
 K = Hydraulic conductivity *K_h*, *VANI*, or fault factor
Kx = Multiplication factor for *K* parameter of *K* group

RCH-ME = Maxey-Eakin recharge efficiency
RCH-RO = In-place / runoff recharge efficiency
SFR = Stream flow routing riverbed conductance
SPR = Spring drain conductance factor

SE ROA 50981

JA_16382

Table 6-6
Model Composite-Scaled Sensitivities for Grouped Model Parameters

Position		Parameter Name	Composite-Scaled Sensitivity	Parameter Type	Group Composition
x	1	CARBK_FACT	7.0475	*K*	All carbonate horizontal *K* parameters
x	2	HFBC_FACT	2.6403	*K*	All HFB parameters
x	3	UVF_K_FACT	2.4493	*K*	All UVF horizontal *K* parameters
x	4	OTHRK_FACT	1.4098	*K*	All non-carbonate and non-UVF horizontal *K* parameters
x	5	SFRC_FACT	1.0197	SFR	All SFR river bed conductance parameters
x	6	UVF_SY_VAL	0.2824	*Sy*	All UVF *Sy* parameters
x	7	CARBSY_VAL	0.0710	*Sy*	All carbonate *Sy* parameters
---	8	UVF_SS_VAL	0.0416	*Ss*	All UVF *Ss* parameters
---	9	OTHRSS_VAL	0.0297	*Ss*	All non-UVF *Ss* parameters
---	10	OTHRSY_VAL	0.0235	*Sy*	All non-carbonate and non-UVF *Sy* parameters

Note: x indicates parameter optimized using UCODE_2005 parameter estimation

- RE parameters were not optimized using parameter estimation. During early model work and work up to the final calibration, attempts were made to estimate RE parameters. Typically the optimization process added unreasonable volumes of water to the model, but RE parameters were not allowed to exceed two times their starting values. Part of the problem may be related to efforts to raise hydraulic heads in the   mountain blocks to m atch potentially perc hed hydraulic-head observations.

- Recharge runoff efficiencies were not optimized as they were being unreasonably estimated during calibration. During calibration, the R_ROLVF_WT parameter was manually adjusted to control hydraulic heads in Clover Valley. Other parameters could control heads in this area without the wider impacts across the model.

In late-stage model testing, attempts were made to optimize several sets of parameters (Table 6-7).

Table 6-7
Late-Stage Parameter Optimization Runs

Run Number	Description
Run 1	A set of 7 of the 20 most sensitive, non-CHD and nonrecharge parameters (Table 6-5)
Run 2	A set of 7 grouped parameters (Table 6-6)
Run 3	The 20 most sensitive, non-CHD and nonrecharge parameters (Table 6-5)

Run 1 included some of the lower-sensitivity parameters that were selected over higher-sensitivity parameters listed in Table 6-5 based on information from previous sensitivity runs, including:

- The HFB_HK conductance was fixed nea r the end of the calibration process because (1) it was not cha nging by lar ge amounts, and (2) in some cases, even small cha nges in t his parameter were causing the model to fail to converge in the steady-state stress period because of issues with the SFR2 module in the area near the Pahranagat Shear Zone.

- Some parameters, while sensitive, did not always improve model results in acceptable ways. While improving one section of the model, another area might be significantly degraded. Because of the different observation types and the une ven distribution of observations, properly balancing observation weights was difficult.

These parameters were also relatively uncorrelated (< 85 percent correlation). The optimized values from Run 1 were used as inputs into the remaining two optimizations.

Run 2 included a set of 7 of the most sensitive of the 10 grouped parameters listed in Table 6-6. The three least sensitive parameters were dropped because of their relatively small CS Ss. Two of the included parameters, UVF_SY_VAL and CARBSY_VAL, while also having fairly small sensitivities, were known to be very important in calculating proper drawdowns in pumping areas.

Run 3 included the 20 most sensitive, non-constant head and non-recharge parameters listed in Table 6-5.

Both Runs 2 and 3 failed to converge.

- Run 2 failed to converge after 30 iterations. It was apparent that more iterations would not result in c onvergence. The convergence criteria measure (maximum calculated parameter change) in this run was also oscillating. The principal parameter being adjusted in this case was CARBSY_VAL. It was oscillating between 1 and 6 percent, at what appeared to be more or less random adjustments. The SoSWR was reduced by several percent in this run, but this was mainly due to an increase in the UVF Sy value. The UVF Sy value was limited to 23 percent, as previous tests estimated values closer to 40 percent, which was unreasonably large.

- Run 3 was terminated after 19 iterations (five days) because of large oscillations in parameter values.

These final estimated parameters are interpreted as representing the most important system characteristics. Thi s analysis helps ensure t hat the measures of prediction uncertainty, calculated using the numerical model, reflect most of the uncertainty in the system; all measures of prediction uncertainty presently available propagate to t he uncertainty of t he estimated parameter values. Uncertainty in other aspects of the model is not propagated into the uncertainty measures; therefore, the total uncertainty as estimated here is considered to be underestimated.

If a model represents a physica l system a dequately and the observations used in the re gression provide substantial information about the parameters being estimated, it is reasonable to think that the

parameter values that produce the best match between the observed and simulated values would be realistic. Thus, model err or would be indicated by unreasonable estimates of parameters for which the data provide substantial information.

A measure of the amount of information provided by the observations for any parameter is the CSS value and the linear confidence interval on the parameter. Generally, a parameter with a large CSS value will have a small confidence interval relative to a parameter with a smaller CSS value. If an estimated parameter value is unreasonable and the data provide enough information so that the linear 95 percent confidence interval on the parameter estimate also excludes reasonable parameter values, the problem is less likely to be lack of data or insensitivity and more likely to be model error or misinterpreted hydraulic-conductivity data.

The model's calibrated parameter values and the 95 percent linear confidence intervals are presented in Table 6-8. The 95 per cent confidence intervals for the selected parameters were calculated assuming a log-normal distribution at ±2 standard deviations from the geometric mean (Helsel and Hirsch, 1992, p. 73-74). In most cases, the estimated parameter values and related model-calculated 95 percent linear confidence intervals are within the range of K values determined by baseline data analysis. As st ated in Section 6.1.5, the model statistics are very clear that this model is highly nonlinear; therefore, the 95 per cent linear confidence intervals are not ve ry meaningful for this model.

Table 6-8
95 Percent Linear Confidence Intervals
for Calibrated Parameters

Parameter	Description	Upper 95% Confidence Interval	Final Estimated Value	Lower 95% Confidence Interval
UVF_AF_HK	UVF K_h Alluvial Fan	14.2	13.31	12.5
LV_CCCMB_H	LVF K_h Caliente Caldera Mountain Block	0.0425	0.04075	0.0391
LC_MB_D_HK	LC K_h Mountain Block Detachment Zone	0.13	0.1261	0.122
LC_MB_S_HK	LC K_h Mountain Block Slight Extension Zone	0.0941	0.09085	0.0878
CA_SBSD_HK	LC K_h Structural Basin (All)	0.0567	0.05217	0.048
KDEP_UVF	UVF KDEP λ	0.00142	0.001311	0.00121
KDEP_LCLVF	LC LDF KDEP λ	0.000215	0.0001979	0.000182

Even with a nonlinear model, however, linear confidence intervals are useful when t he range of possible values for the optimized parameter does not overlap with reasonable values for the parameter (Hill, 1998). This generally indicates there is a problem with the conceptual model represented in the numerical model. The model-estimated confidence intervals on the parameter estimates shown in Table 6-8 appear unrealistically small. This is largely because they represent the confidence interval for the mean hydraulic-conductivity value of the defined hydrogeologic unit or zone. As pointed out by Hill (1998), confidence intervals on mean values are rapidly reduced from the entire range of the population as data are applied to the estimati on of the mean. The v alidity of the idea that the

hydrogeologic units have uniform mean or effective values is, of course, a basic assumption of the modeling approach used in this work.

No prior information was included in the objective function to restrict the estimation process; only the model design and the observation data influenced parameter estimation. Estimation of the most important parameters without prior information has the advantage of allowing a more direct test of the model using the observation data. In this approach, the available information on reasonable parameter values was used to evaluate the estimated parameter values.

Partly because of the numerical model's nonlinearity, the CSS values change somewhat as the parameter values change. As a result, the evaluation of CSS values was repeated frequently. The final values changed somewhat but were still quite similar to initial values and generally indicate that the parameters being estimated were the most important parameters. Exceptions occur for parameters that were correlated with parameters with larger CSS values and for parameters that mostly influence model fit to a single observation.

6.3   Evaluation of Estimated Parameter Values

This section contains an evaluation of the modeling parameters, including hydraulic conductivity, storage, and recharge.

6.3.1   Hydraulic Conductivities

The calibrated hydraulic-conductivity values fall within, or are near, literature ranges. The calibrated hydraulic-conductivity values are shown in Figures 6-43 through 6-49 and are compared to published ranges for like materials (left-most bar) and to the range of values in the adjacent DVRFS model and study area (second bar on left).

Quantitatively, the estimated values of K appear reasonable. They fall within published ranges. From a qualitative perspective, the spatial distribution of K is consistent with the conceptual model. Mountain-block areas are generally less disturbed and therefore have lower K and T values. Valley basins tend to have higher K and T values because they are more disturbed and contain higher-K alluvial deposits. Areas with volcanic, plutonic, or basement clastic rocks also tend to have lower K. Fault zones tend to be of higher K and T, sometimes significantly higher.

A list of all MODFLOW HUF2 parameters is provided on the DVD. Note that most MODFLOW HUF2 parameters are not directly estimated. There are over 2,000 HUF2 HGU-named HK and $VANI$ parameters. Most are derived from one or more UCODE parameters. This allows for a great deal of flexibility when manually calibrating because relatively isolated areas of the model can be tested independently of the rest of the model. If necessary, a new UCODE factor parameter can be added to act as a modifier to the base parameter. During the automated calibration process, though, a few parameters can still be adjusted to influence the overall model. This approach was used to allow model flexibility without drastically overparameterizing the model.
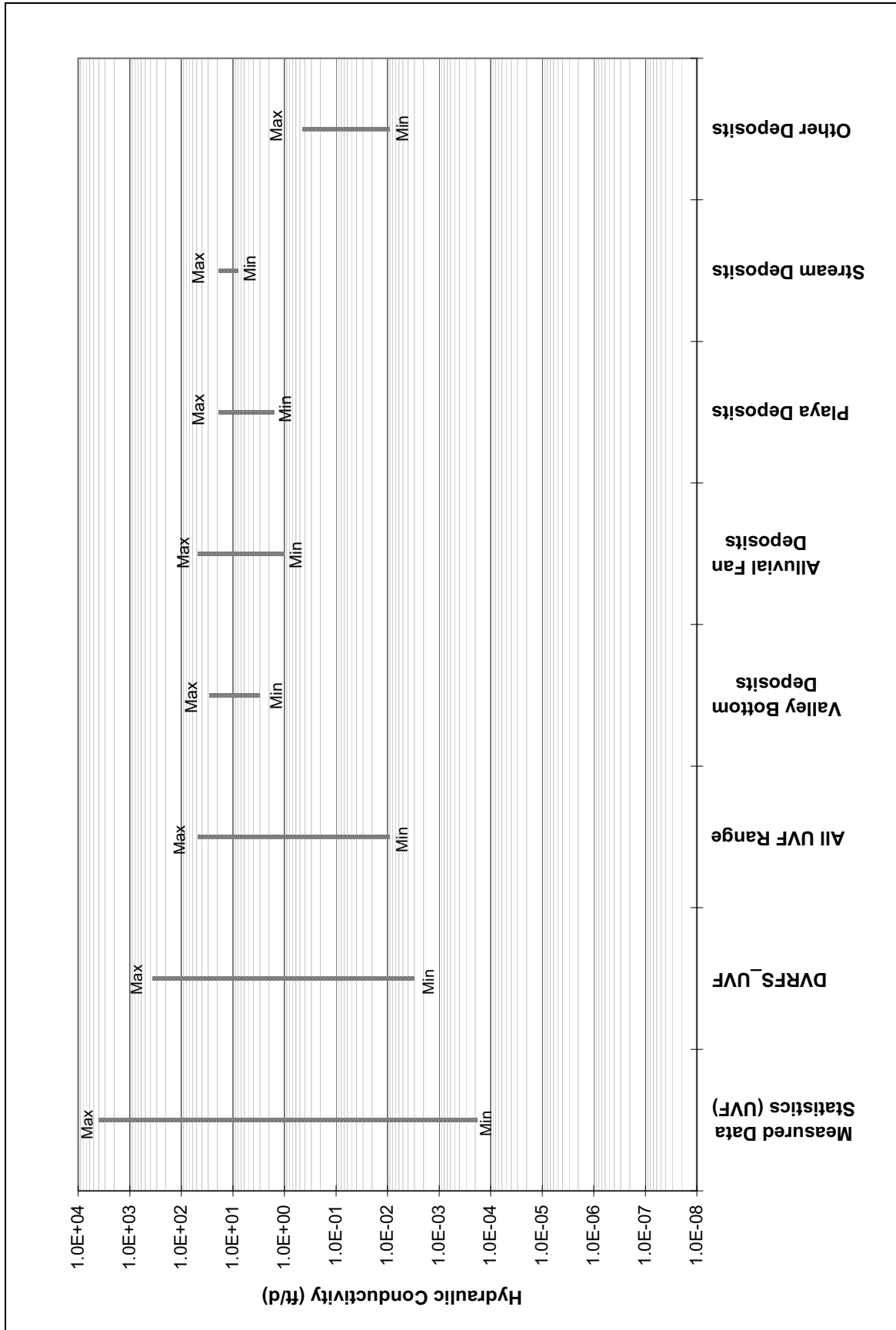
Figure 6-43
Parameters Defining Hydraulic Conductivity for UVF

SE ROA 50986

JA_16387
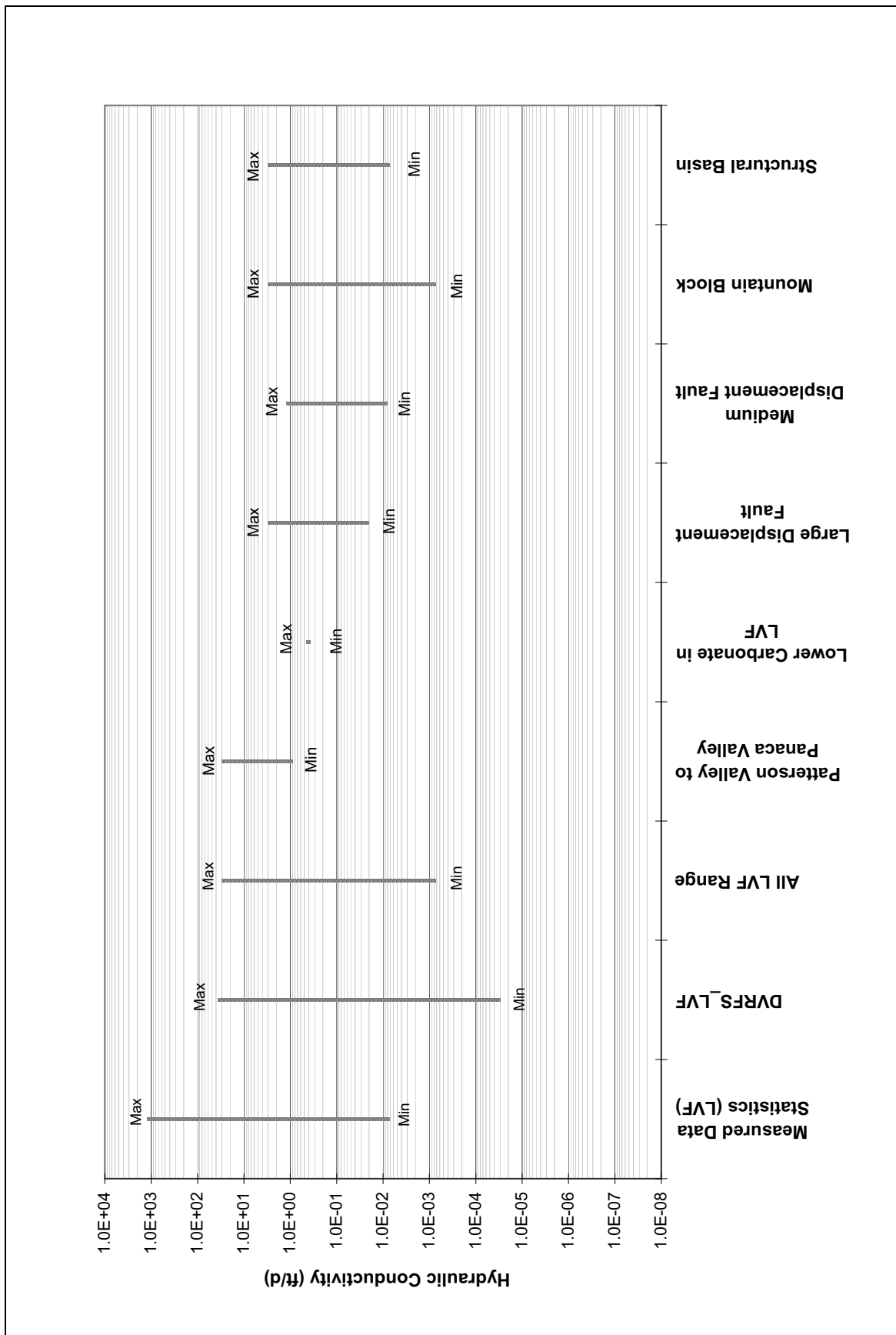
Figure 6-44
Parameters Defining Hydraulic Conductivity for LVF

SE ROA 50987

JA_16388
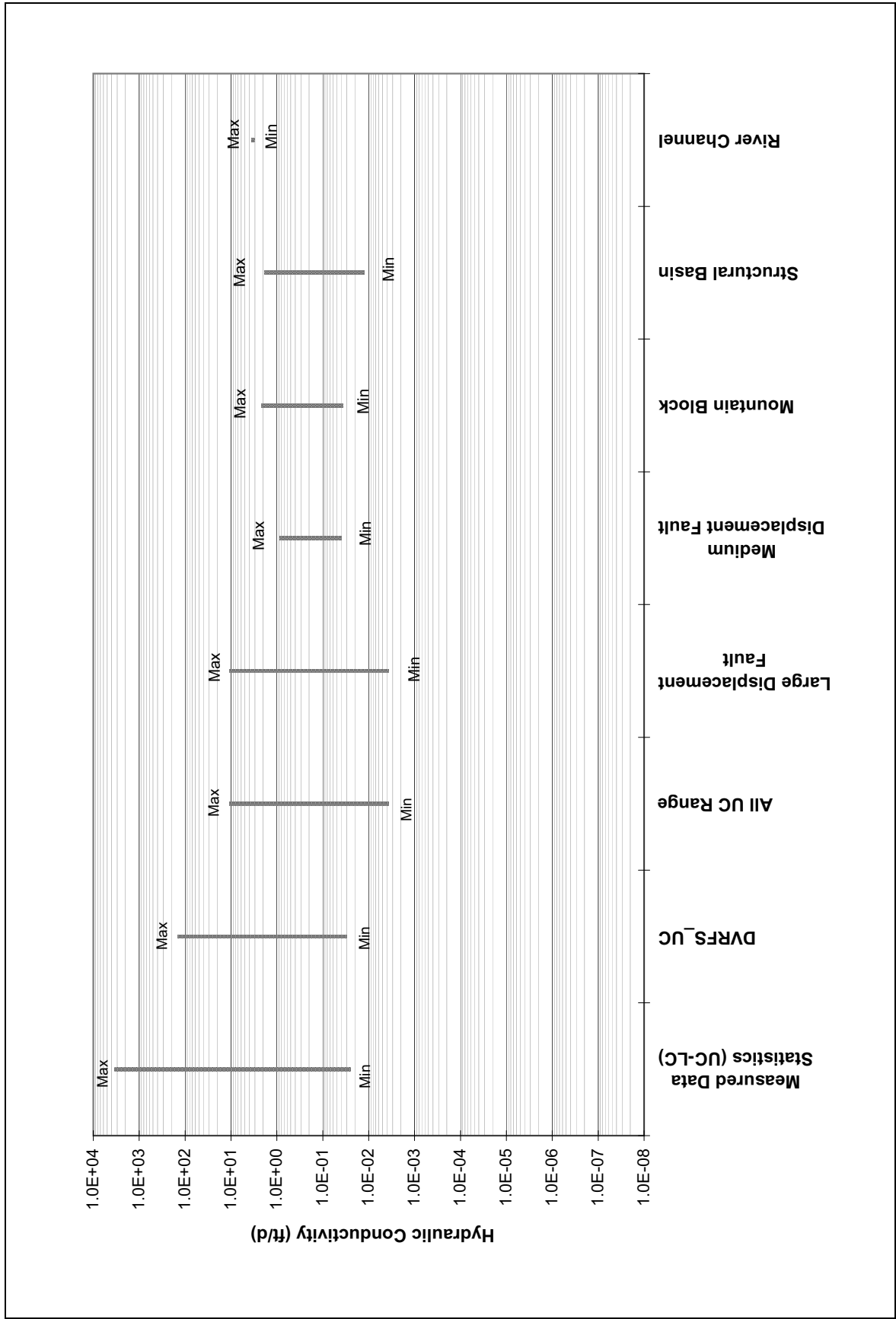
Figure 6-45
Parameters Defining Hydraulic Conductivity for UC

SE ROA 50988

JA_16389
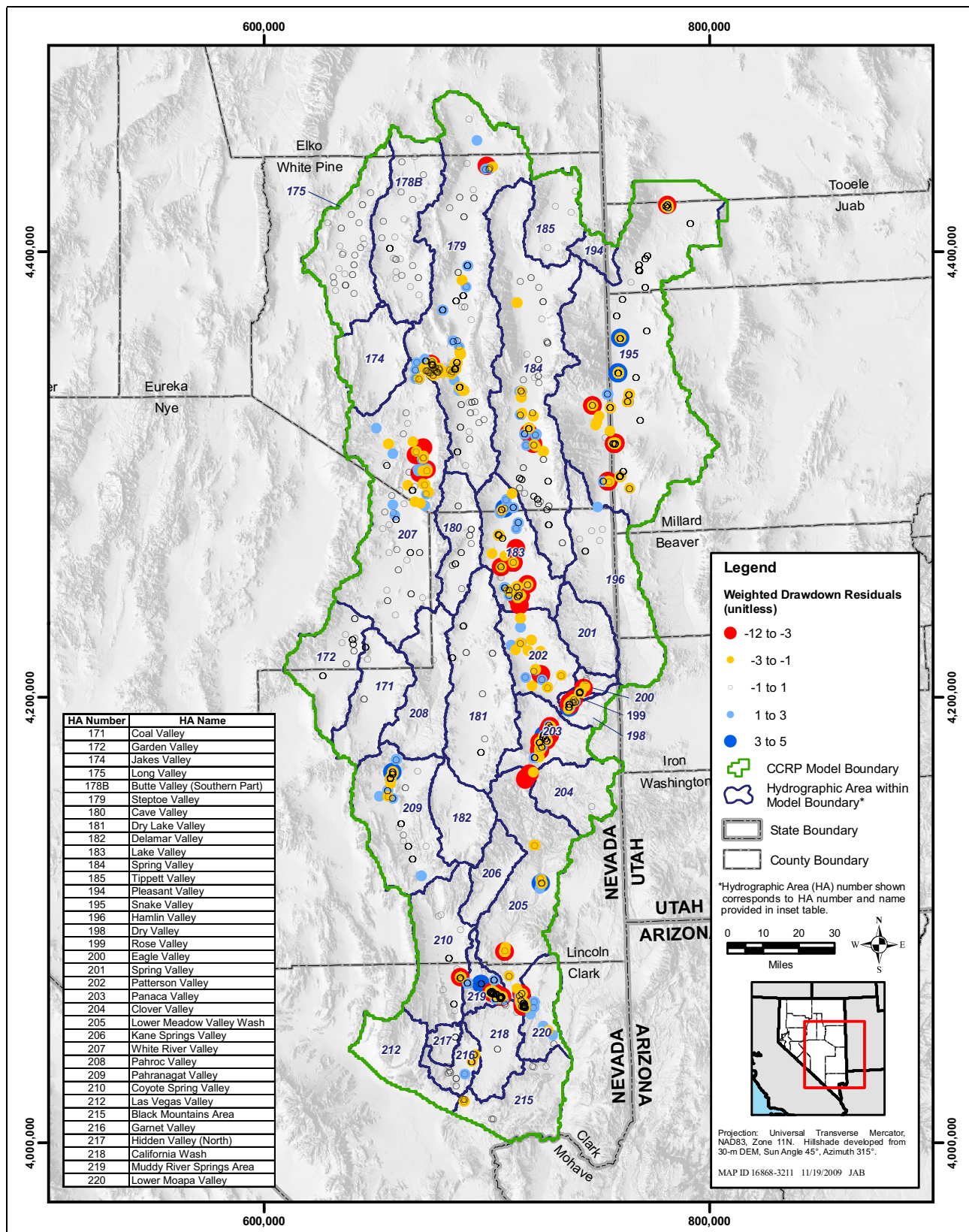
Figure 6-12
Spatial Distribution of Weighted Drawdown Residuals
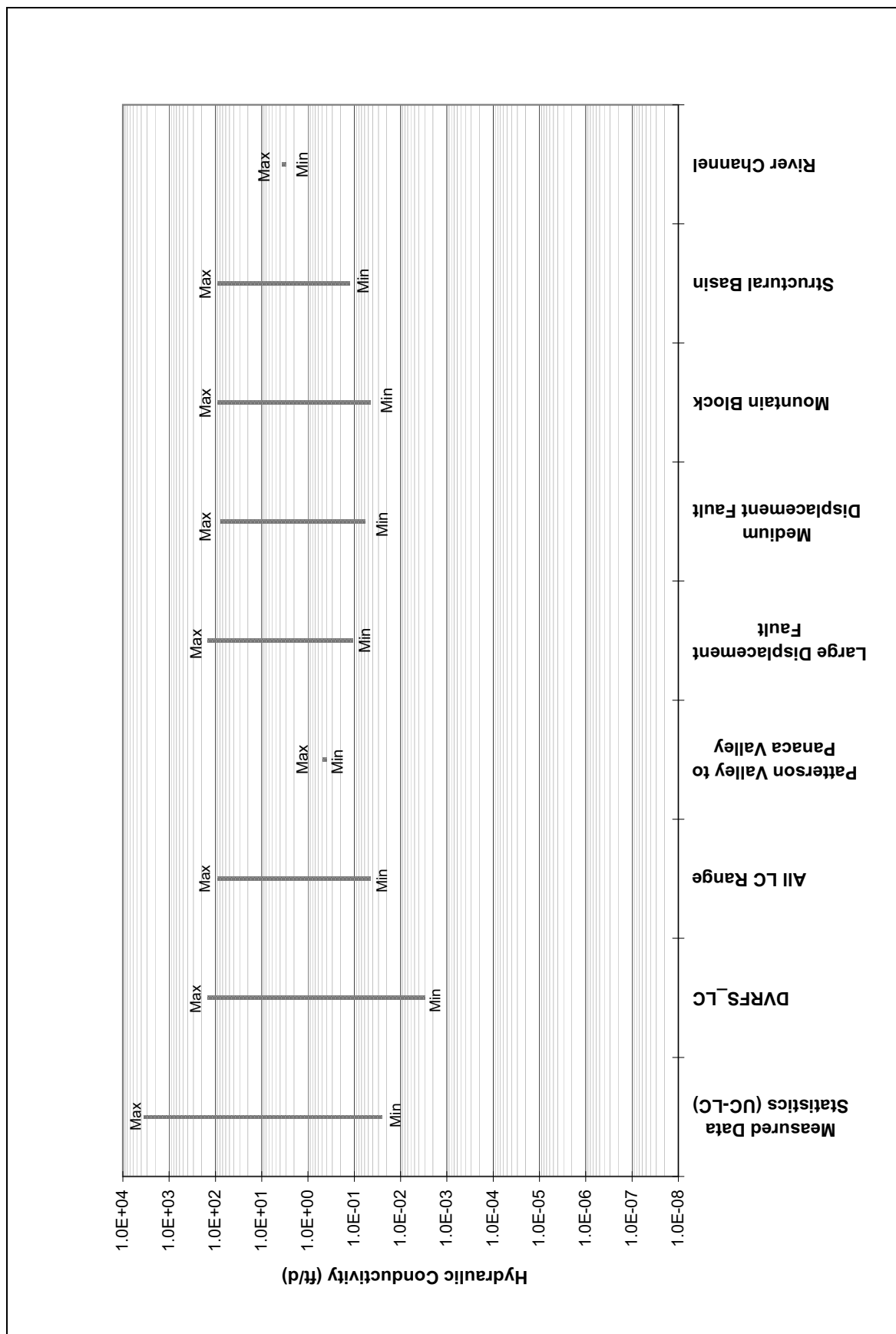
**Figure 6-46
Parameters Defining Hydraulic Conductivity for LC**

JA_16390
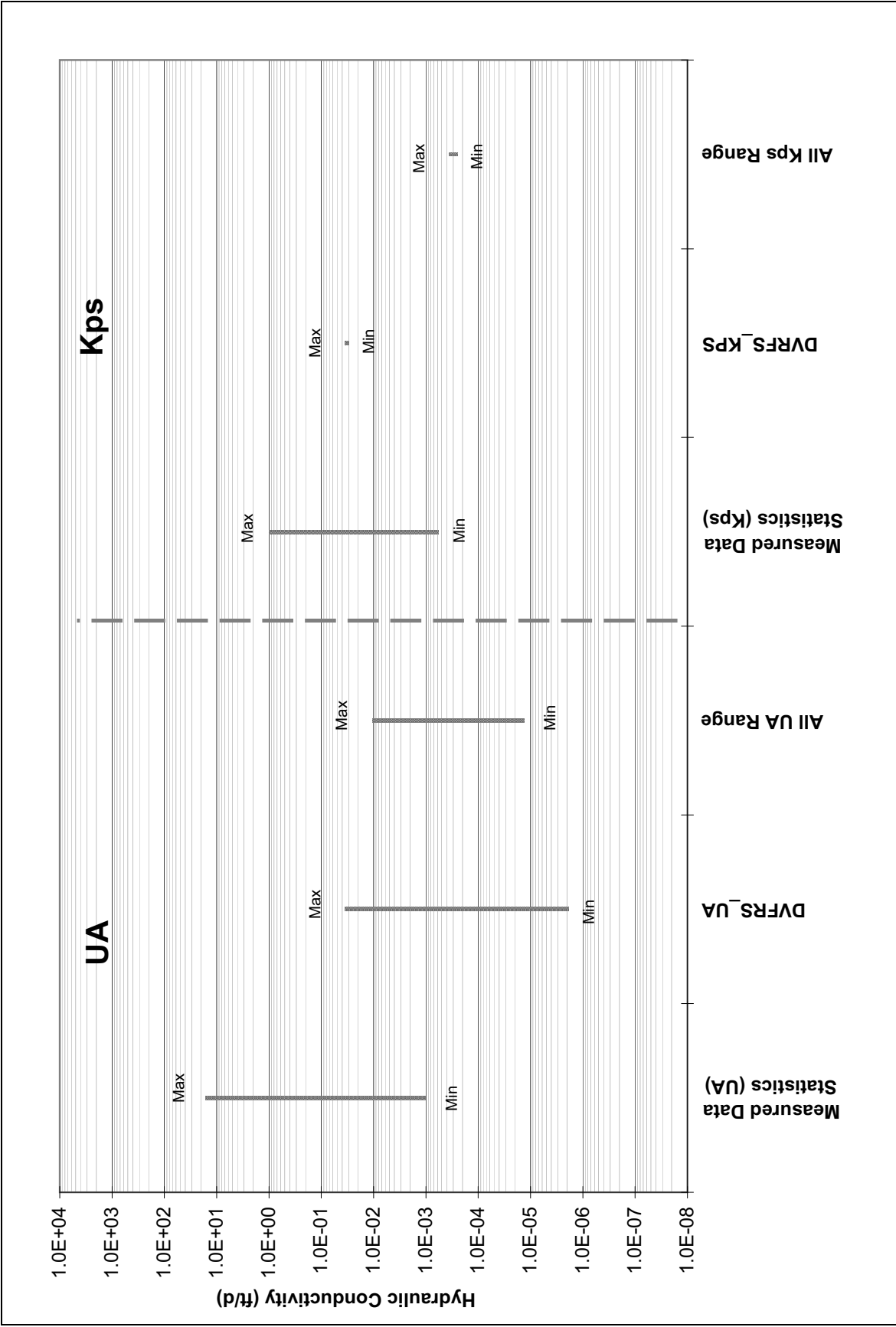
Figure 6-47
Parameters Defining Hydraulic Conductivity for UA and Kps

SE ROA 50990

JA_16391
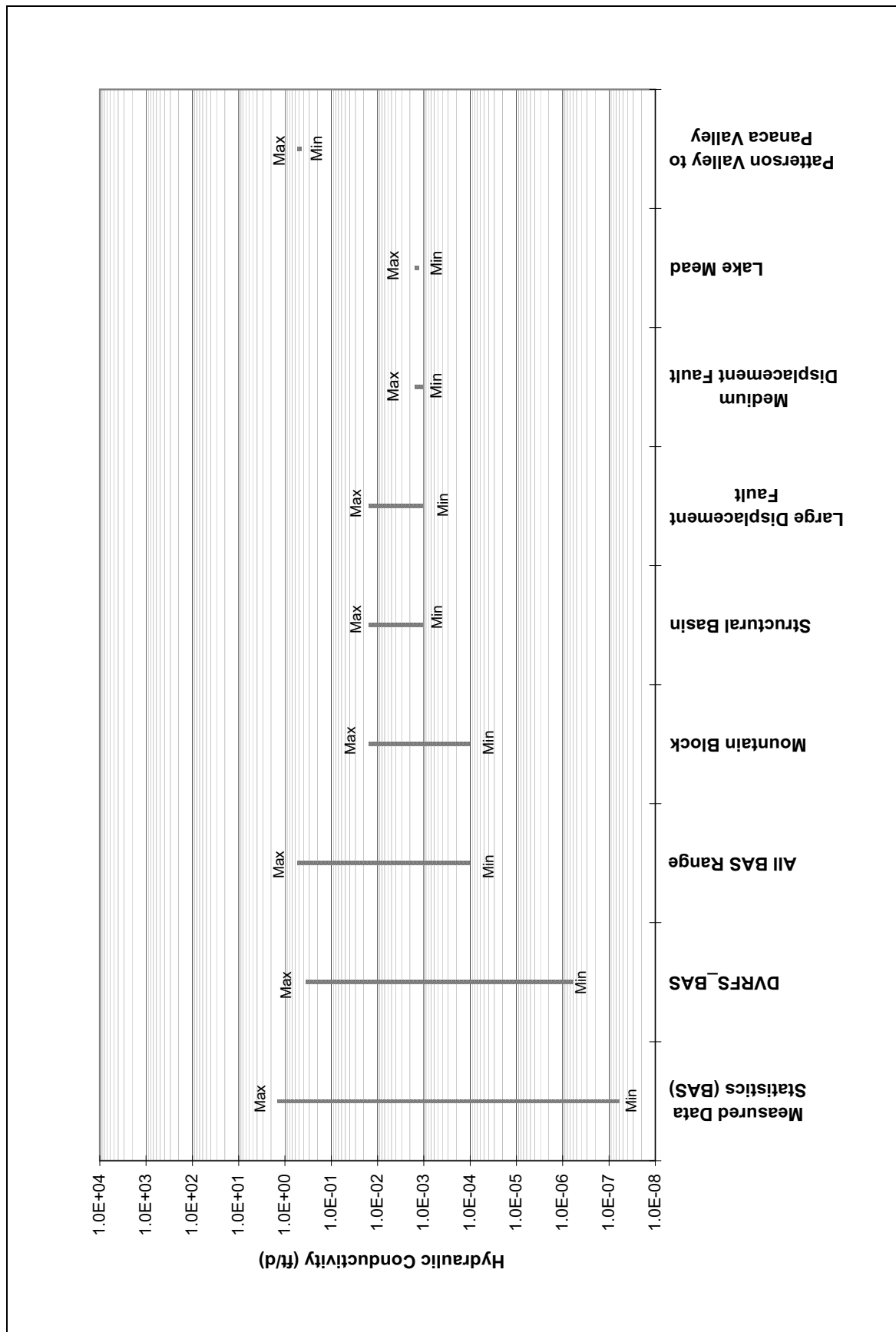
Figure 6-48
Parameters Defining Hydraulic Conductivity for BASE (BAS)

SE ROA 50991

JA_16392
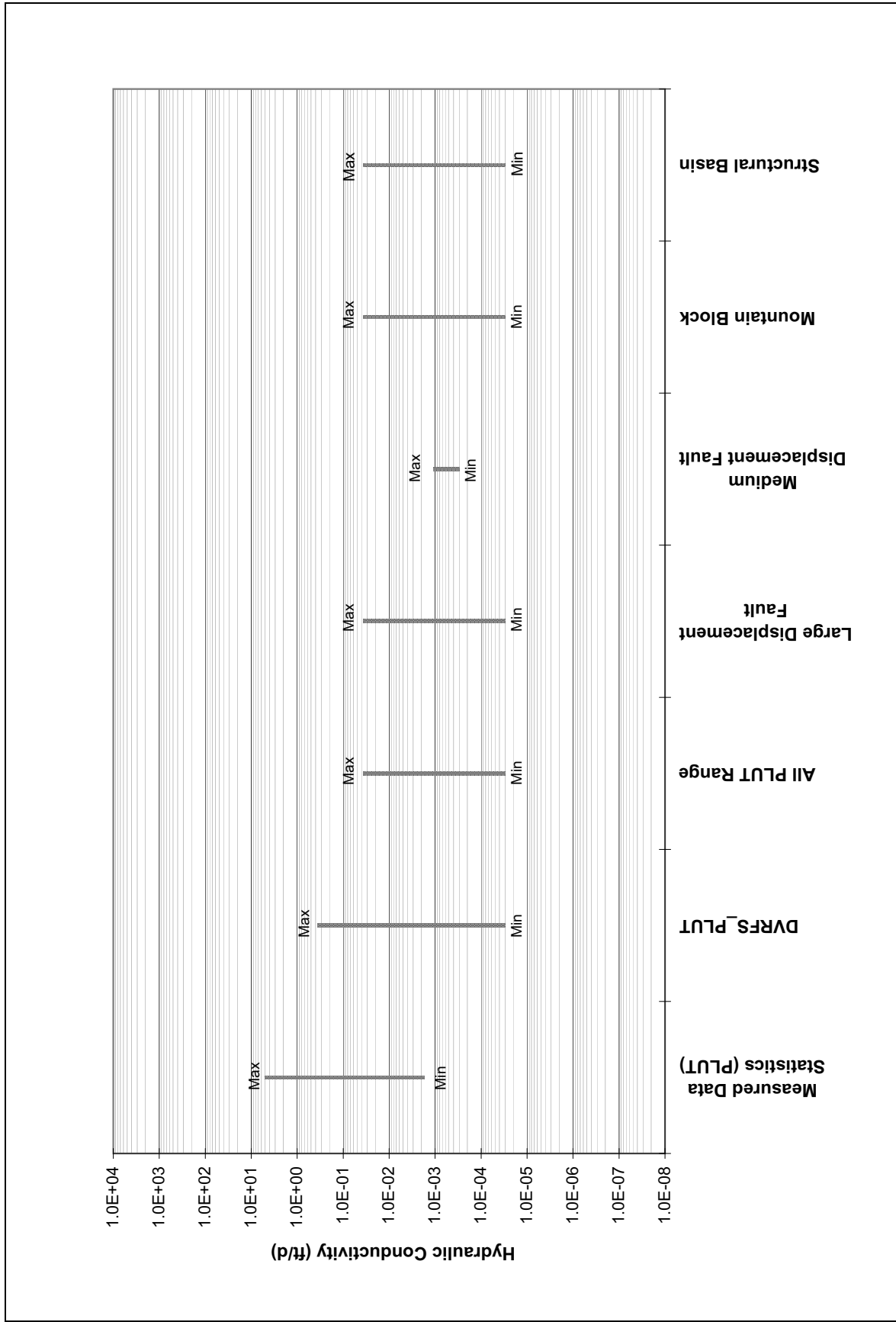
Figure 6-49
Parameters Defining Hydraulic Conductivity for PLUT

Section 6.0

SE ROA 50992

JA_16393

6.3.1.1   *KDEP Values*

The *K* values presented in Figures 6-43 through 6-49 all reference the *K* of materials at or near the ground surface. For UVF and presented faulted carbonate materials, it is assumed that *K* decreases up to two orders of magnitude with depth. Two KDEP parameters, KDEP_UVF and KDEP_LCLDF were optimized using parameter estimation. The KDEP values used in the model are presented in Table 6-9, and the influence on *K* is shown in Figure 6-50. KDEP for the unfaulted carbonates was essentially zero (1.0E-7).

Table 6-9
Estimated KDEP Values

Parameter Name	Calibration Method	Estimated Value (1/m)
KDEP_UVF	UCODE Optimization	1.311E-03
KDEP_LC_NF	Manual	1.000E-07
KDEP_LCLDF	UCODE Optimization	1.979E-04
KDEP_LCMDF	Manual	2.500E-04
KDEP_PANAC	Manual	7.000E-03
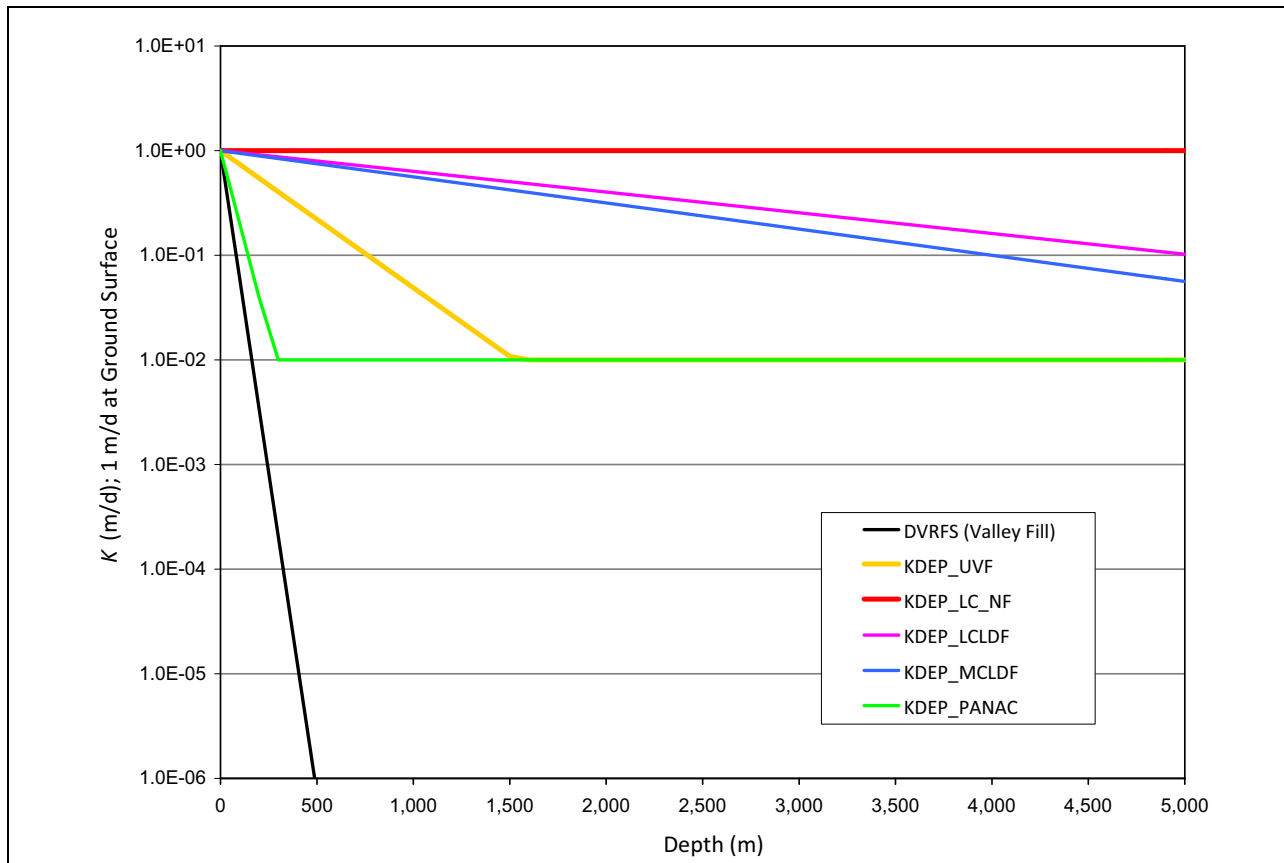
Figure 6-50
KDEP Influence on Hydraulic Conductivity

SE ROA 50993

JA_16394

6.3.1.2   Spatial Distribution

The spatial distribution of hydra ulic conductivity for each numerical model laye r is pre sented in electronic form (see DVD). Transmissivity for the entire saturated thickness of the numerical model is shown in Figure 6-51. Figure 6-51 also illustrates the transmissivity of the DVRFS transient flow model (Faunt et al., 2004) for comparative purposes. As shown in Figure 6-51, the range of transmissivity of the numerical model compares well to that of the DVRFS model.

6.3.2   Storage

While storage parameters significantly influence the magnitude of dra wdowns in the study area, particularly in the UVF, the *Ss* and *Sy* parameters are not the most sensitive parameters. In fact, the UVF_SYTP CSS is the most sensitive *Ss* or *Sy* parameter but is the 40th most sensitive parameter (Table 6-5). The UVF_SYTP (*Sy*) was initially set at 10 percent. After manual calibration and review of other studies in the area (Appendix A), UVF_SYTP was increased to 18 percent. No other *Ss* and *Sy* parameters were adjusted. As shown in Figures 6-52 and 6-53, these values lie well within published ranges. The S_s and S_y spatial distribution is also provided by model layer in electronic form (see DVD).

6.3.3   Recharge

Recharge is the most significant component of groundwater budgets in the nu merical model. As expected, recharge efficiencies are sensitive parameters. Unfortunately, applying parameter-estimation methods to RE parameters resulted in efficiencies increasing to unreasonable rates. Underestimated spring flow s and hydraulic heads i n mountain blocks appear to drive this behavior. As a result, RE were not estimated; these parameters were manually calibrated. The results achieved are reasonable. The final RE are reported in Tables 6-10 and 6-11.

Figures 6-54 and 6-55 show the simulated recharge, target recharge, and range of recharge from literature sources for flow systems and hydrographic areas. The simulated recharge (580,700 afy) is within 1 percent of the target recharge (571,000 afy) for the entire numerical model. Moreover, the simulated recharge in each flow system is within literature ranges. Simulated recharge in the GVFS is 28,400 afy above target recharge, mostly due to simulated recharge in Steptoe Valley which is overestimated by 21,900 afy, as compared to the target value. While it is overestimated based on the target value, simulated Steptoe Valley recharge is still well within the literature range provided in the conceptual model (SNWA, 2009a). Thus , Steptoe Valley accounts for the majority of the recharge difference in the GVFS.

Figures 6-56 through 6-58 illustrate the simulated in-place and runoff recharge components for flow systems, hydrographic areas, and sub-basins. The potential recharge is also shown (see Section 4.0 for a dis cussion of t he development of these recharge components). At the flow-system scale, potential recharge is equivalent to the sum of runoff and in-place recharge. At the hydrographic-area and sub-basin scale, the potential rec harge can slightly deviate from the sum of runoff and in-place recharge. This deviation results from a small component of runoff moving down-gradient to an adjacent hydrographic area or sub-basin. The notable feature of the graphs in Figure 6-56 is the larger
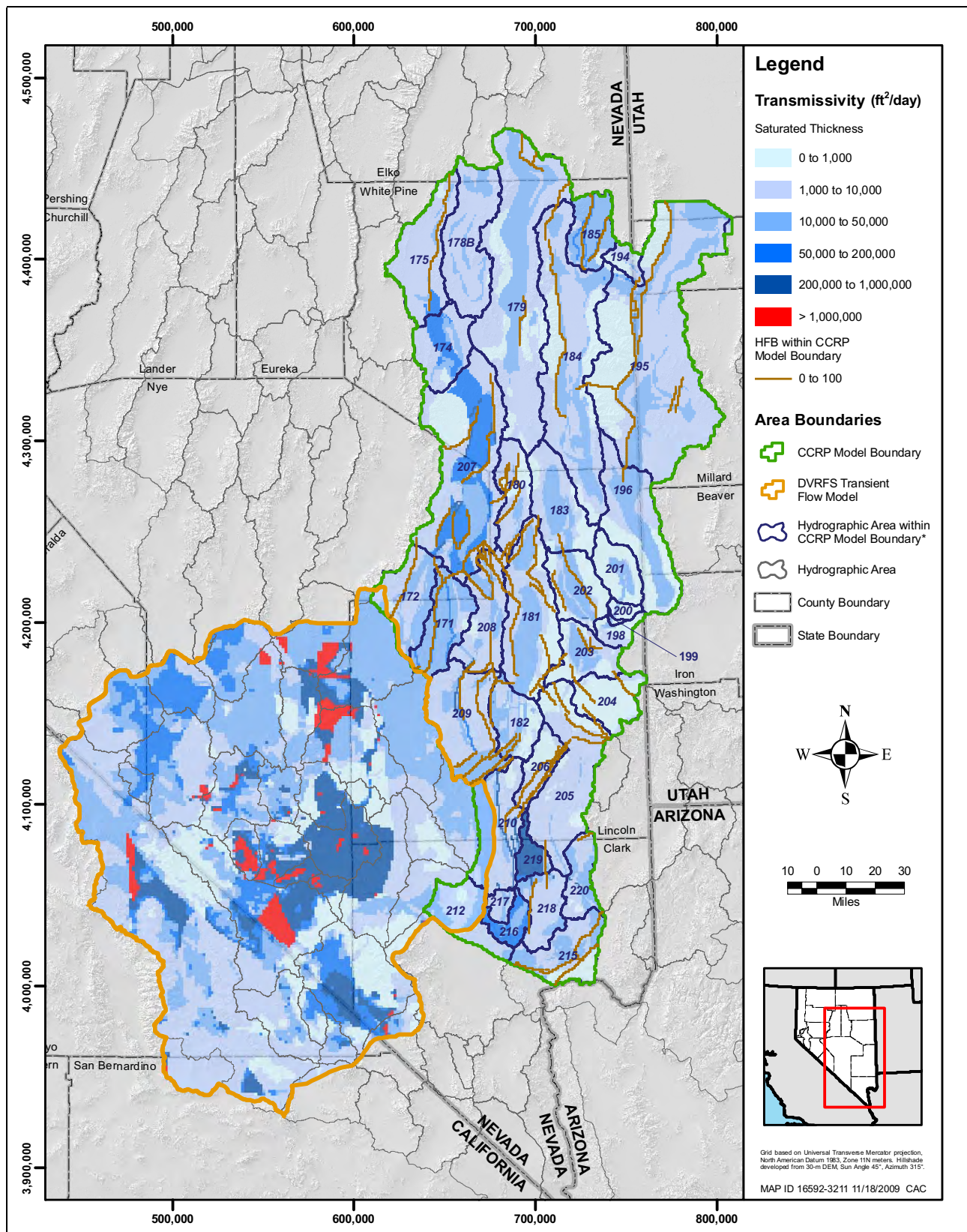
Figure 6-51
Cumulative Transmissivity Distributions of CCRP and DVRFS Models

SE ROA 50995

JA_16396
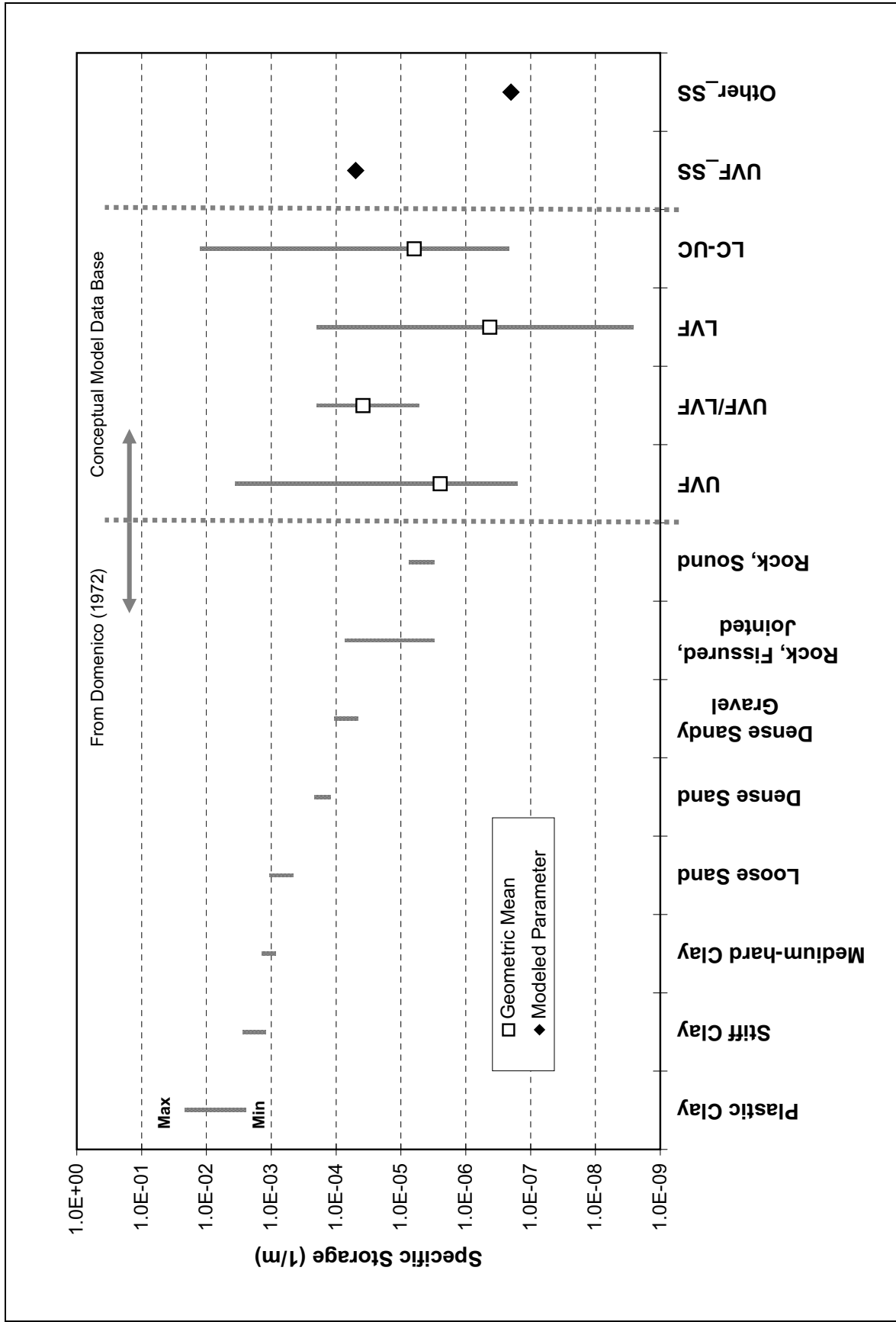
Figure 6-52
Specific-Storage Parameter Values

JA_16397
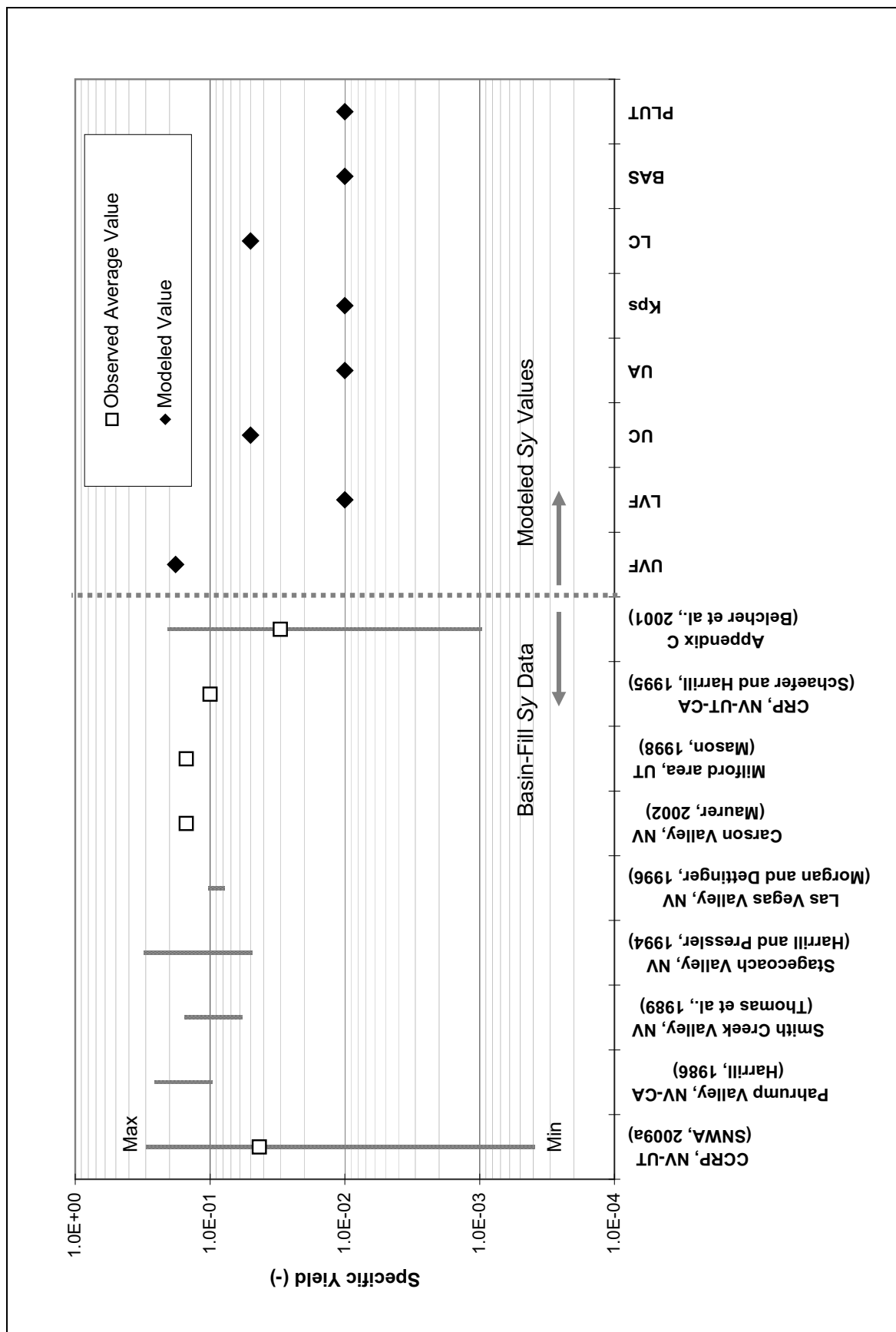
Figure 6-53
Specific-Yield Parameter Values

SE ROA 50997

JA_16398

Table 6-10
Manually Estimated Recharge Efficiencies as Fraction of Precipitation

Precipitation Zone (in./yr)	Parameter Name	Estimated Parameter Value (-)	Final Recharge Efficiency (fraction of precipitation)	UCODE-Derived Parameter Name
Goshute Flow System				
<8	NE	1	0.000	NE
8 to 12	RSC_ME_GV	1.25	0.018	R_ME2_GV_R
12 to 15	RSC_ME_GV	1.25	0.066	R_ME3_GV_R
15 to 20	RSC_ME_GV	1.25	0.158	R_ME4_GV_R
>20	RSC_ME_GV	1.25	0.396	R_ME5_GV_R
Great Salt Lake Desert Flow System				
<8	NE	1	0.000	NE
8 to 12	RSC_ME_GSL	1	0.011	R_ME2_GSLD
12 to 15	RSC_ME_GSL	1	0.050	R_ME3_GSLD
15 to 20	RSC_ME_GSL	1	0.120	R_ME4_GSLD
>20	RSC_ME_GSL	1	0.328	R_ME5_GSLD
Las Vegas Flow System				
<8	NE	1	0.000	NE
8 to 12	RSC_ME_WR	1.052	0.006	R_ME2_LV_R
12 to 15	RSC_ME_WR	1.052	0.037	R_ME3_LV_R
15 to 20	RSC_ME_WR	1.052	0.125	R_ME4_LV_R
>20	RSC_ME_WR	1.052	0.392	R_ME5_LV_R
Meadow Valley Flow System				
<8	NE	1	0.000	NE
8 to 12	RSC_ME_MVW	1.1	0.001	R_ME2_MVW_
12 to 15	RSC_ME_MVW	1.1	0.010	R_ME3_MVW_
15 to 20	RSC_ME_MVW	1.1	0.054	R_ME4_MVW_
>20	RSC_ME_MVW	1.1	0.193	R_ME5_MVW_
Newark Valley Flow System				
<8	NE	1	0.000	NE
8 to 12	RSC_ME_WR * 0.5	1.052	0.003	R_ME2_NE_R
12 to 15	RSC_ME_WR * 0.5	1.052	0.018	R_ME3_NE_R
15 to 20	RSC_ME_WR * 0.5	1.052	0.062	R_ME4_NE_R
>20	RSC_ME_WR * 0.5	1.052	0.196	R_ME5_NE_R
White River Flow System				
<8	NE	1	0.000	NE
8 to 12	RSC_ME_WR	1.052	0.006	R_ME2_WR_R
12 to 15	RSC_ME_WR	1.052	0.037	R_ME3_WR_R
15 to 20	RSC_ME_WR	1.052	0.125	R_ME4_WR_R
>20	RSC_ME_WR	1.052	0.392	R_ME5_WR_R

NE: Not Estimated

SE ROA 50998

JA_16399

Table 6-11
Manually Estimated Recharge Efficiencies for
Recharge Subzone as Fraction of Precipitation

Precipitation Zone (in./yr)	Parameter Name	Estimated Parameter Value (-)	Final Recharge Efficiency (fraction of precipitation)	UCODE-Derived Parameter Name
Great Salt Lake Desert Flow System (Fish Springs)				
<8	NE	NE	0.000	NE
8 to 12	R_ME2_GSLD	1	0.011	R_ME2_GSFS
12 to 15	R_ME3_GSLD	1	0.050	R_ME3_GSFS
15 to 20	R_ME4_GSLD	1	0.120	R_ME4_GSFS
>20	R_ME5_GSLD	1	0.328	R_ME5_GSFS
Great Salt Lake Desert Flow System (Gandy Area Watershed)				
<8	NE	NE	0.000	NE
8 to 12	R_ME2_GSLD * 1.25	1	0.013	R_ME2_GSGY
12 to 15	R_ME3_GSLD * 1.25	1	0.062	R_ME3_GSGY
15 to 20	R_ME4_GSLD * 1.25	1	0.150	R_ME4_GSGY
>20	R_ME5_GSLD * 1.25	1	0.410	R_ME5_GSGY
Great Salt Lake Desert Flow System (Garden Valley)				
<8	NE	NE	0.000	NE
8 to 12	R_ME2_WR_R	1.052	0.006	R_ME2_GSGD
12 to 15	R_ME3_WR_R	1.052	0.037	R_ME3_GSGD
15 to 20	R_ME4_WR_R	1.052	0.125	R_ME4_GSGD
>20	R_ME5_WR_R	1.052	0.392	R_ME5_GSGD
Great Salt Lake Desert Flow System (Hamlin Valley - North)				
<8	NE	NE	0.000	NE
8 to 12	R_ME2_GSLD * 0.50	1	0.005	R_ME2_GSHM
12 to 15	R_ME3_GSLD * 0.50	1	0.025	R_ME3_GSHM
15 to 20	R_ME4_GSLD * 0.50	1	0.060	R_ME4_GSHM
>20	R_ME5_GSLD * 0.50	1	0.164	R_ME5_GSHM
Meadow Valley Flow System (Hamlin Valley - South)				
<8	NE	NE	0.000	NE
8 to 12	R_ME2_MVW_ * 0.50	1.1	0.0003	R_ME2_MVHM
12 to 15	R_ME3_MVW_ * 0.50	1.1	0.004	R_ME3_MVHM
15 to 20	R_ME4_MVW_ * 0.50	1.1	0.025	R_ME4_MVHM
>20	R_ME5_MVW_ * 0.50	1.1	0.088	R_ME5_MVHM
White River Flow System (Dry Lake)				
<8	NE	NE	0.000	NE
8 to 12	R_ME2_WR_R	1.052	0.006	R_ME2_WRDL
12 to 15	R_ME3_WR_R	1.052	0.037	R_ME3_WRDL
15 to 20	R_ME4_WR_R	1.052	0.125	R_ME4_WRDL
>20	R_ME5_WR_R	1.052	0.392	R_ME5_WRDL

NE: Not Estimated
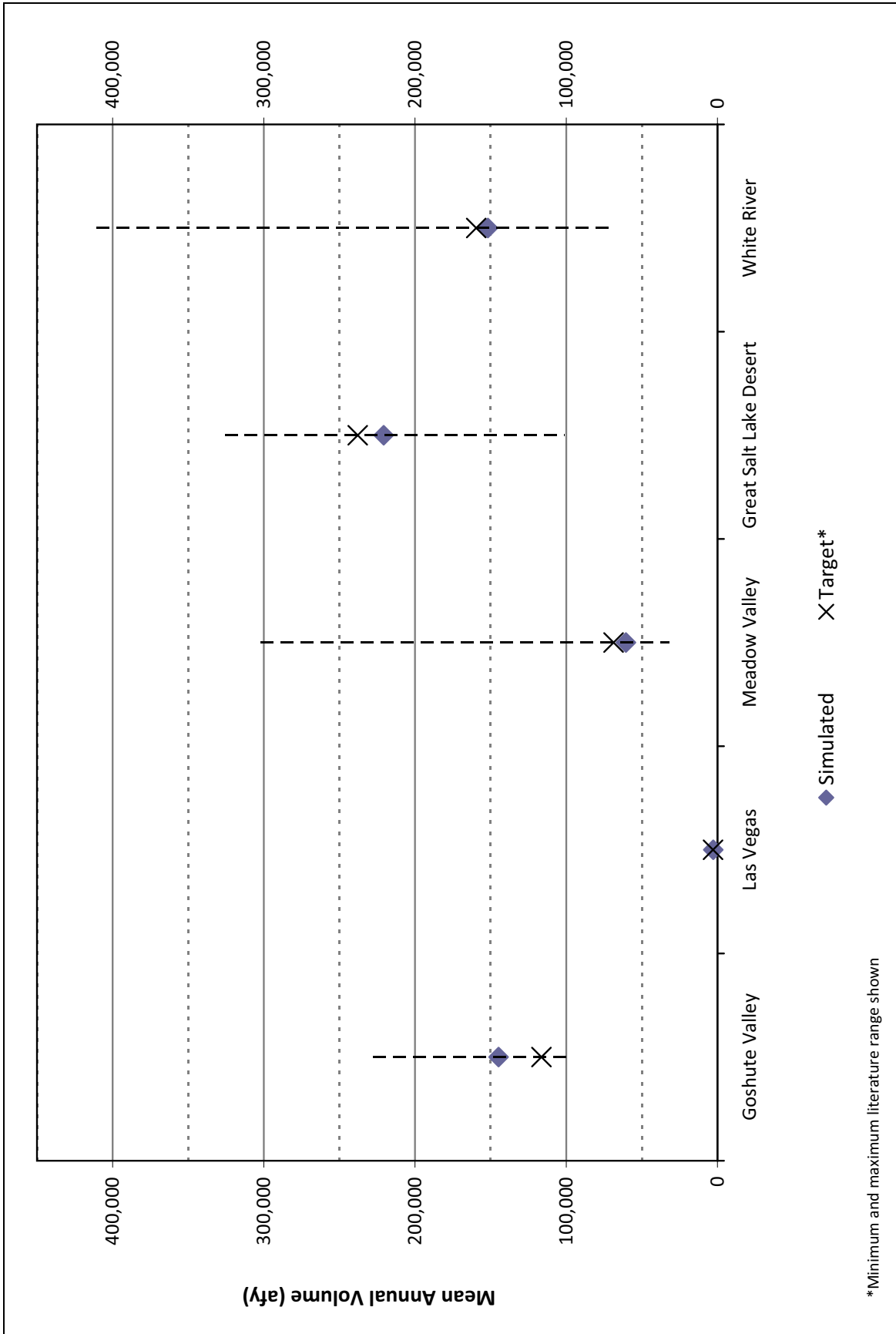
Figure 6-54

Simulated Recharge, Target Recharge, and Range of Recharge from Literature Sources for Flow Systems

◆ Simulated   ✕ Target*

*Minimum and maximum literature range shown

SE ROA 51000

JA_16401
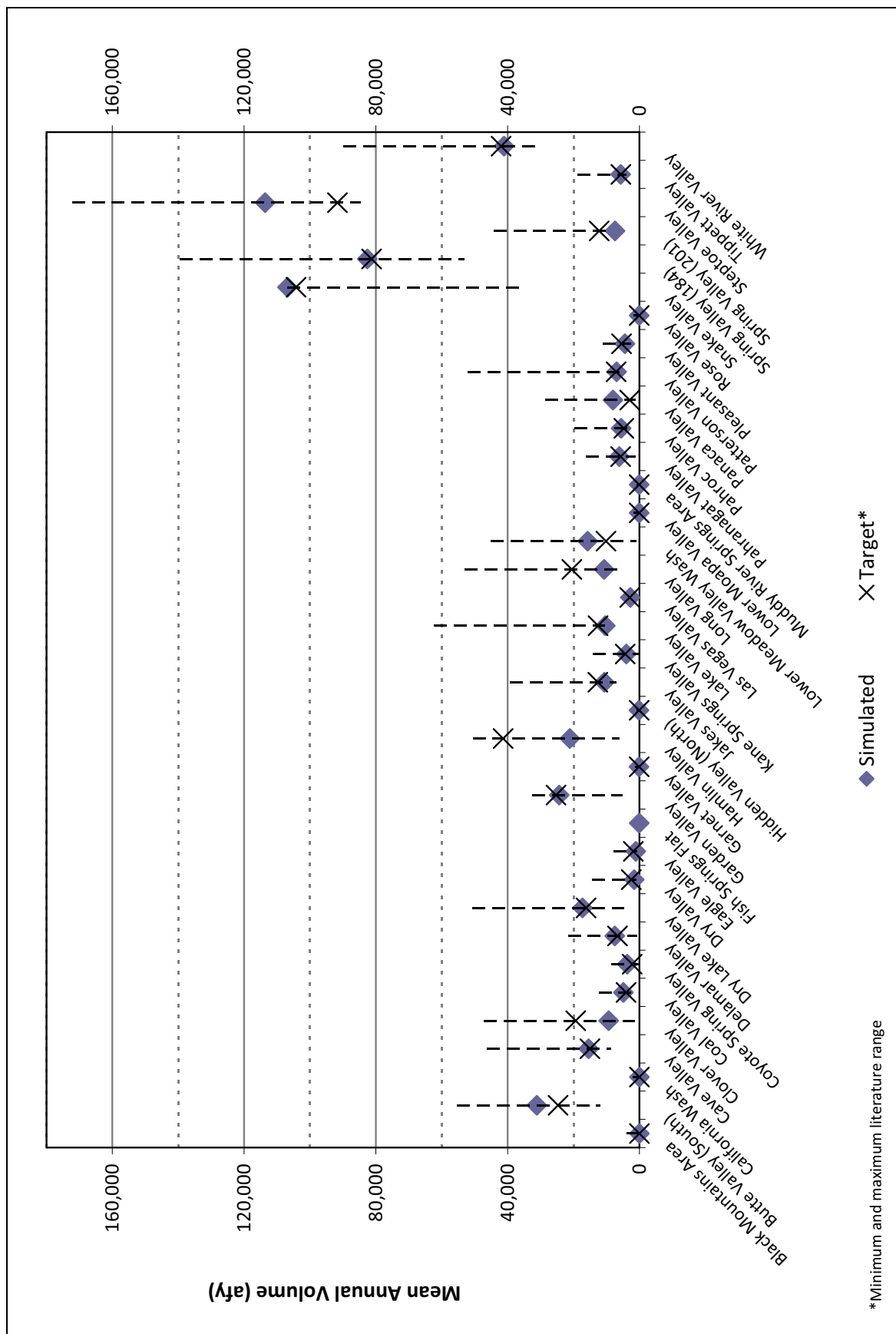
Figure 6-55
Simulated Recharge, Target Recharge, and Range of Recharge from Literature Sources for Hydrographic Areas

*Minimum and maximum literature range
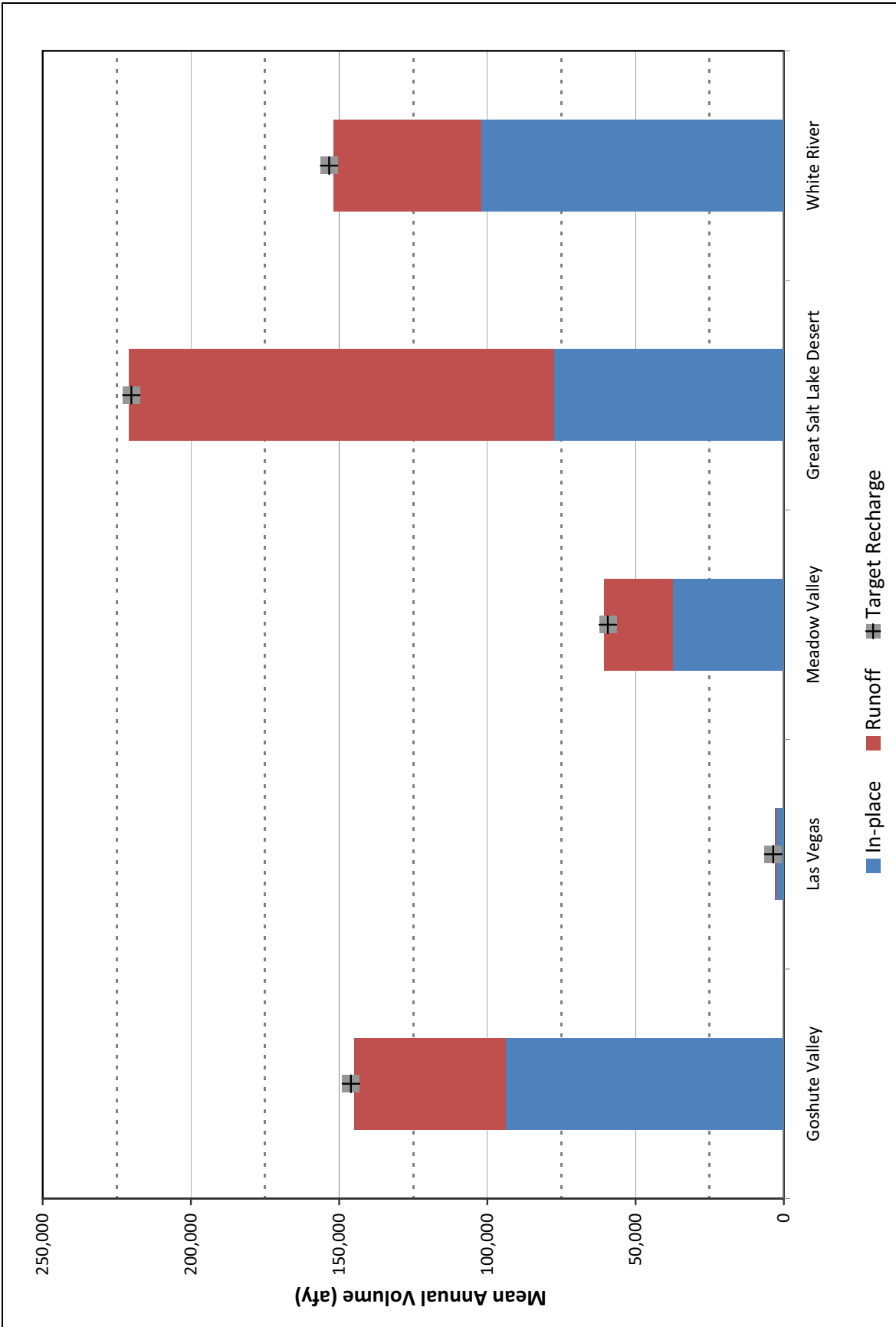
Figure 6-56

Simulated In-Place and Runoff Recharge Components and Target for Flow Systems

SE ROA 51002

JA_16403
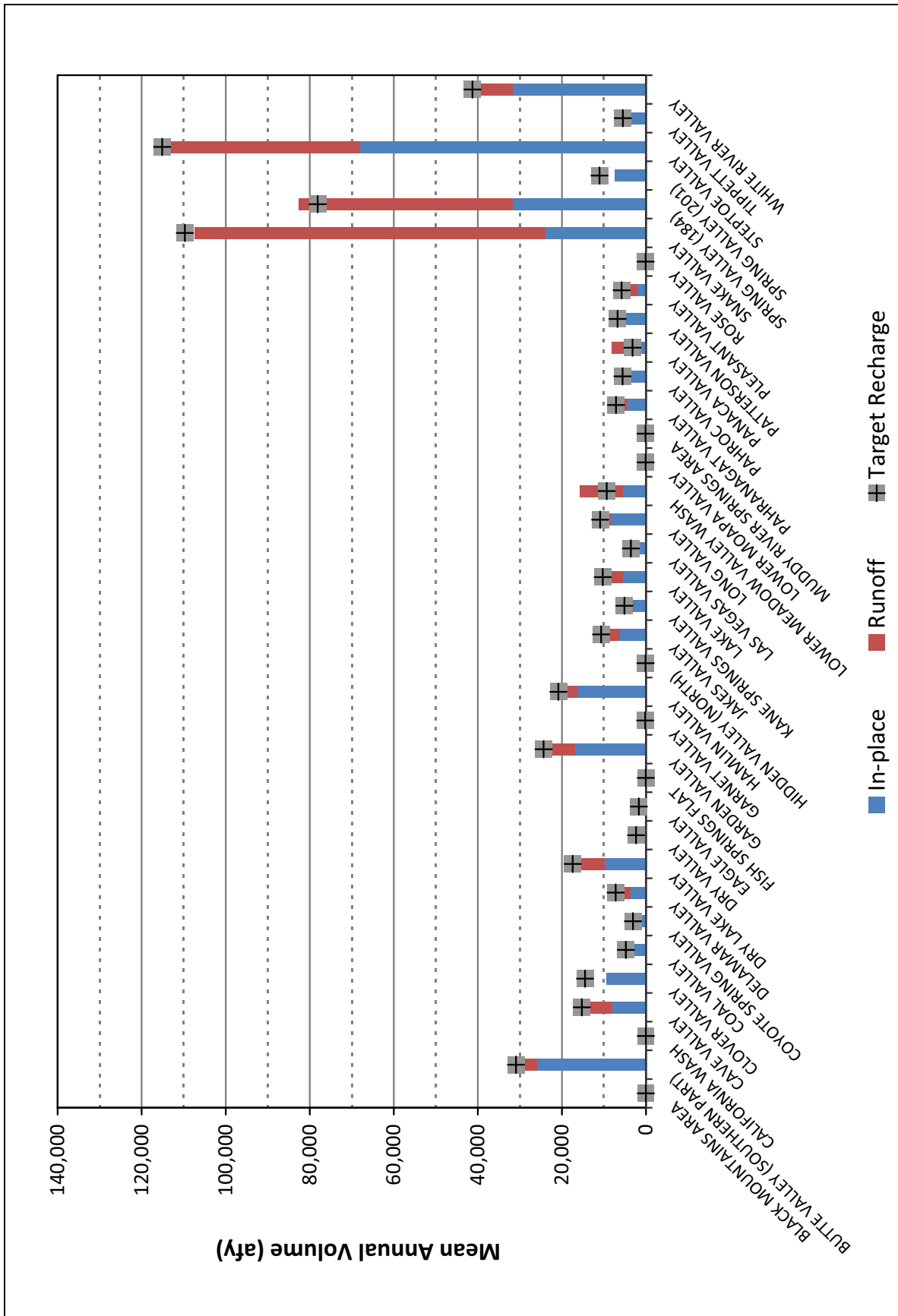
Figure 6-57

Simulated In-Place and Runoff Recharge Components and Target for Hydrographic Areas

SE ROA 51003

JA_16404
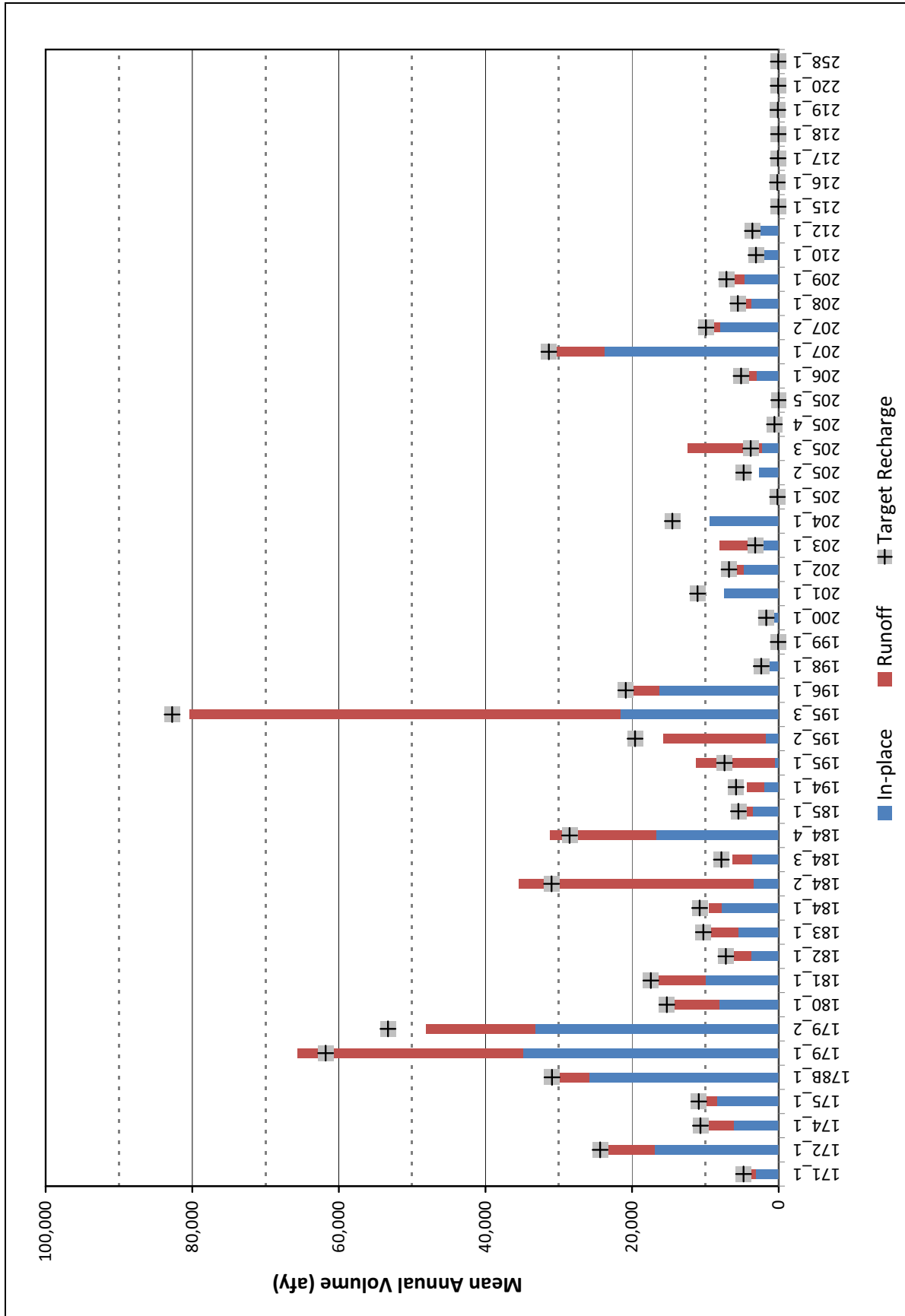
Figure 6-58
Simulated In-Place and Runoff Recharge Components and Target for Sub-Basins

SE ROA 51004

JA_16405

percentage of runoff in the GSLDFS. This is consistent with the less permeable rock types (PLUT and BASE) associated with the Snake and Deep Creek ranges.

6.4   Evaluation of Simulated Flow Systems

The flow systems simulated in the numerical model, including interbasin flow, flow regions, and groundwater budget, are discussed in this subsection. The discussion contains many details that are solely based on model interpretation. Modeling results are not unique and may not be representative of reality in many portions of the model domain because of sparse or nonexistent data.

6.4.1   Simulated Interbasin Flow

Simulated interbasin flow between basins (hydrographic areas) for predevelopment and 2004 conditions are presented in Tables 6-12 and 6-13, respectively. The net groundwater flows between flow-system boundaries for predevelopment and 2004 conditions are presented in Table 6-14. Interbasin flow between two given basins represents the net groundwater flow between the two basins. Totals of interbasin flows simply demonstrate the balance of the inflow and outflow components into a given flow system.

The interbasin flow rates simulated by the numerical model (Table 6-14) are shown on Plates 2 and 3. These two plates also illustrate simulated potentiometric surfaces and simulated groundwater flow regions for the shallow (water table) (Plate 2) and regional (carbonate) (Plate 3) portions of the flow system. The shallow portion of the flow system represents the water table, and the deep portion represents the potentiometric surface of the LC3 RMU. The hydraulic heads simulated in the LC3 RMU were selected to represent the regional carbonate aquifer because the LC3 RMU is the most areally-extensive carbonate unit.

As shown on Plates 2 and 3, simulated flow regions differ slightly from the flow-system boundaries adopted in the simplified conceptual model but are within the uncertainty envelope of the conceptual model (SNWA, 2009a). Plates 2 and 3 show that the simulated flow regions differ between the shallow and deep (regional) portions of the flow system. For example, the southeast boundary of Steptoe Valley and southern end of South Goshute Valley show shallow flow regions generally coincident with hydrographic-area boundaries, while the deep flow region extends toward central Steptoe and central South Butte valleys.

Interbasin flows, illustrated on Plates 2 and 3, are calculated for the entire saturated thickness of the numerical model. Therefore, interpretation of the interbasin flows should consider shallow and deep flow-region information and shallow and deep potentiometric surfaces to understand where flows occur across boundaries (i.e., vertically and laterally). Section 6.4.2 provides additional discussion of regional flows simulated by the numerical model.

6.4.2   Simulated Flow Regions

This section describes the characteristics of the flow systems as simulated by the numerical model (see Plates 2 and 3) and compares them to flow systems defined by previous studies. As similarly

Table 6-12
Net Groundwater Flow Between Hydrographic Areas (Steady-State)
(Page 1 of 2)

From Hydrographic Area	Interbasin Flow afy (m^3/d)	To Hydrographic Area
Butte Valley (South)	3,300 (11,300)	Jakes Valley
	5,600 (18,900)	Long Valley
	12,800 (43,200)	Steptoe Valley
Steptoe Valley	500 (1,800)	Tippett Valley
	2,600 (8,800)	Cave Valley
	3,600 (12,200)	Jakes Valley
	4,400 (14,900)	Lake Valley
	8,800 (29,900)	Spring Valley
	15,500 (52,500)	White River Valley
Las Vegas Valley	700 (2,300)	Coyote Spring Valley
	1,000 (3,200)	Garnet Valley
Clover Valley	2,000 (6,900)	Panaca Valley
	5,400 (18,200)	Lower Meadow Valley Wash
Dry Valley	1,900 (6,500)	Panaca Valley
Eagle Valley	0 (100)	Dry Valley
	4,600 (15,400)	Rose Valley
Lake Valley	1,900 (6,400)	Cave Valley
	3,000 (10,000)	Dry Lake Valley
	3,700 (12,500)	Spring Valley
	4,500 (15,100)	Patterson Valley
Lower Meadow Valley Wash	13,600 (45,800)	Lower Moapa Valley
Panaca Valley	800 (2,700)	Lower Meadow Valley Wash
Patterson Valley	200 (500)	Eagle Valley
	800 (2,700)	Dry Valley
	1,600 (5,400)	Dry Lake Valley
	9,500 (32,000)	Panaca Valley
Rose Valley	4,300 (14,500)	Dry Valley
Spring Valley	700 (2,300)	Patterson Valley
	800 (2,700)	Lake Valley
	1,500 (5,000)	Hamlin Valley
	3,700 (12,500)	Eagle Valley
Fish Springs Flat	2,300 (7,600)	Snake Valley
Hamlin Valley	0 (0)	Dry Valley
	100 (200)	Eagle Valley
	29,400 (99,300)	Snake Valley
Pleasant Valley	0 (0)	Spring Valley
	4,400 (14,800)	Snake Valley

JA_16407

Table 6-12
Net Groundwater Flow Between Hydrographic Areas (Steady-State)
(Page 2 of 2)

From Hydrographic Area	Interbasin Flow afy (m^3/d)	To Hydrographic Area
Spring Valley	7,600 (25,700)	Hamlin Valley
	11,800 (40,000)	Snake Valley
Tippett Valley	0 (0)	Pleasant Valley
	2,000 (6,900)	Spring Valley
California Wash	700 (2,300)	Black Mountains Area
	1,600 (5,500)	Lower Meadow Valley Wash
	4,100 (13,900)	Lower Moapa Valley
Cave Valley	1,300 (4,300)	Dry Lake Valley
	1,600 (5,300)	Pahroc Valley
	17,100 (57,700)	White River Valley
Coal Valley	10,800 (36,400)	Pahroc Valley
	29,200 (98,600)	Pahranagat Valley
Coyote Spring Valley	2,400 (8,000)	Hidden Valley (North)
	49,200 (166,200)	Muddy River Springs Area
Delamar Valley	0 (100)	Lower Meadow Valley Wash
	27,300 (92,300)	Pahranagat Valley
	2,400 (8,114)	Coyote Spring Valley
Dry Lake Valley	100 (400)	Panaca Valley
	300 (1,200)	Lower Meadow Valley Wash
	900 (3,000)	Pahroc Valley
	21,800 (73,500)	Delamar Valley
Garden Valley	25,300 (85,300)	Coal Valley
Garnet Valley	3,400 (11,300)	California Wash
Hidden Valley (North)	3,000 (10,000)	Garnet Valley
Jakes Valley	19,600 (66,200)	White River Valley
Kane Springs Valley	200 (800)	Delamar Valley
	1,800 (6,000)	Coyote Spring Valley
	2,000 (6,800)	Lower Meadow Valley Wash
Long Valley	2,000 (6,700)	Jakes Valley
Lower Moapa Valley	9,300 (31,400)	Black Mountains Area
Muddy River Springs Area	2,500 (8,600)	Lower Meadow Valley Wash
	8,600 (29,200)	California Wash
Pahranagat Valley	41,700 (140,700)	Coyote Spring Valley
Pahroc Valley	25,700 (86,900)	Pahranagat Valley
White River Valley	3,200 (10,700)	Garden Valley
	7,300 (24,500)	Pahroc Valley
	9,800 (33,200)	Coal Valley

Table 6-13
Net Groundwater Flow Between Hydrographic Areas (2004)
(Page 1 of 2)

From Hydrographic Area	Interbasin Flow afy (m^3/d)	To Hydrographic Area
Butte Valley (South)	3,300 (11,300)	Jakes Valley
	5,600 (18,900)	Long Valley
	12,800 (43,400)	Steptoe Valley
Steptoe Valley	500 (1,700)	Tippett Valley
	2,600 (8,800)	Cave Valley
	3,600 (12,200)	Jakes Valley
	4,400 (14,900)	Lake Valley
	8,800 (29,600)	Spring Valley
	15,500 (52,300)	White River Valley
Las Vegas	700 (2,300)	Coyote Spring Valley
	1,100 (3,600)	Garnet Valley
	1,100 (3,700)	Black Mountains Area
Clover Valley	2,100 (7,100)	Panaca Valley
	5,500 (18,700)	Lower Meadow Valley Wash
Dry Valley	1,900 (6,400)	Panaca Valley
Eagle Valley	0 (100)	Dry Valley
	4,800 (16,200)	Rose Valley
Lake Valley	1,700 (5,900)	Patterson Valley
	1,900 (6,300)	Cave Valley
	2,900 (9,700)	Dry Lake Valley
	3,700 (12,300)	Spring Valley
Lower Meadow Valley Wash	13,100 (44,100)	Lower Moapa Valley
Panaca Valley	900 (3,100)	Lower Meadow Valley Wash
Patterson Valley	200 (500)	Eagle Valley
	800 (2,900)	Dry Valley
	1,600 (5,300)	Dry Lake Valley
	9,400 (31,900)	Panaca Valley
Rose Valley	4,500 (15,200)	Dry Valley
Spring Valley	700 (2,300)	Patterson Valley
	800 (2,700)	Lake Valley
	1,500 (5,000)	Hamlin Valley
	3,800 (12,800)	Eagle Valley
Fish Springs Flat	2,300 (7,600)	Snake Valley
Hamlin Valley	0 (0)	Dry Valley
	100 (300)	Eagle Valley
	30,100 (101,600)	Snake Valley
Pleasant Valley	0 (0)	Spring Valley
	4,400 (14,800)	Snake Valley

JA_16409

Table 6-13
Net Groundwater Flow Between Hydrographic Areas (2004)
(Page 2 of 2)

From Hydrographic Area	Interbasin Flow afy (m³/d)	To Hydrographic Area
Spring Valley	7,600 (25,600)	Hamlin Valley
	11,800 (40,000)	Snake Valley
Tippett Valley	0 (0)	Pleasant Valley
	2,100 (6,900)	Spring Valley
California Wash	800 (2,600)	Black Mountains Area
	1,900 (6,300)	Lower Meadow Valley Wash
	4,100 (13,800)	Lower Moapa Valley
Cave Valley	1,300 (4,400)	Dry Lake Valley
	1,600 (5,300)	Pahroc Valley
	17,100 (57,700)	White River Valley
Coal Valley	10,900 (36,800)	Pahroc Valley
	29,400 (99,300)	Pahranagat Valley
Coyote Spring Valley	2,400 (8,000)	Hidden Valley (North)
	50,000 (168,900)	Muddy River Springs Area
Delamar Valley	0 (100)	Lower Meadow Valley Wash
	27,300 (92,400)	Pahranagat Valley
	2,400 (8,114)	Coyote Spring Valley
Dry Lake Valley	200 (600)	Panaca Valley
	300 (1,200)	Lower Meadow Valley Wash
	900 (3,100)	Pahroc Valley
	21,800 (73,500)	Delamar Valley
Garden Valley	25,300 (85,400)	Coal Valley
Garnet Valley	3,300 (11,300)	California Wash
Hidden Valley (North)	3,100 (10,500)	Garnet Valley
Jakes Valley	19,700 (66,400)	White River Valley
Kane Springs Valley	200 (800)	Delamar Valley
	1,800 (6,100)	Coyote Spring Valley
	2,000 (6,800)	Lower Meadow Valley Wash
Long Valley	2,000 (6,700)	Jakes Valley
Lower Moapa Valley	9,300 (31,400)	Black Mountains Area
Muddy River Springs Area	2,100 (7,200)	Lower Meadow Valley Wash
	8,300 (27,900)	California Wash
Pahranagat Valley	41,700 (140,700)	Coyote Spring Valley
Pahroc Valley	26,000 (87,700)	Pahranagat Valley
White River Valley	3,200 (10,700)	Garden Valley
	7,300 (24,500)	Pahroc Valley
	9,800 (33,200)	Coal Valley

Table 6-14
Net Groundwater Flow Between Flow Systems

From Flow System	Net Groundwater Flow (Predevelopment) afy (m³/d)	Net Groundwater Flow (2004) afy (m³/d)	To Flow System	Comment
Goshute Valley	4,400 (14,900)	4,400 (14,900)	Meadow Valley	Steptoe Valley to Lake Valley
	9,400 (31,600)	9,300 (31,300)	Great Salt Lake Desert	Steptoe Valley to Spring Valley (HA 184); Steptoe Valley to Tippet Valley
	30,700 (103,700)	30,600 (103,500)	White River	Butte Valley to Jakes Valley; Steptoe Valley to Jakes Valley; Steptoe Valley to White River Valley; Steptoe Valley to Cave Valley
Las Vegas Valley	2,800 (9,300)	3,300 (11,100)	White River	Las Vegas Valley to Coyote Springs Valley, Hidden Valley (North), Garnet Valley, and Black Mountains Area
Meadow Valley Wash	5,200 (17,600)	5,200 (17,400)	Great Salt Lake Desert	Lake Valley to Spring Valley (HA 184); Spring Valley (HA 201) to Hamlin Valley
	13,700 (46,100)	13,100 (44,200)	White River	Meadow Valley Wash to Lower Moapa Valley, and Muddy River Springs Area; Patterson Valley to Dry Lake Valley; Lake Valley to Dry Lake Valley; Lake Valley to Cave Valley

stated by Prudic et a l. (1995), it is important to recognize that even though the simulated directions and amounts of groundwater flow are provided in detail in Plates 2 and 3, they constitute but one solution to groundwater flow within the model domai n. Because data are scarce in the model area, groundwater flow patterns and, therefore, flow-system boundaries, are uncertain. In fact, several interpretations exist as described by SNWA (2009a). The conceptualization resulting from the CCRP model is discussed for the following flow syst ems: Great Salt Lake Desert, Goshute Valley and Newark Valley, Meadow Valley, White River, and Las Vegas.

6.4.2.1   Great Salt Lake Desert Flow System

The GSLDFS is si mulated to pre dominantly include Tippett, Pleasant, Spring, S nake, a portion of Lake, and Hamlin valleys hydrographic areas. The characteristics of the simulated GSLDFS shown in Plates 2 and 3 are as follows:

- Simulated groundwater recharge is derived from precipitation dominantly on the Schell Creek, Snake, and Deep Creek ranges with lesser amounts derived on the W hite Rock Mountains and Indian Peak Range above Hamlin Valley.

- Simulated groundwater discharge to the surface occurs both in the form of ET and spring flow throughout the flow system. Simulated groundwater ET occurs in Spring and Snake valleys and to a lesser degree in Tippett and Hamlin valleys.

SE ROA 51010

JA_16411

- Simulated outflow occurs at northern Tippett Valley, at northern Snake Valley, out of Snake Valley at the southern Confusion Range, out of Snake Valley to Wah Wah Valley, and out of Snake Valley to Pine Valley.

The simulated flow patterns and flow-system boundaries are very similar to those described in BARCASS (Welch et al., 2008) and in the RASA model (Prudic et al., 1995) but are somewhat different from the interpretations of Harrill et al. (1988) and Eakin (1966).

6.4.2.2   Goshute Valley and Newark Valley Flow Systems

The GVFS is simulated to predominantly include the northern part of South Butte Valley and most of Steptoe Valley. The Newark Valley Flow System is simulated to predominantly include the southern part of South Butte Valley, Long Valley, and northern Jakes Valley. The characteristics of the simulated GVFS and Newark Valley Flow System shown in Plates 2 and 3 are as follows:

- Much of the groundwater recharge in these flow systems is derived from precipitation predominantly on the Cherry Creek, northern Egan, and White Pine ranges and the Butte Mountains.

- Simulated groundwater discharge in the GVFS occurs both in the form of ET and spring flow. Simulated ET occurs along the valley bottom throughout Steptoe Valley and northern Butte Valley South. Simulated groundwater discharge in the Newark Valley Flow System occurs predominantly in the form of ET in southern Butte Valley South and Long Valley.

- Simulated outflow from the GVFS occurs at northern South Butte Valley and at northern Steptoe Valley. Simulated outflow from the Newark Valley Flow System occurs at northern Long Valley and at southwestern Long Valley.

- The simulated flow patterns and flow-system boundaries are somewhat different from those described by Harrill and Prudic (1998). They are, however, similar to those described by Bedinger and Harrill (2004) and Welch et al. (2008). Similarities also exist with the CRP model (Prudic et al., 1995) in the northwestern part of the CCRP model domain.

6.4.2.3   Meadow Valley Flow System

The MVFS is located in the southeastern part of the CCRP model domain. The simulated MVFS includes a small part of southern Lake Valley and all or most of Dry, Rose, Eagle, Spring (HA 201), Patterson, Panaca, Clover, and Lower Moapa valleys, and Lower Meadow Valley Wash. Only the southernmost portion of Lake Valley is simulated as part of the MVFS. The general characteristics of the simulated MVFS shown in Plates 2 and 3 are as follows:

- Much of the groundwater recharge is derived from precipitation on the White Rock Mountains, the Wilson Creek Range, and the Clover Mountains.

- Simulated groundwater discharge occurs both as ET and spring flow a long Meadow Valley Wash.

- Groundwater flowpaths are predominantly toward and a long Meadow Valley Wash. Groundwater outflow is to Lower Moapa Valley and the Muddy River Springs Area.

- Simulated groundwater flow patterns ar e very similar to those des cribed by Bedinger and Harrill (2004) and those simulated by Prudic et al. (1995) in the CRP model.

6.4.2.4   White River Flow System

The WRFS is located in t he western part of the CCRP model domain. The simulated WRFS predominantly includes Jakes, White Ri ver, Cave, Garden, Coal, Pahr oc, Dry Lake, Pahranagat, Delamar, Kane Springs, C oyote Spring, Hidden (North), and Garnet valleys and Muddy Ri ver Springs Area, California Wash, parts of South Butte Valley, Steptoe Valley, Lower Moapa Valley, and the Black Mountains Area. The general characteristics of the simulated WRFS shown in Plates 2 and 3 are as follows:

- Groundwater recharge is derived from precipitation predominantly on the White Pine, Egan, Schell Creek, Quinn Canyon, Seaman, Bristol and Sheep ranges with lesser amounts derived from the Delamar Mountains and Hiko, Pahranagat, and Pahroc ranges.

- Simulated groundwater discharge to the surface occurs both by ET and spring flow throughout the flow system. The largest areas of simulated ET occur along the valley bottom in White River Valley and along Pahranagat Wash in Pahranagat Valley.

- Flowpaths from the WRFS ultimately converge with groundwater flow from the MVFS at Muddy River that is either discharged to the r iver or e vapotranspired into Lower Moapa Valley. Outflow is from t he Muddy River Springs Area to Lower Moapa, the B lack Mountains Area to Lake Mead, from Garden Valley to Penoyer Valley, and from Pahranagat Valley to Tikaboo Valley South.

- Flow patterns in the northern part of the WRFS are comparable to interpretations in BARCASS (Welch et al., 2008). As si mulated, shallow flowpaths in Lake Valley contribute flow to the WRFS, and deep flowpaths in Lake Valley contribute flow to the GSLDFS.

6.4.2.5   Las Vegas Groundwater Basin

The extreme southern e nd of the CC RP model domain contains an area of simul ated flow that originates predominantly as recharge on the Sheep Range. This groundwater flows east to southeast along the model boundary at the Las Vegas Valley Shear Zone and ultimately discharges to Las Vegas Valley or as spring flow at Rogers and Blue P oint springs or as outflow to Lake Mead through the Black Mountains Area.

6.4.3   Simulated Groundwater-Budget Components

The large areal extent of the numerical model and the large uncertainties associated with external boundary conditions preclude a comprehensive and accurate assessment of all groundwater inflows and outflows. As a result, comparing the simulated volumetric budget to conc eptual groundwater-budget estimates is difficult. Thus, when e valuating the groundwa ter budget, it is important to not e that significant uncertainti es still exist with regard to t he groundwater-budget components of the flow system, including external boundary flows, groundwa ter discharge, and indirectly, groundwater recharge. A discussion of the simulated groundwater budget, however, is warranted.

Tables 6-15 and 6-16 list the simulated groundwater budget for the model area for the steady-state and 2004 stress periods. The budgets are organized by hydrographic area and flow system. A grand total for the model domain is also provided. Groundwater-inflow components are positive values; groundwater-outflow components are negative values.

As shown in Table 6-15, totals of interbasin-flow components are provided only to demonstrate the balance of in and out components.

As shown in Table 6-15, Constant Head is the net groundwater flow through exter nal boundaries in each hydrographic area and flow system. ET and Springs is the discharge from ET zones and springs in each hydrographic area and flow system. Rec harge is t he total rec harge (sum of in-place and runoff recharge components) in e ach hydrographic area and flow system. S tream Flow is t he net groundwater flow from stream flow routing cells in each hydrographic area and flow system.

6.5   Summary of Model Calibration Evaluation

The results presented in this section suggest that the numerical model reproduces the measured hydraulic heads and estimated groundwater-budget components reasonably accurately but with noted levels of uncertainty. In addition, the estimated parameter values are reasonable. The *K* distribution patterns are generally consistent with the conceptual model. The transmissivities across the model area, while high in some locations, are reasonable.

Because the we ighted residuals are not enti rely random, some model e rror is indicate d. This is mostly related to the occurrence of large positive-weighted residuals for some hydr aulic-head observations located predominantly in large hydraulic-gradient areas and large weighted residuals for intermediate spring discharge and groundwater discharges in areas such as Pahranagat Valley. These errors are largely the result of sparse data and the way in which these areas relate to the regional flow system.

In addition, weighted residuals a re not normally distributed. Previous groundwater modeling exercises in other parts of the southern Great Basin (D'Agnese et al., 1997, 2002; Faunt et al., 2004) suggest that additional calibration and re duction in conceptual model uncertainty may significantly improve model ac curacy. This ana lysis suggests that the numer ical model is a reasonable representation of the physical system, but evidence of model error exists.

Table 6-15

Simulated Groundwater-Budget Components Organized by Hydrographic Area

HA Number and Name	Net Interbasin Flow	Change in Storage	Groundwater Withdrawals	Constant Head	ET and Springs	Recharge	Stream Flow
	afy						
178B Butte Valley (South)	-21,700	0	0	-500	-8,900	31,100	0
179 Steptoe Valley	-22,800	0	0	-2,100	-88,700	113,600	0
Goshute Valley Total	**-44,500**	**0**	**0**	**-2,600**	**-97,600**	**144,700**	**0**
212 Las Vegas Valley	-2,800	0	0	0	0	2,800	0
Las Vegas Valley Total	**-2,800**	**0**	**0**	**0**	**0**	**2,800**	**0**
183 Lake Valley	-7,900	0	---	0	-2,400	10,400	0
198 Dry Valley	3,200	0	---	0	-4,800	1,600	0
199 Rose Valley	300	0	---	0	-400	100	0
200 Eagle Valley	-700	0	---	0	-400	1,100	0
201 Spring Valley	-6,700	0	---	0	-700	7,400	0
202 Patterson Valley	-6,900	0	---	0	0	6,900	0
203 Panaca Valley	12,800	0	---	0	-20,800	8,000	0
204 Clover Valley	-7,400	0	---	0	-1,900	9,400	0
205 Lower Meadow Valley Wash	-1,100	0	---	0	-14,600	15,700	0
Meadow Valley Total	**-14,400**	**0**	**0**	**0**	**-46,000**	**60,600**	**0**
184 Spring Valley	-4,900	0	0	0	-77,700	82,600	0
185 Tippett Valley	-1,500	0	0	-4,200	0	5,700	0
194 Pleasant Valley	-4,400	0	0	0	0	4,400	0
195 Snake Valley	47,900	0	0	-31,900	-122,600	106,900	-200
196 Hamlin Valley	-20,300	0	0	0	-800	21,100	0
258 Fish Springs Flat	-2,300	0	0	2,200	0	100	0
Great Salt Lake Desert Total	**14,500**	**0**	**0**	**-33,900**	**-201,100**	**220,800**	**-200**
171 Coal Valley	-4,900	0	0	0	0	4,900	0
172 Garden Valley	-22,100	0	0	-2,300	0	24,300	0
174 Jakes Valley	-10,700	0	0	0	0	10,700	0
175 Long Valley	3,600	0	0	-13,500	-800	10,700	0
180 Cave Valley	-15,400	0	0	0	0	15,400	0
181 Dry Lake Valley	-17,300	0	0	0	0	17,300	0
182 Delamar Valley	-7,500	0	0	0	0	7,500	0
206 Kane Springs Valley	-4,000	0	0	0	0	4,000	0
207 White River Valley	32,000	0	0	0	-73,100	41,100	0
208 Pahroc Valley	-5,500	0	0	0	0	5,500	0
209 Pahranagat Valley	40,600	0	0	-9,500	-23,000	6,100	-14,200
210 Coyote Spring Valley	-5,700	0	0	2,000	0	3,700	0
215 Black Mountains Area	11,600	0	0	-7,500	-2,100	0	-2,000
216 Garnet Valley	-200	0	0	0	0	200	0
217 Hidden Valley (North)	-200	0	0	0	0	200	0
218 California Wash	6,400	0	0	0	-7,500	0	1,200
219 Muddy River Springs Area	38,000	0	0	0	-4,200	100	-33,900
220 Lower Moapa Valley	8,400	0	0	-6,700	-21,300	100	19,500
White River Total	**47,100**	**0**	**0**	**-37,500**	**-132,000**	**151,800**	**-29,400**
Grand Total	**-100**	**0**	**0**	**-74,000**	**-476,700**	**580,700**	**-29,600**

JA_16415

Table 6-16
Simulated Groundwater-Budget Components Organized by Hydrographic Area (2004)

HA Number and Name	Net Interbasin Flow	Change in Storage	Groundwater Withdrawals	Constant Head	ET and Springs	Recharge	Stream Flow
	afy						
178B Butte Valley (South)	-21,800	0	-200	-500	-8,800	31,100	0
179 Steptoe Valley	-22,600	2,500	-11,900	-2,100	-79,600	113,600	0
Goshute Valley Total	**-44,400**	**2,500**	**-12,100**	**-2,600**	**-88,400**	**144,700**	**0**
212 Las Vegas Valley	-3,300	500	0	0	0	2,800	0
Las Vegas Valley Total	**-3,300**	**500**	**0**	**0**	**0**	**2,800**	**0**
183 Lake Valley	-5,000	10,600	-13,600	0	-2,400	10,400	0
198 Dry Valley	3,500	300	-3,500	0	-1,900	1,600	0
199 Rose Valley	300	100	-400	0	-100	100	0
200 Eagle Valley	-800	100	-100	0	-200	1,100	0
201 Spring Valley	-6,800	100	0	0	-700	7,400	0
202 Patterson Valley	-9,700	6,000	-3,300	0	0	6,900	0
203 Panaca Valley	12,700	4,900	-9,300	0	-16,400	8,000	0
204 Clover Valley	-7,600	300	-200	0	-1,800	9,400	0
205 Lower Meadow Valley Wash	-500	800	-3,100	0	-13,000	15,700	0
Meadow Valley Total	**-13,900**	**23,200**	**-33,500**	**0**	**-36,500**	**60,600**	**0**
184 Spring Valley	-4,900	2,000	-5,600	0	-74,100	82,600	0
185 Tippett Valley	-1,600	0	0	-4,200	0	5,700	0
194 Pleasant Valley	-4,400	0	0	0	0	4,400	0
195 Snake Valley	48,600	2,800	-21,600	-31,800	-104,700	106,900	-200
196 Hamlin Valley	-21,000	600	0	0	-700	21,100	0
258 Fish Springs Flat	-2,300	0	0	2,200	0	100	0
Great Salt Lake Desert Total	**14,400**	**5,400**	**-27,200**	**-33,800**	**-179,500**	**220,800**	**-200**
171 Coal Valley	-5,200	300	0	0	0	4,900	0
172 Garden Valley	-22,100	0	0	-2,200	0	24,300	0
174 Jakes Valley	-10,700	0	0	0	0	10,700	0
175 Long Valley	3,600	0	0	-13,500	-800	10,700	0
180 Cave Valley	-15,500	0	0	0	0	15,400	0
181 Dry Lake Valley	-17,500	100	0	0	0	17,300	0
182 Delamar Valley	-7,500	0	0	0	0	7,500	0
206 Kane Springs Valley	-4,000	0	0	0	0	4,000	0
207 White River Valley	32,000	3,400	-10,900	0	-65,600	41,100	0
208 Pahroc Valley	-5,700	100	0	0	0	5,500	0
209 Pahranagat Valley	41,100	400	-2,800	-9,500	-21,800	6,100	-13,500
210 Coyote Spring Valley	-6,500	800	0	2,000	0	3,700	0
215 Black Mountains Area	12,100	1,200	-1,700	-7,400	-2,100	0	-2,000
216 Garnet Valley	100	700	-1,000	0	0	200	0
217 Hidden Valley (North)	-300	200	0	0	0	200	0
218 California Wash	5,700	400	0	0	-7,500	0	1,400
219 Muddy River Springs Area	39,600	700	-8,100	0	-2,100	100	-30,200
220 Lower Moapa Valley	7,800	100	-2,700	-6,700	-20,900	100	22,200
White River Total	**47,000**	**8,400**	**-27,200**	**-37,300**	**-120,800**	**151,800**	**-22,100**
Grand Total	**-200**	**40,000**	**-100,000**	**-73,700**	**-425,200**	**580,700**	**-22,300**

Some of the simulated flow-system boundaries in the calibrated transient numerical model are similar to those described in BARCASS (Welch et al., 2008) and in the RASA model (Prudic et al., 1995). They do differ, however, from the interpretations of Harrill et al. (1988) and Eakin (1966) adopted in the simplified conceptual model as described in Sections 3.0 and 5.0. Because of the lack of regional data in the northwestern region of the model area, particularly in Jakes Valley, and the uncertainty associated with the recharge estimate, different interpretations of flow patterns and, therefore, flow-system boundaries are possible. This area of the model is located a significant distance away from the Project basins, and the locations of these flow-system boundaries should not affect the EIS analysis for which the numerical model is intended. Previous studies like Belcher (2004), for example, have shown that drawdowns are mostly sensitive to the hydraulic properties of the aquifers. The distribution of hydraulic conductivities derived from this model appears to be reasonable.

7.0 MODEL LIMITATIONS AND UNCERTAINTIES

The numerical model contains th e most up-to-date representation of hydroge ologic data for the Central Carbonate-Rock Province of the Great Basin region. However, it is still a model cove ring a vast portion of re mote Nevada where data are limited. This lack of da ta causes limitations and uncertainties in values simulated by the numerical model. The se limitations and uncertainties are common for models develope d in this region, as the DV RFS model describes many of the same (Belcher, 2004). Uncertainties are unavoidable but can be reduced with additional data collected in the future. Inhe rent model limitations result from uncertainty in five basic aspects of the model, including inadequacies in (1) the hydrogeologic framework, (2) the p recipitation recharge, (3) the historical anthropogenic da ta, (4) the obser vations, and (5) the representation of hydrologic conditions. These limitations are disclosed below.

7.1 Hydrogeologic Framework

Accurate simulation of many of the important flow-system characteristics depends on a n accurate understanding and representation of the hydrogeologic framework. Limitations exist in the numerical model because of the difficulties inherent in the interpretation and re presentation of the c omplex geometry and spatial variabilit y of hydrogeologic materials and structures in a hydrogeologic framework and numerical model. The hydrogeologic framework is further complicated by the lack of data within the model area.

7.1.1 Complex Geometry

Geometric complexity of hydroge ologic materials and structures is appa rent throughout the model domain. Notable large-scale examples that have a significant effect on regional groundwater flow are (1) the fault system at the Muddy River Springs Ar ea, (2) the lateral faults of the Pahranagat Shear Zone, and (3) the calderas of the Caliente Caldera complex.

A system of a pparent regional-scale normal a nd lateral faults likely provides the mechanisms for groundwater discharge at the Muddy River Springs Area. The complexity of this system is not fully known; however, the current understanding suggests that the hydrogeologic framework represented in the model is grossly simplified because of the coarse numerical model resolution.

Regional-scale lateral faults associated with the Pahranagat shear zone give rise to hydrogeologic features that contribute to a generally southward stair-stepping of the regional water table. The lack of available knowledge on t his fault system adds uncertainty to t he simulation of directions and quantities of groundwater flow out of Pahranagat Valley.

East and northeast of the Pahranagat shear zone, a series of calderas and intracaldera intrusions cause regional discontinuities in the flow system. The complex geometries associated with these calderas are not fully known a nd cause uncertainties in si mulating the re gional, large-hydraulic gradient coincident with these volcanic features.

7.1.2 Complex Spatial Variability

As with complex h ydrogeologic geometries, spatial variability of m aterial properties of the hydrogeologic units and structures i s also a l imitation in the CCR P model. The ass umption of homogeneity within a given RMU in the hydrogeologic framework model, or hydraulic-conductivity parameter zone in the numerical model, limits the simulation by re moving the potential effects of variability in gr ain-size distribution, degree of welding, and fracture density and or ientation. This limitation is the direct result of data limitations and simplifications due to hydrogeologic framework and flow model construction and discretization.

The LVF RMU is a good example of a hydrogeologic unit that has significant spatial variability. This highly heterogeneous unit consists of (1) older Tertiary sediments, which possess varying grain- size distributions and degr ees of lithification and (2) Tertiary volcanic rocks, which possess units of varying composition, degrees of welding, and hydrothermal alterations. These heterogeneities, which can affect hydraulic properties and consequently groundwater flow, cannot be repr esented in the hydrogeologic framework and numerical models. In fact, many of the limitations of the simulation within the Caliente Caldera complex and related calderas are in part due to the underrepresentation of local-scale hydrogeologic complexities in the regional-scale hydrogeologic framework and numerical models.

7.1.3 Hydrogeologic Model Representation

Discretization and abstra ction of the physi cal hydrogeologic fra mework impose limitations on all components of the hydrogeologic framework and numerical models. While the 3,281 ft (1,000 m) resolution is appropriate to represent regional-scale conditions, it presents dif ficulty in a ccurately simulating areas of geologic complexity. The grid cells tend to gene ralize important local-scale complexities that have an impact on r egional hydrologic conditions. This sit uation is pa rticularly prevalent in large-hydraulic-gradient areas where sharp geologic contacts or loc al-scale fault characteristics can influence regional hydraulic heads and groundwater discharges. The current level of understanding of the geology throughout the mode l area does not w arrant a highe r-resolution regional flow model at this time.

7.2 Precipitation Recharge

Limitations in precipitation recharge stem from the approximate methods used to esti mate recharge and the assumption that the effects of climate variability on recharge are negligible.

Groundwater recharge cannot be measured directly in the field for areas as large as the mode l area. Furthermore, groundwater recharge is spatially and temporally variable. The yearly rates and spatial distribution of the mean recharge were estimated through model calibration. Although a solution was

JA_16419

obtained in this manner, the actual annual rates and particularly the spatial distribution of recharge remain very uncertain. Another source of uncertainty is the assumption that recharge does not vary with time. This assumption constitutes an important limitation, particularly in the simulations of the groundwater development scenarios. Under this assumption, potential variations in recharge due to climate change or the lowering of the water table by pumping, for example, cannot be simulated.

Climate variability over the course of the simulation affects precipitation and therefore groundwater recharge. The numerical model simulates a constant average recharge from precipitation rates averaged over 30 years (PRISM normal precipitation grid) and does not consequently account for climate variability over the simulation period.

7.3   Historical Anthropogenic Data

No historical groundwater-pumping or surface-water diversion records from which historical stress data sets can be derived exist for most of the hydrographic areas in the model area. Therefore, the historical anthropogenic data sets were estimated from the available information. The estimation process has important limitations leading to uncertainties in the data set.

As historical records of actual groundwater use are sparse, the consumptive water-use estimates were derived using estimates of consumptive water use based on water-rights information obtained from NDWR and the Utah Division of Water Rights (UDWR). Reported groundwater-production or surface-water diversion data were used where available to support the estimation process.

In many of the croplands, irrigation with groundwater could not be clearly identified because irrigation water is supplied by both surface water and groundwater. In these areas, groundwater is commonly pumped to supplement surface-water sources used to irrigate crops. This adds another layer of complexity to estimating groundwater use in that supplemental groundwater pumping generally only occurs when conditions warrant it, such as in low runoff years.

7.4   Observations

Hydraulic-head and groundwater-discharge observations constrain model calibration through the parameter-estimation process; therefore, uncertainty in these observations results in uncertainty in the numerical model. All available hydraulic-head-observation data were thoroughly analyzed prior to and throughout the calibration process. However, uncertainty still exists in (1) the quality of the observation data, (2) the appropriateness of the hydrogeologic interpretations, and (3) the way in which the observation was represented in the numerical model.

7.4.1   Quality of Observations

The sparse distribution and high concentration, or clustering, of hydraulic-head observations are numerical model limitations. Because available data in the overall region are scarce and available multiple observations in isolated areas are overemphasized, biasing occurs in those parts of the model. Water-level-data scarcity is particularly noticeable in Long, Jakes, Coal, Garden, Dry Lake, and Delamar valleys and Lower Meadow Valley Wash because of the lack of wells in those valleys.

SE ROA 51019

JA_16420

High clustering of observa tions occurs along ripar ian areas of Pahr anagat Wash, Meadow Valley Wash, and the Muddy River. A declustering method was used to address this situation; however, this declustering only applies to situations where multiple water levels occur in a given model cell.

7.4.2   Interpretation of Observations

It is difficult to determine whether hydraulic-head observations represent regional versus perched or localized conditions. Field testing is often not sufficient to distinguish conclusively between regional or localized conditions. The d ata necessary to determine unequivocally the presence of perc hed or local groundwater are rarely, if ever, available. Because large simulated hydraulic-head residuals in recharge areas often suggest the possibil ity of perched water, either the hydraulic-head observations in this category were removed or the observation weight was dec reased. Fewer observations, or observations with lower weights, result in higher uncertainty in the numerical model.

Large-hydraulic-gradient areas also are difficult to interpret. Limited water-level data in these areas exacerbate the situation. Hydraulic-head observations defining large hydraulic gradients are also typically associated with perched or localized water.

The model al so does not account for climate variabilit y over th e course of the simulation. Approximately 6 pe rcent of the water-level hydrographs and 16 per cent of the hydra ulic-head or drawdown observations in the mode l are clearly influenced by climate variability. The majority of these (85 out of 1 12 climate-affected wells and 919 out of 1,225 observa tions) occur in S teptoe Valley. The se wells and their associated observations however, only occ ur in isolated geographic locations within Steptoe Valley and occ ur within the time period of an extre mely wet cycle in the region. The value of, or the abili ty to, extrapolate this climate var iability information to the remainder of the 1,751 wells and 6,322 hydraulic-head and drawdown observations was not practical or considered valuable.

Accurate groundwater-discharge estimates for many of the springs and ET areas are not available and are thus numerical model limitations. Highe r quality, spatially distributed, groundwater-discharge observations for the re gion only began to be collected in 2002 (SNWA, 2008; SNWA 2009a; Welch et al., 2008). The lack of estimates as well as the variability in the estimates, based on long-term data, limits how well these groundwater-discharge areas and related areas can be sim ulated. In addition, the assumptions necessary to use present-day groundwater discharge to approximate predevelopment groundwater-discharge conditions may introduce error. Reliable historical groundwater-discharge estimates are an unrec overable data ga p in the model that will add uncertainty to any groundwate r flow simulation of this region.

7.4.3   Representation of Observations

Although the vol umetric discharge from ET is reasonably matched, the model does not accurately simulate the areas where ET occurs. This is due to the limitations associated with the representation of groundwater ET areas in the model, including the course resolution and the setup of the drains.

SE ROA 51020

JA_16421

Simulating small discharge volumes less than 296 afy (less than 1,000 m^3/d) was difficult in the CCRP numerical model. For instance, incised drainages and other focused discharge areas are difficult to simulate accurately. This difficulty is particularly noticeable along Meadow Valley Wash and Pahranagat Wash. In many cases, the hydraulic conductivity of the hydrogeologic units present at the land surface and the geometry of these topographic features control the simulated discharge.

The elevations assigned to define drains in the numerical model also affects the ability to simulate groundwater conditions more accurately. The elevations of drains in ET areas were set to values of land-surface elevation reduced by one of two values of extinction depth depending on location. The values of land-surface elevation were based on a 1:24,000-scale digital elevation model, and the extinction depth values were set to either 16.4 ft (5 m bgs) or 32.8 ft bgs (10 m bgs). This simplified method of representing drain elevations in the numerical model may not accurately approximate the extinction depth for all discharge areas, particularly in areas with highly variable rooting depths and discontinuous areas of capillary fringe. Snake Valley is an example of a discharge area that may have a zone of extensive capillary fringe. In areas of the model where these conditions exist, observed hydraulic heads may be lower than the drain elevations. The consequence of this limitation is that the numerical model has difficulty simulating groundwater discharge within the delineated ET areas.

In summary, in several cases, the distribution of ET is not simulated accurately; however, the total ET from a given ET area matches well. This limitation will cause drawdowns to propagate faster between the basin edge and simulated ET areas until ET is captured. Errors in ET simulation minimally affect drawdown propagation after capture starts because simulated discharge volumes are approximately correct.

7.5   *Hydrologic Conditions Representation*

The hydrologic conditions that, perhaps, most influence the CCRP numerical model are the representation of external and internal boundary conditions. Limitations in external-boundary-condition definition are the result of both incomplete understanding of natural conditions and associated poor representation of the natural conditions in the numerical model. Because very little data exist in the areas defined as lateral flow-system boundaries, the boundaries are highly uncertain. Also, defining these boundaries in the numerical model is effectively limited to either a no-flow or a constant-head boundary. Both types of boundary definitions impose significant constraints on model results.

This Page Intentionally Left Blank

SE ROA 51022

JA_16423

8.0 SUMMARY

A numerical groundwater flow model was developed for the CCRP in Nevada and Utah. A summary of the objectives, approach, model construction and calibration, evaluation of results, and limitations is presented, followed by a statement of the conclusions.

The numerical model described in this document was developed to s upport the environmental analysis for the Clark, Lincoln, and White Pine Counties Groundwater Development Project. Specifically, the numerical model was used to simulate groundwater development scena rios to evaluate the potential water-related effects of the Project's groundwater production at the regional scale (SNWA, 2009b). As pumping, monitoring, and testing data become available in the future, this numerical model will be improved and used as a management tool.

The modeling approach was consistent with the model-calibration guidelines established by Hill and Tiedeman (2007) and incorpor ated a nonlinear, regression technique to estim ate aquifer parameters. The numerical model was developed using the computer program MODFLOW-2000 and was calibrated using a combination of trial-a nd-error and automatic parameter-estimation methods. The parameter-estimation code UCODE_2005 was used to implement the automatic parameter-estimation method and assist in the c alibration process. The numerical model was constructed based on a conceptual model described mainly in S NWA (2009a). Addit ional information supporting the conceptual model may be found in the Baseline Report (SNWA, 2008) and in Appendixes A through C of this report.

The finite-difference numerical model c onsists of 474 rows, 202 columns, and 11 layers. The grid cells are oriented north-south and are of unifor m size, with side dimensions of 3,281 f t (1,000 m). The model grid encompasses about 20,688 mi^2 (53,581 km^2), and the layers vary in thicknesses from 328 ft (100 m) to 6,562 ft (2,000 m) each. The required grid-cell values, including initial parameter values, were supplied by di scretization of a 3D hydrogeologic fr amework model and digital representations of the remaining hydrologic model components. The initial conditions of the aquifer system used in the transient model were obtai ned through preliminary test simulations conducted to refine the numerical representation of the conceptual model.

During model calibration, techniques available in MODFLOW-2000 and UCODE_2005 allowed for estimation of a series of parameters that provided a best fit to observed hydraulic heads, groundwater discharge, and boundary flows. As part of calibration, numerous conceptual models were evaluated to test the validity of various interpretations about the flow systems. For e ach hypothesis tested, a new set of parameters was estimated using MODFLOW-2000 and UCODE_2005, and the re sulting simulated hydraulic heads and groundwater-discharge rates were compared to observed values. Only those conceptual model changes contributing to a significant improvement in model fit, as indicated by a reduction in the sum of weighted squared errors, were retained in the final calibrated model.

The final calibrated numerical model was evaluated to assess the likely accuracy of its results by comparing simulated values to measured and expected quantities for hydraulic heads, drawdowns, and groundwater discharge. Resulting model fit and calibration accuracy were assessed and reported. An evaluation of the calibrated parameter values was performed to assess their level of reasonableness. The calibrated parameter values were found to be within the range of expected values. In addition, the simulated general regional flow directions were found to be similar to previous interpretations (Prudic et al., 1995; Welch et al., 2008; SNWA, 2009a). Despite important remaining uncertainties due to sparse data and model error, the evaluation process indicates that the numerical model is a reasonable representation of the natural flow system.

The inherent, unavoidable limitations result from uncertainty in five basic aspects of the model:

1. Lack of geologic and hydraulic-property data and limitations on the ability to represent the complex geometry and spatial variability of hydrogeologic materials and structures in the hydrogeologic framework and numerical models.

2. Limitations on the ability to measure and represent precipitation recharge in the numerical model.

3. Lack of an accurate historical record of the anthropogenic stresses imposed on the aquifer system.

4. Lack of observation data and associated difficulties in the interpretation and representation of these in the numerical model.

5. Limitations on the ability to represent hydrologic conditions, particularly external and internal boundary conditions, in the numerical model.

In conclusion, given that (1) the current numerical model contains the most up-to-date representation of hydrogeologic data for this part of the Great Basin, (2) the model was calibrated and evaluated using state-of-the-art methods, (3) the model fit the observations reasonably well, and (4) the estimated aquifer parameters are comparable to the available data, this numerical model is a reasonable representation of the flow system at the regional scale. Therefore, this numerical model achieves the primary objective of the CCRP model, which is to simulate estimates of potential drawdowns from groundwater withdrawals from the Project basins.

9.0 REFERENCES

Anderman, E.R., and Hill, M.C., 2000, MOD FLOW-2000, the U.S. Geological Survey modu lar ground-water model—Documentation of the H ydrogeologic-Unit Flow (HUF) Packa ge: U.S. Geological Survey Open-File Report 00-342, 94 p.

Anderman, E.R., and Hill, M.C., 2003, MOD FLOW-2000, the U.S. Geological Survey modu lar ground-water model—Three additions to the Hydrogeologic-Unit Flow (HUF) Package: Alternative storage for the uppermost active cells (SYTP pa rameter type), Flows in hydrogeologic units, and the hydraulic- conductivity depth-dependence (KDEP) capability: U.S. Geological Survey Open-File Report 03-347, 42 p.

Bard, Y., 1974, Nonlinear parameter estimation: New York, Academic Press.

Bear, J., 1979, Hydraulics of Groundwater: New York, McGraw-Hill Book Company, 269 p.

Bedinger, M.S., and Harrill, J.R., 2004, Appendix 1—Regional potential for interbasin flow of ground water, *in* Belcher, W.R., ed., Death Valley Regional Ground-Water Flow System, Nevada and California—Hydrogeologic framework and transient ground-water flow model: U.S. Geological Survey Scientific Investigations Report 2004-5205, p. 355–374.

Belcher, W.R., ed., 2004, Death Valley Regional Ground-Water Flow System, Ne vada and California—Hydrogeologic framework and transient ground-water flow model: U.S. Geological Survey Scientific Investigations Report 2004-5205, 402 p.

Belcher, W.R., Elliott, P.E., and Geldon, A.L., 2001, Hydraulic-property estimates for use with a transient ground-water flow mod el for the Death Valley regional ground-water flow system, Nevada and California: U.S. Geological Survey Water-Resources Investigations Report 01-4210, 28 p.

Bolke, E.L., and Sum sion, C.T., 1978, H ydrologic reconnaissance of the Fis h Springs Fl at area, Tooele, Juab, and Mil lard counties, Utah: Utah Department of Natura l Resources, Technical Publication No. 64, 36 p.

Bredehoeft, J.D., 2003, From models to per formance assessment—The conceptualization problem: Ground Water, Vol. 41, No. 5, p. 571–577.

Brothers, K., Bernholtz, A.J., Buqo, T .S., and Tracy, J.V., 1994, H ydrology and steady state ground-water model of Spring Valley, Lincoln a nd White Pin e counties, Nevada: Las Vegas Valley Water District, Cooperative Water Project, Report No. 13, 111 p.

Brothers, K., Buqo, T.S., and Tracy, J.V., 1993, Hydrology and steady state ground-water model of Snake Valley, east-central Nevada, and west-central Utah, Las Vegas Valley Water District, Cooperative Water Project, Report No. 9, 97 p.

Brothers, K., Katzer, T., and Johnson, M., 1996, Hydrology and steady state ground-water model of Dry Lake and Delamar valleys, Lincoln County, Nevada: Las Vegas Valley Water District, Cooperative Water Project Report No. 16, 71 p.

Carlton, S.M., 1985, Fish Springs Multibasin Flow System, Nevada and Utah [Master's thesis]: University of Nevada, Reno, 112 p.

Christensen, S., and Cooley, R.L., 1996, Simultaneous confidence intervals for a steady-state leaky aquifer groundwater flow model, *in* Kovar, K., and van der Heijde, P.K.M., eds., Calibration and reliability in groundwater modelling: Proceedings of the ModelCARE96 Conference, Golden, Colorado, September 24–26, 1996, International Association of Hydrological Sciences Publication No. 237, p. 561–569.

Christensen, S., and Cooley, R.L., 2006, User guide to the UNC process and three utility programs for computation of nonlinear confidence and prediction intervals using MODFLOW-2000: U.S. Geological Survey Techniques and Methods Report 6-A10, 193 p.

Cooley, R.L., 2004, A theory for modeling ground-water flow in heterogeneous media: U.S. Geological Survey, Professional Paper 1679, 234 p.

Cooley, R.L., and Naff, R.L., 1990, Chapter B4—Regression modeling of ground-water flow: U.S. Geological Survey Techniques of Water-Resources Investigations, Book 3—Applications of Hydraulics, 242 p.

D'Agnese, F.A., Faunt, C.C., Turner, A.K., and Hill, M.C., 1997, Hydrogeologic evaluation and numerical simulation of the Death Valley Regional Ground-Water Flow System, Nevada and California: U.S. Geological Survey Water-Resources Investigations Report 96-4300, 131 p.

D'Agnese, F.A., O'Brien, G.M., Faunt, C.C., Belcher, W.R., and San Juan, C., 2002, A three-dimensional numerical model of predevelopment conditions in the Death Valley Regional Ground-Water Flow System, Nevada and California: U.S. Geological Survey Water-Resources Investigations Report 02–4102, 122 p.

DeMeo, G.A., Smith, J.L., Damar, N.A., and Darrell, J., 2008, Quantifying ground-water and surface-water discharge from evapotranspiration processes in 12 hydrographic areas of the Colorado Regional Ground-Water Flow System, Nevada, Utah, and Arizona: U.S. Geological Survey Scientific Investigations Report 2008-5116, 34 p.

Dettinger, M.D., 1989, Reconnaissance estimates of natural recharge to desert basins in Nevada, U.S.A., by using chloride-balance calculations: Journal of Hydrology, Vol. 106, p. 55–78.

Dettinger, M.D., and Scha efer, D.H., 1996, Hydrogeology of structurally extended t errain in the eastern Great Basin of Nevada, Utah, and adjacent states, from geologic and geophysical models: U.S. Geological Survey Hydrologic Investigations Atlas HA-694-D, scale 1:100,000.

DOE/NV, see U.S. Department of Energy.

Eakin, T.E., 1966, A re gional interbasin groundwater system in the W hite River area, southeastern Nevada: Water Resources Research, Vol. 2, No. 2, p. 251–271.

Faunt, C.C., Blainey, J.B., Hill, M.C ., D'Agnese, F.A., and O'Brie n, G.M., 2004, Chapter F—Transient numerical model, *in* Belcher, W.R., ed., Death Valley Regional Ground-Water Flow System, Nevada and California—Hydrogeologic framework and transient ground-water flow model: U.S. Geological Survey Scientific Investigations Report 2004-5205, p. 257-352.

Freeze, R.A., and Cherry, J.A., 1979, Groundwater: Englewood Cliffs, New Jersey, Prentice-Hall.

Frick, E.A., 1985, Quantitative analysis of groundwater flow in valley-fill deposits in Steptoe Valley, Nevada [M.S. thesis]: University of Nevada, Reno, 208 p.

Gates, J.S., and Kruer, S.A., 1981, Hydrologic reconnaissance of the southern Great Salt Lake Desert and summary of the hydrology of west-central Utah: Utah Department of Natural Resources Technical Publication No. 71, 64 p.

Halford, K.J., and Hanson, R.T., 2002, User guide for the drawdown- limited, multi-node well (MNW) package for the U.S. Geol ogical Survey's modular three-dimensional finite-difference ground-water flow model, versions MODFLOW-96 and MODFLOW -2000: U.S. Geological Survey Open-File Report 2002-293.

Harbaugh, A.W., 1990, A computer program for calculating subregional water budgets using results from the U.S. Geological Survey modular three-dimensional finite-difference ground-water flow model: U.S. Geological Survey Open-File Report 90-392, 25 p.

Harbaugh, A.W., Banta, E.R., Hill, M.C., and McDonald, M.G., 2000, MODFLOW-2000, the U.S. Geological Survey modular ground-water model—User guide to modul arization concepts and the ground-water flow process: U.S. Geological Survey Open-File Report 00-92, 127 p.

Harbaugh, A.W., and McDonald, M.G., 1996, User's documentation for MODFLOW-96, an update to the U.S. Geological Survey modular finite-difference ground-water flow model: U.S. Geological Survey Open-File Report 96-485, 62 p.

Harrill, J.R., 1986, Ground-wa ter storage depletion in P ahrump Valley, Nevada-California, 1962-75: U.S. Geological Survey Water-Supply Paper 2279, 53 p.

Harrill, J.R., Gate s, J.S., and Thoma s, J.M., 1988, Major ground-water flow systems in the Gre at Basin region of N evada, Utah, a nd adjacent states: U.S. Geological Surve y Hydrologic Investigations Atlas HA-694-C, 4 p., scale 1:1,000,000, two sheets.

Harrill, J.R., and Preissler, A.M., 1994, Ground-water flow and s imulated response to several developmental scenarios in Stagecoach Valley- a small partly-drained basin in Lyon and Storey Counties, Nevada: U.S. Geological Survey Professional Paper 1409-H, 74 p.

Harrill, J.R., and Prudic, D.E., 1998, Aquifer systems in the Great Basin region of Nevada, Utah, and adjacent states—Summary report: U.S. Geological Survey Professional Paper 1409-A, 75 p.

Helsel, D.R., and Hirsch, R .M., 1992, Statistical methods in water resources: Studies in Environmental Science No. 49, El sevier Science Publishers, Amsterdam, The Ne therlands, 529 p.

Hill, M.C., 1992, A computer program (MODFLOWP) for estimating pa rameters of a transient, three-dimensional, ground-water flow mod el using nonlinear regression: U.S . Geological Survey Open-File Report 91-484, 366 p.

Hill, M.C., 1994, Five computer programs for testing weighted residuals and calculating linear confidence and pre diction intervals on results from the ground-water parameter-estimation computer program MODFLOWP: U.S. Geological Survey Open-File Report 93-481, 85 p.

Hill, M.C., 1998, Methods and guidelines for effective model calibration: U.S. Geological S urvey Water-Resources Investigations Report 98-4005, 90 p.

Hill, M.C., Banta, E.R., Ha rbaugh, A.W., and Anderman, E.R., 2000, MODF LOW-2000, the U.S. Geological Survey modular gr ound-water model—User guide to the O bservation, Sensitivity, and Parameter-Estimation Processes and thre e post-processing programs: U.S. Geological Survey Open-File Report 00-184, 219 p.

Hill, M.C., and Tiedeman, C.R., 2007, Effective groundwater model calibration—With analysis of data, sensitivities, predictions, and uncertainty: Hoboken, New Jersey, John Wiley and Sons, Inc.

Hood, J.W., and Waddell, K.M., 1968, Hydrologic reconnaissance of Skull Valley, Tooele County, Utah: State of Utah Department of Natural Resources Technical Publication No. 18, 54 p.

Hsieh, P.A., and Fre ckleton, J.R., 1993, Documentation of a computer program to simul ate horizontal-flow barriers using the U.S. Geol ogical Survey's modular thre e-dimensional finite-difference ground-water flow mo del: U.S. Geological Survey Open-File Report 92-477, 37 p.

Kirk, S.T., and Campana, M.E., 1990, A deuterium-calibrated groundwater flow model of a r egional carbonate-alluvial system: Journal of Hydrology, Vol. 119, p. 357–388.

Las Vegas Valley Water District, 2001, W ater resources and gr ound-water modeling i n the White River and Meadow Valley flow systems, Clark, Lincoln, Nye, and White Pine counties, Nevada: Las Vegas Valley Water District, Las Vegas, Nevada, 297 p.

JA_16429

Leake, S.A., and Prudic, D.E., 1991, Documentation of a computer progr am to simulate aquifer-system compaction using the modular finite-difference ground-water flow model: U.S. Geological Survey Techniques of Water-Resources Investigations, 6-A2, 74 p.

Leeds, Hill and Jew ett, Inc., 1983, White Pi ne Power Project—Groundwater investigation phase 3—Technical report: Los Angeles Department of Water and Power, Los Angeles, California, 259 p.

LVVWD, see Las Vegas Valley Water District.

Mankinen, E.A., 2008, Personal c ommunication of July 9 to G . Dixon (Southwest Geology, Incorporated) regarding Confusion Range gravity survey.

Mankinen, E.A., and Mc Kee, E.H., 2009, Geophysical setting of western Uta h and eastern Nevada between latitudes 37°45' and 40°, *in* Tripp, B.T., Krahulec, K., and Jordan, J.L., editors, Geology and geologic resources and issues of western Utah: Utah Geological Association Publication 38.

Mason, J.L., 1998, Ground-water hydrology and simulated effects of development in the Milford area, an arid basin in southwestern Utah, Professional Paper 1409-G accessed http://pubs.er.usgs.gov/usgspubs/pp/pp1409G.

Maurer, D.K., 2002, Groundwater flow and numerical simulation of recharge from streamflow infiltration near Pine Nut Creek, Douglas County, Nevada: Water Resources Investigation Report 2002-4145

Maxey, G.B., and Eakin, T.E., 1949, Groundwater in the White River Valley, White Pine, Nye, and Lincoln counties, Nevada: State of Nevada, Office of t he State Engineer, Water Resources Bulletin No. 8, 61 p.

McDonald, M.G., and H arbaugh, A.W., 1988, A modular three-dimensional finite-difference ground-water flow model: U.S. Geological Survey Techniques of W ater-Resources Investigations 06-A1, 588 p.

Morgan, D.S., and Dettinger, M.D., 1996, Ground-water conditions in La s Vegas Valley, Clark County, Nevada- Part 2 Hydrogeology and simulation of ground-w ater flow: U.S. Geological Survey Water Supply Paper 2320-B, 124 p.

Niswonger, R.G., and Prudic, D.E., 2006, Documentation of the Streamflow-Routing (SFR2) Package to include unsaturated flow beneath streams—A modification to SFR1: U.S. Geological Survey Techniques and Methods 6-A13, 57 p.

Poeter, E.P., and Hill, M.C., 1998, Documentation of UCODE, a computer code for universal inverse modeling: U.S. Geological Survey Water-Resources Investigations Report 98-4080, 116 p.

Poeter, E.P., and Hill, M.C., 2008, SIM_ADJUST—A computer c ode that adjust s simulated equivalents for observations or predictions [Computer Software]: GWMI 2008-01.

SE ROA 51029

JA_16430

Poeter, E.P., Hill, M.C., Banta, E.R., Mehl, S., and Christensen, S., 2005, UCODE_2005 and six other computer codes for universal sensitivity analysis, calibration, and uncertainty evaluation: U.S. Geological Survey Techniques and Methods 6-A11, 300 p.

Prudic, D.E., Harrill, J.R., and Burbey, T.J., 1993, Conceptual evaluation of regional ground-water flow in the carbonate-rock province of the Great Basin, Nevada, Utah, and adjacent states, U.S. Geological Survey Open File Report 93-170, 103 p.

Prudic, D.E., Harrill, J.R., and Burbey, T.J., 1995, Conceptual evaluation of regional ground-water flow in the Carbonate-Rock Province of the Great Basin, Nevada, Utah, and adjacent states—Regional aquifer-system analysis—Great Basin, Nevada–Utah: U.S. Geological Survey Professional Paper 1409-D, 117 p.

Prudic, D.E., Konikow, L.F., and Banta, E.R., 2004, A new streamflow-routing (SFR1) package to include simulated stream-aquifer interaction with MODFLOW-2000: U.S. Geological Survey Open-File Report 2004-1042, 105 p.

San Juan, C.A., Belcher, W.R., Laczniak, R.J., and Putnam, H.M., 2004, Hydrologic components for model development, *in* Belcher, W.R., ed., Death Valley Regional Ground-Water Flow System, Nevada and California—Hydrogeologic framework and transient ground-water flow model: U.S. Geological Survey Scientific Investigations Report 2004-5205, p. 99–136.

Schaefer, D.H., and Harrill, J.R., 1995, Simulated effects of proposed ground-water pumping in 17 basins of east-central and southern Nevada; U.S. Geological Survey Water-Resources Investigations Report 95-4173, 73 p.

Smales, T.J., and Harrill, J.R., 1971, Water for Nevada—Report 2—Estimated water use in Nevada: Nevada Department of Conservation and Natural Resources, Division of Water Resources, 38 p.

SNWA, see Southern Nevada Water Authority.

Southern Nevada Water Authority, 2004, Five Year Conservation Plan, 2004–2009—Submitted to the U.S. Bureau of Reclamation in fulfillment of the requirements for Section 210(b) of the Reclamation Reform Act of 1982: Southern Nevada Water Authority, Las Vegas, Nevada, 31 p.

Southern Nevada Water Authority, 2006, Water resources assessment for Spring Valley—Presentation to the Office of the Nevada State Engineer: Southern Nevada Water Authority, Las Vegas, Nevada, 176 p.

Southern Nevada Water Authority, 2008, Baseline characterization report for Clark, Lincoln, and White Pine Counties Groundwater Development Project: Southern Nevada Water Authority, Las Vegas, Nevada, 1146 p.

Southern Nevada Water Authority, 2009a, Conceptual model of groundwater flow for the Central Carbonate-Rock Province—Clark, Lincoln, and White Pine Counties Groundwater Development Project: Southern Nevada Water Authority, Las Vegas, Nevada, 416 p.

SE ROA 51030

JA_16431

Southern Nevada Water Authority, 2009b, Simulation of groundwater development scenarios using the transient numerical model of groundwater flow for t he Central Carbonate-Rock Province—Clark, Lincoln, a nd White Pine Count ies Groundwater Development: Prepared by Southern Nevada Water Authority, in cooperation with the U.S. Bureau of Land Management. Las Vegas, Nevada, 82 p.

Southern Nevada Water Authority, 2009c, Water resource plan: Southern Nevada Water Authority, Las Vegas, Nevada, 71 p.

Thomas, J.M., Calhoun, S.C., and Apambire, W.B., 2001, A deuterium mass-balance interpretation of groundwater sources and flows in southeastern Nevada: Desert Research Institute, Publication No. 41169, 52 p.

Thomas, J.M., Carlton, S.M., and Hines, L.B., 1989, Ground-water flow and simulated response to selected develop-mental alternatives in Sm ith Creek Valley, a hydrologically c losed basin in Lander County, Nevada: U.S. Geological Survey Professional Paper 1409-E, 57 p.

Thomas, J.M., and Mihevc, T.M., 2007, Stable isotope evaluation of wa ter budgets for the White River and Meadow Valley Wash regional groundwater flow systems in east-central and southeastern Nevada: Desert Research Institute, Las Vegas, Nevada, 189 p.

Thomas, J.M., Welch, A.H., and Dettinger, M.D., 1996, Geochemistry and isotope hydrology of representative aquifers in the Great Basin region of Ne vada, Utah, a nd adjacent states: U.S. Geological Survey Professional Paper 1409-C, 108 p.

Tóth, J.A., 1963, A t heoretical analysis of ground-water flow in small dra inage basins: Journal of Geophysical Research, Vol. 68, No. 16, p. 4795–4812.

USBR, see U.S. Bureau of Reclamation.

U.S. Bureau of Reclamation, 2007, Lower Colorado Region, Lake Mead at Hoover Dam [Internet], available from http://www.usbr.gov/lc/region/g4000/hourly/mead-elv.html.

U.S. Department of Energy, 1997, Regional groundwater flow and tritium transport modeling and risk assessment of the underground test area, Nevada Test Site, Nevada: U.S. Department of Energy Report DOE/NV–477. U.S. De partment of Energy, Nevada Operations Office: Las Vegas, Nevada, 66 p.

U.S. Geological Survey, 2006a, 09419547 Blue Point Spring near Valley of Fire State Park, Nevada, Lower Colorado, Lake Mead Basin, Lake Mead Subbasin: U.S. Geological Survey Water-Data Report, Water Year October 2005 to September 2006, 3 p.

U.S. Geological Survey, 2006b, 09419550 Rogers Spring near Overton Beach, Nevada, Lower Colorado, Lake Mead Basin, Lake Mead Subbasin: U.S. Geological Survey Water-Data Report, Water Year October 2005 to September 2006, 3 p.

USGS, see U.S. Geological Survey.

Walton, W.C., 1988, Practical aspects of groundwater modeling; flow, mass and heat transport, and subsidence analytical and computer models; 3rd edition. Library of Congress Cataloging-in-Publications Data.

Welch, A.H., Bright, D.J., and Knochenmus, L.A., eds., 2008, Water resources of the Basin and Range Carbonate-Rock Aquifer System, White Pine County, Nevada, and adjacent areas in Nevada and Utah: U.S. Geological Survey Open-File Report 2007-5261, 112 p.

Wells, J.V.B., 1954, Compilation of records of surface waters of the United States through September 1950—Part 9, Colorado River Basin: U.S. Geological Survey Water-Supply Paper 1313, 756 p.

Winograd, I.J., and Friedman, I., 1972, Deuterium as a tracer of regional ground-water flow, Southern Great Basin, Nevada and California: Geological Society of America Bulletin, v. 83, p. 3691-3708.

Winograd, I.J., and Thordarson, W., 1975, Hydrogeologic and hydrogeochemical framework, south-central Great Basin, Nevada-California, with special reference to the Nevada Test Site: U.S. Geological Survey Professional Paper 712-C, 131 p.

JA_16433

Appendix A

Estimation of Large-Scale Hydraulic Properties

A.1.0 INTRODUCTION

Hydraulic-property estimates have been derived from many types of tests, but only a few of these sometimes yield hydraulic properties of the aquifer system a t scales large enough for use in large-scale numerical groundwater flow models. Th is appendix desc ribes an alternate approach to deriving large-scale hydraulic properties and its application to portions of the model a rea. The se activities were conducted independently by the USGS, in cooperation with SNWA, in support of the CCRP numerical model described in the main report. Preliminary results are included in this appendix. The final results will be made available on a USGS website: http://nevada.usgs.gov/water/ aquifertests/index.htm (Halford, 2009).

A.1.1 Limitations Associated with Aquifer Tests

The best type of aquifer test to derive transmissivity (T) and hydraulic-conductivity (K) values for the numerical model is the multiple-well, constant-rate aquifer test. Although estimates of T and K can also be derived from single-well tests, a quifer-storage properties can only be estimated from da ta collected from observa tion wells in multi ple-well, constant-rate aquifer tests. This type of test is considered to be the best but us ually has two primary issues, both of which are associated with the limited duration of testing. Such tests are usually conducted for short periods of time for logistical reasons.

The first issue pertains to the scale of the aquifer tests. If te sting time is l imited, then the aquifer volume tested must be limited too. Therefore, the properties derived from these tests only represent small portions of t he aquifer. This presents a problem for the estimates of T, K, and storage coefficients (S), as the derived values may not be representative of the areas located outside the tested area. Regiona l effects due to long-term pumping cannot be a ccurately predicted with the use of hydraulic properties derived from the typical pumping tests. To derive hydraulic properties at the appropriate scale, the multiple-well aquifer tests would have to be conducted for larger areas and longer times. It is extremely impractical to conduct aquifer tests at such scales.

The second issue arises for estimates of specific yield, as this property has been observed to vary with time during aquife r testing. Nwankwor et al. (1984) re ported a compara tive study of Sy determinations for a sha llow sand aquifer. The results from the study indicate that the Sy values derived from a pum ping test increase with the time of pum ping. The Sy values derived from a pumping test at 15, 40, 600, 1,560, 2,690, and 3,870 minutes are 0.02, 0.05, 0.12, 0.20, 0.23, and 0.25, respectively. The Sy of 0.25 at 3,870 minutes c losely approaches the Sy of 0.30 derived from the laboratory drainage curve. Nwankwor et al. (1984) concluded that the Sy derived from the short pumping duration based on the type-curve models is not suitable for use in the context of long-term aquifer-yield analysis, but the Sy derived from the pumping test at late times with the volume-balance

method or the *Sy* derived from the laboratory drainage curve provides a more reasonable estimate of the long-term *Sy* of the aquifer.

An approach to derive hydraulic properties at large scales from the existing anthropogenic data (stress and response) was applied to the modeled area and is described in the next section.

A.1.2 Approach

The response of wells (water-level changes) that are located in an area where groundwater pumping occurs was analyzed to derive reasonable ranges of *T* and *S,* which were used to simulate the regional effects of pumping. In essence, the available stress/response data associated with human activities, such as irrigation with groundwater, constitute large-scale aquifer-test data that can be analyzed to derive *T* and *S* values for large portions of the aquifer system. Two solution methods were used and are described in the following sections, including a list of the steps necessary to complete the analysis.

A.1.2.1 Method 1 - Analytical Model

In Method 1, estimates of *T* and *S* are derived by applying the Theis equation (Theis, 1935), the principle of superposition, and an optimization method to historical pumping and water-level data.

In this method, the water-level changes caused by one or more pumping wells in a single observation well are simulated and compared to observed water-level changes. Adjustments are made to *T* and *S* until an acceptable fit is obtained between the simulated and observed values. Because there are two unknown parameters, *T* and *S*, a solution cannot be derived analytically. However, a solution may be derived using the Theis equation as implemented in " Function.xls" and the Excel solver. "Function.xls" (Hunt, 2005) was developed as a tool to facilitate the analysis of groundwater problems. It is a collection of user-defined functions written in Visual Basic grouped into modules for use in Excel spreadsheets. The Theis solution for flow to a well is part of the hydraulics module. The input consists of the locations of the observation and pumping wells, pumping schedules, time-water-level changes for the observation well, and initial values for *T* and *S*.

A.1.2.2 Method 2 - Local Numerical Model

Method 2 estimates of *T* and *S* are derived by calibration of a local numerical flow model using MODFLOW-96 (Harbaugh and McDonald, 1996) and MODOPTIM (Halford, 2006). In this method, the water-level changes caused by one or more pumping wells in one or more observation wells are simulated and compared to observed water-level changes. In addition to *T* and *S*, other parameters may be adjusted during calibration, depending on the flow-system features and processes incorporated in the numerical model.

A.1.2.3 Steps

The steps of the approach are as follows:

1. Compile relevant historical data.

   - Water-level data
   - Water-use data
   - Precipitation data

2. Identify potential sites suitable for analysis.

   - Identify wells with detailed hydrographs located within historically irrigated areas.

   - Identify relatively dry time periods for which sufficient water levels and groundwater-use estimates are available or have available information from which to derive them.

   - Perform preliminary calculations using one or both methods to evaluate site conditions.

   - Eliminate sites that are not suitable for this analysis.

3. Perform final calculations for selected sites and present results.

A.2.0 DATA COMPILATION

The necessary historical data available for the study area were first compiled. Data of interest consist of water-level, water-use, and precipitation data obtained from the following sources:

- USGS National Water Information System (NWIS) for the historical water levels
- BARCASS Reports, NDWR pumpage inventories and water-rights database for historical water-use information
- Western Regional Climate Center (WRCC) for precipitation station data

The water-level data were compiled from the NWIS database (USGS, 2009). These data indicate that most of the available information is for the UVF RMU. The surface extent of the UVF RMU is about 4,993,486 acres, as compared to the total area of the model of 14,085,099 acres, or is about 35 percent of the model area. Data for about 1,245 wells are in the NWIS database (USGS, 2009), of which 985 wells are completed in the UVF RMU. The NDWR water-right database contains 9,325 points of diversion (POD) in the model area, of which 5,378 are associated with the UVF RMU. The basin-fill aquifer is generally shallow and unconfined within the model area.

The NDWR maintains Nevada's water-right database and has also conducted pumping inventories for some of the basins in the study area. The records of historical water rights are available for all basins beginning when significant water use was initiated. The pumping inventories are available for Dry, Rose, Panaca, Pahranagat, and Garnet valleys and the Black Mountains Area starting in 1989. As

SE ROA 51036

JA_16437

part of BARCASS, Welborn and Moreo (2007) delineated irrigated acreage for basins in the BARCASS area using satellite imagery for the 2000, 2002, and 2005 growing seasons. Welborn and Moreo (2007) supplemented the a creages derived from the satellite imagery with information collected during field reconnaissance visits (water source, irrigation system, and crop type) in 2005. Spatial distributions of the croplands, including the acreage, the irrigation water sources, the irrigation system, and the crop types, were derived for Butte, Cave, Jakes, Long, Tippett, Snake, and White River valleys. The net groundwater volumes affecting water levels were estimated by multiplying the acreages by a low and high estimate of net use rates of 2 and 3 ft/yr. The approximate locations of irrigation pumping were obtained from the NDWR water-right database (NDWR, 2009).

Precipitation data compiled by the National Climatic Data Center were obtained from the WRCC website (DRI, 2009). Historical precipitation data were obtained for the following precipitation stations located in the study area:

- Pioche
- Caliente
- Great Basin National Park
- Callao

A.3.0 SITE SELECTION

This section describes the process of site selection, followed by the data used to select the sites and descriptions of sites eliminated from the process.

A.3.1 Process

Sites that qualify for the analysis approach described in this appendix m ust meet the following criteria: (1) the observation well must exhibit a continuously declining water-level trend that correlates with groundwater pumping for irrigation for a per iod of two years or longer; (2) the observation well must be located within 6 to 10 mi of lands irr igated with groundwater and be far enough from recharge areas so as to not be significantly affected by seasonal fluctuations in water levels due to natural responses; (3) the amount of water pumped for the irrigation must be known or can be estimated from satellite imagery and consumptive-use rates; and (4) the time period for which the needed types of da ta are available must contain a period of below-average precipitation. The process consists of the following steps:

1. Generate water-level hydrographs for wells that have more than 10 measurements made after 1980. A cutoff date of 1980 was selected for several reasons: (1) the water-level data are of better quality and therefore are more reliable than older measurements, (2) the effects of pumping are more pronounced a nd can therefore be identified; and (3) pumping data are available or can be reliably estimated.

2. Identify wells with 10 measurements or more located within 10,000 ft of one or more irrigated areas.

3. Select sites for which historical pumping data are available for long periods of time (two years or more).

4. Identify hydrographs exhibiting effects of pumping

   - Compare water-level hydrograph to precipitation record
   - Compare water-level hydrograph to water-use trend

5. Identify a relatively dry time period for which pumping schedules can be estimated.

A.3.2 Potential Site Selection and Elimination

The total number of wells located within the model area that have historical water-level records in the NWIS database is 1, 245. Only 190 of these we lls have 10 or more water-level measurements recorded after 1980. Among the 190 wells, only 55 wells are within 10,000 ft of an irrigation area. After a detailed examination of each of the 55 wells, 9 well s that satisfy the criteria listed in Section A.3.1 were initially selected for the analysis. Two wells are located in northe rn Steptoe Valley; one well is located in northern Snake Valley; three wells are located nea r Baker, Nevada (central Snake Valley); one well is located in Lake Valley; one well is located in White River Valley; and the last well is located in Pahranagat Valley (Figure A-1).

Preliminary calculations were conducted using Method 1 to evaluate the nine potential sites. All sites were deemed to be ac ceptable for further analysis, except for those located in Steptoe, White River, and Pahranagat valleys. The unacceptable sites were eliminated based on the following findings.

A.3.2.1 Pahranagat Valley Site

The hydrograph of Well 209 S03 E60 35dabd1 (USGS ID 373808115124301) in Pahranagat Valley exhibits a significant drawdown consistent with pumping from Marc h 18, 1992, t o December 16, 1993. How ever, only four water-level measurements are available during this period, making it difficult to identify the start and t he end of the annual pum ping cycle. Another is sue with this observation well is that it is loc ated in the narrow alluvial floor whe re the alluvial deposits ar e bounded by bedrock on both sides at distances less than 5,000 ft. Therefore, the water levels at the observation well are probably affected by these boundaries, but the extent of the effect is unknown. Accounting for the ef fect of these boundaries in the analysis would introduce large uncertainties in the resulting T and S values.

A.3.2.2 White River Valley Site

The hydrograph of Well 207 N12 E62 18ddaa1, also known as USGS W ell 24 (USGS ID 385400115024001), exhibits the effects of a pumping cycle from March 22, 1962, to September 16, 1966. However, this well was not used i n the an alysis because no reliable re cords of hist orical pumping exist for this period. Furthermore, no reliable pumping estimate could be derived from satellite imagery because the agricultural lands around thi s observation well are irrigated with both groundwater and surf ace water. The N evada State Engineer water-right database indicates the
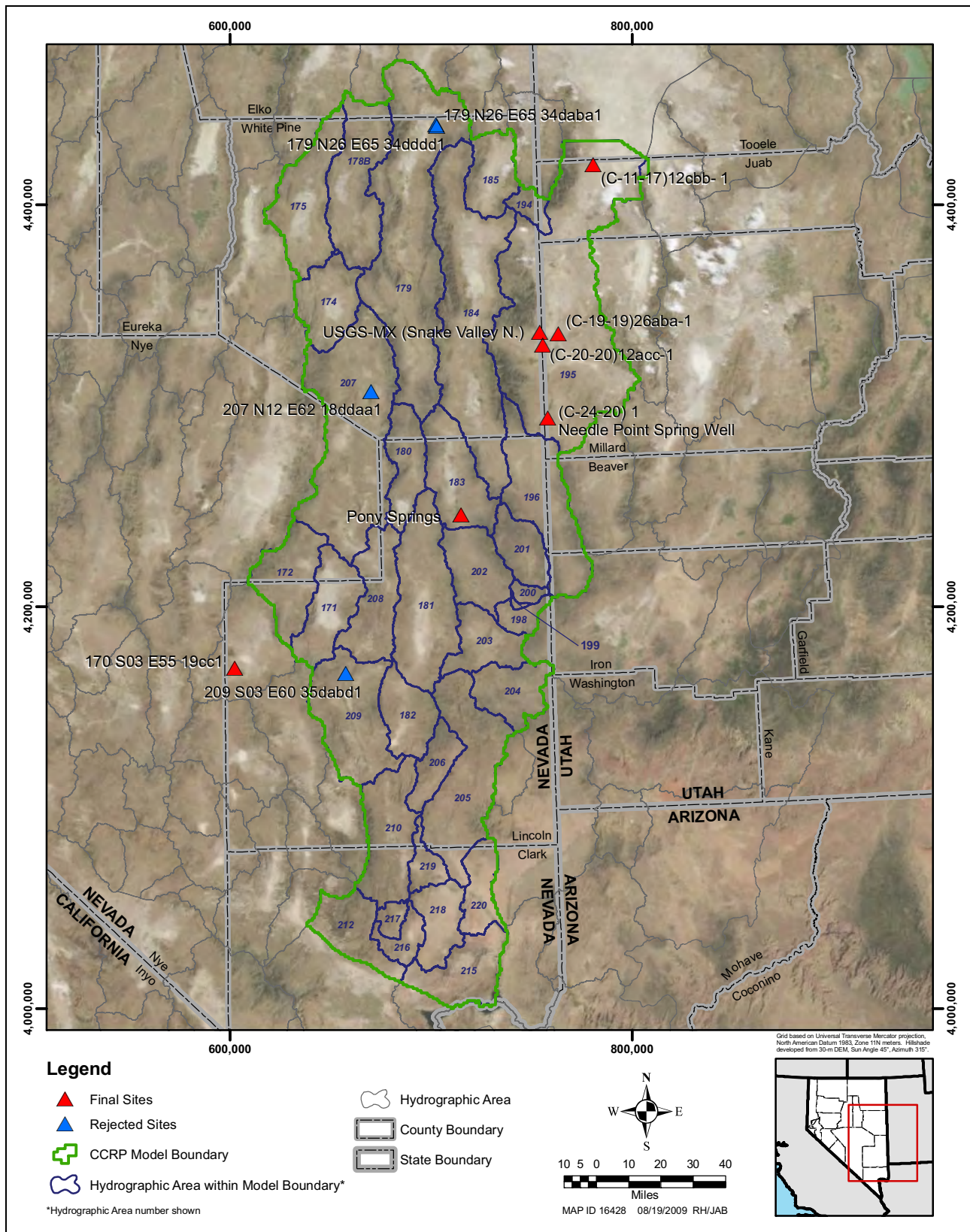
Figure A-1
Location of Sites Evaluated for Analysis

SE ROA 51039

JA_16440

presence of both groundwater and surface-water rights in the area (NDWR, 2009). A lthough a percentage of gr oundwater use c ould be derived from the wa ter rights, it is dif ficult to define the actual value of this percentage for the 1962 to 1966 time period, as the source of water use may vary depending on climatic and other conditions.

A.3.2.3 Steptoe Valley Sites

Two of the hydrographs selected from Steptoe Valley are for Wells 179 N26 E65 34daba1 (USGS ID 400504114373101) and 179 N26 E65 34dddd1 (USGS ID 400446114371501). The distance between the first t wo wells is about 3,000 ft, but t heir hydrographs show opposi te trends (up and down) between the periods of 1984 to 1987 and 1981 t o 1983. The refore, it is difficult to distinguish the effects of groundwater pumping on their water-level hydrographs.

A.3.3 Final Site Selection

The five wells that were acceptable for further analysis were used to derive estimates of *T* and *S* (Figure A-2). Two additional wells were then selected for analysis: Needle Point Spring Well and well 170 S03 E55 19cc 1 (USGS ID 373955115490201). Needle Point Spring Well was added to the analysis because it has good wate r-level measurements and is close to a major irrigation area located at the southern end of Snake Valley (Summers, 2001). Well 170 S03 E55 19cc 1 is located in Penoyer Valley and is outside of the model area. This well was added to the analysis for comparison purposes. Information on each of the sele cted wells is provided in Table A-1. Descriptions of the observation wells and the time periods selected for inclusion in the analysis are provided in the remainder of this section.

A.3.3.1 Baker Sites (Central Snake)

The three selected observation wells near the town of Baker, Nevada, are (C-19-19) 26aba 1, (C-20-20) 12acc 1, a nd 195 N15 E70 25dd 1, a ll of which are located in central Snake Valley (Figure A-2).

Well 195 N15 E70 25dd 1 is completed in basin fill near the mountain block to a depth of 94 ft bgs. The depth to water in this well was at 14 ft bgs in 1981. The la test recorded measurement was 16.73 ft bgs in 2008. The water level in this well not only exhibits a declining trend but also distinct seasonal variations.

Wells (C-19-19) 26aba 1 and (C-20-20) 12acc 1 are located 4 to 6 mi away from Well 195 N15 E70 25dd 1 toward the centra l part of the valley in bottom valley fill. The depth of Well (C-19-19) 26aba 1 is 103 ft bgs, and the well i s completed in alluvial deposits. The NW IS database contains water-level measurements for these wells from 1973 to 2008 (USGS , 2009). The hydrogr aphs of these wells show good seasonal variations prior to 1993. The water levels for these wells decline in subsequent years and do not exhibit the seasonal variations observed in Well 195 N15 E70 25dd 1.

The water-level measurements taken at t he three observation wells between 2000 and 2004 wer e selected for this analysis for the following reasons:
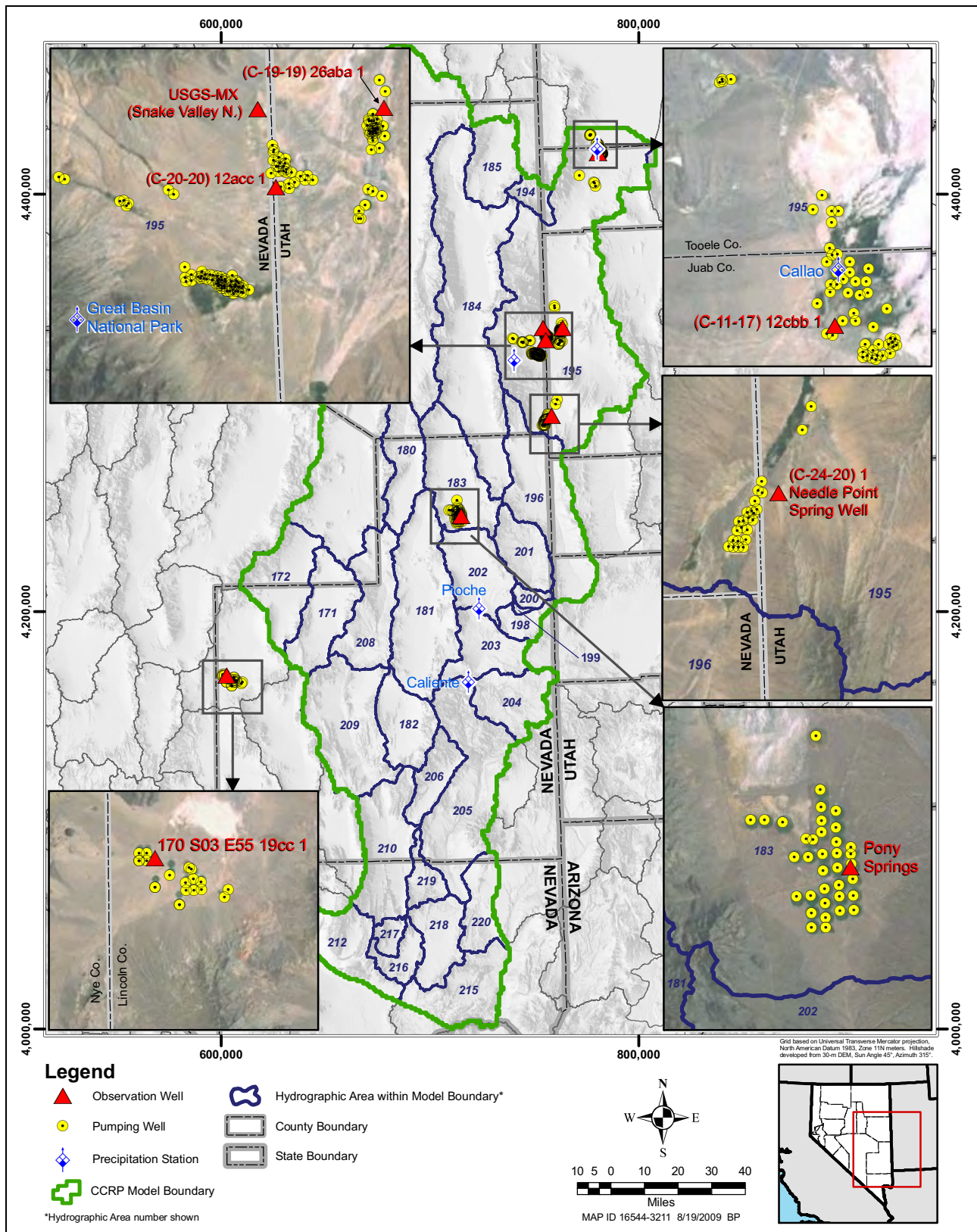
Figure A-2
Location of Selected Sites in Study Area

Table A-1
Selected Site Information

Observation Well	USGS ID	HA	UTM Northing[a] (m)	UTM Easting[a] (m)	Latitude[b]	Longitude[b]	Land-Surface Elevation[c] (ft amsl)	Time Period Available	Time Period Analyzed	Well Depth (ft bgs)
(C-20-20)12acc 1	3905001140245501	195	4,330,171	755,459	39°05'00"	114°02'45"	5,120	1972–2009	2000–2003	300
(C-19-19)26aba 1	3907581135655501	195	4,335,938	763,685	39°07'58"	113°56'55"	4,945	1977–2009	2000–2003	---
USGS-MX (Snake Valley N.)	390812114033601	195	4,336,051	754,041	39°08'12"	114°03'36"	5,068	1981–2009	2000–2003	94
(C-24-20) 1 Needle Point Spring	---	195	4,293,863	758,107	38°45'21"	114°01'47"	5,450	2002–2008	2002–2003	46
(C-11-17)12cbb 1	395259113430401	195	4,419,927	780,604	39°52'59"	113°43'04"	4,390	1986–2009	1989–1991	126
Pony Springs	382003114322501	183	4,245,749	714,916	38°20'03"	114°32'25"	5,950	1946–2008	2000–2004	161
170 S03 E55 19cc 1	373955115490201	170	4,169,399	602,402	37°39'58"	115°50'17"	4,850	1963–2002	1997–2002	238

[a]North American Datum of 1983 (NAD83), Zone 11
[b]North American Datum of 1927 (NAD27)
[c]National Geodetic Vertical Datum of 1929 (NGVD29)

- The extents of the c roplands in the area where the three observation wells are located have been estimated as part of BARCASS from satellite imagery for 2000, 2002, and 2005 (Welborn and Moreo, 2007).

- The annual precipitation rates measured for the same period of time at nearby stations ar e below the long-term annual average.

A.3.3.2 Northern Snake Valley Site

The selected observation well, (C-11-17) 12cbb 1, located in northern Snake Valley is close to the northern hydrographic boundary of Snake Valley.

The observation well is completed in alluvial deposits to a depth of 126 ft bgs. The Utah water-right database indicates that this well was drilled for domestic use. It has a duty of 10.86 afy, which is less than 1 pe rcent of the estimated irrigation consumptive water use in the area around t he selected observation well. No pumping inventory is available for this site.

Welborn and Moreo (2007) reported irrigated acreages for Snake V alley in 2000, 2002, and 2005. The irrigated acreage for Snake Valley in 2002 is about the same as the ave rage of the a creages for 2000, 2002, and 2005.

The depth-to-water measurements in this observation well are available from 1986 to 2008 (U SGS, 2009). The measur ements indicate consistently declining water levels. The depth to water was 48.84 ft bgs on March 10, 1987, and 55.29 ft bgs on March 4, 2008.

The water-level measurements taken at this observation well between 1989 and 1991 were selected for this analysis for the following reasons:

- The most detailed portion of the hydrographs occurs between 1989 and 1991.

- Based on the nearest precipitation stations, this time period is relatively dry.

- The observation well's hydrograph exhibits drawdowns of similar magnitudes for the periods 1989 to 1991 and 2000 to 2004. Thus, it was deemed r easonable to use the ac reage of the irrigated areas obtained fr om 2002 satellite imagery to estimate irrigation pumping for the period 1989 to 1991.

A.3.3.3 Southern Snake Valley Site

The selected observation well, (C-24-20) 1 Needle Point Spring Well, is a BLM m onitoring well located in southern Snake Valley, about 6 mi from the hydrographic boundary of S nake Valley and Hamlin Valley.

The observation well log indicates that the well is completed in alluvial basin fill (Summers, 2001). However, the basin fill at this location is interpreted to be thin and underlain by carbonate rocks.

Water-level measurements for this we ll are available from 2002 to 2008, and the corresponding hydrograph shows very good seasonal variation that appears to correlate to irrigation pumping. The total decrease in wa ter levels from 2002 to 2008 is only 1.65 ft. The declining water levels in this well may be due to both irrigation pumping and below-normal levels of precipitation. The acreages of the irrigated areas were derived from satellite imagery by Welborn and Moreo (2007) for 2000, 2002, and 2005. The acreages are consistent for these years.

The water-level measurements taken at this observation well between 2002 and 2003 were selected for this analysis for the following reasons:

- The acreages of irrigated areas are available for that time period (Welborn and Moreo, 2007).
- The time period between 2002 and 2003 is relatively dry.

A.3.3.4 Lake Valley Site

The selected observation well, Pony Springs Well, is located in southern Lake Valley. This well is completed in alluvial deposits t o a tot al depth of 161 ft bgs. Based on driller's well logs from NDWR, the alluvial deposits extend to a depth greater than 545 ft bgs around this well.

Depth to water in the P ony Springs Well was 1 30.3 ft bgs on J uly 26, 1946; 130.0 ft bgs on September 9, 1949; and 130.4 ft bgs in July 17, 1963 (Rush and Eakin, 1963). The water level observed during th at span of 17 ye ars was consistent with insignificant pumping. Beca use groundwater is th e only resourc e for irrigation, the water level in Pony Springs Well has be en declining since 1963; the water level continuously declined from 130.4 ft bgs in 1963 to 153.85 ft bgs in 2006, which is consistent with seasonal irrigation pum ping starting in the 1960s. During that period, the irrigated land around this we ll increased from 1,600 acres in the 1960s to 4,600 a cres in the 2000s. The water-level hydrograph for this well also exhibits irrigation pumping cycles.

Rush and Eakin (1963) also reported that a bout 1,900 afy was pumped from wells 6/66-22b1 and 22b2 for irrigation. These two wells were drilled to depths of 410 and 450 ft bgs, respectively, and approximately 2,400 gpm was yi elded with a drawdown of 30 ft (Rush and Eakin, 1963). The transmissivity estimated with the associated specific capacity is about 21,000 ft^2/d. These two wells are located about 3 mi from Pony Springs Well.

The water-level measurements taken at this observation well between 2000 and 2004 were selected for this analysis for the following reasons:

- The acreages of irrigated areas are available for that time period (Welborn and Moreo, 2007).
- The time period between 2000 and 2004 is relatively dry.

A.3.3.5 Penoyer Valley Site

The selected observation well, 170 S03 E55 19cc 1, is located in Penoyer Valley, which is outside of the model boundary and within the DVFS. The selec ted observation well is completed to a depth of 238 ft bgs in coarse alluvial deposits. Wells present around this observation well are also completed

in alluvial deposits. Water-level measurements and the pumping inventory for Penoyer Valley, including those for Well 170 S03 E55 19cc 1, are available in the USGS NWIS database and Moreo and Justet (2008), respectively. The sele cted observation well water-level hydrograph covers the period of 1963 to 2002.

The water-level measurements taken at this observation well between 1997 and 2002 were selected for this analysis for the following reasons:

- The acreages of the irrigated areas are available for that time period (Moreo and Justet, 2008).
- The time period between 1997 and 2002 is relatively dry.

A.4.0 DERIVATION OF T AND S

This section describes the estimates of net pumping rates, the solution process using the two methods described in Section A.1.2, preliminary results, and comparison to literature ranges.

A.4.1 Net Pumping Estimates

The volume of groundwater pumpage that is directly linked to the drawdown (also referred to as effective withdrawal rate) is calculated as follows:

$$Q_{DD} = Q_{Pump} - RF \qquad \text{(Eq. A-1)}$$

where,

Q_{DD} = Pumpage directly linked to the drawdown
Q_{Pump} = Total pumpage
RF = Return flow or water that percolates past the root zone and returns to the aquifer

RF is estimated to be about 20 percent of t he sum of t he water available (total pumpage + precipitation). Therefore, Q_{DD} may be expressed as follows:

$$Q_{DD} = 0.8 \times Q_{Pump} - 0.2 \times P \qquad \text{(Eq. A-2)}$$

where,

P = Precipitation falling in the irrigated area

Welch et al. (2008) examined the same equation expressing it in terms of rates with different variable names. In t heir study, the application rate, AR (ft/yr), co rresponds to the pumping rate, and the net pumping rate, $Pump_{net}$ (ft/yr), corresponds to the portion of groundwater withdrawal causing the drawdown. The precipitation rate P_r (ft/yr) is equivalent to the prec ipitation rate used in this study. Using the BARCASS variable names, Equation A-2 can be written as follows:

JA_16446

$$Pump_{net} = 0.8 \times AR - 0.2 \times P_r \qquad \text{(Eq. A-3)}$$

The crop application and precipitation rates reported by Welch et al. (2008) for BARCASS are listed in Table A-2. The net pumping rate can be calculated using this information and Equation A-3. The results are presented in Table A-2.

Table A-2
Application Rates, Precipitation Rates, and Derived Net Pumping Rates

Hydrographic Area	Average Application Rate[a] (af/acre)	Area Weighted Precipitation[a] (ft/yr)	Net Pumping Rate (ft/yr)
Lake Valley	3.0	1.0	2.2
Snake Valley	3.7	0.6	2.8
Spring Valley	3.5	0.8	2.7
Steptoe Valley	3.4	0.7	2.6
White River Valley	3.6	0.8	2.7
		Average	2.6

[a] Welch et al. (2008)

The rounded net pumping rates listed in Table A-2 range from 2 to 3 ft/yr. This range could change if a different percentage of return flow is used. This range was used at each site selected for the Theis superposition analysis.

A.4.2 Solutions and Preliminary Results

The results of the analysis using Method 1 for all selected sites and Method 2 for the Baker, Lake Valley and Penoyer Valley sites are described in this section.

The estimated ranges of T and Sy derived from the available stress/response data associated with agricultural activities, using Method 1, are summarized in Table A-3. Because of the large uncertainty associated with the estimated groundwater pumping and the actual correlation of the fluctuations in the hydrographs to the irrigation pumping, these estimates carry different levels of uncertainty depending on the site. In fact, as the optimization method could yield different solutions depending on the initial estimates for the parameters, it was necessary to assign initial values of T and Sy based on the available data for the study area. Initial values assigned to T and Sy were 3,500 ft^2/d and 0.07, respectively. The T and Sy ranges derived from the Lake Valley and Penoyer Valley sites carry less uncertainty than the other sites because of the following reasons: (1) the groundwater is the only source of irrigation water in these two basins; (2) the estimated irrigation acreages are more accurate; (3) the hydrographs exhibit continuous declines and distinct annual pumping cycles; and (4) the site conditions are more consistent with the assumptions of the Theis equation because the observation wells are located on the valley floors. Major sources of uncertainty for the other sites include the sources of irrigation water, acreages of the irrigated areas, measurement errors in the water levels, and the potential presence of subsurface boundaries affecting the hydrographs.

SE ROA 51046

JA_16447

Table A-3
Summary of *T* and *Sy* Values Derived with Method 1

Site	Observation Wells	UTM Northing[a] (m)	UTM Easting[a] (m)	*T* (ft²/d) Low	*T* (ft²/d) High	*Sy* Low	*Sy* High
Baker	(C-20-20)12acc 1	4,330,171	755,459	11,073	16,610	0.14	0.21
	(C-19-19)26aba 1	4,335,938	763,685	16,494	24,742	0.07	0.10
	USGS-MX (Snake Valley N.)	4,336,051	754,041	162,664	243,996	0.05	0.08
Needle Point Spring	(C-24-20) 1 Needle Point Spring	4,293,863	758,107	48,000	72,000	0.03	0.05
North Snake Valley	(C-11-17)12cbb 1	4,419,927	780,604	23,000	34,000	0.15	0.23
Lake Valley	Pony Springs	4,245,749	714,916	22,000	33,000	0.19	0.28
Penoyer Valley	170 S03 E55 19cc 1	4,169,399	602,402	19,000	29,000	0.09	0.13
			Average[b]	18,000	27,000	0.13	0.19

[a]North American Datum of 1983 (NAD83), Zone 11
[b]The average doesn't include the Needle Point Spring Well and USGS-MX well in Baker because the *T* and *S* derived for the former observation well mainly represent carbonate-aquifer properties and the location of the later observation well is close to mountain block.

Thus far, Method 2 (loca l numerical model) has be en applied only to the Bake r, Lake Valley and Penoyer sites. Water-level changes observed in se veral observation wells a nd related to irrigation pumping were analyzed using a local numerical flow model to derive ranges of transmissivity and specific yield of the basin fill in these sites.

The values of *T* and *Sy* derived through model calibration are presented in Table A-4. Details will be provided in Halford (2009).

Table A-4
Solutions for Baker, Lake Valley and Penoyer Valley Sites with Methods 2

Lithology	Site	Number of Monitoring Wells	Duration (Years)	Volume Pumped (afy) Low	Volume Pumped (afy) High	*T* (ft²/d) Low	*T* (ft²/d) High	*Sy* Low	*Sy* High
Basin Fill	170_Penoyer	12	11	57,000	95,000	11,000	19,000	0.09	0.16
Basin Fill	183_Lake	7	42	210,000	310,000	9,000	13,000	0.12	0.18
Basin Fill	195_Baker	8	4	31,000	46,000	5,600	9,000	0.12	0.18

A.4.3 Comparison to Literature Ranges

The values obtained f or *Sy* in Me thods 1 a nd 2 compar e favorably with those f rom the lit erature. Published values of specific yield, ge nerally derived from aquifer tests or laboratory tests, for unconsolidated materials were compiled by Johnson (1967) and are summarized in terms of minimum, average, and maximum values for each type of ma terial in Table A-5. The range of all reported *Sy* values, excluding zero values, is 0.02 to 0.35 for all samples (Table A-5). The last row in Table A-5 consists of t he average values of each column. The se average values serve as approximations of the overall mean and its range of unc ertainty. Thus, the ar ithmetic mean of the

**Table A-5
General Value of Specific Yield**

Material	Sy (-) Minimum	Sy (-) Average	Sy (-) Maximum
Clay	0	0.02	0.05
Sandy clay (mud)	0.03	0.07	0.12
Silt	0.03	0.08	0.19
Fine sand	0.10	0.21	0.28
Medium sand	0.15	0.26	0.32
Coarse sand	0.20	0.27	0.35
Gravelly sand	0.20	0.25	0.35
Fine gravel	0.21	0.25	0.35
Medium gravel	0.13	0.23	0.26
Coarse gravel	0.12	0.22	0.26
Average	**0.12**	**0.19**	**0.25**

Source: Johnson, 1967

averages (center column of Table A-5) is 0.19 with a range of uncertainty of 0.12 to 0.25 (arithmetic means of the minimum and maximum values located in the first and last columns of Table A-5).

Table A-6 contains the ranges of *T* for alluvial aquifers in Nevada as reported in Halford (2009). The values obtained for *T* in Methods 1 and 2 compare favorably to those reported in Table A-6.

SE ROA 51048

JA_16449

Table A-6
Transmissivity of Alluvial Aquifer from Pumping Tests in Nevada

USGS Site ID	Local Name	Altitude (ft)	Uppermost Opening (ft)	Lowermost Opening (ft)	Opening Interval (ft)	Transmissivity (ft^2/d)
390136119451501	N. Nowlin	4,689	80	374	294	1,000
395734119595601	Knox Well	4,405	100	440	340	1,200
385338119415801	Hatchery#3	4,901	90	440	350	2,000
385749119432701	Minden#7	4,807	175	500	325	2,000
385419119451001	Ranchos 9	4,796	230	658	428	3,300
364708115574401	WW-5C	3,082	887	1,187	300	2,500
390118119451501	S. Nowlin	4,694	60	330	270	2,300
390206119440001	S. Clapham	4,727	55	220	165	1,900
385634119433801	g-ville No. 9	4,797	140	400	260	3,000
390219119440001	N Clapham	4,727	55	220	165	2,250
385646119451101	g-ville No. 2	4,742	40	290	250	5,000
364922115580101	RNM-2s	3,130	1,038	1,119	81	1,900
385926119451201	Airport	4,700	150	450	300	7,300
390018119462901	Aldax	4,687	100	400	300	8,300
385444119453301	Ranchos Rocky Terrace	4,761	240	390	150	5,900
385611119435601	g-ville No. 4	4,785	125	305	180	7,700
385738119433601	Minden#8	4,800	110	510	400	23,000
390321119465301	Brown's	4,654	100	400	300	20,000
385604119445201	g-ville No. 7	4,761	95	300	205	18,000
385604119435601	g-ville No. 6	4,785	100	300	200	19,000
385505119435901	Ranchos 8	4,795	260	500	240	23,000
385738119465301	Minden#4	4,701	200	400	200	31,000

Source: Halford (2009)

SE ROA 51049

JA_16450

A.5.0 *SUMMARY*

The *T* and *Sy* values shown in Table A-3 and Table A-4 for alluvial deposits reflect a wide variation, especially for the re sults from Method 1.   Because of the lim itations of Method 1, th e *T* and *Sy* derived from Method 2 is generally more representative. Therefore, the *T* of 5,600 to 13,000 ft^2/d and the *Sy* of 0.12 to 0.18 from Method 2 for the sites within the study model area could be a representative range of me an *T* and *Sy*. However, the *T* and *Sy* derived from M ethod 1 may still reflect a range of site-spec ific data. The *T* and *Sy* derived from Me thods 1 a nd 2 fa ll within the literature range (see Tables A-5 and A-6), except for the *T* derived for the USGS_MX obs ervation well at Baker, Nevada, using Method 1, which may re flect that thi s well has a connection with the underlying carbonate aquifer.

A.6.0 REFERENCES

Desert Research Institute, 2009, Western U.S. Climate Historical Summaries [Internet], [accessed August 11], available from http://www.wrcc.dri.edu/Climsum.html.

DRI, see Desert Research Institute.

Halford, K.J., 2006, MODOPTIM: a general optimization program for ground-water flow model calibration and groundwater management with MODFLOW, U.S. Geological Survey Scientific Investigation Report 2006-5009.

Halford, K.J., 2009, Aquifer-test analyses of water level fluctuations from pumpage for irrigation during multiple drought years in selected basins of east-central Nevada [Internet], available from http://nevada.usgs.gov/water/aquifertests/index.htm.

Harbaugh, A.W., and McDonald, M.G., 1996, User's documentation for MODFLOW-96, an update to the U.S. Geological Survey modular finite-difference ground-water flow model: U.S. Geological Survey Open-File Report 96-485, 62 p.

Hunt, B., 2005, Visual basic programs for spreadsheet analysis. Ground Water. Vol. 43, No. 1, p. 138-141.

Johnson, A.I., 1967, Specific yield compilation of specific yields for various materials: U.S. Geological Survey Water-Supply Paper 1662-D, 80 p.

Moreo, M.T., and Justet, L., 2008, Update to the ground-water withdrawals database for the Death Valley regional ground-water flow system, Nevada and California, 1913–2003: U.S. Geological Survey Data Series 340, 10 p.

NDWR, see Nevada Division of Water Resources.

Nevada Division of Water Resources, 2009, Well Log Database [Internet], [accessed June], available from http://water.nv.gov/Engineering/wlog/wlog.cfm.

Nwankwor, G.I., Cherry, J.A, and Gillham, R.W., 1984, A comparative study of specific yield determinations for a shallow sand aquifer, Ground Water, Vol. 22, No. 6, p. 764-772.

Rush, F.E., and Eakin, T.E., 1963, Ground-water appraisal of Lake Valley in Lincoln and White Pine counties, Nevada: Nevada Department of Conservation and Natural Resources, Ground-Water Resources Reconnaissance Series Report 24, 43 p.

SE ROA 51051

JA_16452

Summers, P., 2001, Hydrologic analysis of Needle Point Spring. Fillmore Field Office, Utah.

Theis, C.V., 1935, The relation betwee n the lowering of the piezometric surface and the rate and duration of di scharge of a well using groundwater storage: American Geophysical Union Transactions, Vol. 16, p. 519-524.

U.S. Geological Survey, 2009, N ational water information system data base [Internet], [accessed February], available from http://waterdata.usgs.gov/nwis.

USGS, see U.S. Geological Survey.

Welborn, T.L., and Moreo, M.T., 2007, Delineated irrigated acreage overlying the Basin and Range carbonate-rock aquifer system, White Pine County, Nevada, and adjacent areas in Nevada and Utah: U.S. Geological Survey Data Series 273, 18 p.

Welch, A.H., Bright, D.J., and Knochenmus, L.A., eds., 2008, Water resources of t he Basin and Range Carbonate-Rock Aquifer System, White P ine County, Nevada, and a djacent areas in Nevada and Utah: U.S. Geological Survey Scientific Investigations Report 2007–5261, 96 p.

SE ROA 51052

JA_16453

This Page Intentionally Left Blank

Appendix B

Transient Data Compilation and Analysis

B.1.0 INTRODUCTION

Transient observations of hydrologic data are necessary for the calibration of the numerical model. This appendix details the development of model observations for select springs, stream gages, and well locations in the study area.

B.1.1 Purpose and Scope

The purpose of the work described in this appendix is to derive hydrologic model observations for the study area. To derive these observations, a series of steps were required that included the following:

- Update hydrologic data sets previously compiled and reported in SNWA (2008, 2009).
- Conduct a preliminary analysis on the updated hydrologic data.
- Derive transient flow observation data sets for calibration of the numerical model.

B.2.0 DATA COMPILATION

Data sets previously compiled and reported in SNWA (2008, 2009) were updated to include additional measurements to existing sites or to add completely new sites along with new hydrologic data. The updating of the data sets reported in SNWA (2008) was not a systematic effort to amend every well, spring, or stream gage location with data current to the end of 2008. Specific data sets were updated, however, in an effort to fill in potential data gaps or to enhance existing data sets to improve calibration of the transient model. The following sections discuss the incorporation of additional hydrologic data into the spring, stream flow, and water-level data sets originally documented in SNWA (2008).

B.2.1 Spring Discharge

The spring discharge data sets included in SNWA (2008, 2009) documented spring discharges as either individual miscellaneous measurements or as average discharges over the period of record for a given spring. For calibration of the transient model, however, calendar year average measurements of spring discharge were necessary. As a result, springs from the Conceptual Model Report (SNWA, 2009, Table G-1) were identified that had continuous discharge measurements available. For these springs, daily mean discharge data were obtained from the USGS 's NWIS website (http://waterdata.usgs.gov/nwis) for the entire period of record available. In addition, the calendar year annual statistics for each site were also downloaded. The daily mean discharge data for all of the continuously monitored springs were then combined into one data set for further analysis. The springs that had continuous discharge measurements available and their calendar year periods of record are listed in Table B-1.

Table B-1
Continuously Monitored Spring Discharge Locations
and Calendar Year Periods of Record

HA Number	USGS Site Number	USGS Site Name	Period of Record
195	10243224	BIG SPGS CK SOUTH CHANNEL NR BAKER, NV	2008
195	102432241	BIG SPGS CK NORTH CHANNEL NR BAKER, NV	2006–2007
195	10172860	WARM CREEK NEAR GANDY, UT	2006–2007
207	09415558	HOT CK NR SUNNYSIDE, NV	2007
207	09415510	PRESTON BIG SPRG NR PRESTON NV	1983–1984, 2001–2008
209	09415639	ASH SPGS DIV AT ASH SPGS, NV	2004–2007
209	09415640	ASH SPGS CK BLW HWY 93 AT ASH SPGS, NV	2000–2007
209	09415589	CRYSTAL SPGS DIV NR HIKO, NV	2005–2007
209	09415590	209 S05 E60 10 1 CRYSTAL SPGS NR HIKO, NV	1986–1987, 1991–1993, 1999–2007
215	09419547	BLUE POINT SPG NR VALLEY OF FIRE STATE PARK, NV	2000–2007
215	09419550	ROGERS SPNG NR OVERTON BEACH, NV	1986–2007
219	09415900	MUDDY SPGS AT LDS FARM NR MOAPA, NV	1986–1993, 1997–2007
219	09415908	PEDERSON E SPGS NR MOAPA, NV	2003–2004, 2007
219	09415910	PEDERSON SPGS NR MOAPA, NV	1987–1993, 1997–2007

B.2.2 Muddy River Stream Flow

Similar to the spring discharge data sets, the Muddy River stream flow data sets documented in SNWA (2008) were reported as water-year annual discharges for gaging stations or as a series of miscellaneous discharge measurements for ungaged streams in the study area. For calibration of the transient numerical model, however, calendar year discharge measurements of the stream flow along the Muddy River were necessary. As a result, the stream flow discharge data sets for the Moapa and Glendale gages were updated so that calendar year average discharge measurements could be derived. These updates included obtaining daily mean discharge data from the USGS's NWIS website (http://waterdata.usgs.gov/nwis) for the entire period of record available for each of the gages. In addition, the calendar year annual statistics for each site were downloaded. The daily mean discharge data were combined into one data set for further analysis. The stream gage locations that had continuous discharge measurements available and their calendar year periods of record are provided in Table B-2.

B.2.3 Water Levels

The water-level data set described in SNWA (2008) was updated to include both new water-level measurements for existing sites and new well locations and water-level measurements. The new